Early structural connectivity in preterm infants' brain and how music might shape it

ALVES SA DE ALMEIDA, Joana Rita

Abstract

La naissance prématurée expose les enfants à des stimuli nocifs pendant une période critique de maturation cérébrale, entraînant des conséquences néfastes sur leur neurodéveloppement. La musicothérapie a été proposé comme intervention précoce visant à enrichir l'apport sensoriel des prématurés pendant cette période de plasticité et ainsi améliorer la maturation cérébrale. En s'appuyant sur l'IRM de diffusion, cette thèse a évalué les effets d'une intervention musicale sur le développent structurel cérébral des enfants très prématurés. Les résultats démontrent que d'importantes modifications de la microstructure e de l'organisation du cerveau du prématuré ont lieu entre la 33ème semaine de gestation jusqu'à l'âge équivalent du terme (TEA), lesquelles sont affectées par la naissance prématurée. L'intervention musicale postnatale précoce a conduit à une maturation microstructurelle significativement supérieure de plusieurs fibres de la substance blanche, ainsi que de diverses régions corticales impliquées dans le traitement des émotions et la cognition, en [...]

Reference

UNIVERSITÉ DE GENÈVE

UNIVERSITÉ DE GENÈVE

DOCTORAT EN NEUROSCIENCES
des Universités de Genève
et de Lausanne

UNIVERSITÉ
DE GENÈVE

UNIL | Université de Lausanne

UNIVERSITÉ DE GENÈVE   FACULTÉ DE MEDECINE

Professeure Petra S. Hüppi, directrice de thèse

TITRE DE LA THÈSE

EARLY STRUCTURAL CONNECTIVITY IN PRETERM INFANTS'
BRAIN AND HOW MUSIC MIGHT SHAPE IT

THÈSE
Présentée à la
Faculté de Médecine

de l'Université de Genève

pour obtenir le grade de
Docteure en Neurosciences

par

Joana SA DE ALMEIDA

de Lisbonne, Portugal

Thèse N° 283

Genève

Editeur ou imprimeur : Université de Genève

2020

ACKNOWLEDGMENTS

"Life is either a daring adventure, or nothing at all"

Helen Keller

In this journey of emotions, that has been carrying out this project for the last (almost) four years, with some moments making me happy, and many others making me cry, I could not pass without a deep and warm "Thank you!" to all the people that, in a way or another, have crossed my path and have been part of, probably, one of the best periods of my life.

First of all, I would like to acknowledge my supervisor, Prof. Petra S. Hüppi, who has offered me the unique opportunity to work with her on the best phD project ever (true story). Thank you for your unconditional support and for trusting in my capabilities, even if one could initially question (myself included!) if I would be the ideal person for handling this project. You have always encouraged me and pushed me forward, giving me strength and motivation, what ideally every supervisor should do, but so rarely actually happens. I once overheard you referring to me in the neonatology unit (during a period when the subjects' recruitment was not going very well), as "*ma chère Joana*". I might not be very expensive as a phD student, but maybe to your heart, and you know you are also to mine.

I would like also to express my sincere gratitude to the jury members of my thesis, Prof. Serena Counsell, Dr. Jessica Dubois and Prof. Dimitri Van De Ville for having accepted to be part of it, for their consideration towards my work and their constant kindness and good humour.

As one may imagine, this work would not have been possible without the support from a countless number of amazing people.
I would like to acknowledge all the clinical staff from the services of neonatology and development and growth, who have helped me in the recruitment, data acquisition and implementation of the intervention.
Thank you, Dr. Olivier Baud and Dr. Francisca Barcos, for your unstoppable research motivation and for "making it happen". Thank you, Dr. Sebastien Fau, for helping producing the adapted headphones used in this project, as well as improvement of all the logistics regarding the MRI transport. Thank you, Dr. Marlene de Abreu, for your help and support throughout so many MRI exams. Thank you, Dr. Riccardo Pfister, for supporting this research and being always available when needed.

And because the company makes the journey more valuable than the actual destination, a huge thank you to all my friends, that have been there for me, for the best and for the worst, turning Geneva into a new home.

Thank you, Marta M., for your true friendship, all the support, help, company and encouragement, which you have unconditionally given to me throughout all these years. Although sharing the same age, life gave you probably more wisdom xD You are the closest I have to a family in Geneva and I'm very lucky to have you here. :)

Thank you, Nikita, also a sister of the heart and best companion of so many adventures. It's difficult to imagine Geneva without you, our spontaneous decisions and your psychologic support and astrological advices (Ahaha). We have grown up together during these last years and, even if life is guiding you towards a new destination, distance will not keep us apart.

Thank you, Elsa, Diana, Vânia, Luisa, Vasia, Thomas, Alessandro, as well as to all the rest of the "tuga crew" plus the "adopted ones", and to all the friends I have made in Geneva. Thank you all for all the amazing travels, hikings, runs, culinary and life (or death, like skiing…) experiences that we have shared! You have definitely make this journey better and worth it!! Thank you also to my friend Diana Gonçalves, who, despite the distance, has always managed to join me in lovely travels whenever our crazy lives were giving us some time to discover a bit the world.

Last but not the least, I would like to express my love for my family, that, not matter how far, is always with me. Thank you to my mum and dad, Fatima and Altino, for never neglecting anything that is important to me in this life. Words are not enough to express my gratitude and recognition towards the love you have always given to me. Thank you for being there, for having made my education a priority and for always push me to be better. Thank you to my grandma, Maria, for being the best grandma in the universe. You have given me everything, in all possible ways. Thank you for your infinite patience and unconditional love. My heart is with you. And thank you to my little brother (now much bigger than me!), João, for being the best and the kindest brother ever. I miss not having been able to see you growing these last years. I know mum and dad are, in any case, doing a great job. Thank you for making everything better. I love you all infinitely.

And, as emotions make us feel truly alive, and this musical project has offered me more of them than one could ask for, I'm very pleased to share with you the results of these thesis, which show how music may influence our emotional brain already very early in our life.

<div align="right">Joana Sa de Almeida</div>

ABSTRACT

Preterm birth occurs during a critical period of brain maturation and plasticity, the third trimester of pregnancy, interfering with important processes of structural brain development. By exposing the preterm infants to a dramatic change in the environment, namely noxious stimuli and events that can injure the brain, as well as by denying the expected intrauterine factors and meaningful sensory inputs relevant for activity-dependent plasticity, preterm birth may lead to an altered brain development and neurodevelopmental impairments, with an increased risk for those born before 32 weeks of gestational age (GA).

The neonatal intensive care unit (NICU) environment is recognised to be stressful and to lack of meaningful sensory input, leading to premature infant's physiologic instability and altered brain development. For such reasons, there has been an increasing interest in developmentally oriented care to modulate preterm infants' sensory input during NICU stay. Music therapy has been one of the investigated early interventions aimed to enrich preterm infants sensory input and thus enhance maturation of distinct brain neural networks, including regions important for cognitive and emotional processing, during a period when neural remodelling is particularly experience-dependent.

Capitalizing on the latest technological advances regarding dMRI acquisition and analysis, this thesis project aims to study the impact of prematurity on early brain structural connectivity and maturation, as well as the effectiveness of an early postnatal music intervention in enhancing preterm infants' brain structural development.

Two cohorts of very premature infants participating in similar randomised controlled clinical trials investigating the effects of an early postnatal music intervention on brain development have been studied. In the first cohort, premature infants have undergone an MRI at term-equivalent age (TEA), after the intervention. In the second cohort, evaluated longitudinally, two MRI were acquired, a first one during the 33th week GA and a second one at TEA, before and after the intervention, respectively. Full-term infants were recruited in parallel and have undergone a single MRI shortly after birth, at term age. The music used for the intervention was especially created for the project by the composer Andreas Vollenweider, based on the infants' behavioral responses, assessed by

developmental specialists, to various instruments and tunes. This music was played daily during NICU stay, from the 33th week GA to TEA, by means of adapted headphones manufactured for the project, accordingly to the premature infants' behavioral state (waking up, being awake, falling asleep).

Using a longitudinal whole-brain fixel-based analysis, we demonstrate that important micro and macrostructural maturational changes take place from the 33th week GA to TEA of preterm brain development, in both WM and GM. Preterm birth leads to an impaired fiber density of major WM fiber bundles at TEA, in comparison to full-term birth, what is further supported by an alteration also of diffusion tensor parameters in premature infants' WM fibers at TEA, evaluated by means of region-of-interest and seed-based tractography analysis. Such impairments in WM microstructure may lead to the measured diminished connectivity strength of several connections and diminished rich-club connectivity and global efficiency observed in the preterm brain networks at TEA, as shown by whole-brain connectomic analysis.

We further show that an early postnatal music intervention leads to an improved maturation of several functionally important WM tracts, namely the acoustic radiations and uncinate fasciculus, an increased amygdala volume at TEA, as well as to a longitudinal accelerated microstructural cortical maturation of the left insulo-orbito-temporopolar complex, right middle temporal gyrus and right precuneus/posterior cingulate gyrus, regions that were shown to have an impaired microstructural maturation and/or connectivity in preterm infants at TEA in comparison to full-term newborns. Both WM tracts and cortical regions affected are and known to be involved in auditory, congnitive and socio-emotional processing.

Overall, our results support that an early music postnatal intervention can enhance the maturation of brain regions undergoing important developmental changes during early brain development and known to be impaired by premature birth. Therefore, preterm infants can benefit from music, as a non-invasive approach to enhance their brain development, with a particular effect on the orbitofrontal-temporal pole circuitry, what might help to mitigate the later socio-emotional deficits frequently observed in this population and prevent loss of potential and lifelong impairments associated with premature birth.

RÉSUMÉ

La naissance prématurée a lieu pendant une période critique de maturation et de plasticité cérébrale, raison pour laquelle la prématurité a un impact sur le développement normal du cerveau. Elle expose les enfants à des stimuli et événements nocifs, tout en les privant des sollicitations intra-utérines et informations sensorielles adaptées pendant une importante période de plasticité cérébrale dépendante de l'activité, ce qui peut avoir des conséquences néfastes sur le développement du cerveau. La prématurité peut ainsi conduire à des troubles neuro-développementaux, avec un risque accru pour les enfants nés avant 32 semaines d'âge gestationnel (AG).

L'environnement dans l'unité de soins intensifs néonataux (USIN) peut être stressant et avec un manque d'informations sensorielles adaptées, entraînant une instabilité physiologique chez l'enfant prématuré et contribuant à un développement cérébral altéré. Pour ces raisons, au cours des dernières années, il y a eu un intérêt croissant concernant les soins de développement, axée sur l'apport sensoriel des nourrissons pendant le séjour à l'USIN. La musicothérapie est l'une des interventions précoces proposées visant à enrichir l'apport sensoriel des prématurés, pendant une importante période de plasticité cérébrale dépendante de l'activité, et ainsi améliorer la maturation de réseaux neuronaux cérébraux, incluant des régions importantes pour le traitement cognitif et émotionnel.

En s'appuyant sur les dernières avancées technologiques en matière d'acquisition et d'analyse de l'IRM de diffusion, ce projet de thèse vise à étudier l'impact de la prématurité sur la connectivité et la maturation structurelles du cerveau, ainsi que l'efficacité d'une intervention musicale postnatale précoce pour améliorer le développement structurel du cerveau des prématurés.

Deux cohortes de nourrissons prématurés, participant à des essais cliniques contrôlés randomisés similaires visant examiner les effets d'une intervention musicale postnatale précoce sur le développement cérébral, ont été étudiés dans le cadre de ce travail. Dans la première cohorte, des images IRM ont été acquises chez des prématurés après l'intervention, à l'âge équivalent du terme (TEA). Dans la seconde cohorte, évaluée longitudinalement, deux IRM ont été acquises, une première peu de temps après la naissance : lors de la 33ème semaine d'AG, et une deuxième, à l'âge du terme, respectivement avant et après l'intervention. Des

nouveau-nés nés à terme ont également été recrutés et des images IRM ont été acquises à la naissance. La musique utilisée pour l'intervention a été spécialement créé pour le projet par le compositeur Andreas Vollenweider. Pour ce faire, les instruments et mélodies ont été choisies en se basant sur les réponses comportementales des nourrissons, évaluées par des spécialistes du développement. Les bébés prématurés ayant bénéficié de l'intervention musicale ont ainsi écouté, grâce à des écouteurs adaptés et fabriqués pour ce projet, cette musique tous les jours pendant leur séjour à l'USIN, et ce dès la 33ème semaine d'AG jusqu'à TEA. Chaque moment musical était choisi et adapté en fonction de l'état d'éveil des enfants prématurés (réveil, éveil, endormissement).

En utilisant une analyse longitudinale fixel-based évaluant l'ensemble du cerveau, nous avons montré d'importantes altérations maturationelles, de la micro et macrostructure, de la substance blanche et substance grise du cerveau du prématuré, ayant lieu entre la 33ème semaine d'AG jusqu'à TEA. De plus, en utilisant une analyse longitudinale fixel-based, nous avons également montré qu'une naissance prématurée entraîne une altération de la densité des fibres de substance blanche à TEA, en comparaison avec celles des enfants nés à terme. Ce résultat est confirmé par l'observation d'une modification des paramètres du tenseur de diffusion des fibres de substance blanche des prématurés à TEA, évalués en utilisant une analyse avec des régions d'intérêt et la tractographie. Ces altérations de la microstructure de la substance blanche peuvent être à l'origine de la diminution de la connectivité détectée dans plusieurs connexions cérébrales, notamment entre les régions appartenant au "rich-club", ainsi que la diminution de l'efficacité globale du réseau neuronal du prématuré à TEA, comme nous démontrons en utilisant une analyse connectomique.

De plus, nos résultats démontrent qu'une intervention musicale postnatale précoce conduit à une maturation microstructurelle significativement supérieure de plusieurs fibres de la substance blanche notamment impliquées dans la cognition et les émotions. Nous avons ainsi observé un effet de l'intervention musicale sur la maturation microstructurelle des radiations acoustiques et du faisceau unciné, ainsi qu'une augmentation du volume de l'amygdale à TEA, et une maturation longitudinale accélérée du complexe insulo-orbito-temporopolaire cortical gauche, du gyrus temporal moyen droit et du précunéus/gyrus cingulaire postérieur droit. Cette amélioration de la maturité microstructurelle est d'autant plus importante car elle survient dans des régions présentant une altération due à la naissance prématurée et qui sont connues pour être impliquées dans l'audition, cognition et traitement des émotions.

En résumé, nos résultats soutiennent qu'une intervention musicale précoce peut améliorer la maturation des régions du cerveau subissant des importants changements pendant le développent du cerveau du prématuré et connues pour être altérées par une naissance prématurée. Par conséquent, les nourrissons prématurés peuvent bénéficier de la musique, en tant qu'approche non invasive pour améliorer leur développement cérébral, avec un effet particulier sur le circuit orbitofrontal-temporopolaire, ce qui pourrait aider à atténuer les déficits socio-émotionnels fréquemment observés dans cette population et à prévenir la perte de potentiel et les troubles neuro-développementaux associées à la prématurité.

x

TABLE OF CONTENTS

1.   INTRODUCTION

1.1. Motivation and aims

Preterm birth, accounting for approximately 15 million newborns yearly, besides being a major cause of death, impacts clinical outcome and is associated with numerous long-term complications. In particular, it may lead to a disruption of neural structures typical developmental trajectory and, consequently, neurodevelopmental impairments, affecting motor, sensory, cognition, language, attention and behavioral and socio-emotional domains (Anderson and Doyle, 2003; Bhutta et al., 2002; Marlow, 2004; Montagna and Nosarti, 2016; Spittle et al., 2009; Spittle et al., 2011; Williams et al., 2010; Witt et al., 2014), with an augmented risk for those born before 32 weeks' gestational age (GA) (Blencowe et al., 2013). Causes for these neurodevelopmental problems are multiple and include factors linked to early life events and environment. In fact, preterm birth is associated with complications such as hypoxic-ischemic events, intracranial hemorrhage, periventricular leukomalacia, sepsis, hypoglycaemia and malnutrition, which may lead to direct brain damage (Back and Miller, 2014; Duvanel et al., 1999; Feldman et al., 1990). Furthermore, during NICU stay, preterm infants are exposed routinely to multiple noxious stimuli (Vinall et al., 2012) and denied meaningful sensory inputs relevant for activity-dependent plasticity (Kiss et al., 2014b; Radley and Morrison, 2005), what also impacts on brain maturation (Brummelte et al., 2012; Smith et al., 2011).

In the last years, neonatal intensive care units (NICU) have been in search for developmentally oriented care to modulate preterm infants' sensory input, aiming to prevent preterm infants' loss of potential and lifelong impairments, which constitute a heavy burden on families, society and health system.

Music has been one of these early interventions introduced into NICU as an approach for sensory stimulation potentially influencing cognitive and emotional development. The sound environment was shown to shape the auditory system during early brain development (Chang and Merzenich, 2003; Pineda et al., 2014; Ponton and Eggermont, 2001; Zhang et al., 2002) and music listening is thought to be relevant for activity-dependent brain plasticity during early auditory and brain networks maturation (Graven and Browne, 2008; Kiss et al., 2014b; Lasky and

Williams, 2005), by triggering a rich brain processing, with the recruitment of regions implicated in cognitive and emotional processing, which are functions typically affected by prematurity (Koelsch, 2014; Zatorre et al., 2009).

However, to date, studies evaluating the effect of music on preterm newborn's brain development are still scarce and, in particular, there is little to no evidence regarding the influence of music on early brain structural maturation.

Diffusion Magnetic Resonance Imaging (dMRI) is a non-invasive MRI method with high sensitivity to water movements within the architecture of the tissues (Beaulieu, 2002; Le Bihan, 1991) that allows the reconstruction of WM fiber pathways and to study its microstructure and connectivity properties. dMRI has allowed the detection of early developmental abnormalities in brain microstructure and structural network organisation holding a negative impact on clinical development after preterm birth (Fischi-Gomez et al., 2015; Pecheva et al., 2018; Rogers et al., 2012). Besides the study of WM development, dMRI also allows the study of cortical maturation and has revealed an altered cortical development in relation to prematurity (Ball et al., 2013b; Rogers et al., 2012).

Capitalizing on the latest technological advances regarding analysis of dMRI, this thesis project was designed to study the impact of prematurity on whole-brain early structural maturation and connectivity, both at term-equivalent age (TEA) in comparison to full-term newborns, and longitudinally from the 33th week GA to TEA of preterm brain developmental (which corresponds to the third trimester of pregnancy) as well as to evaluate the effectiveness of an early postnatal music intervention for enhancing preterm infants' brain structural maturation and connectivity, both longitudinally and at TEA.

1.2. Brain development

The human brain can be seen as a complex network, comprising around 100 billion (10^{11}) neurons connected by about 100 trillion (10^{14}) synapses (Ackerman, 1992). Neurons, the basic units of the brain, are electrically excitable cells that process and transmit information by electro-chemical signalling. A typical neuron consists of a cell body with dendrites (which conduct signals from postsynaptic terminals to the cell body) and a single axon with branches (that conducts signals from the cell body to the presynaptic terminals) (Ramón y Cajal, 1899). The synapse, a complex membrane junction or gap, is the structure that permits a neuron to pass an electrical and chemical signal to another neuron. When stimulated by an electrical pulse, neurotransmitters of various types are released into the synaptic gap between neurons and then bind to chemical receptors in the dendrites of the post-synaptic neuron, being able to modulate the potential of the receiving neuron (Pereda, 2014), to enhance the target recognition or to supply nutrition, by providing chemical compounds needed by the axon (as the nerve growth factor, NGF) (Ackerman, 1992; Pereda, 2014; Petruska and Mendell, 2009). In addition to neurons, glial cells are the second major cell type in the brain. They are known to play important roles, such as trophic and metabolic support to neurons, neuronal guidance, neurite outgrowth and synaptogenesis, among others (Kettenmann and Ransom, 2004).

1.2.1. Emergence of brain connectivity

The development of the central nervous system (CNS) is a protracted and asynchronous process, dependent on a complex interaction between genetic, epigenetic and environmental factors. During early development, the brain is composed by different transient laminar components: the poliferative zones (ventricular and subventricular), the intermediate zone (which will become mature white matter, WM), the subplate, the cortical plate (that will become the mature cortex) and the marginal zone. Various processes may overlap in time during CNS development, namely neuronal proliferation, neuronal and glial migration, synaptogenesis, organization and myelination. Neuronal proliferation, occurring in the ventricular and subventricular zones, is mostly prominent during the first trimester of pregnancy, achieving its maximal rate between 12 and 18 weeks' gestational age (GA). It is followed by neuronal migration from the germinal matrix

to grey matter (GM) regions, which occurs mainly during the second trimester (Volpe, 2001a). By the end of the second trimester most cortical neurons have reached their sites in the developing cortex, including the thalamocortical afferents that accumulate in the superficial subplate, "waiting" zone, prior to their ingrowth into the cortical plate. The subplate, containing postmigratory neurons, migratory neurons, glial cells, extra-cellular matrix and "waiting" thalamocortical axons, is a key connectivity compartment and a major site of synaptic interactions during this period (Kostovic and Judas, 2010a). Between 24 and 26 weeks GA, the brain starts receiving thalamic input: thalamocortical afferents from the subplate invade the cortical plate in a deep-to-superficial manner, mainly in sensory and associative cortical regions (frontal, auditory, visual and somatosensory) and the first synapses are formed. Therefore, besides the endogenous activity, also extrinsic input from sensory thalamic nuclei starts shaping brain development during this period (Kostovic and Judas, 2007; Milh et al., 2007). The establishment of thalamocortical connectivity represents thus a "developmental window" for structural cortical plasticity since it constitutes an anatomical substrate for extrinsic sensory-expectant cortical activation, leading to a crucial impact of the environment on ultimate brain development. Approximately by the beginning of third trimester, from 26 to 34 weeks GA, thalamocortical axons establish synapses with cortical layer IV neurons, becoming sensory-driven and, in parallel, there is an intense dendrite and axonal branching growth, accompanied by synaptogenesis and regulated by early synaptic activity (Mire et al., 2012; Mizuno et al., 2010). This leads to a complexification of the cortical dendritic tree structure, which is firstly predominantly radially organized, perpendicular to the cortical surface and, later on, characterized by a denser and more complex structure with an increasing number of neural connections running parallel to the surface (Bystron et al., 2008). There is also an important axonal development through the WM, corresponding at first mainly to the projection fibers of the corona radiata, which comprise principally thalamocortical axons (Dubois et al., 2014; Dubois and Dehaene-Lambertz, 2015; Kostović et al., 2019). In order to reach their target structure, axons are guided by their extremity growth cones, which can be attracted or repulsed by contact or chemical signals, neurotransmitters or growth factors from other neurons and glia. The end of the third trimester, from 35 weeks GA to term age, is essentially characterized by a gradual resolution of the subplate and maturation of long intra-hemispheric association and inter-hemispheric commissural cortico-cortical connections (Kostovic and Judas, 2010a). Long-distance WM bundles can be classified according to their connection patterns in: commissural fibers, which

connect the cerebral hemispheres (e.g. corpus callosum (CC)); projection fibers, bi-directional fibers between the cortex and thalamus/brainstem/spinal cord (e.g. cortico-spinal tract (CST)); and association fibers, which are cortico-cortical fibers between intra-hemispheric regions (e.g. superior longitudinal fasciculus (SLF)).

1.2.2. Brain connectivity maturational phenomena

Different maturational phenomena take place during early development, comprising synaptogenesis, refining of synapses (maturation and pruning) and myelination. In fact, the connections between neurons are not static and do change over time during brain development. Synapse formation and elimination during early development allow the emergence of circuitry complexity, with changes in the relationships and relative strengths of the connections (Hofman, 2019), contributing to brain organization, a process by which the brain takes on the capacity to operate as an integrated network (Knickmeyer et al., 2008; Volpe, 2001a).

Synaptic overproduction is generally followed by programmed cellular death, axonal retraction and synaptic pruning (Stiles and Jernigan, 2010). Pruning corresponds to the selective elimination of redundant or under-used connections, leading to the preservation of only the functionally relevant ones and thus neuronal circuit refinement (Huttenlocher and Dabholkar, 1997a).

Neuronal survival is strongly dependent on activity, target-derived trophic factors and axonal guidance molecules, and their deprivation might therefore induce cell death (Singh et al., 2008). Changes at the synaptic level, namely in synaptic efficiency, induced by long-term potentiation or long-term depression, may lead to structural stabilization or weakening of pre-existing synapses and therefore growth or pruning of axonal and dendritic branches (Erzurumlu and Gaspar, 2012; Hensch, 2005). The more signals are sent between two neurons, the stronger the connection becomes. During the early developmental stages, this neuronal plasticity is mainly intrinsic (experience-independent), whereas later on, during critical developmental windows, it is essentially driven by experience, leading to remodelling and proper development of circuits (Hensch, 2005). The fetus itself, by kicking, turning or sucking its thumb, leads to a stimulation of synapses growth. In addition, some environmental conditions can also act directly on the fetal senses, namely temperature, pressure and sounds (Ackerman, 1992). Therefore, experience can rewire brain's structure and thus impact brain connectivity and neuroplasticity.

Myelination starts during the second trimester, with the wrapping of oligodendrocytes around nerve fibers in CNS, and continues through postnatal period into adulthood. It follows the axonal pruning and pre-myelinating stages (Thomas et al., 2000) and is responsible for favouring the conduction of the nerve impulse and thus the communication across the neural systems (Baumann and Pham-Dinh, 2001; Volpe, 2001a). It has a particular spatial and temporal pattern: occurs primarily in proximal pathways than in distal, in central regions than in peripheral, in projection fibers than in association, in sensory pathways than in motor ones and in occipito-parietal regions before temporo-frontal regions (posterior-to-anterior) (Kinney et al., 1988). By term-age histological and neuroimaging studies have shown that most WM tracts appear to be in place, with myelination being observed in the rostral part of brain stem, cerebellar peduncles and in the posterior limb of the internal capsule (PLIC), where passes the CST (Sie et al., 1997). The rate of WM myelination increases after term age, with intense changes in the first post-natal months: myelination of acoustic and optic radiations is observed soon after term age, the spino-thalamic tract, fornix, splenium and body of CC and rolandic area around 4 months, the anterior limb of internal capsule and genu of CC around 6 months, the external capsule around 10 months, the occipital pole by the 15th month and the frontal and temporal pole WM by 1 year of age. The myelination peak occurs during the first post-natal year (Baumann and Pham-Dinh, 2001; Dubois et al., 2008; Paus et al., 1999). Less rapid modifications are observed during toddlerhood and subsequently slower changes until young adulthood (Forbes et al., 2002; Hermoye et al., 2006; Meng et al., 2012; Mukherjee et al., 2001; Sadeghi et al., 2013).

It has been suggested that this asynchrony in the maturation sequence might be related to the fact that extending myelination in longer WM bundles may be necessary to compensate for brain growth and maintain similar communication latencies between brain regions across ages (Salami et al., 2003). Additionally, these discrepancies might be relevant to the hierarchy of connections between cortical areas: the early maturation of receptive sensory areas (low-level processing) would enable a stabilization of the information used by integrative areas (high-level processing) that develop later (Guillery, 2005).

1.3.   Diffusion Magnetic Resonance Imaging

Magnetic resonance imaging (MRI) is a non-invasive nuclear medical imaging technique that allows in-vivo imaging of human tissue, with high contrast and resolution.

Approximately 60% to 70% of the human body is composed of water. Conventional MRI uses magnetic fields and electromagnetic energy to generate signals from hydrogen nuclei. By applying a radio frequency pulse in a homogeneous magnetic field, it is possible to measure the resulting signal emitted by hydrogen atoms in the water molecules of the tissue being scanned. Different combinations of a number of radiofrequency pulses and gradients result in a set of different images with a particular appearance, constituting the MRI sequences.

The following sections focus on dMRI, a MRI sequence that has emerged as an important and valuable instrument to study brain structure in-vivo, namely WM morphology, whole-brain brain structural connectivity and microstructural properties of both GM and WM.

1.3.1. Diffusion Weighted Imaging

Diffusion Weighted Imaging (DWI) is a non-invasive MRI method with high sensitivity to water movements within the architecture of the tissues (Soares et al., 2013). In biological tissues, the diffusion of water is primarily caused by random thermal fluctuations ("Brownian motion") and modulated by the interactions with cellular membranes, subcellular structures and organelles. In a perfectly homogenous medium, like in cerebrospinal fluid (CSF), diffusion is random and isotropic (e.g., equal probability in all directions). In cerebral GM, although internal cellular structures and cell membranes slow the rate of diffusion in comparison to CSF, diffusion remains isotropic. However, in a tissue with a regularly ordered microstructure, like the WM, diffusion respects the tissue orientation and is anisotropic: unhindered in the direction parallel to the axon fibers and hindered in the perpendicular direction to axonal orientation (Beaulieu, 2002; Le Bihan, 1991).

The signal contrast generation provided is based on the differences in Brownian motion. The emitted signal decreases as a function of the movement of water molecules in the direction of this gradient: the higher the degree of random motion (e.g. isotropic medium), the greater MRI signal loss, whereas the lower the

degree of random motion (e.g. anisotropic medium), the lower the MRI signal loss (Bammer, 2003).

The MRI method the most used for diffusion measurements is the "pulsed gradient spin-echo", introduced by Stejskal and Tanner. In this method, after a 90 degree excitation pulse, two diffusion-sensitizing linear magnetic-field gradients are placed each on either side of a 180 degree radio-frequency refocusing pulse (Stejskal and Tanner, 1965). Only motion in the direction of the gradient causes a change in the phase of the spin. When there is no diffusion, the phase difference is zero: phase shift is cancelled out, because the 180 degree pulse in the spin-echo sequence reverses the sign of the phase angle. This causes the static spins to be all in phase with respect to other spins at the same spatial location, which gives a maximum echo signal. Diffusing spins, on the other hand, will not be in phase with respect to the other spins at the same spatial location, which leads to signal attenuation: the signal from diffusing molecules is lost, generating darker voxels (Basser and Pierpaoli, 1996). This means that, for example, WM fiber tracts parallel to the gradient direction will appear dark in the DWI for that direction.
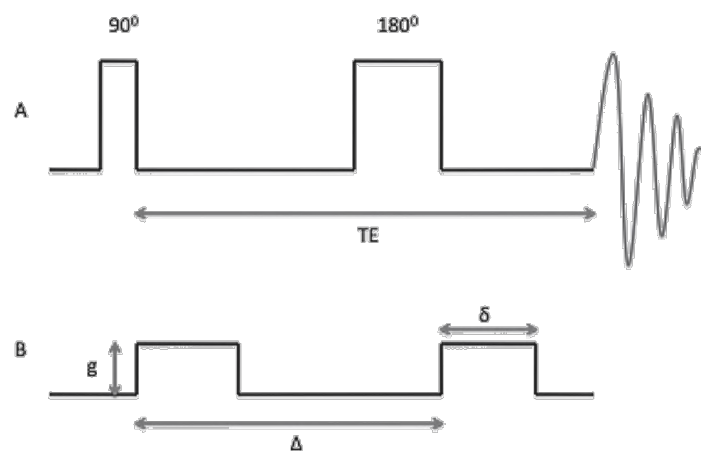
Figure 1.3.1 – **Diffusion sensitized spin-echo sequence.** (A) The 90 degree excitation and 180 degree refocusing pulses form a spin-echo at the echo-time (TE). (B) The pulse sequence can be sensitized for diffusion by applying a pair of pulsed-field gradients, with amplitude g, surrounding the 180 degree pulse. Gradient pulse duration, δ, and time separation between the gradient pulses, Δ, are indicated. Adapted from (Dudink, 2010).

From a series of DWI images, it is possible to calculate an apparent diffusion coefficient (ADC) of water molecules in the direction of the diffusion sensitizing gradient. The amount of attenuation caused by diffusion is determined by the ADC

and by the "b-value", which describes the strength of the diffusion sensitivity and is expressed in s/mm^2 (Chilla et al., 2015; Le Bihan et al., 1986).

Determining the behaviour of water diffusion in tissues allows the study of its microstructure: in tissues with a random microstructure ADC appears to be the same in all directions (isotropic diffusion), while in tissues that have a regularly ordered microstructure ADC varies with the tissue orientation (anisotropic diffusion). However, the assessment of diffusion in anisotropic tissues as in brain WM requires a knowledge of molecular displacements in different directions, whereas the ADC only provides a measure of the displacement of molecules in one direction. The dependency of the ADC on one gradient direction introduces thus an orientation bias into the anisotropy indices, which can lead to erroneous conclusions about tissue microstructure (Pierpaoli et al., 1996).

The diffusion tensor model has been proposed to overcome this problem and characterize diffusion in anisotropic and heterogeneously oriented tissues. In this model the rate of water diffusion in other directions is measured by changing the direction of the gradient (Basser et al., 1994a; Basser et al., 1994b).

1.3.2. Diffusion Tensor Imaging

Diffusion Tensor Imaging (DTI) provides information about the degree of water diffusion in multiple directions within individual voxels. Indeed, when diffusion is anisotropic, it can't be described by a single scalar coefficient but is, instead, dependant on a three-dimensional (3D) direction.

The introduction of this model provided, for the first time, a rotationally invariant description of the shape of water diffusion, allowing to study complex anatomic tissues, like brain WM fiber tracts, by measuring principal diffusivities regardless the position of fibers in space.

The diffusion tensor (DT) is a 3 × 3 symmetric, positive-definite matrix, calculated at each voxel, that fully characterizes diffusion in 3D space, assuming that the displacement distribution is Gaussian:

$$DT = \begin{bmatrix} D_{xx} & D_{xy} & D_{xz} \\ D_{yx} & D_{yy} & D_{yz} \\ D_{zx} & D_{zy} & D_{zz} \end{bmatrix} \quad (2.1)$$

To obtain the directional information, DWI images along several gradient directions need to be collected. The diagonal elements D_{xx}, D_{yy} and D_{zz} represent the ADC along the axes x, y and z, in which the gradients are applied. The off diagonal elements allow the calculation of the principal diffusion direction when it is different from one of the main axes x, y and z in the frame. At least seven images, comprising the six diffusion different directions using gradient pulses, plus one image that is not diffusion weighted (b=0), are needed to calculate the six independent numbers in the 3x3 symmetric DT matrix, and thus characterize diffusion rate in all directions. The b-value generally used in DTI for studying human adults brain is 1000 s/mm^2 (Le Bihan et al., 2001). Although it is not necessary to use more than six diffusion directions for the model, such is advantageous, in order to cover the space more uniformly in many directions, especially when aiming fiber orientation mapping.

The DT is usually represented by an ellipsoid (Figure 3.2) or an orientation distribution function (ODF). The ellipsoid has its specific reference frame, the eigensystem. Diagonalization of the diffusion tensor yields the eigenvectors and the corresponding eigenvalues of the diffusion tensor, which describe the directions and the apparent diffusivities along the axes of principle diffusion. Eigenvalues are ordered as $\lambda_1 \geq \lambda_2 \geq \lambda_3$ and each corresponds to one eigenvector. The ellipsoid is oriented such that its long axis is parallel with the direction of greatest (fastest) diffusion (the principal diffusion direction). The largest eigenvalue, λ_1, represents thus the diffusion coefficient along the direction parallel to the fibers. The two additional vectors represent the rate of diffusion perpendicular to the principal diffusion direction, with λ_2 and λ_3 representing the transverse diffusion coefficients (O'Donnell and Westin, 2011).

$$
\begin{array}{ccc}
\vec{e}_1 & \vec{e}_2 & \vec{e}_3 \\
\end{array}
\begin{pmatrix}
\lambda_1 & 0 & 0 \\
0 & \lambda_2 & 0 \\
0 & 0 & \lambda_3
\end{pmatrix}
$$
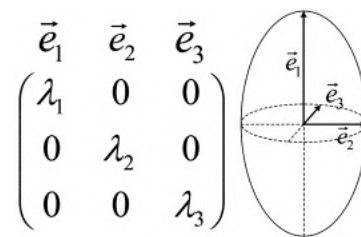
Figure 1.3.2 – **3D ellipsoid representing the DT**. The DT 3D ellipsoid represents the diffusion isoprobability surface at the voxel level. The ellipsoid axes are oriented according to the DT eigenvectors and their length depends on the tensor eigenvalues. (Adapted from Huppi and Dubois, 2006).

The relationship between the eigenvalues reflects the characteristics of the diffusion in the tissues. Diffusion in WM is less restricted along the axon, tending to be anisotropic, whereas in GM is usually less anisotropic and in the CSF is unrestricted in all directions (isotropic) (Hagmann et al., 2006).

Several indices are described to infer the amount of diffusion anisotropy of the DT in each voxel, and subsequently in a region, such as: Axial Diffusivity (AD), Radial Diffusivity (RD), Mean Diffusivity (MD) and Fractional Anisotropy (FA) (Basser and Pierpaoli, 1996; Soares et al., 2013).

AD (λ_1) measures the diffusion rate along the main axis of diffusion within a voxel and is thought to reflect fiber coherence and structure of axonal membranes. It is more specific of axonal degeneration (Song et al., 2002).

RD (($\lambda_1+\lambda_3$)/2) is the rate of diffusion in the transverse direction, being calculated as the mean of the diffusivities perpendicular to the primary axis of diffusion. It is thought to represent degree of myelination (Song et al., 2002).

MD (($\lambda_1+\lambda_1+\lambda_3$)/3) provides the overall magnitude of water diffusion, along the three main axes, and is independent of anisotropy. It relates to the total amount of diffusion in a voxel, which is related to the amount of water in the extracellular space. High signal (white areas) represents high diffusion (e.g. CSF), whereas low signal (gradations of dark areas) represents reduced diffusion (e.g. GM and WM). It can be a useful measure for assessing WM maturation and/or injury (Snook et al., 2007).

FA describes the degree of anisotropy of water diffusion in tissues and is by far the most widely used measure of anisotropy in DTI literature. It can be calculated by comparing each eigenvalue with the mean of all the eigenvalues and is essentially a normalized variance of the eigenvalues. It can be described by the following equation:

$$\text{FA} = \sqrt{\frac{(\lambda_1-\lambda_2)^2+(\lambda_2-\lambda_3)^2+(\lambda_1-\lambda_3)^2}{2(\lambda_1{}^2+\lambda_2{}^2+\lambda_3{}^2)}} \quad (2.2)$$

FA is broadly used to quantify the shape of the diffusion and to locate voxels likely to contain single WM tracts (without crossing fibers). Its values range from 0 (isotropic diffusion) to 1 (anisotropic diffusion) in a non-directional proportion. FA values are thought to be determined by fiber diameter, density, myelination, extracellular diffusion, inter-axonal spacing and intra-voxel fiber-tract coherence, being thus closely correlated with the microstructure of the fibers. A high degree of myelination, for example, would cause axons to be more tightly packed, increasing

FA, whereas light axonal packing would lead to more intercellular water, resulting in less restriction of diffusion and lowering FA (Beaulieu, 2002).

DTI provides therefore tissue fiber orientation and diffusion summary measures, being a sensitive tool to investigate microstructural tissue properties and to explore WM tracts anatomy and structure in vivo (Assaf and Pasternak, 2008).
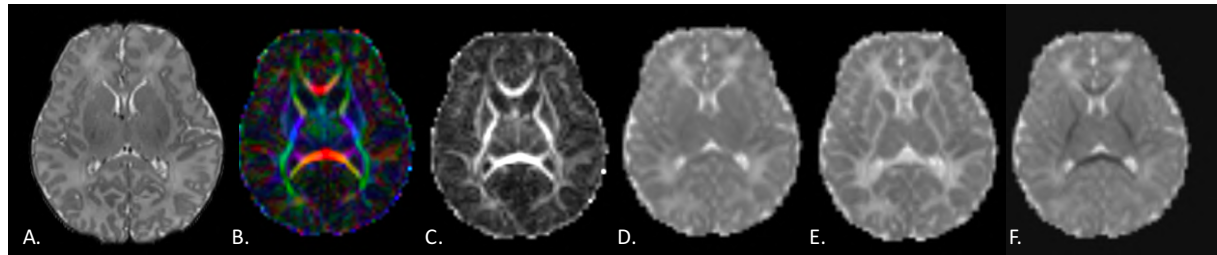
Figure 1.3.3 – **T2-weighted imaging and DTI images from a healthy full-term newborn scanned at 40 weeks GA, axial views.** (A) Conventional T2-weighted anatomical image. (B) Red-Green-Blue (RGB) map calculated from DTI data. Voxels are coloured by diffusion main tensor direction (left-right: red, anterior-posterior: green, superior-inferior: blue). (C) FA map calculated from DTI data. High signal areas (white) correspond to high FA whereas low signal areas (dark) to reduced anisotropy. (D) MD map calculated from DTI data. High signal areas (white) correspond to high MD, whereas low signal areas (dark) to reduced diffusivity. (E) AD map calculated from DTI data. High signal areas (white) correspond to high AD, whereas low signal areas (dark) to reduced diffusion in the principal direction. (F) RD map calculated from DTI data. High signal areas (white) correspond to high RD, whereas low signal areas (dark) to reduced diffusion in the transverse direction.

However, changes in the measured DT should be cautiously interpreted. Many studies focus on the diffusion anisotropy (mostly FA), which may not be enough to characterize tissue changes. For example, different eigenvalue combinations can give the same values of FA and therefore FA does not describe the full DT shape or distribution (Alexander et al., 2007). Interpretation might be further complicated by other factors, including: image noise, artifacts, partial volume averaging between tissues and regions of crossing WM tracts. In fact, although the DT model performs well in regions where there is only one fiber population (e.g. large fiber bundles containing fibers aligned along a single axis) it fails in regions with several fiber populations aligned along intersecting axes (e.g. where two tracts with different principal diffusion directions cross, merge, branch or touch within a voxel), since it cannot be used to map several diffusion maxima at the same time.

1.3.3. New diffusion acquisition protocols

Recently, some alternatives to the DTI model have been proposed, such as diffusion spectrum imaging (DSI) and single-shell or multi-shell high-angular resolution diffusion imaging (HARDI). These techniques enable multiple fiber orientations within a voxel to be resolved, but they require longer acquisition times and higher diffusion-weighting, both of which may result in a poorer SNR-to-scan time relationship and higher sensitivity to motion-related artifacts.

DSI allows to measure the diffusion spectrum, requiring specific diffusion encoding schemes by which 3D q-space is sampled following a Cartesian grid (Hagmann et al., 2006; Wedeen et al., 2005). This technique permits the obtention of accurate information about the neural architecture. It calculates the diffusion orientation distribution function (dODF) analytically and represents accurately multiple fiber orientations. However, it is extremely time demanding, as it measures the diffusion signal on a 3D Cartesian lattice. It requires more than 512 gradient directions and generally more than an hour to scan each subject using a spatial resolution of 2 mm^3, which makes it impractical to use in clinical settings and specially in newborns.

HARDI acquisitions are characterized by a large number of diffusion encoding gradients for a b-value uniformly spread on a sphere in q-space. It may employ many directions on a sphere with a single (single-shell) or multiple diffusion weightings (multi-shell) (Tuch et al., 2003). Several reconstruction schemes can be used to analyse HARDI data, such as Q-Ball Imaging (QBI), which provides the dODF via Funk-Radon transform and spherical harmonics reconstruction (Tuch et al., 2003), or Constrained Spherical Deconvolution (CSD), which provides the fiber ODF (fODF) (Tournier et al., 2007). CSD has been proven to provide an estimate of fODF that is robust and able to resolve multiple fiber orientations in a voxel, allowing reliable tractography results (Tournier et al., 2007).

Although single-shell HARDI allows resolving the angular structure of the neural fibers, it does not provide information about the radial signal decay, which is sensitive to WM anomalies. Multi-shell HARDI, comprising the acquisition of multiple shells (at least two), besides providing accurate local estimates of fibre orientations within a clinic realistic time, allows to acquire important information about neural tissues by means of multi-compartment modelling techniques, which provide information regarding differentiation between WM, GM and CSF compartments, missed by DTI and single-shell HARDI methods (Jbabdi et al., 2012; Rathi et al., 2011).
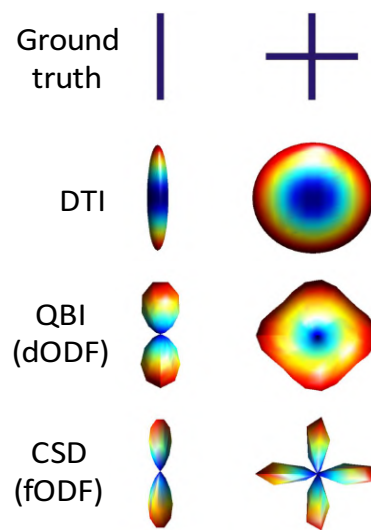
Figure 1.3.4 – **Example of 3D DT and ODF profiles obtained using different dMRI methods for both single fiber and fiber crossing configurations.** In the case of DTI, the single fiber is reconstructed accurately, but when two fibers cross DTI doesn't discriminate the two main orientations. QBI and CSD reconstruct ODF more accurately. dODF is less sharply defined when compared to the fODF. (Adapted from Bastiani and Roebroeck, 2015).

1.3.4. Multi-compartment and fixel-based diffusion models

The DWI signal in each voxel combines the signal arising from a variety of microstructural environments, including multiple cell types (not only axons, but also glia) and extra-cellular space; such is known to lead to an overall non-exponential decay in each voxel.

DTI assumes that the diffusion in tissues is Gaussian, what is not true in many biological tissues. Indeed, biological tissues, including the brain, are characterized by complex intra and extracellular in vivo environments, marked by the presence of barriers (e.g. cell membranes) and different compartments. Other approaches have emerged to try to overcome this limitation and quantify the non-Gaussianity of diffusion. In particular, Diffusion Kurtosis Imaging (DKI), which is an extension of DTI, is a model that accounts for the non-Gaussian signal decay, estimating the kurtosis (skewed distribution) of water diffusion. The Diffusion Kurtosis (DK) tensor is characterized by a symmetric 3 x 3 x 3 x 3 positive-definite matrix, with 15 independent elements, representing a more complex spatial distribution. DKI requires thus a dMRI acquisition with at least 3 b-values and 15 distinct diffusion directions. In addition to the DTI diffusion metrics, DKI provides estimates of

diffusional kurtosis and therefore allows a more complete characterization of water distribution in the brain. The most common DKI parameters are: mean kurtosis (MK), the average of the diffusion kurtosis along all diffusion directions; axial kurtosis (AK), the kurtosis along the axial direction of the diffusion ellipsoid; and radial kurtosis (RK), the kurtosis along the radial direction of the diffusion ellipsoid (Jensen et al., 2005). Kurtosis values were shown to be more sensitive, providing more information regarding the microstructural barrier complexity within the tissues than DTI (Cheung et al., 2009; Paydar et al., 2014). However, since DTI and DKI parameters are calculated voxel-wise, they lack of specificity for individual tissue microstructure features.

Multi-compartment and fixel-based diffusion models have been proposed, providing additional microstructural parameters in order to complete the characterization of cerebral tissue complexity (Jelescu and Budde, 2017; Panagiotaki et al., 2012; Pierpaoli and Basser, 1996a; Raffelt et al., 2017).

Examples of these models comprise NODDI (Neurite Orientation Dispersion and Density Imaging), DIAMOND (Distribution of Anisotropic Microstructural Environments in Diffusion-Compartment Imaging) and Fixel-based analysis (FBA).

NODDI is a three-compartment model, based on the local diffusion process. It englobes three mediums: the intracellular, corresponding to neurites represented as sticks (where diffusion is unhindered parallel to the sticks and highly restricted in the perpendicular direction, following a non-Gaussian distribution); the extracellular, space around neurites with glial cells and somas (where diffusion is hindered, following an anisotropic Gaussian distribution); and CSF (where diffusion is isotropic, unhindered, following an isotropic Gaussian distribution). NODDI provides parameters such as the intra-cellular volume fraction (v_{ic}, relating to neurite density index, NDI), isotropic volume fraction (v_{iso}) and orientation dispersion index (ODI; degree of incoherence in fiber orientations). Besides modelling coherent structures like WM tracts, it also has the advantage of modelling highly dispersed structures, such as GM. This model has been validated by histological examinations in both GM and WM of rats and ferrets (Jespersen et al., 2010; Jespersen et al., 2012). However, it has some key assumptions that are inconsistent with the known tissue microstructure. In particular, it assumes prefixed compartment diffusivities and it considers only a single fascicle compartment per voxel (Zhang et al., 2012).
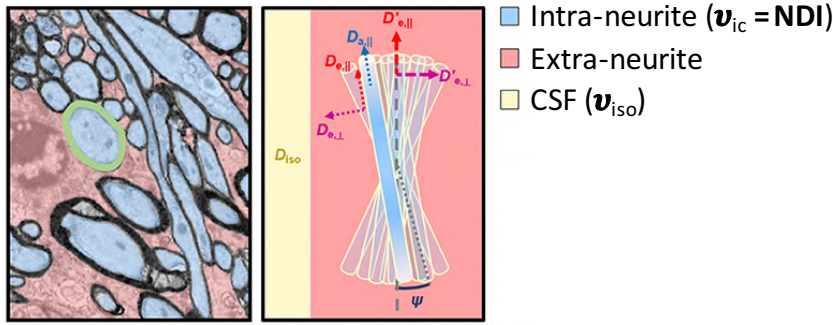
Figure 1.3.5 – **WM bundle tissue components and its correspondence with the compartments from NODDI model.** Left: cross-sectional electron microscopy image of a WM bundle. Right: Schematic of NODDI three-compartment model and relevant parameters. (Adapted from Jelescu and Budde, 2017).
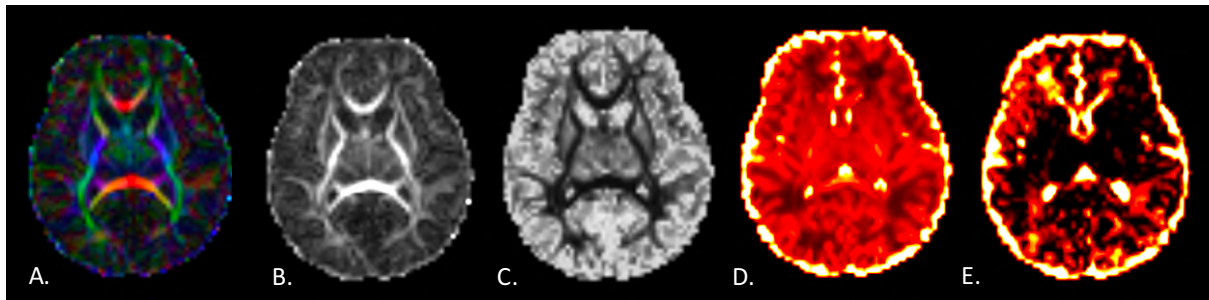
Figure 1.3.6 – **DTI and NODDI images from healthy full-term newborn scanned at 40 weeks GA, axial views.** (A) Red-Green-Blue (RGB) map calculated from DTI data. Voxels are coloured by diffusion tensor direction (left-right: red, anterior-posterior: green, superior-inferior: blue). (B) FA map calculated from DTI data. (C) ODI map calculated from multi-shell diffusion imaging (MSDI) using NODDI model. (D) v_{ic} map calculated from MSDI using NODDI model. (D) v_{iso} map calculated from MSDI using NODDI model.

DIAMOND is also a multi-compartment model that has emerged as a new alternative to NODDI, combining a 3-compartment biophysical model with a statistical modelling to represent also restricted, hindered and isotropic compartments both in WM and GM. In each voxel, using model selection techniques, is evaluated the presence of each of the 3 compartments and compartment-specific diffusion characteristics are calculated (cAD, cRD, cMD). Additionally, it provides also an overall measure of heterogeneity for each compartment (cHEI, heterogeneity index) (Scherrer et al., 2016). Although it allows the representation of multiple fascicles with heterogeneous orientations, it does not enable the assessment of the intra-axonal volume fraction (IAVF), which is critical for

better assessing axonal loss. Plus, microstructure metrics estimated using DIAMOND still need to undergo validation studies.

FBA model enables fiber pathways to be studied, including regions with crossing fibers, and to discriminate micro and/or macrostructural alterations within the WM fiber bundles. A "fixel" refers to a single fiber population and thus FBA allows to describe different fibre bundles with different orientations within a voxel (Raffelt et al., 2015). The model assumes that the apparent fiber density (AFD), which reflects the volume of the intra-axonal compartment, can be estimated from the fiber orientation densities (FOD). The FOD amplitude is proportional to the radial DWI signal, providing thus a measure of fiber density (FD). Additionally, using FOD registration, FBA method investigates the macroscopic changes in the fiber bundle occurring perpendicular to the main fiber orientation, which provide a measure of fiber cross-section (FC). The fixel metrics include thus FD, FC and a combined measure of fibre density and cross-section (FDC) (Raffelt et al., 2017). Changes in tissue microstructure characterized by a reduced number of axons per voxel can be detected by a reduction of FD, whereas changes in tissue macrostructure characterized by a diminution of the spatial extent of the fiber bundle (without reduction of the number of axons per voxel) can be reflected by FC. The combination of the two mechanisms implying microstructure and macrostructural changes in conjunction can be assessed using FDC.

These multi-compartment and fixel-based models allow to relate DWI signals directly to the underlying cellular microstructure and thus to reveal the microstructural effects underlying FA values alterations (Assaf and Basser, 2005; Barazany et al., 2009; Behrens et al., 2003; Zhang et al., 2011; Zhang et al., 2012). They have therefore the potential to provide new biomarkers to the complex process of human brain development.
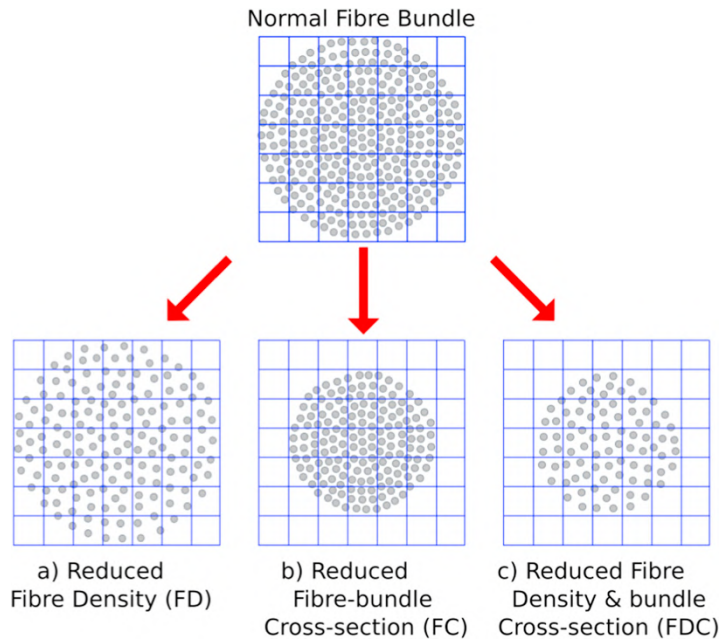
Figure 1.3.7 – **Fixel-based metrics.** Schematic representation of FC (grey circles represent axons, whereas grid represents voxels). Altered intra-axonal volume may manifest as: (a) change in tissue microstructure with diminution of FD; (b) macroscopic altered FC; (c) combination of both altered FD and FC area, FDC. (Adapted from Raffelt et al., 2017).

1.3.5. Tractography

DWI protocols allow to perform fiber tracking, by means of tractography, in order to obtain 3D representations of WM fiber tracts. Fiber tracking is, at the moment, the only available tool to visualise WM bundles trajectories in vivo and non-invasively. Tractography requires two main steps: the first is to fit a diffusion model at each voxel of the image; the second is to sequentially piece together the estimates, within each voxel, of the ODF from the direction of diffusion (fiber tracking across voxels) in order to reconstruct the WM tracts.

There are two main classes of fiber tracking methods: deterministic and probabilistic. Deterministic tractography estimates at every voxel the "most likely" fiber orientation (e.g. based on the major eigenvector of the DT or on anatomical assumptions). In this method, each seed point yields a unique streamline, and thus it tends to be simpler and faster. However, it lacks of information regarding the implicit errors in the tracking procedure. Probabilistic tractography, on the other hand, rather than estimating a single "peak" orientation, follows a random orientation sample within a range of possible orientations. It estimates a distribution

representing "how likely" each other orientation is to lie along a fiber, tracing the connections thousands of times, each time using slightly different orientations according to their likelihood. It attempts thus to estimate the range of connections that the seed point might be connected to, given the various sources of uncertainty, and characterizes the confidence with which connections may be established through the dMRI dataset (Behrens et al., 2014).

Tractography allows the identification of fiber bundles that connect specific cortical or subcortical structures, within and across individuals, and has become the method of choice for investigating quantitative MRI parameters in specific WM tracts. Diffusion measures can be averaged over the entirety of each tract (Lebel et al., 2008) or calculated for different segments of a tract, in order to reveal variations within it (Berman et al., 2009). This technique allows therefore not only to localize tracts on a subject, but to study its microstructural characteristics and compare them among different populations of subjects. Tractography may therefore contribute to the better understanding or even prediction of dysfunction caused by structural WM bundles alterations in specific locations.
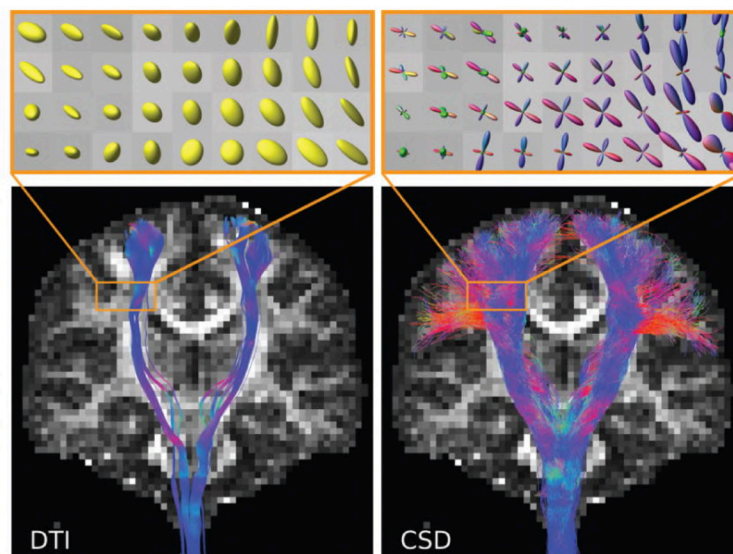
Figure 1.3.8 – **Coronal FA images overlaid with fiber tracking results from DTI using deterministic tractography (left) and from CSD using probabilistic fiber-tracking (right) from a representative healthy control subject.** The magnified regions in the orange boxes show the fiber orientation estimates within individual voxels. The CSD fiber orientation estimates (upper right image) confirm the presence of many voxels containing multiple fiber orientations, which are not well represented using DTI (upper left image), leading in this case to incomplete delineation of the lateral aspects of the cortico-spinal tracts when using DTI fiber-tracking (bottom left). (Adapted from Farquharson et al., 2013).

1.3.6. Connectomics

The mapping of brain networks, at different scales of space and time, has been a central focus of modern neuroscience and has led to the rise of the field of connectomics, which aims to study, describe and quantify the whole-brain network connections between neural elements of the brain.

With the development of tractography, one can construct whole-brain structural connectivity matrices (connectomes) describing WM fibers anatomical connections between all brain regions and providing measures of "connectivity" between brain regions.

The connectome can be seen as a network (equivalently, a graph), where the nodes represent brain regions and the edges represent the anatomical connections formed by WM fiber paths between the different brain regions (Bullmore and Bassett, 2011; Meskaldji et al., 2013; Sporns, 2012). The connectivity between every pair of nodes is represented as a connectivity matrix, which is a two-dimensional matrix where each row and column correspond to a different node and each matrix element represents an edge. In this matrix, the element at the intersection of the row i and column j will thus encode information about the connection between regions i and j. While diagonal elements can be interpreted as representing the connectivity of each node with itself, off-diagonal elements of the connectivity matrix represent the connectivity between pairs of distinct neural elements and provide estimated measures of pairwise connectivity (Sporns et al., 2005). Edges can be represented as binary, describing the existence or not of a connection, or weighted, for example by the number of streamlines connecting two regions (SC) or by microstructural features, such as fractional anisotropy (FA), providing a measure of the "strength" of connectivity between two regions. Indeed, not all connections between neural elements are the same: some pairs of neural elements might communicate via denser axonal bundles or have more myelinated fibers facilitating faster signal transmission, what can be differentiated via the connectivity weight. Regarding the directionality of the connectivity matrix, non-invasive methods such as dMRI do not presently allow to resolve the direction of an axonal projection, providing thus undirected networks.

Graph-based analysis network measures allow the study of whole-brain network topology, revealing meaningful information regarding integration, segregation, small-worldness, modular organization, the presence of hubs and rich-club connectivity (Bullmore and Sporns, 2009; He and Evans, 2010; Meunier et al., 2010; van den Heuvel and Sporns, 2013). These network measures can be applied

to both unweighted and weighted connectivity matrices and have been shown to be reliable biomarkers for discriminating normal and abnormal brain networks (Lo et al., 2010; Owen et al., 2013; Shu et al., 2011).

Measures of integration refer to the ability of communication between distributed nodes, reflecting the global information transfer efficiency of the network (Rubinov and Sporns, 2010). They comprise the characteristic path length, which is computed as the average of shortest path lengths between all pairs of nodes in the network (Watts and Strogatz, 1998), and the network global efficiency, which is the average inverse of the shortest path lengths (Rubinov and Sporns, 2010).

Network segregation relates to its organization into a collection of sub-networks and can be measured by means of average clustering coefficient and local efficiency. The clustering coefficient is computed as the fraction of a node's neighbors that are also connected to each other. These fractions at each node are averaged over all the nodes of the network to give the overall network average clustering coefficient (Watts and Strogatz, 1998). Local efficiency is computed as the average of the global efficiency of each node's neighborhood sub-graph, reflecting the ability of information exchange of a subnetwork consisting of itself and its all direct neighbors (Latora and Marchiori, 2001; Wu et al., 2018).

An optimal balance between segregation and integration is ideal to allow high capacity for local and global information transfer. This aspect is quantified by the small-world network topology, which is computed as the ratio between the normalized average clustering coefficient and normalized characteristic path length (Rubinov and Sporns, 2010). Small-world networks are highly clustered but with short path lengths (Watts and Strogatz, 1998) and are characteristic of both functional and structural human brain networks (Bassettt et al., 2006; Sporns et al., 2005).

In brain networks, nodes might aggregate into densely connected subgroups called modules. Modularity measures a network's modular structure, namely how much nodes are highly connected to one another within the same community and sparsely connected to nodes from other communities (Newman, 2004). The modularity index is computed as the ratio between the number of connections (or sum of edge weights) within the modules and the number of connections (or sum of edge weights) exiting the same modules, taking the maximum of these ratios across all possible modules (Newman, 2004). Modular networks generally have small-world properties. Indeed, a strong within-module connectivity results in a high clustering coefficient, whereas a small number of inter-

modular links is sufficient to maintain a low characteristic path length of the network. Both structural and functional human brain networks have been described as modular (Sporns and Betzel, 2016).

In a connectome, certain nodes may possess a larger number of connections than others, which makes of them network hubs (van den Heuvel and Sporns, 2013). This heterogeneous distribution implies that different nodes serve distinct topological roles in the network, with highly connected nodes exerting a particularly important influence over the network. To detect networks hubs, one can use measures of centrality, such as nodal degree. In a binary undirected network, the nodal degree is the number of edges connecting a node with all others. A network with hubs will reveal a right-tailed distribution of the nodal degree. The hubs will be the nodes with the highest score in nodal degree. They can be calculated, for example, as the 10% nodes with the highest nodal degree, or as the nodes scoring more than the average nodal degree plus 1 standard deviation. Other measures of centrality, such as the nodal strength, nodal betweenness centrality and nodal closeness centrality can also be used to identify hubs. These measures capture the capacity of a node to influence (or be influenced by) other network elements, given its connection topology (Rubinov and Sporns, 2010; van den Heuvel and Sporns, 2013).

Some hub regions tend to be densely connected to each other, forming a "rich-club" organization, which is thought to be important for efficient global information transfer (van den Heuvel et al., 2012). Rich-club brain regions have a high number of connections, being more connected to each other than would be expected by chance. They play a central role in intra-modular connectivity and in maintaining network global integration (van den Heuvel and Sporns, 2011; van den Heuvel et al., 2012). The rich-club coefficient can be calculated as follow: for a given a nodal degree κ, we identify the subset of nodes E > κ with a nodal degree > κ; the RC coefficient is computed as the ratio between the number of connections present in E > κ, and the maximal number of connections possible within E> κ if the nodes were fully connected. The concept can also be applied to weighted networks (Opsahl et al., 2008).

Besides graph-analysis, connectome differences can also be evaluated at the connection level, by means of whole-brain edge-wise connectivity strength differences between groups. Connection-level group analyses reveal local effects in the connectome, providing thus information regarding the connections with different connectivity strength between distinct groups, what complements the more abstract graph-theoretical topological parameters.

When performing such group-level comparisons, given the large number of univariate tests undertaken, a multiple testing correction is necessary. Examples are Bonferroni's method (or other methods) to control the family-wise error rate (FWER) or false discovery rate (FDR), but these greatly reduce the statistical power due to the large number of comparisons (Benjamini and Hochberg, 1995; Dunn, 1961; Kim et al., 2014b). Network Based Statistic (NBS) is an alternative global test that can be applied to assess significance of overall network differences by summarizing individual connection differences. NBS controls the FWER by considering a global statistic measuring the clustering structure of changed edges (cluster-based thresholding) based on mass-univariate statistics, each performed at every connection included in the graph, avoiding therefore the multiple comparisons issue (Zalesky et al., 2010). However, NBS weakly controls the FWER at the connections level and its results strongly depend on the choice of the initial threshold on the p-values, which is of arbitrary nature (Meskaldji et al., 2013; Meskaldji et al., 2015).

1.4. Diffusion MRI applied to early brain development

1.4.1. Technical limitations regarding application of dMRI to the neonatal brain

The developing human brain presents several challenges for dMRI applications compared to the adult brain.

One of the challenges is related to the fact that the neonatal brain has increased water content than the adults' brain. In adult brain, for example, the water content of WM is substantially lower than that of GM (65% versus 85%) (Maas et al., 2004). Nevertheless, diffusivity values for both WM and GM are virtually identical, meaning that, at a given water content, WM is less restrictive to water motion that GM (Ulug et al., 1997). On the other hand, in the immature brain the water content is higher and similar in both WM and GM. The higher diffusivity values in WM than GM in the immature brain are also in agreement with the idea that WM is less restrictive to water motion than GM. The increased water content and low myelination in the immature brain lead to very different diffusion properties (e.g. higher diffusivity and lower anisotropy values), when compared to brains of older children and adults (Dubois et al., 2014). The different diffusion properties in early brain might require an adjustment of the optimized b-value. Since neonates and young infants' brain have a much higher water content than adults, there is an increased diffusivity and increased signal attenuation in the immature brain. These reasons justify why the b-value is often made shorter: b-values on the order of 700–1000 mm^2/s are usually preferred for DTI sequences, for example. Given the very low anisotropy of WM, there is still little knowledge about the appropriate FA threshold values needed for discriminating WM tracts, particularly in preterm population. The relationship between tissue microstructure, diffusivity and anisotropic diffusion is complex, multifactorial and most likely involves a combination of a decreasing tissue water content and increasing complexity of WM structures with age, during development. The changes in diffusion metrics during development, although imposing technical limitations, provide a unique insight into the structural basis of brain maturation.

Besides the different diffusion properties accompanying early brain development, there are other limitations to be considered. Indeed, the very low anisotropy of pre-myelinated WM and the very small size of WM tracts, principally in premature newborns, present serious technical challenges for dMRI due to

signal-to-noise ratio (SNR) and spatial resolution constraints. Since cerebral structures are smaller, spatial resolution should be higher than in adults, what would result in a longer scan time and worse SNR. Additionally, the movement during sequence acquisition is more frequent in scans from young subjects. This requires an important post-acquisition step of pre-processing, in order to correct for motion artefacts, comprising signal drop-out from major movement and intra-slice or within-volume motion. The acquisition time is thus a crucial point for image quality in this particular population. Therefore, new dMRI sequences that do not rely on the tensor model and aim to overcome the limitations of DTI, although providing more accurate WM tracts reconstructions, require a longer scan time and higher diffusion-weighting, both of which result in a poorer SNR-to-scan time relationship and higher sensitivity to motion-related artifacts in neonatal and pediatric population. The application of these new sequences remains thus difficult in most settings.

1.4.2. dMRI WM microstructural changes in early brain development

During early brain development, myelination, which contributes significantly to the gradual maturation and functionality of WM fibers, leads to important changes in WM anisotropy and diffusivity.

DTI metrics have been widely used to study changes in WM maturation throughout development, allowing to quantify differences across different WM bundles and also within a specific WM tract. Evidence suggests that changes in FA occur in tandem with changes in MD during early brain development. Although these two parameters are theoretically independent of one another, with increasing brain maturation FA has been shown to increase, while MD decreases (Aeby et al., 2009; Huppi et al., 1998a; Neil et al., 2002; Partridge et al., 2004).

Regarding diffusivity parameters, in the immature unmyelinated brain, due to the larger extracellular space in the WM, the average MD values are higher than in adult brain. MD is higher for WM than GM, leading to MD maps with evident contrast between these two tissues. During brain development, MD values in the WM decrease with the increasing age, until they reach the adult values (Mukherjee et al., 2002). The exact reason is not known, although it has been shown to be influenced by a decrease in water content, related to a reduction of extracellular spaces and increased complexity of WM structures. DTI has shown that this decrease in MD is principally driven by a decrease in λ_2 and λ_3 diffusion, but less in λ_1. Such reflects a change in water diffusion perpendicular to WM fibers and may

indicate alterations due both to pre-myelination (change of axonal width) and myelination (Mukherjee et al., 2002). Quantitative changes in MD have a regional variation in brain WM, as measured in diverse studies: in general, MD values are higher in the superior, anterior and peripheral regions of the brain, compared to inferior, posterior and central regions (Dubois et al., 2006; Hermoye et al., 2006; Huang et al., 2006; Mukherjee et al., 2001; Mukherjee et al., 2002; Oishi et al., 2011; Partridge et al., 2004; Provenzale et al., 2007). In particular, among WM structures, the lowest MD values were found in the projection fibers of the internal capsule and the cerebral peduncles, with decreasing values from 30 weeks GA to term age (Huppi et al., 1998a; Partridge et al., 2004).

Anisotropy values also differ between adult and pediatric brain (Hermoye et al., 2006; Sakuma et al., 1991). Since WM tracts in neonatal brain are only partially developed and myelinated (Rose et al., 2014), the developing WM has lower FA values than adult WM (about 40-60% lower), which increase steadily with increasing age during development (Dubois et al., 2008; Huppi et al., 1998a; Huppi et al., 2001; Klingberg et al., 1999; Neil et al., 2002). Indeed, with increasing GA, the brain water content decreases dramatically and new barriers to water mobility are formed, such as axonal cell membranes, development of WM structural coherence and increasing myelination, which hinders and restricts water motion, justifying the increasing FA values throughout development (Dubois et al., 2008; Neil et al., 1998; Nossin-Manor et al., 2013).

The increase in WM anisotropy values during development appears to take place in three steps: 1) fiber organization into fascicles, 2) proliferation and maturation of glial cell bodies and intracellular compartments and 3) myelination (Dubois et al., 2008).

The first stage, fiber organization, occurs largely in utero. It is evidenced by the presence of anisotropy in late intrauterine and premature infants WM fibers (Partridge et al., 2004), in the absence of changes in T1- or T2-weighted imaging, before the histologic appearance of myelin (Huppi et al., 1998a). This stage is characterized by changes in WM structure representative of "pre-myelination" (Wimberger et al., 1995), namely an increase in: axon calibre and membrane density, microtubule-associated proteins in axons, axonal membrane conduction velocity and developmental proliferation of immature oligodendrocytes (Drobyshevsky et al., 2005). The initial extension of oligodendrocytes processes has been suggested to be anisotropic in favor of the axonal direction (Nossin-Manor et al., 2013; Zanin et al., 2011). This stage constitute thus the earliest indication of impending myelination and is reflected by an increase in anisotropy due to an

increase in AD and a decrease in RD (Beaulieu, 2002). The fibers that express the highest FA values in the immature brain are the commissural fibers of the splenium and genu of CC (Partridge et al., 2004), which are largely unmyelinated in the newborn period and therefore their high anisotropy is in part due to a high degree of parallel organization. In addition to the CC, the internal capsule, as well as external capsule, optic radiation and other tracts within the cerebral hemispheres show anisotropy clearly long before they are seen to be myelinated on T1- or T2-weighted images (Nomura et al., 1994; Rutherford et al., 1991; Takeda et al., 1997).

The second stage includes the maturation of glial cell bodies and their processes, as well as the development of the cytoskeleton and various intracellular structures. This may be linked to a decrease in water content of the brain and an increase in membrane density, leading to a reduction in water diffusivity. A decrease in MD without increasing anisotropy is predominant at this stage (Yoshida et al., 2013).

The third stage, where the increase in anisotropy is continuous and sustained, is associated with the histologic appearance of myelin and its maturation. In this third stage, there is an increase of FA and decrease on RD and MD, related to a decrease in membrane permeability and extracellular distance between membranes. The increase in WM anisotropy takes place at different rates for different brain areas (Brody et al., 1987), following typically a "high FA in the central and posterior WM and low FA in the peripheral and anterior WM" rule (Zhai et al., 2003). In the brain, the earliest signs of this third stage are observed in the projection fibers of the PLIC. In fact, from 36 weeks GA, the first evidences of myelination have been found in PLIC, corona radiata and CST around the central sulcus, as well as in the inferior and superior cerebellar peduncles (Counsell et al., 2002). At birth, almost all prominent WM bundles can be detected and tracked despite its low anisotropy values (Hermoye et al., 2006).

Overall, in neonates WM fibers, FA has been found to increase, while MD, AD and RD decrease with age, likely due to increased fiber organization, axonal coherence and preliminary myelination (Aeby et al., 2009; Dubois et al., 2008; Mukherjee et al., 2002; Shim et al., 2012). In most tracts, FA increases significantly each week, whereas weekly decreases in MD values are smaller and less discriminative in the majority of regions (Partridge et al., 2005). Regional patterns of higher FA and lower RD, suggestive of more advanced microstructural development, were found in posterior compared to anterior and in central compared to peripheral WM regions (Oishi et al., 2011; Rose et al., 2014).

Besides DTI, the NODDI model has also been used to study WM microstructural changes during brain development. Indeed, NODDI has been successfully applied to the newborn brain and was proven to describe more accurately the diffusion mechanisms than DTI in the WM, providing derived parameters that agreed with the newborn's brain cellular architecture known from histology (Kunz et al., 2014). NDI has been shown to increase in WM during early brain development, parallel with increasing WM maturation, in particular between deep GM (DGM) and central cortical regions (Batalle et al., 2017). At TEA and one-month of age, central fibers, namely commissural fibers (splenium, genu and body of CC) and projection fibers (PLIC) showed the highest NDI and diminished ODI, reflecting a highly-organized axonal structure, whereas peripheral fibers exhibited the higher ODI values and association fibres the lowest NDI values (Dean et al., 2017; Kunz et al., 2014). Moreover, central fibers evidenced a non-linear increase in NDI and in tortuosity of the extra-axonal space as a function of age during the first three years of life, in agreement with the progressive myelination process (Jelescu et al., 2015).

Additionally, FBA has also been applied to study brain development during early and late childhood. An increase in FD, FC and FDC has been found in major WM fibers, namely CC, forceps major, forceps minor, SLF, inferior longitudinal fasciculus (ILF), inferior fronto-occipital fasciculus (IFOF), uncinate fasciculus, cingulum, fornix and CST. These findings suggest an increase in fibers axonal density, as well as in fibers cross-sectional bundle size throughout childhood (Dimond et al., 2020; Genc et al., 2018).

1.4.3. dMRI GM microstructural changes in early brain development

GM microstructural changes during early brain development have also been studied by means of dMRI, namely using DTI parameters.

From mid-gestation, the cortical plate is initially anisotropic, given the radial orientation of the main tensor, which is thought to be related to the apical dendrites and radial glia fibers creating a highly directional, coherent and columnar microstructure setting (Ball et al., 2013b; McKinstry et al., 2002; Ouyang et al., 2019a). Then, there is a subsequent increase in complexity of the neural connections, with formation of basal dendrites cross-connections, parallel to the surface, obscuring the underlying radial structure and leading to an isotropic diffusion in the cortical plate (Bystron et al., 2008). There is thus a decrease of FA in

the cortical plate during prenatal development, which stabilizes around term-age (Batalle et al., 2019). This decrease is higher and faster in gyri than sulci and in frontal, temporal pole and parietal association cortex compared with other brain regions (Ball et al., 2013b). On the other hand, MD decreases in cortical plate throughout development, including after tem-age, presenting higher values in gyri than in sulci and in frontal compared with occipital lobes (Ball et al., 2013b; Batalle et al., 2019). Such findings are in agreement with a consistent increase in cellular and synaptic complexity starting earlier in sulci than gyri, and being initially more pronounced in the frontal pole, temporal pole and the parietal association cortices (Ball et al., 2013b).

The decrease of anisotropy (FA) and diffusivity (MD, AD, RD) indices in the cortex has been related to the elaboration of the radial glial cells, increased dendritic density, cellular maturation and a general increase in complexity (Ball et al., 2013b; delpolyi et al., 2005; McKinstry et al., 2002). In particular, evaluation of cortical anisotropy in preterm infants from 25 to 40 weeks GA has shown that the reduction in AD (λ_1) was the major contributor for the loss of anisotropy observed throughout cortical maturation (delpolyi et al., 2005). Indeed, studies in developing rodents and ferrets have shown that the reductions of MD and FA co-localize and correlate with increased dendritic density, fewer radial glia and more orthogonal dendrites (Bock et al., 2010; Sizonenko et al., 2007). Specifically, decreasing MD has been related to increased tissue density subsequent to an increased neurite number, cellular complexity and synaptogenesis, whereas decreasing FA predominantly to an increased dendritic elongation and branching orthogonal to cortical columns (Dean et al., 2013; Sizonenko et al., 2007).

Longitudinal microstructural cortical maturation during early development has also been investigated using DIAMOND compartment diffusivities and a "radiality index" parameter, measuring how orthogonal to the cortical surface the principal diffusion is. Evidence has shown that there is decrease in cFA and in cortical radiality with increasing GA, in all cortical lobes, with region specific rates. Such is in agreement with an increased complexity of the cortical microstructural environment, which passes from a highly ordered and radial structure to a more complex setting, with increased number of fibers overlying to the radial structure and reduction of extra-cellular space (Eaton-Rosen et al., 2017).

The NODDI model was also applied to study GM microstructure during early brain development. In this model, increases in NDI can be interpreted as increases in neurite and organelle density, while increases in ODI are generally related to an increased dendritic arborisation and consequent alteration of cortical

geometrical structure. Evidence has proven that ODI increases during early brain development until term age and then stabilizes, while NDI initially decreases, rising only after 38 weeks, mainly in motor and sensory areas. These results support that until term-age cortical maturation is dominated by an increase in dendritic arborisation, congruent with the increase on cortical volume and curvature, whereas after term predominates an increase in neuronal an organelle density (Batalle et al., 2019).

Literature suggests that these cortical microstructural changes might be associated to the maturation of WM tracts (Ouyang et al., 2019b) and gyrification process (Batalle et al., 2019).

1.4.4. Early development of brain structural connectivity

Recent studies have evaluated whole-brain structural connectivity during early brain development using connectomic analysis.

A fetal MRI study has shown that the early brain evidences already a topological small-world organization at 20 weeks GA, which is typical of the adult human brain (Song et al., 2017). Small-world organization was shown to increase significantly in the preterm brain during early brain development, from 30 weeks GA to TEA (van den Heuvel et al., 2015).

Literature suggests that the typical developmental course of the brain structural network is characterized by a continuously increasing integration and decreasing segregation with age, favouring thus an integrative topology (Hagmann et al., 2010; Huang et al., 2015; Tymofiyeva et al., 2013; Yap et al., 2011). From the second trimester of brain development to term age, various studies have shown an increase in network strength and integration capacity, with a decrease of the characteristic path length and increase of network global efficiency (Ball et al., 2014; Batalle et al., 2017; Brown et al., 2014; Song et al., 2017; van den Heuvel et al., 2015; Zhao et al., 2019). In fact, during fetal brain development, there is a dramatic growth of major long association WM fibers from 20 to 40 weeks GA, which is thought to underlie the dramatic increases of network strength and efficiency (Song et al., 2017). On the other hand, clustering coefficient has been shown to decrease from 20 to 40 weeks GA (Ball et al., 2014; Song et al., 2017). Modularity index has been also shown to decrease along development, with an increase of communications between different modules from birth to adolescence (Huang et al., 2015). These

findings support the increasing integration and decreasing segregation properties of brain networks during brain development.

Regarding the presence of hubs, studies have shown that structural hubs are present already during the prenatal period and have a consistent spatial topography throughout development (Ball et al., 2014; Chen et al., 2013; Hagmann et al., 2010). During early brain development, most of the studies have identified hubs in posterior midline regions, such as the precuneus and cingulate gyrus (namely the posterior cingulate gyrus), as well as in frontal, temporal and subcortical areas, many of them overlapping with typical adult hubs and others being more infant specific, namely those in sensorimotor and temporal areas (Ball et al., 2014; Huang et al., 2015; Oldham and Fornito, 2019; van den Heuvel et al., 2015).

Additionally, literature has shown that the developmental window between 30 and 40 weeks GA corresponds to an essential period for the establishment of connections between rich-club regions and the rest of the cortex, contributing to an increase in rich-club connectivity (Ball et al., 2014). Moreover, rich-club coefficient has been shown to increase during brain development, from adolescence to adulthood (Dennis et al., 2013).

Regarding spatio-temporal connectivity maturational differences occurring during early brain development, whole-brain connectome analysis has shown that cortical-subcortical connections, namely thalamo-cortical, are the ones maturing faster, whereas intra-frontal, frontal-cingulate, frontal-caudate and inter-hemispheric connections mature slower (Batalle et al., 2017), in agreement with typical WM development and myelination progression histological findings (Kostovic and Jovanov-Milosevic, 2006).

1.5. Prematurity impacts structural brain maturation and connectivity

1.5.1. Effects of preterm birth on early brain maturation and associated neurodevelopmental outcomes

Preterm birth, accounting for approximately 15 million newborns yearly, besides being a major cause of death, may result in a range of long-term complications which hold a considerable impact on families, society and health system (Blencowe et al., 2013).

A preterm infant is an infant that was born before the full gestation was completed, by definition before 37 weeks GA. Despite the multiple advances in neonatal medicine, the borders of life viability have not changed since 1980, remaining around 24 weeks GA (Richardson et al., 1998). Preterm infants can be sub-categorized, according to their GA at the time of birth, into: extremely preterm (born before 28 weeks GA), very preterm (born between 28 and 32 weeks GA) and moderate to late preterm (born between 32 and 37 weeks GA).

The third trimester of gestation, when preterm birth occurs, is characterized by a rapid and important growth of the fetal brain (Brody et al., 1987; Dubois et al., 2008; Huang et al., 2006; Huppi et al., 1998b; Nossin-Manor et al., 2013). During this period, important processes take place, such as axonal and dendritic growth and arborisation, synaptogenesis, neural organization, cortical gyration and sulcation and myelination (Knickmeyer et al., 2008; Volpe, 2001a). Indeed, there is an important expansion of GM and WM volumes, leading to a linear increase of the total brain tissue volume. In particular, there is a fourfold increase of the cortical GM contributing to the rapid total GM increase (Huppi et al., 1998b) and an important organization and maturation of axonal pathways, which are highly vulnerable to injury during this period, in particular between 23 and 32 weeks GA (Kostovic and Jovanov-Milosevic, 2006; Volpe, 2009a).

Preterm birth, by predisposing to pathological events that injure directly the brain and by interfering abruptly with the normal intrauterine brain development occurring during the third trimester, may thus impact the typical development of neurological structures, leading to important neurological morbidity, with an augmented risk for those born before 32 weeks (Dubois et al., 2014; Huppi and Dubois, 2006).

In fact, prematurity might expose the infant to numerous complications, such as hypoxic-ischemic events, sepsis (Back and Miller, 2014), intracranial hemorrhage (Papile et al., 1983), periventricular leukomalacia (Feldman et al., 1990), hypoglycemia (Duvanel et al., 1999) and malnutrition (Hack and Breslau, 1986), which may lead to direct brain damage. These disorders can impact neurogenesis and the balance between excitatory and inhibitory neuronal circuitry, and lead, as well, to WM injury. Analysis of brain autopsy samples from preterm infants have proven that neurogenesis continues until 28 weeks GA and preterm birth was shown to be responsible for supressing glutamatergic neurogenesis in a rabbit model, proving the important impact of prematurity on brain development (Malik et al., 2013). Indeed, neuropathological observations in preterm infants' brains with lesions such as periventricular leukomalacia have shown a decreased number of neurons in WM, subplate and cerebral cortex (Andiman et al., 2010; Kinney et al., 2012). Also, hypoxic-ischemic injury was shown to lead to a decreased number of dendritic branches and synapses in preterm fetal sheep brains (Dean et al., 2013) and is thought to cause a loss of subplate neurons in the immature brain, resulting in an inappropriate formation of thalamocortical and intracortical circuits (McQuillen et al., 2003). WM injury is known to be the most common cause of chronic neurological morbidity of diverse neurobehavioral disabilities following preterm birth, including cerebral palsy. These alterations might explain the abnormal neurodevelopmental outcome accompanying preterm birth. Furthermore, during NICU stay, preterm infants are also exposed routinely to multiple noxious, painful and stressful stimuli or procedures (Vinall et al., 2012), as well as denied the expected intrauterine factors and meaningful sensory inputs relevant for activity-dependent plasticity (Kiss et al., 2014b; Radley and Morrison, 2005), what has also been associated with disturbances in postnatal brain growth and maturation (Brummelte et al., 2012; Smith et al., 2011). Indeed, the third trimester is a period marked by an important activity-dependent brain dendritic and axonal growth and branching, regulated by early synaptic activity (Kostovic and Rakic, 1990; Mrzljak et al., 1992), reason why the environment and early experience may play a crucial role in shaping brain maturation and development.

Although advances in neonatal medicine have improved survival rates and outcome among preterm infants, still up to 40% of very preterm infants experience a broad spectrum of neurodevelopmental impairments evident in childhood, including motor and sensory deficits, attention and socio-emotional impairments, as well as language and cognitive delays (Anderson and Doyle, 2003; Bhutta et al., 2002; Marlow, 2004; Montagna and Nosarti, 2016; Spittle et al., 2009; Spittle et al.,

2011; Williams et al., 2010; Witt et al., 2014), with 25% evidencing behavioral impairments, characterized by inattention, anxiety, internalizing and socio-emotional problems (Anderson and Doyle, 2003; Arpi and Ferrari, 2013; Bhutta et al., 2002; Marlow, 2004; Montagna and Nosarti, 2016; Spittle et al., 2009; Spittle et al., 2011; Williams et al., 2010; Witt et al., 2014), and 10% presenting permanent motor impairment ranging from mild to profound spastic motor deficits, such as cerebral palsy (Beaino et al., 2010; Miller et al., 2005; Vohr, 2014). Moreover, these infants are also at higher risk of developing psychiatric disorders, such as attention deficit and hyperactivity disorder (ADHD), autism spectrum disorder (ASD), anxiety and depression (Johnson and Marlow, 2011; Nosarti et al., 2012; Treyvaud et al., 2013).

Given this considerable risk of lifelong impairment, it is therefore imperative to understand the long-lasting consequences of prematurity on neurodevelopment and define the timing and mode of early interventions aiming to improve and maintain brain functions in preterm infants.

1.5.2. MRI reveals preterm brain structural alterations

By TEA and also later in childhood and adulthood, the preterm brain has been found to be structurally different from that of a healthy full-term born infant.

Preterm birth has been shown to be associated with an impaired cortical growth and maturation, with consequent overall brain volume reduction, of both GM and WM, increased CSF volume, less GM/WM differentiation, WM alterations and reduced anisotropy and poor myelination in comparison with full-term newborns (de Kieviet et al., 2012; Huppi et al., 1996; Huppi et al., 1998a; Inder et al., 1999b; Mewes et al., 2006; Mewes et al., 2007; Peterson et al., 2000; Volpe, 2009a).

In fact, MRI brain volumetric analysis have shown that preterm infants, even in the absence of severe perinatal complications, have reduced volumes of various regions and structures, including cortical GM, namely the orbitofrontal cortex (OFC) and posterior cingulate cortex, as well as subcortical GM, as the thalamus, amygdala, hippocampus, basal ganglia, and also WM fibers, like the CC and internal capsule, besides the cerebellum, cerebral peduncles and brainstem (Cismaru et al., 2016; Huppi and Dubois, 2006; Ment et al., 2009; Mewes et al., 2006; Nosarti, 2013; Padilla et al., 2015; Peterson et al., 2000; Srinivasan et al., 2007). Indeed, lower GA was associated with lower growth rates of cortical GM,

cerebellum and total tissue volume (Gui et al., 2019). Additionally, in comparison to term-born age-matched peers, cortical thickness was also found reduced in children and adolescents born preterm, namely in frontal lobes (Kesler et al., 2008; Nagy et al., 2011; Zubiaurre-Elorza et al., 2012) with some studies also reporting it in the parietal, occipital and temporal lobes (Frye et al., 2010; Kesler et al., 2008; Nagy et al., 2011; Soria-Pastor et al., 2009; Zubiaurre-Elorza et al., 2012).

Preterm infant's WM is known to be highly vulnerable to inflammatory and oxidative processes, being at a high risk of injury during the postnatal preterm period, in particular in periventricular regions (Volpe, 2001b). In fact, cerebral WM injury is considered to be the major form of brain injury in preterm infants (Volpe, 2009a). Using MRI, brain research studies report that 50% to 80% of extremely and very preterm neonates have diffuse WM abnormalities, in particular necrotic lesions of periventricular leukomalacia (Bax et al., 2006; Inder et al., 2003; Inder et al., 2005; Woodward et al., 2006). Indeed, WM injury and abnormal maturation have been identified in several WM tracts of the preterm brain using MRI, and are thought to be the major contributor to the neurodevelopmental disabilities observed later in preterm infants' childhood and adolescence (Ment et al., 2009; Volpe, 2009a).

dMRI provides unique information about preterm WM tracts anatomy, which are not yet myelinated and for which relaxation-based contrast is still inadequate (Hermoye et al., 2006; Huppi et al., 1998a; Neil et al., 1998). dMRI studies have contributed for understanding the nature of neural injury prior to its detection on conventional MRI (Inder et al., 1999a), as well as the neurodevelopmental outcome variation following preterm birth.

DTI has been the most widely used dMRI analysis approach in the developing preterm brain. Studies using this model have proven that, in comparison to full-term newborns, WM microstructure alterations in children born prematurely are already evident at TEA and persist into school age and beyond (Anjari et al., 2007; Nagy et al., 2003; Vangberg et al., 2006). In fact, when compared to age matched full-term born infants, preterm infants without evidence of lesions on conventional MRI present an immaturity of several WM tracts (defined by an inferior FA and increased MD), namely in the CC, anterior commissure, forceps minor, forceps major, frontal gyrus WM, cingulum, uncinate fasciculus, PLIC, external capsule, corona radiata, ILF, SLF, acoustic radiations and medial temporal gyrus WM (Akazawa et al., 2016; Anjari et al., 2007; Dyet et al., 2006; Huppi et al., 1998a; Loe et al., 2013; Rose et al., 2008; Skranes et al., 2007; Thompson et al., 2011; Young et al., 2019). The decreased FA has been shown to be mainly related to a significantly increase in RD, without changes of AD (Young et al., 2019),

reflecting a defect of pre-myelination and myelination events, such as increased membrane permeability, decreased axonal diameter or a greater spacing between axons of the WM fascicles (Counsell et al., 2006; Huppi et al., 1998a). Additionally, increased prematurity (lower GA at birth) has been shown to be associated with a lower FA and increased MD in various WM tracts (Ouyang et al., 2019a; Partridge et al., 2004).

Connectomic analysis and multi-compartment models have also been used to study the impact of prematurity on whole-brain structural connectivity and preterm infants brain WM. Structural connectomes have been constructed, describing the presence of connections between different brain regions, as well as the strength of these connections, using SC, FA, NDI and ODI as measures. Neonatal FA and NDI-weighted connectome analysis revealed that lower GA at birth was correlated with lower FA and NDI, and that there was a negative correlation between brain network global efficiency and GA at birth, suggesting an impact of prematurity on FA and NDI-weighted brain networks (Batalle et al., 2017). Additionally, short-range connections were altered in relation to the degree of prematurity (Batalle et al., 2017). In comparison to full-term newborns, graph-analysis has proven that preterm infants brain networks at TEA present an increased clustering coefficient, increased shortest path length (Ball et al., 2014) and decreased brain network small-worldness and global efficiency (Lee et al., 2019), suggesting an increase in network segregation and decrease in network integration following preterm birth. Furthermore, preterm infants at TEA brain networks revealed a reduced network capacity of DGM, namely a diminished thalamocortical connectivity, towards the frontal cortices, supplementary motor areas, occipital lobe and temporal gyri, in comparison to full-term newborns (Ball et al., 2013a; Ball et al., 2014; Ball et al., 2015). At school-age, extreme preterm children FA-weighted brain networks revealed also an increased characteristic path length and diminished global efficiency, as well as a diminished average nodal degree and nodal strength, in comparison to control infants. In addition, preterm infants have been shown to present altered FA-weighted connectivity in WM frontal brain networks, namely pre-frontal and medial orbito-frontal-cortico-striatal networks, as well as temporal regions, in comparison to age-matched control infants (Fischi-Gomez et al., 2016; Pannek et al., 2013).

NODDI analysis have revealed that, in comparison to full-term children, very preterm children had various WM regions with increased ODI, comprising CC (genu, body and splenium), corona radiata, cingulum, anterior limb of the internal capsule, external capsule, uncinate fasciculus, ILF and SLF (Kelly et al., 2016; Young

et al., 2019). This ODI increase in multiple WM tracts of preterm infants is thought to be related to a disruption of the organization of the densely packed parallel WM fibers leading thus to an axonal dispersion (Young et al., 2019).

FBA analysis of WM tracts in preterm born infants revealed that a lower FD, FC and FDC in WM pathways such as CC (in particular its splenium), anterior commissure, CST, IFOF, ILF, SLF, cingulum and fornix, were associated with lower GA at birth, proving an impact of the degree of prematurity in the maturation of these structures (Pannek et al., 2018; Pecheva et al., 2019). Moreover, when compared to full-term age-matched controls, preterm infants at TEA, 7 years and at 13 years of age demonstrated a reduced FD, FC and FDC in similar regions, namely in the CST, CC, anterior commissure, cingulum, optic radiations, IFOF and fornix, revealing an impact of prematurity in both WM micro and macrostructure during early brain development (Kelly et al., 2020; Pannek et al., 2018). The decrease of these metrics might be related to a diminished axonal number of WM fibers and/or an impact on myelination (Pannek et al., 2018; Raffelt et al., 2012).

In addition to assessing the WM, dMRI studies on cortical GM have identified altered cortical development in preterm infants. During early brain development, DTI studies have shown typically a decrease of both FA and MD in cortical regions, reflecting mostly an increased dendritic arborisation and cellular density leading to a shift from a radial neuronal organisation to a more complex and dense structure, with a large number of neural connections parallel to the cortical plate surface (Ball et al., 2013b; Batalle et al., 2019; McKinstry et al., 2002; Ouyang et al., 2019a; Yu et al., 2016). This complex microstructural development was shown to be impaired in a dose-dependent manner by premature exposure to the extra-uterine environment (Ball et al., 2013b). Furthermore, in comparison to full-term newborns, preterm infants at TEA were shown to present a superior FA and MD in various cortical regions, namely the frontal cortex, including the OFC (Rogers et al., 2012), and also parietal, occipital and temporal areas, suggesting an impaired cortical development in this population (Ball et al., 2013b).

1.5.3. MRI features correlate with clinical outcome in preterm infants

MRI use has been increasing exponentially in premature infants, namely at TEA, with the objective of identifying cerebral lesions and predict long-term developmental outcomes.

In general, total and regional volumetric reductions in premature infants at TEA, mainly in central and parieto-occipital regions, cerebellum and CSF, have been related to poorer neurodevelopmental impairments in early childhood (Inder et al., 2005; Lind et al., 2011; Thompson et al., 2008). Preterm infants' brain tissue volumes at TEA were shown to contribute to the prediction of motor outcomes at 18–24 months and, together with volume growth rates, to the prediction of cognitive scores at 5 years of age (Gui et al., 2019). Significant associations were detected at TEA between WM volume reductions in the right sensorimotor and mid-temporal regions and measures of cognitive and motor development assessed between 18 and 20 months of corrected age (Peterson et al., 2003). Additionally, reduced volumes in premotor, sensorimotor and parieto-occipital regions, as well as increased CSF, were shown to correlate with performance in an object working memory task (Woodward et al., 2005). Thus, alterations in brain tissue volumes due to preterm birth appear to be associated with later neurodevelopmental impairments.

Besides brain tissue volumes alterations, moderate to severe WM abnormalities on MRI at TEA were shown to predict cerebral palsy and motor function in very preterm neonates (van't Hooft et al., 2015).

Diffusion-based WM microstructural measures have also been used to link WM maturation features to brain function, offering a potential as biomarkers for early prognosis of subsequent neurodevelopmental outcome (Arzoumanian et al., 2003; Limperopoulos, 2010; Rose et al., 2007; Rose et al., 2009).

In normal pediatric population, WM maturation evaluated by DTI has been correlated with the development of cognitive functions. For example, in 12-month-old infants and in children between 8 and 18 years, working memory was correlated with DTI parameters in left frontal lobe regions and WM tracts connecting brain regions involved in working memory (such as the genu of CC, anterior and superior thalamic radiations, anterior cingulate gyrus and arcuate fasciculus), whereas reading ability was correlated with FA in the left temporal lobe and tempo-parietal WM (Beaulieu et al., 2005; Deutsch et al., 2005; Klingberg et al., 2000; Nagy et al., 2004; Short et al., 2013). Positive correlations have also been reported in normal pediatric population between IQ (intelligence quotient) and FA in several structures, such as the left arcuate fasciculus, genu of CC and right parietal and frontal regions, suggesting that increases in fiber organization are related to increased cognitive capacity (Schmithorst et al., 2005).

In prematurely born infants, DTI measures indicative of WM microstructural alterations have been generally associated with cognitive, motor and socio-

behavioral impairments. A positive association has been reported between FA and NDI in several WM tracts, with intelligence, socio-behavioral, gross-motor, fine-motor and visuomotor skills, whereas a negative association was found between ODI, MD, AD and RD and these abilities (Fischi-Gomez et al., 2015; Kelly et al., 2016; van Kooij et al., 2012; Young et al., 2019).

Regarding cognitive function, DTI parameters within the CC and fronto-striatal WM fibers have shown associations with later cognitive capacity in preterm infants (Counsell et al., 2008; Duerden et al., 2013; Rose et al., 2009). FA values within the CC, in particular, have been shown to be linearly correlated with developmental quotient at 2-years corrected age (Counsell et al., 2008), while whereas diffusivity in superior temporal gyrus was correlated with language scores at 2-years corrected age (Aeby et al., 2013). In addition, mean FA of the whole-brain WM was correlated with mathematical ability and working memory at 5 years (Ullman et al., 2015) and with full IQ scores in preterm children aged between 8 and 11 years (Yung et al., 2007). In preterm born adolescents, a low IQ was associated with low FA in the external capsule, ILF and SLF, whereas performance IQ was positively correlated with FA in the right PLIC and right SLF (Skranes et al., 2007).

Regarding motor function, DTI parameters within CST/PLIC have shown associations with later motor impairment (Drobyshevsky et al., 2007; Rose et al., 2007; Rose et al., 2009). In particular, in preterm infants with cerebral palsy, DTI has shown that, in addition to lower FA in CST/PLIC, also thalamocortical connections were disrupted, correlating with poor motor and sensory outcome measures (Arzoumanian et al., 2003; Hoon et al., 2009). Fine motor impairment was related to low FA in the internal, external capsule and SLF in preterm born adolescents (Skranes et al., 2007).

Behavioral and socio-emotional function has also been related to DTI parameters. In particular, alterations in FA-weighted structural connectivity in the cortico-basalganglia-thalamo-cortical loop and in short cortico-cortical connectivity (involving namely the superior frontal gyrus, lateral OFC and cingulate gyrus), following preterm birth, were associated with poorer social behavior, recognition of social context and simultaneous information processing at school age (Fischi-Gomez et al., 2015). Additionally, increased diffusivity in right orbitofrontal cortex has been associated with an increased rate of peer problems at 5 years old (Rogers et al., 2012). In preterm born adolescents, mild social deficits were correlated with reduced FA in the external capsule and SLF, while inattention symptoms and the diagnosis of ADHD were related to lower FA in several WM areas. In fact, impairments in more complex functioning such as attention, arithmetic and visual

motor integration seemed to be related to more extensive WM injury (Skranes et al., 2007).

Furthermore, an impaired visual function in premature infants at TEA has been associated with lower FA values in the optic radiations (Bassi et al., 2008).

NODDI parameters have also been applied to study preterm brain development and correlation with clinical outcomes. A higher axon dispersion was found in very preterm infants in various tracts, comprising the CC, CST, corona radiata, internal capsule, external capsule, cingulum, ILF, SLF and uncinate fasciculus. Lower axon density of these WM tracts was correlated with worse neurodevelopmental outcomes in these infants, whereas a worse behavioral/emotional outcome was associated with lower axon density and higher axon dispersion in tracts such as the CC and forceps minor (Kelly et al., 2016).

Regarding structural whole-brain network topology in preterm infants at TEA, global efficiency and clustering coefficient have been found, respectively, to be significantly correlated with later cognitive performance (Keunen et al., 2017) and internalizing and externalizing behaviours assessed in early childhood (Wee et al., 2017).

1.6. Music as an intervention to promote early brain structural maturation

1.6.1. The environment matters: preterm period as a key moment for neuroplasticity

Cognition and socio-emotional competencies rely not only on an intact brain structure, but are also influenced by the environment, which modulates functions formed early in development, both pre- and postnatally. Indeed, the development of neural networks in the perinatal period is highly dependent on intrinsic and extrinsic multisensory activity driving the maturation of neuronal circuits (Kiss et al., 2014b; Sameroff, 2010; Shonkoff, 2010; Swingler et al., 2015). During early brain development, the brain is extremely plastic, given the possibility of massive overproduction of new neural connections and presence of exuberant connections with multiple brain regions, which are no longer observed in the mature brain (Bourgeois and Rakic, 1993; Innocenti and Price, 2005). After the initial neuronal formation and migration until reaching its target, the elaboration and

remodelling of neuronal connections has been shown to be activity-dependent (Goodman and Shatz, 1993; Katz and Shatz, 1996). Indeed, thalamocortical neurons, by bridging the cortical circuitry with sensory periphery, allow sensory-driven activity to modulate neuronal formation and remodelling. The environment, for providing appropriate patterns of neural activity, is thus thought to be crucial for infant's brain development.

Preterm birth occurs during a critical period of brain organization when cortical wiring and activity-dependent neuroplasticity are taking place. It exposes the preterm infant to diverse clinical complications that may lead to brain damage (Back and Miller, 2014), as well as to different noxious stimuli and procedures in the NICU, and it denies the expected intrauterine factors and meaningful sensory inputs relevant for activity-dependent plasticity (Kiss et al., 2014b; Radley and Morrison, 2005), interfering consequently in a negative way with the typical brain developmental processes and being thus associated with disturbances in postnatal brain development (Brummelte et al., 2012; Smith et al., 2011).

The activity-dependent dendritic and axonal remodelling occurring during this critical period will refine the initial brain network formation, being regulated mainly by the early cortical synaptic activity and leading to an increase in network complexity and growth, specially between 27 and 32 weeks GA (Kiss et al., 2014b). The integrity of the brain developmental processes depends therefore upon the presence of the right neural elements appearing at the appropriate developmental moment, with an optimal interaction between endogenous activity and environmental stimulations (Stiles and Jernigan, 2010). Environmental experiences may thus hold significant effects on neural plasticity during this important organizational period by impacting synaptic efficiency via long-term potentiation or long-term depression (Baroncelli et al., 2010; Chun et al., 2013; Isaac et al., 1997; Pouchelon and Jabaudon, 2014). In fact, enrichment and deprivation studies support an important role of experience on brain development. In particular, enrichment studies suggest widespread effects of experience on brain complexity and function, including changes in synapse number and morphology persisting beyond the period of exposure, as well as in myelination (Black et al., 1987; Greenough et al., 1987; Markham and Greenough, 2004), while deprivation studies evidence the capacity for neural reorganization, namely within particular sensory systems (Hubel and Freeman, 1977; Hubel and Wiesel, 1977).

The NICU environment and practices have been typically recognized to be a font of stress to the preterm infant. In contrast to uterine environment, NICU stay is characterized by the presence of painful events, medical and nursing procedures,

as well as strong light, absence of day-night differentiation and a sound environment characterized by direct, erratic, non-biological, unpredictable and excessive noise (Goldson, 1999). Such environment has been related to premature infant's physiologic instability (Freedman et al., 2001; Maschke et al., 2000), increased concentration of stress hormones (Lagercrantz et al., 1986), as well as altered brain development (Akazawa et al., 2016; Anjari et al., 2007; Ball et al., 2010; Gimenez et al., 2008; Qiu et al., 2015) and later poor clinical outcome (Bregman, 1998; Perlman, 2001).

In order to counteract the negative effects of NICU environment on preterm infants' development, during the last years there has been an increasing interest and research regarding developmentally oriented care to modulate preterm infants' sensory input. "Early interventions" refer to prevention-focused programs occurring soon after birth when the infant's brain is plastic and thus interventions are more likely to have maximal impact (Blackman, 2002).

Early developmental care intervention programs designed for preterm infants, such as NIDCAP (Newborn Individualized Developmental Care and Assessment Program) and Kangaroo care (skin-to-skin contact) have proven a beneficial impact on premature infants' clinical outcome, as well as on brain functional and structural maturation, in comparison to standard-of-care (Als et al., 2004; Conde-Agudelo et al., 2011; McAnulty et al., 2009; Soleimani et al., 2020; Spittle et al., 2015; Spittle et al., 2016).

However, given the important burden that prematurity still represents for the health and social system, new interventions and definition of their right timing and mode, aiming to improve and maintain brain functions in preterm infants, are still needed. The preterm period constitutes a window of opportunity in brain development and neuroplasticity and, hence, specifically designed early interventions might have the potential of neuro-enhancement and to recover the loss of function observed in premature infants later in life.

1.6.2. Rational behind using Music to promote early brain development

The sound environment that is present during perinatal period contributes not only for the maturation of the auditory circuits, which require a particular auditory input, but influences also the maturation of distinct brain neural networks. This process is highly dependent on intrinsic and extrinsic multisensory activity: during initial developmental stages, spontaneous activity from the immature

cochlea drives the maturation of networks in the auditory cortex, whereas further remodelling is experience-dependent (Blankenship and Feller, 2010; Kiss et al., 2014b; Sameroff, 2010; Shonkoff, 2010; Swingler et al., 2015). Indeed, from 24-26 weeks GA, with the invasion of the thalamocortical afferents into the cortical plate, the brain starts receiving thalamic input and becomes sensory-driven, mainly in sensory cortical regions as the auditory cortex, what results in an intense dendrite and axonal growth accompanied by synaptogenesis and remodeling (Mire et al., 2012; Mizuno et al., 2010). Also by the third trimester, all the major auditory structures are developed and anatomically functional (Hall, 2000; Polin et al., 2011). The cochlea matures slowly during the third trimester, undergoing "tuning", which is sensitive to changes in sound environment (Benfield, 2004). During this period occurs myelination of the auditory pathway, running from the cochlea, through the auditory nerve, to the cochlear nuclei in brainstem, passing then mainly via the superior olivary complex, the inferior colliculus of the midbrain and the auditory thalamus and from the thalamus, through the acoustic radiations, to the contralateral areas of the primary auditory cortex in the temporal lobe (Moore and Linthicum, 2007).
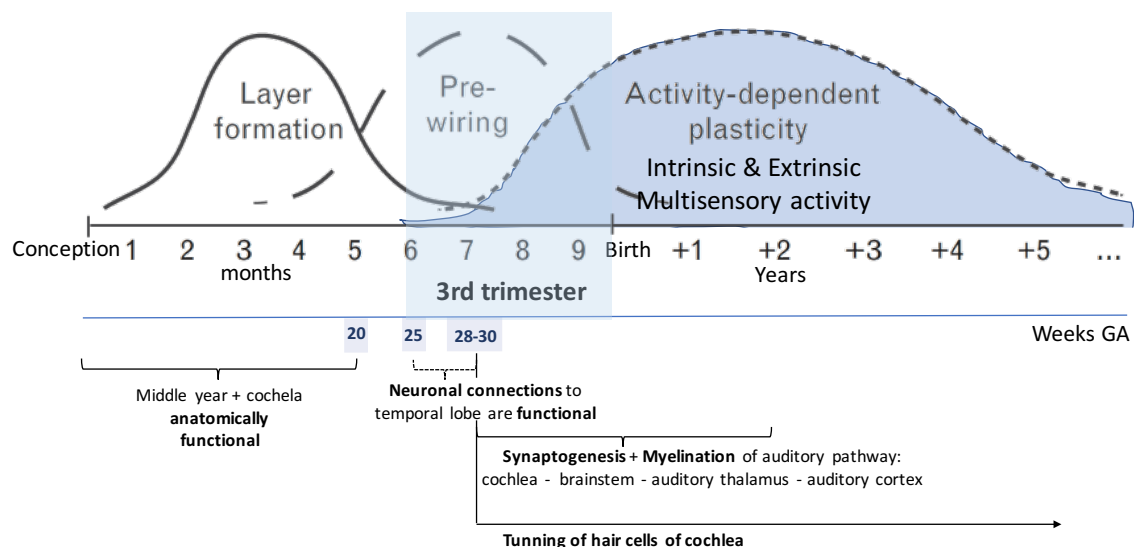
Figure 1.6.1 – **Timing of main developmental stages in the human cerebral cortex and auditory circuitry.** Prematurity occurs during the third trimester of pregnancy, a period of important cortical wiring, activity-dependent neuroplasticity and auditory circuitry development. The activity-dependent dendritic and axonal growth occurring during this period are mainly regulated by the early cortical synaptic activity. The auditory environment contributes thus not only for the maturation of the auditory circuits, which require a particular auditory input, but influences also the maturation of distinct brain neural networks, a process dependent on extrinsic multisensory activity. (Adapted from Kiss et al., 2014b).

Studies measuring fetal movement or heart rate response to sound have shown that, although not fully mature yet, the developing auditory system enables responses to sound in utero from around 25 weeks GA (Birnholz and Benacerraf, 1983) and fetal auditory-evoked responses, evaluated with magnetoencephalography (MEG), have been identified from 27 weeks GA in preterm infants (Draganova et al., 2007).

By the third trimester, preterm infants are thus capable of processing sound, which will be crucial for the normal development of the auditory system, and consequently for the maturation of distinct related brain neural networks.

The sound environment in the NICU is one of the environmental drastic changes that preterm infants have to face, exposing them to direct, erratic, unpredictable and noisy sounds, different from the rhythmical, coherent and familiar auditory stimuli inside the mother's womb. The high noise associated with premature infant's basic care in the NICU can damage the infant's auditory system and impact early brain development. Indeed, studies using pulsed noise exposition in rat pups have shown a substantial impairment in the formation of cortical tonotopic maps and local cortical circuits (Zhang et al., 2002), while sound deprivation studies in rat pups have proven that is necessary to experience spectrally and temporally patterned rich sound to wire brain circuits for pitch processing (Chang and Merzenich, 2003). Deprivation of meaningful sounds or exposition to specific auditory stimuli in the NICU have also been shown to impact auditory cortex maturation (Pineda et al., 2014). On the other hand, auditory experience has been shown to shape the auditory system in the developing brain, namely through studies on reintroduction of the auditory sensation via a cochlear implant in profoundly deaf children, which enabled to restore some or all aspects of normal cortical function (Ponton and Eggermont, 2001).

Music, in contrast to the auditory stressors present in the NICU, is a rich auditory stimulus with elements such as melody, rhythm, harmony, timbre, form and style, comprising both sound and silence expressively organized in time. Through its acoustic properties, music may serve as a masking agent for much of the typical noise present in the NICU (Standley, 2003). Additionally, music listening implies a complex brain processing (Phillips-Silver and Trainor, 2005), triggering both cognitive and emotional components with distinct neural substrates (Zatorre et al., 2009). Indeed, besides brain areas analysing the basic acoustic cues of sound, music is known to activate areas involved in higher order musical features, attention, working memory, episodic memory, experiencing of emotions and sensory-motor regions (Sarkamo et al., 2013). The human neural processing of music involves thus

a widespread bilateral network of cortical and subcortical areas, extending well beyond the auditory cortex and including temporal, frontal, parietal, subcortical and limbic and paralimbic regions, integrating several auditory, cognitive, sensory-motor and emotional functions (Koelsch et al., 2004; Koelsch, 2010; Popescu et al., 2004). In particular, functional neuroimaging studies have proven that music listening triggers many neural substrates involved in socio-emotional functions, comprising amygdala, hippocampal formation, ventral striatum (including nucleus accumbens), cingulate cortex, insula and the OFC, which constitute brain core regions involved in emotion processing (Koelsch et al., 2004; Koelsch, 2010; Koelsch, 2014; Popescu et al., 2004; Zatorre et al., 2009) and are also key areas of deficits in preterm infants (Fischi-Gomez et al., 2015; Lordier et al., 2019b; Spittle et al., 2009; Witt et al., 2014). In fact, literature shows that premature newborns present an atypical socio-emotional development, comprising diminished social competences and self-esteem, emotional dysregulation, shyness and timidity (Bhutta et al., 2002; Hille et al., 2001; Hughes et al., 2002; Montagna and Nosarti, 2016; Spittle et al., 2009), accompanied by structural and functional alterations in brain areas involved in processing emotion and social stimuli (Cismaru et al., 2016; Fischi-Gomez et al., 2016; Peterson et al., 2000; Witt et al., 2014).
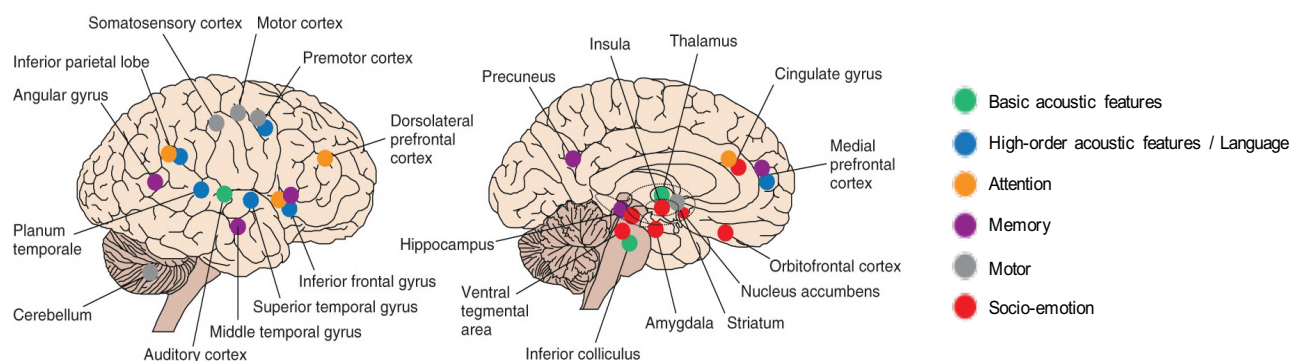
Figure 1.6.2 – **Key brain areas associated with music processing based in neuroimaging studies of healthy subjects.** Each color represents a subgroup of brain areas activated during music processing. In green are regions known to perceive the basic features of music; in blue, regions perceiving higher-order musical features; in yellow, regions implied in attention and working memory, for keeping track of music in time; in purple are areas important for episodic memory, in order to recognize music and recall associated memories; in grey, regions important for motor functions; and in red regions related to emotional processing and experience pleasure and reward. (Adapted from Sarkamo et al., 2013).

Given its rich brain processing, with the recruitment of regions implicated in functions known to be affected by prematurity, music has been implemented in the past years as a meaningful sensory stimulation approach during NICU stay, thought to be relevant for activity-dependent brain plasticity during a critical period of auditory and brain networks maturation (Graven and Browne, 2008; Kiss et al., 2014b; Lasky and Williams, 2005).

An early music therapy program intervention during preterm infants NICU stay might thus impact the auditory system maturation, as well as its associated brain networks, which are important for language processing, attention, memory, emotion, mood and motor skills.

1.6.3. Effects of Music interventions in preterm infants' early brain maturation

For about a decade neonatologists have been investigating the potential role of music in the NICU (Anderson and Patel, 2018). Many authors have evaluated the physiological effects of music listening in premature infants. Most of them have observed a stabilizing effect on heart and respiratory rates, a decrease in daily apnea and bradycardia events, a better feeding outcome, greater weight gain and more mature sleep patterns (Bieleninik et al., 2016; Haslbeck and Stegemann, 2018; van der Heijden et al., 2016). However, literature is still lacking of evidence regarding the effects of music interventions in the brain during early development. Few neurophysiological and neuroimaging studies have been conducted with this purpose.

A neurophysiologic study revealed that, in comparison to control group, fetal exposure to a recorded lullaby presented 5 times per week from the 29th week of pregnancy until birth lead to significantly stronger amplitude event-related potential (ERP) responses at birth and at 4 months, which correlated with the amount of prenatal exposure (Partanen et al., 2013). Such indicates that prenatal music exposure has an effect on the neural responsiveness to sounds, which is still present several months later, supporting a sustained effect on fetal memory during early infancy. Another study has evaluated preterm infants' ERP responses (used as a biomarker of infant speech-sound differentiation during neonatal period), as a measure of the effect of vocal music exposure in preterm infants during NICU stay. It was found that infants exposed to a cappella lullabies (from mother or stranger voice), contingent with infant non-nutritive sucking on a standard pacifier for 20

minutes twice per day for 2 weeks, lead to an increase in speech sound differentiation response on ERP (Chorna et al., 2018).

Some functional neuroimaging studies have also been conducted to unveil brain effects of music interventions. A functional MRI (fMRI) study has shown that preterm infants exposed to a specific music intervention during NICU stay, when at TEA, had an increased functional connectivity between the primary auditory cortex and the thalamus, middle cingulate cortex and striatum, when re-listening to the known music, regions linked to familiarity, pleasant and arousing music processing. This study has proven that the preterm infants at TEA that received an early musical training could already distinguish a known music from the same melody played on a different tempo (Lordier et al., 2018). Additionally, the effect of this music intervention on preterm infants' resting-state functional connectivity was also studied. When compared to full-term infants, premature infants in the control group evidenced a decreased functional connectivity between the salience network (comprising bilateral insula and anterior cingulate) and sensory and high level cognitive networks (auditory, sensorimotor, superior frontal, thalamus and precuneus networks). Conversely, preterm infants that received the music intervention evidenced a higher functional connectivity between these same regions when compared to those in control group (Lordier et al., 2019b).

Another resting-state fMRI study has evaluated the effect of creative music therapy (CMT), which combines individual social contact and musical stimulation in preterm infants' brain. CMT lead to lower thalamocortical processing delay, stronger functional networks and higher functional integration in predominantly left prefrontal, supplementary motor and inferior temporal brain regions in comparison to standard-of-care (Haslbeck et al., 2020).

Regarding the effects of music interventions on brain structure, only an ultrasound study has shown that preterm infants benefited from an early enrichment of their postnatal environment, specifically with cumulative daily 3 hours of audio recordings of maternal sounds (heartbeat, speech, reading and singing) for about a month, which lead to an increase of cortical thickness in their primary auditory cortex (Webb et al., 2015). However, literature is still poor regarding the effects of music interventions on brain macro and microstructure.

1.7. Main research questions and hypothesis

Main research questions:

(i)   Characterize brain microstructural and structural connectivity alterations at TEA resulting from prematurity, in comparison to full-term newborns

(ii)   Study longitudinal whole-brain structural maturation occurring during early brain development in preterm infants, from 33 weeks GA to TEA

(iii)   Evaluate the effectiveness of an early music intervention in modulating preterm infant's brain structural and microstructural maturation during early brain development

Hypothesis:

(i)   Decreased WM microstructural maturation and altered structural connectivity organization in preterm infants at TEA in comparison to full-term newborns.

(ii)   Increase of WM and GM microstructural maturation during preterm infants' early brain development

(iii)   Early postnatal intervention with music during NICU hospitalization will ameliorate preterm infants' macro and microstructural structural brain maturation and connectivity, in particular regarding cortico-limbic networks.

2. BRIEF SUMMARY OF RESULTS

2.2. Resume of contributions

Capitalising on the latest methodological advances, this thesis project aimed to broaden the knowledge regarding the impact of preterm birth on early brain structural connectivity and to study the effectiveness of an early postnatal music intervention as a novel non-invasive approach to enhance brain structural maturation during preterm infant's early brain development.

This section resumes the main resulting contributions in three manuscripts, one published, the other accepted for publication and the third in preparation.

The first manuscript, "Preterm birth leads to impaired rich-club organization and fronto-paralimbic/limbic structural connectivity in newborns", accepted for publication in Neuroimage, describes the impact of preterm birth on whole-brain structural connectivity at TEA, in comparison to full-term (FT) birth. dMRI sequence that had been previously acquired in VPT and FT infants at TEA was used to construct weighted connectomes, describing the number of streamlines connecting the different brain regions, by means of whole-brain probabilistic CSD-based tractography. Graph-based analysis and edge-wise connectivity statistics were employed to unveil brain networks topological alterations and connections with impaired structural connectivity at TEA resulting from preterm birth.

The second manuscript, "Music enhances structural maturation of emotional processing neural pathways in very preterm infants", published in Neuroimage, focused on studying the impact of a music intervention given to VPT infants during NICU stay on regional brain maturation at TEA, in comparison to VPT infants not receiving this intervention. dMRI that had been previously acquired in VPT infants at TEA that had participated in the intervention (as part of the music or control group), as well as in FT infants at TEA, was used to evaluate regional WM microstructural differences between groups, using the DTI model, by means of region-of-interest and seed-based tractography approaches, as well as amygdala volumetric differences between groups.

The third manuscript, "Music impacts brain cortical maturation in very preterm infants: a longitudinal fixel-based and NODDI analysis", in preparation, is the result of a new cohort recruitment and music intervention implementation, that I have conducted during this thesis. It consists in the longitudinal inclusion of VPT infants, which undergo a novel multi-shell dMRI sequence at two time-points, a first at the 33th week GA and a second at TEA. Between the two time-points, VPT infants are included in the intervention protocol, as part of the music or control group. Additionally, also FT infants were recruited and have undergone an MRI at TEA. Using an FBA analysis complemented by NODDI, we unveil the longitudinal whole-brain micro and macrostructural changes occurring both in WM and GM during the third trimester of preterm brain development, we describe the impact of prematurity on whole-brain maturation at TEA, and we reveal the longitudinal impact of an early postnatal music intervention on the whole-brain maturation occurring from the 33th week GA to TEA.

CONTRIBUTIONS

Study 1: Preterm birth leads to impaired rich-club organization and fronto-paralimbic/limbic structural connectivity in newborns

Sa de Almeida et al., *Neuroimage, 2020, Accepted for publication*

- Preterm infants' structural connectome organization is altered already at term age
- Decreased connectome global efficiency and increased modularity in preterm newborns
- Impaired rich-club organization and neonatal hubs connectivity in preterm newborns
- Decreased orbitofrontal-temporal pole circuitry connectivity in preterm newborns
- Evidence of alteration of posterior DMN structural connectivity in preterm newborns
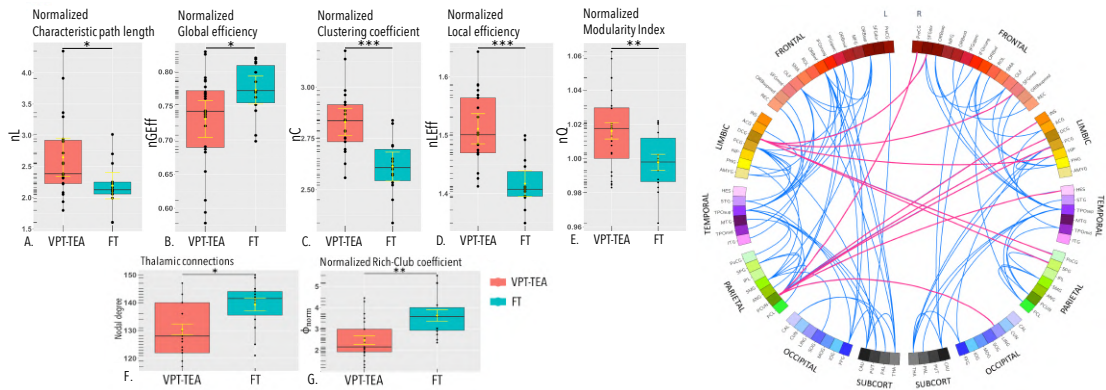
Study 2: Music enhances structural maturation of emotional processing neural pathways in very preterm infants

Sa de Almeida et al., *Neuroimage, 2020*

- VPT infants have a decreased overall brain microstructural maturation at TEA vs FT
- Music enhanced maturation of acoustic and emotional WM pathways in VPT infants
- Amygdala volumes were larger in VPT infants exposed to music than in control group
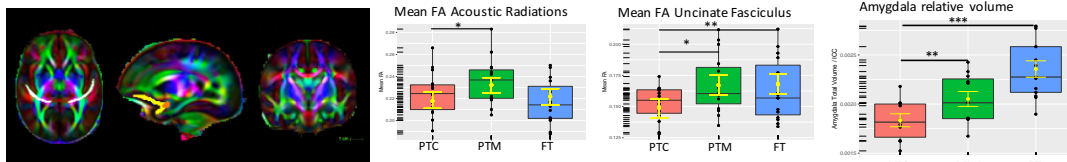
Study 3: Music impacts brain cortical maturation in very preterm infants: a longitudinal fixel-based and NODDI analysis

Sa de Almeida et al., *In preparation*

- The third trimester of preterm brain development is marked an important increase in micro and especially macroscopic maturation of all major cerebral WM fibers, which was higher in the projection fibers, as well as an increase of dendrite arborization and complexity in various cortical GM regions
- An early music intervention led to an increased maturation of cortical regions implied in auditory, cognitive and specially socio-emotional processing.
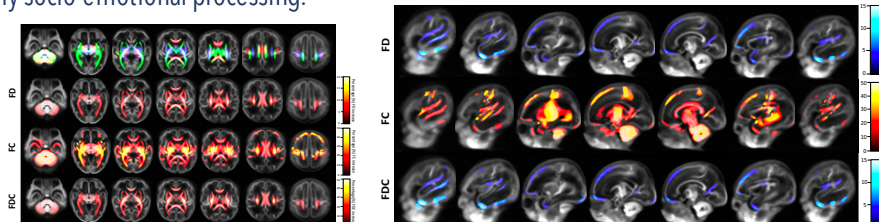
Figure 2.1.1 – **Infographic of thesis contributions resume.**

2.2.1. Preterm birth leads to impaired rich-club organization and fronto-paralimbic/limbic structural connectivity in newborns

Joana Sa de Almeida, Djalel-Eddine Meskaldji, Serafeim Loukas, Lara Lordier, Laura Gui, François Lazeyras, Petra S. Hüppi. *Neuroimage, 2020. Accepted for publication*

Abstract

Introduction: Prematurity disrupts brain development during a critical period of brain growth and organization and is known to be associated with an increased risk of neurodevelopmental impairments. Investigating whole-brain structural connectivity alterations accompanying preterm birth may provide a better comprehension of the neurobiological mechanisms related to the later neurocognitive deficits observed in this population.

Methods: Using a connectome approach, we aimed to study the impact of prematurity on neonatal whole-brain structural network organization at term-equivalent age. In this cohort study, twenty-four very preterm infants at term-equivalent age (VPT-TEA) and fourteen full-term (FT) newborns underwent a brain MRI exam at term age, comprising T2-weighted imaging and diffusion MRI, used to reconstruct brain connectomes by applying probabilistic constrained spherical deconvolution whole-brain tractography. The topological properties of brain networks were quantified through a graph-theoretical approach. Furthermore, edge-wise connectivity strength was compared between groups.

Results: Overall, VPT-TEA infants' brain networks evidenced increased segregation and decreased integration capacity, revealed by an increased clustering coefficient, increased modularity, increased characteristic path length, decreased global efficiency and diminished rich-club coefficient. Furthermore, in comparison to FT, VPT-TEA infants had decreased connectivity strength in various cortico-cortical, cortico-subcortical and intra-subcortical networks, the majority of them being intra-hemispheric fronto-paralimbic and fronto-limbic. Inter-hemispheric connectivity was also decreased in VPT-TEA infants, namely through connections linking to the left precuneus or left dorsal cingulate gyrus – two regions that were found to be hubs in FT but not in VPT-TEA infants. Moreover, posterior regions from Default-

Mode-Network (DMN), namely precuneus and posterior cingulate gyrus, had decreased structural connectivity in VPT-TEA group.

<u>Conclusion:</u> Our finding that VPT-TEA infants' brain networks displayed increased modularity, weakened rich-club connectivity and diminished global efficiency compared to FT infants suggests a delayed transition from a local architecture, focused on short-range connections, to a more distributed architecture with efficient long-range connections in those infants. The disruption of connectivity in fronto-paralimbic/limbic and posterior DMN regions might underlie the behavioral and social cognition difficulties previously reported in the preterm population.

2.2.2. Music enhances structural maturation of emotional processing neural pathways in very preterm infants

Joana Sa de Almeida, Lara Lordier, Benjamin Zollinger, Nicolas Kunz, Matteo Bastiani, Laura Gui, François Lazeyras, Petra S. Hüppi. *Neuroimage, 2020*

Abstract

Introduction: Prematurity disrupts brain maturation by exposing the developing brain to different noxious stimuli present in the neonatal intensive care unit (NICU) and depriving it from meaningful sensory inputs during a critical period of brain development, leading to later neurodevelopmental impairments. Music therapy in the NICU environment has been proposed to promote sensory stimulation, relevant for activity-dependent brain plasticity, but its impact on brain structural maturation is unknown. Neuroimaging studies have demonstrated that music listening triggers neural substrates implied in socio-emotional processing and, thus, it might influence networks formed early in development and known to be affected by prematurity.

Methods: Using multi-modal MRI, we aimed to evaluate the impact of a specially composed music intervention during NICU stay on preterm infant's brain structure maturation. 30 preterm newborns (out of which 15 were exposed to music during NICU stay and 15 without music intervention) and 15 full-term newborns underwent an MRI examination at term-equivalent age, comprising diffusion tensor imaging (DTI), used to evaluate white matter maturation using both region-of-interest and seed-based tractography approaches, as well as a T2-weighted image, used to perform amygdala volumetric analysis.

Results: Overall, WM microstructural maturity measured through DTI metrics was reduced in preterm infants receiving the standard-of-care in comparison to full-term newborns, whereas preterm infants exposed to the music intervention demonstrated significantly improved white matter maturation in acoustic radiations, external capsule/claustrum/extreme capsule and uncinate fasciculus, as well as larger amygdala volumes, in comparison to preterm infants with standard-of-care.

Conclusion: These results suggest a structural maturational effect of the proposed music intervention on premature infants' auditory and emotional processing neural pathways during a key period of brain development.

2.2.3. Music impacts brain cortical maturation in very preterm infants: a longitudinal fixel-based and NODDI analysis

Joana Sa de Almeida, Olivier Baud, Sebastien Fau, Francisca Barcos, Sebastien Courvoisier, Lara Lordier, François Lazeyras, Petra S. Hüppi. *In preparation*

Contribution of J.S.A: Investigation (recruitment, data acquisition, implementation of research protocol), Formal analysis, Software, Methodology, Conceptualization, Writing-Original Draft.

Abstract

Introduction: Dynamic micro and macrostructural changes take place from mid-fetal stage to birth, comprising increasing axon density and myelination in white matter (WM), as well as dendritic growth and arborisation in grey-matter (GM), leading to a significant expansion of brain volumes during the third trimester of brain development. Preterm birth interrupts abruptly the normal brain maturation, exposing preterm infants to multiple pathological events and noxious stimuli, as well as depriving them from meaningful sensory inputs during a critical period of activity-dependent plasticity. Music therapy has been used in neonatal intensive care units (NICU) as a relevant approach for activity-dependent brain plasticity that may influence brain networks formed early in development and affected by prematurity.

Methods: Multi-shell diffusion imaging data was acquired in 24 full-term (FT) newborns and 54 very preterm infants (VPT), 26 without music exposure and 28 exposed daily to a music therapy protocol during neonatal stay, from the 33th week gestational age (GA) to term-equivalent age (TEA). FT newborns underwent the MRI at TEA whereas the VPT underwent an MRI at two-time points: the first during the 33th week GA before starting the intervention and the second at TEA, at the end of the intervention. Using a whole-brain fixel-based analysis (FBA) complemented by NODDI, we aimed to study: the longitudinal whole-brain micro and macroscopic changes occurring in preterm infants from the 33th week GA to TEA; the impact of preterm birth on brain maturation at TEA, in comparison to FT birth; and the longitudinal effect of an early music intervention during neonatal stay on preterm infants' brain maturation, from the 33th week GA to TEA.

Results: Overall, during preterm infants' early brain development, from the 33th week GA to TEA, there is a significant longitudinal increase of fiber density (FD), fiber cross-section (FC) and fiber density cross-section (FDC) in all major cerebral

WM fibers, as well as in the thalamus, brainstem, cerebellum and cerebellar peduncles, whereas in cortical GM there is an increase of FC accompanied by a decrease of FD and FDC. Preterm birth led to a diminished FD in commissural and projection WM fibers at TEA, in comparison to FT birth. An early music intervention from the 33th week GA to TEA has resulted in a significant longitudinal increase of cortical FC in the right middle temporal gyrus, the insulo-orbito-temporopolar complex, and the precuneus and posterior cingulate gyrus, which was accompanied by an increase of ODI, reflecting an increase in dendrite arborisation and cortical geometrical complexity of these regions, undergoing important maturation changes during the third trimester and known to be impaired by prematurity.

Conclusion: Our findings support therefore that: important micro and macroscopic changes are taking place in human brain WM and GM during the third trimester; that preterm birth impairs microscopic WM maturation by TEA in comparison to FT birth; and that an early music intervention can enhance maturation of diverse cortical regions undergoing significant maturational changes during the third trimester and implied in auditory, cognitive and specially socio-emotional processing.

3. DISCUSSION

This thesis project has contributed to: 1) broaden the present knowledge regarding regional and whole-brain structural maturation and connectivity alterations accompanying preterm birth at TEA, using four different methodological techniques: region-of-interest analysis, tractography analysis, connectomic analysis and FBA; 2) unveil whole-brain longitudinal maturational changes occurring both in WM and GM, from the 33th week GA of preterm brain development to TEA, using whole-brain FBA; 3) prove the effectiveness of an early music intervention in enhancing preterm brain structural maturation, by evaluating two different cohorts of preterm infants receiving this intervention during NICU stay, a first one evaluated only at TEA, by means of region-of-interest and tractography based analysis, and a second one, recruited subsequently and analysed by means of whole-brain FBA complemented by NODDI, replicating the first study, but now with longitudinal MRI data acquired before and after the intervention (at the 33th week GA and at TEA).

In this section, I discuss in detail the main findings and possible implications, in the perspective of current literature knowledge. Our results support that: 1) preterm birth is responsible for impairing WM maturation and connectivity at TEA, regionally, affecting in particular the fronto-limbic/paralimbic circuitry, as well as in terms of whole-brain topological organisation, impairing brain network rich-club connectivity and global efficiency; 2) important micro and macrostructural longitudinal changes take place from the 33th week GA to TEA in preterm infant's brain, comprising a general increase in WM density and specially in fiber bundles diameter, in line with pre-myelination and myelination events, as well as an increase in cortical GM complexity, subsequently to an increase in dendritic arborisation; 3) an early music intervention given to very preterm infants during NICU stay may enhance structural maturation of WM fibers and cortical regions implied in sensory, cognitive and specially socio-emotional processing.

To finalise, I also include an overview of the limitations of these studies, as well as future perspectives to further explore the structural connectivity and the effectiveness of early interventions in enhancing preterm brain maturation, in relation with clinical neurodevelopment.

3.1. Preterm birth leads to impaired early brain structural maturation and connectivity at TEA

In comparison to full-term newborns, very preterm infants' brain networks at TEA present a more immature whole-brain topological organisation, characterized by a diminished global efficiency and a delayed shift from a local emphasis to a more distributed and integrated network architecture. Such is accompanied by a decreased connectivity of typical neonatal network hubs (such as the thalamus and the precuneus), decreased rich-club connectivity and decreased connectivity of various cortico-cortical and cortico-subcortical connections, in particular fronto-paralimbic and fronto-limbic. Additionally, there is also an impaired microstructural maturation of WM, characterized by a diminished anisotropy or increased diffusivity of various WM fibers, as well as a diminished fiber density of major WM fiber bundles.

3.1.1. Preterm birth impairs whole-brain network integration

Our results, revealing a decreased global efficiency, increased characteristic path length, and thus an impaired integration of brain networks in prematurely born infants at TEA, support the hypothesis that preterm birth affects the establishment of long-distance WM connections, which are known to undergo a dramatic growth from 20 to 40 weeks GA (Kostovic and Judas, 2010a), when preterm birth occurs, and are thought to underlie the significant increase of network strength and efficiency observed during this period of early brain development (Song et al., 2017). These findings are in line with previous published literature, showing that, both at TEA and later in life during childhood, brain network integration is impaired in preterm infants in comparison to age-matched full-term newborns (Ball et al., 2014; Fischi-Gomez et al., 2015; Lee et al., 2019; Thompson et al., 2016a). The obtained results additionally support that, at TEA, preterm infant's brain is still marked by an important network segregation, with increased clustering coefficient and local efficiency in comparison to full-term infants, suggesting a delayed transition from a local emphasis to the expected more integrated brain network topology. Such is also in line with current literature, showing that structural clustering coefficient tends, in general, to decrease over the preterm period and later in brain development (Ball et al., 2014; Hagmann et al., 2010; Huang et al., 2015; Song et al., 2017; Tymofiyeva et al., 2013), being increased in preterm infants

in comparison to full-term newborns at TEA (Ball et al., 2014). There is still, however, little literature regarding this topic. Our findings support the hypothesis that preterm birth, possibly by impairing WM fibers microstructural maturation and, consequently, the establishment of long-distance WM connections, leads to an impaired brain network integration, what might have as consequence the presence of a still increased network segregation, resulting in a more immature brain network topology at TEA, in comparison to a full-term newborns.

This increased network segregation and impairment in preterm infants' brain network integration is further supported by an increased modularity, dependency on a superior number of hubs but holding a diminished average nodal degree, decreased connectivity of typical neonatal hubs (comprising the thalamus and the precuneus) and a decreased rich-club connectivity in premature infants' brain networks at TEA. Thalamo-cortical connectivity had been already shown to be impaired at TEA in prematurely born infants, correlating with impaired cognitive performance at two years of age (Ball et al., 2015). In fact, premature birth occurs during a critical period of establishment of thalamo-cortical connections, which allow sensory-driven activity to modulate the neuronal circuitry formation. Therefore, the impairment of thalamo-cortical connectivity establishment by preterm birth might impact the brain connectivity remodelling occurring during this critical period of brain development. Such may contribute to the observed decreased integration and increased segregation in premature brain infants' networks. Precuneus connectivity is also particularly impaired in preterm infants at TEA. The precuneus, situated in a strategic location, is known to present a widespread connectivity involving higher association areas and subcortical regions and to support a variety of behavioural functions, including emotional processing and integration of both internally and externally driven stimuli. The precuneus influences thus an extensive network of cortical and subcortical structures involved in the elaboration of highly integrated and associative information (Cavanna and Trimble, 2006). The disruption of precuneus connectivity associated with premature birth, may therefore be at the origin, as well, of the decreased integration observed in premature infants' brain networks. In addition, we show, for the first time, that rich-club structural connectivity is decreased in very preterm infants at TEA, in comparison to full-term newborns. Literature supports that the developmental window between 30 and 40 weeks GA, when preterm birth occurs, corresponds to a crucial period for the establishment of connections between rich-club regions and the rest of the cortex, as well as increase in rich-club connectivity (Ball et al., 2014). A previous fMRI study has also evidenced that preterm infants at TEA exhibit a

significantly reduced functional connectivity within rich-club nodes in comparison to full-term newborns (Scheinost et al., 2016), in line with our structural results.

Integration of distributed neuronal activity across specialized brain systems is required for higher brain function and diverse cognitive processes, such as language (Friederici and Gierhan, 2013), emotion (Pessoa, 2012), cognitive control (Power and Petersen, 2013) and learning (Bassett et al., 2011; Bassett et al., 2015). Indeed, network integration and segregation measures have been found to correlate with clinical features. In particular, an increased global efficiency was found to be significantly positively correlated with increased cognitive performance, whereas a decrease in global efficiency has been related to autism spectrum disorder features, cognitive impairment and aging (Keunen et al., 2017; Lawrence et al., 2014; Lewis et al., 2014; Otte et al., 2015; Shu et al., 2012). Clustering coefficient was found to predict internalizing and externalizing behaviours assessed in early childhood. In particular, a decreased clustering coefficient of the right inferior frontal gyrus and right insula with the rest of the brain was associated with less externalising problems at 48 months of age, whereas a decreased clustering coefficient of the left superior temporal gyrus with the rest of the brain was associated with less internalizing problems in children at 24 months of age (Wee et al., 2017). Therefore, by disrupting integration capacity, what may be at the origin of a more segregated brain network, premature birth predisposes the infants to clinical neurodevelopmental impairments touching various domains of function, including cognitive, behavior and socio-emotional deficits, which have been shown to be present in prematurely born infants later in life (Anderson and Doyle, 2003; Bhutta et al., 2002; Marlow, 2004; Montagna and Nosarti, 2016; Spittle et al., 2009; Spittle et al., 2011; Witt et al., 2014).

3.1.2.   WM microstructure is compromised after preterm birth

The observed impairment of brain networks integration might be due to a disruption of growth and maturation of major long-range WM fibers in association with preterm birth. In fact, we show that, even in the absence of brain lesions, prematurely born infants evidence a decreased microstructural maturation of diverse cerebral WM fibers at TEA.

In particular, in comparison to full-term newborns, a diminished anisotropy and/or higher diffusivity are found in preterm infants at TEA in the following WM fibers: frontal WM, genu, body and splenium of corpus callosum,

interhemispherical auditory callosal fibers, anterior commissure, forceps minor, posterior limb of internal capsule, inferior longitudinal fasciculus, medial temporal gyrus WM, external capsule/claustrum/extreme capsule and uncinate fasciculus. The majority of these regions had been already previously described in literature as affected by preterm birth (Akazawa et al., 2016; Anjari et al., 2007; Dyet et al., 2006; Huppi et al., 1998a; Rose et al., 2008; Thompson et al., 2011). In addition, we show that the inferior FA in most of these WM regions is due to a significant increase in RD, without changes in AD, reflecting most likely a defect in pre-myelination events, such as impaired axonal calibre, delayed or deficient wrapping of the oligodendrocytes around the axons affecting membrane permeability, increased space between axons constituting the WM fascicle and defects in the development of functioning ionic channels (Counsell et al., 2006; Huppi et al., 1998a; Partridge et al., 2004; Qiu et al., 2008; Suzuki et al., 2003; Wimberger et al., 1995).

Furthermore, a reduced fiber density, obtained by means of whole-brain FBA, is also found in major cerebral WM fibers, namely the corpus callosum, fornix and the cortico-spinal tract, passing through the posterior limb of internal capsule. These results are in line with other recently published data (Pannek et al., 2018; Pecheva et al., 2019). In comparison to these prior publications, our cohort of preterm babies did not present any brain lesions which might explain the less extensive changes in fibre density and absence of differences in fiber cross-section, compared to those found by Pannek et al. or Pacheva et al., when evaluating the impact of prematurity in FBA metrics change. Our data supports thus that preterm birth affects mostly WM microstructural fiber density, in comparison to macrostructural fiber cross-section. Indeed, if no significant changes are found in fiber cross-section between full-term newborns and preterm infants at TEA, but these present WM fibers bundles with diminished fiber density, it might be that prematurity has impacted mostly axonal formation, but also pre-myelination events, leading a diminished mass of axons in the fiber bundles and possible increased extra-cellular space. Although offering a more fiber-specific measure of microstructural integrity that aims to overcome the crossing-fibers problem, this whole-brain method implies different registration steps and a complex correction for multiple comparison statistics, given the evaluation at the whole-brain level, being thus less sensitive than the region-of-interest and seed-based tractography analysis to microstructural alterations of specific WM fibers. This might be a possible reason why we obtain an inferior number of affected regions when using FBA than with the previous analysis using the DTI model applied to regions-of-interest or specific tracts to evaluate its microstructure.

These microstructural defects observed in various WM fibers might therefore lead to an impaired communication between disparate brain regions and be at the origin of the impaired brain network integration capacity following preterm birth, what might contribute ultimately to the neurodevelopment impairments observed in preterm infants later in life.

3.1.3. Emotional processing neural pathways are affected in prematurely born infants

The preterm infant's brain reveals specific regional impairments of neural pathways implied in socio-emotional processing, which is observed across different methodological analysis.

Using a connectome approach, whole-brain edge-wise connectivity strength analysis shows that, in comparison to full-term newborns, fronto-paralimbic and fronto-limbic connections are the most frequently affected in very preterm infants, with a particularly noticeable decreased connectivity strength of the orbitofronto-temporal pole circuitry. Additionally, a decreased FA is found in preterm infants' uncinate fasciculus at TEA, which connects the orbitofrontal cortex to the temporal pole, what further supports that preterm birth leads to a decreased microstructural integrity of one of the most relevant WM connections for emotional processing (Oishi et al., 2015; Olson et al., 2015; Von Der Heide et al., 2013). This finding is in agreement with previous studies reporting a decreased FA in the uncinate fasciculus of adolescents (Constable et al., 2008; Mullen et al., 2011) and adults (Rimol et al., 2019) that were born prematurely, as well as a decreased FA-weighted connectivity in the pre-frontal, medial orbito-frontal-cortico-striatal and temporal networks of preterm infants (Fischi-Gomez et al., 2015; Pannek et al., 2013), in comparison to age-matched control infants. In addition, literature has also shown that very preterm infants present volumetric reduction, cortical immaturity and cortical gyrification abnormalities of the orbitofrontal cortex in comparison to full-term newborns (Ganella et al., 2015; Rogers et al., 2012; Thompson et al., 2007), what could be at the origin of the impaired structural connectivity observed in this region following preterm birth.

Since connectivity between the orbitofrontal cortex and temporal pole has been proven to play a role in behavioral and socio-emotional processing (Ghashghaei and Barbas, 2002; Kringelbach, 2005; Wildgruber et al., 2005), it is possible that the observed impaired connectivity strength and microstructural

maturation of this circuitry might be at the origin of the behavioral and socio-emotional difficulties present in prematurely born infants later in development (Bhutta et al., 2002; Hille et al., 2001; Hughes et al., 2002; Lejeune et al., 2015; Montagna and Nosarti, 2016; Spittle et al., 2009; Witt et al., 2014). In fact, alterations in FA-weighted structural connectivity in the orbitofrontal-basalganglia-thalamo-cortical loop following preterm birth, were associated with poorer social behavior, recognition of social context and simultaneous information processing at school age (Fischi-Gomez et al., 2015).

Additionally, we show that brain amygdala volumes are decreased in premature infants at TEA, in comparison to full-term newborns, which is agreement with previous literature findings (Cismaru et al., 2016; Peterson et al., 2000). Such might be associated with the decreased structural connectivity and impairment in WM microstructure found between the temporal pole and orbitofrontal cortex. Indeed, the amygdala is a primary structure of the brain limbic network and constitutes a central component of emotional processing network (Aggleton and Saunders, 2000).

Our findings support therefore that premature birth leads to structural alterations at TEA in brain areas involved in emotional processing, what may constitute a structural basis for the later neurodevelopmental impairments touching socio-emotional deficits observed in the preterm population (Bhutta et al., 2002; Fischi-Gomez et al., 2015; Hille et al., 2001; Hughes et al., 2002; Lejeune et al., 2015; Montagna and Nosarti, 2016; Spittle et al., 2009; Witt et al., 2014).

3.2. Important WM and GM maturational changes occur in the preterm infant's brain from the 33th week GA to TEA

Preterm birth offers a unique window of opportunity to study early brain development. Using the recently established FBA approach applied to longitudinal dMRI data of very preterm infants, we reveal the important whole-brain WM and GM maturational changes occurring from the 33th week GA of early brain development to TEA.

FBA has the advantage of being able to characterize multiple fiber orientations within the voxel, providing microstructural metrics that are more fiber-specific than the ones obtained with the DTI model, and to perform whole-brain comparisons of the fiber-specific properties. Furthermore, we have acquired longitudinal data, what strengthens the statistical power of our analysis.

Regarding WM maturation, from the 33th week GA of preterm brain development to TEA, we show a significant longitudinal increase in fiber density and in fiber cross-section, and thus an increase in micro and macroscopic maturation of all major cerebral WM fibers, bilaterally, in line with the important axonal growth, neural organization and maturational processes known to occur during this developmental period (Batalle et al., 2017; Kostovic and Jovanov-Milosevic, 2006; Kostovic and Judas, 2010a; Kostovic et al., 2014; van den Heuvel et al., 2015). Increases in WM fiber cross-section throughout this period can reach 50%, while fiber density augments by 20%, what suggests that, beyond the augmentation in intra-axonal volume/packing, there is a particularly important augmentation in fiber bundles spatial extent. Such can be due to the maturational processes taking place during this period, such as myelination, leading to an important increase of fiber bundles diameter (Baumann and Pham-Dinh, 2001; Volpe, 2001a). Projection fibers are the ones exhibiting the highest increase in fiber density and, specially, in fiber cross-section, which supports the hypothesis that the observed increases in these metrics might be related to myelination processes, known to have a particular spatial-temporal pattern, starting in the central projection fibers (Kinney et al., 1988).

Fiber density and fiber cross-section metrics increase significantly also in the brainstem, cerebellum and cerebellar peduncles, where projection fibers pass and early myelination occurs. Furthermore, also deep GM undergoes important maturational changes. In fact, there is a significant increase regarding FBA metrics in the thalamus, from where main ascending projection fibers originate, leading to the establishment of functional thalamo-cortical connections during this critical developmental period (Batalle et al., 2017; Kostovic and Jovanov-Milosevic, 2006; Kostovic and Judas, 2010a; Krsnik et al., 2017; Pouchelon and Jabaudon, 2014).

In addition, important maturational changes occur in the cortical GM, as is unveiled by this longitudinal FBA analysis. From the 33th week GA to TEA, there is a significant increase of fiber cross-section, accompanied by a decrease of fiber density in various cortical regions, distributed among frontal, parietal, temporal, insula, cingulate and occipital cortices. In fact, in terms of cortical brain development, the third trimester of pregnancy is characterized by a significant increase in cortical plate complexity, marked by an important growth of the dendritic tree structure, with basal dendrites cross-connections running in parallel to the cortical surface, an increasing number of neuronal connections, including in-growth of thalamo-cortical afferents, transformation of the radial glial cells into astrocytes and proliferation of glial cells (Bystron et al., 2008). There is, therefore,

an important configurational change, from a highly structured cortical plate, with the apical dendrites and radial glia fibers creating a directional and columnar microstructure setting (Ball et al., 2013b; McKinstry et al., 2002; Ouyang et al., 2019a), to a more complex multidirectional microstructural environment, what could justify the observed decrease of fiber density. Fiber density is a directionally-dependent metric, being proportional to the volume of the fibers aligned in that direction (Raffelt et al., 2017), which, in GM, may comprise multiple cellular components sharing the same orientation, namely apical dendrites, axons and astrocytes processes (Budde et al., 2011; Budde and Annese, 2013). Therefore, its calculation might be affected by the increase in cortical geometric complexity, similarly to what is observed when evaluating cortical FA changes during early brain development, which is known to diminish throughout early cortical maturation (Ball et al., 2013b; Batalle et al., 2019; Eaton-Rosen et al., 2015; McKinstry et al., 2002). Furthermore, this decrease of fiber density in cortical GM is also in agreement with the observed decrease in cortical NDI, which has been described during early brain development until TEA (Batalle et al., 2019). This reduction of NDI in cortical GM has been related to the cortical expansion occurring during this period (Huttenlocher, 1990), as well as cell death or apoptosis, what could explain a reduction of the neuronal density in the cortical plate (Chan and Yew, 1998; Lossi and Merighi, 2003). The observed regional significant increase in cortical FC might be related to an augmentation of the number of basal dendrites and glial cells in cortical GM areas, as well as myelination of intracortical axons. Indeed, a decreased FC has been related to decreased myelination (Gajamange et al., 2018), what has been confirmed by histological staining (Malhotra et al., 2019). Furthermore, the highest FC increase was observed in primary sensorial and motor processing areas, which have been proven to be the first cortical regions to demonstrate the presence of intra-cortical myelin (Huttenlocher and Dabholkar, 1997b; Rowley et al., 2017).

The observed longitudinal increase of fiber cross-section accompanied by a decrease of fiber density in various cortical GM regions was complemented by a NODDI analysis, showing that, from the 33th week GA to TEA there is a significant ODI increase in cortical GM, what has been related to increased dendritic branching and cortical complexity (Batalle et al., 2019).

The fact that the primary motor, somatosensory, visual and auditory cortices are among the various cortical regions undergoing significant maturational changes is in line with the establishment of the activity-dependent thalamo-cortical connectivity during this period, transmitting the environmental extrinsic input (from sensory periphery) through the sensory thalamic nuclei to the cerebral cortex,

holding therefore the potential to modulate cortical maturation (Kostovic and Judas, 2007; Milh et al., 2007).

Our data acquired longitudinally throughout this early period of preterm brain development has allowed thus, for the first time, to measure cortical FBA metrics, providing new in vivo imaging biomarkers of major maturational microstructural cortical changes.

Our results, specifying the major brain WM and cortical GM maturational changes occurring typically during the third trimester of pregnancy, complement and are in line with previous findings. In WM fibers, in particular, previous findings have revealed mainly an increase of NDI and FA, in parallel to a decrease of MD and RD during early brain development, consequently to an increase in fiber organization and preliminary myelination (Aeby et al., 2009; Batalle et al., 2017; Dean et al., 2017; Dubois et al., 2008; Huppi et al., 1998a; Kunz et al., 2014; Mukherjee et al., 2002; Nossin-Manor et al., 2013; Shim et al., 2012). On the other hand, in cortical GM, studies have shown mostly a decrease of FA and an increase in ODI during early brain development, in relation with the increased dendritic density and general increase in cortical complexity (Ball et al., 2013b; Batalle et al., 2019; McKinstry et al., 2002). Such significant maturational processes may underlie the important brain growth and significant increase of both GM and WM volumes observed during the third trimester of pregnancy and brain development (Brody et al., 1987; Dubois et al., 2008; Huang et al., 2006; Huppi et al., 1998b; Nossin-Manor et al., 2013).

3.3. Music enhances maturation of brain correlates of emotional processing

To the best of our knowledge, this is the first study investigating the effects of a postnatal music intervention on early brain structure using MRI.

Preterm birth, in particular, constitutes a window of opportunity for early interventions aiming to promote brain plasticity, since it occurs during a critical period of brain development, the third trimester of pregnancy, when cortical wiring and activity-dependent neuroplasticity are taking place. Indeed, during this period, thalamocortical neurons will bridge the cortical circuitry with the sensory periphery, allowing sensory-driven activity to modulate neuronal formation and remodelling, and thus the environment to influence brain development (Goodman and Shatz, 1993; Katz and Shatz, 1996).

In this thesis, two different cohorts of infants receiving the music intervention were evaluated, a first one scanned only at TEA and a second one undergoing a longitudinal MRI evaluation, before and after the intervention, and benefiting from a multi-shell dMRI sequence allowing higher-order diffusion modelling and multi-compartment analysis.

Overall, our results support that an early postnatal music intervention, given to premature infants during NICU stay, will enhance the maturation of both WM and GM, with a particularly remarking effect on emotional processing neural pathways.

Regarding WM evaluation, by means of region-of-interest and seed-based tractography analysis, we show, in our first cohort, that the music intervention enhances preterm infants' WM fibers microstructural maturation at TEA, as revealed by an increased FA in the acoustic radiations, uncinate fasciculus and in the external capsule (constituted dorsally by claustro-cortical fibres and ventrally by the uncinate fasciculus) in the preterm infants receiving the music intervention, in comparison to the preterm control group. These findings prove a structural effect of the early music intervention on WM fibers connecting areas involved in auditory and emotional processing (Koelsch, 2014). In particular, the uncinate fasciculus is a WM bundle that connects parts of the limbic system in the temporal pole, comprising the hippocampus and amygdala, with frontal regions, such as the orbitofrontal cortex, involved in sensory integration, processing of affective stimuli (Kringelbach, 2005) and evaluation of emotional association (Wildgruber et al., 2005). Both the temporal pole and orbitofrontal cortex were shown to be activated during music evoked emotions (Koelsch, 2014). Evidence suggests that training, as well as experience during development, may influence myelination, by promoting neural firing across axons (Demerens et al., 1996; Ishibashi et al., 2006; Zatorre et al., 2012), what can lead to an alteration of WM diffusion parameters, typically marked by a diminished RD and increased FA (Engvig et al., 2012; Hu et al., 2011; Keller and Just, 2009; Moore et al., 2017; Tang et al., 2012). In fact, training has been found to result in higher FA measured in specific WM tracts, what has been related to improved performance (Engel et al., 2014; Ruber et al., 2015; Taubert et al., 2012). Therefore, an early music training, by promoting neural firing across specific WM pathways, may contribute to WM maturation, leading thus to an increased FA and, ultimately, to an increase function of these pathways.

Additionally, a volumetric analysis of amygdala, a central component of the emotional processing network (Aggleton and Saunders, 2000) and emotion modulation during music processing (Ball et al., 2007; Blood and Zatorre, 2001; Koelsch et al., 2013; Koelsch, 2014) shows that the early music intervention leads to

an increased amygdala volume in comparison to the control group, what further supports our hypothesis that listening to music during early brain development might influence networks involved in emotional processing.

In what concerns cortical GM maturation, FBA and NODDI longitudinal analysis applied to data from our second cohort of recruited infants, suggest that the early music intervention leads to an enhanced maturation of some cortical GM brain areas undergoing important maturational changes from the 33th week GA to TEA. These cortical maturational changes are evidenced by a decrease of fiber density, accompanied by an increase of fiber cross-section and of ODI, reflecting an increase in dendritic arborisation and consequent complexification of cortical geometrical structure, as well as a probable increase in intra-cortical myelination. In particular, in comparison to preterm infants in the control group, we observe a longitudinal significantly improved cortical maturation in the preterm infants exposed to the music intervention, from the 33th week GA to TEA, in the left orbitofrontal cortex, left temporal pole and left insula. These paralimbic brain regions constitute the insulo-orbito-temporopolar complex, which is involved in sensory integration, processing of affective stimuli and evaluation of emotional association (Chang et al., 2013; Kringelbach, 2005; Mackes et al., 2018; Olson et al., 2007; Wildgruber et al., 2005), and is known to be activated when musical stimuli elicit emotions (Koelsch et al., 2018). These results complement our previous ones from the first cohort, since they further support a significantly enhanced maturation of the orbitofronto-temporal pole circuitry by the early music intervention, which is found to have an increased maturation in both cortical GM, as well as in the WM pathway connecting these cortical regions.

In addition, preterm infants that have listened to music during NICU stay also present a significantly superior longitudinal maturation of the right middle temporal gyrus, part of the auditory association cortex, known to be activated during passive music listening (Ohnishi et al., 2001) and when musical stimuli elicit emotions (Koelsch et al., 2018), as well as of the right precuneus and posterior cingulate gyrus. These last two brain regions have been shown to be activated when musical stimuli elicit emotions (Koelsch et al., 2018) and they constitute the posterior component of "default mode network" (DMN), functionally linked to self-related processes (Cavanna and Trimble, 2006; Fransson and Marrelec, 2008), social cognition (Mars et al., 2012), inhibitory control (Fair et al., 2008; Whitfield-Gabrieli and Ford, 2012) and regulation of attentional states (Leech and Sharp, 2014; McKiernan et al., 2003).

Furthermore, our results are in line with a previous fMRI study from our group, regarding the functional effects of this music intervention on preterm infants' brain, which has revealed that, in comparison to preterm infants in the control group, those that received the intervention had a significantly increased resting-state (rs) functional connectivity between the salience network, in which the insula is a main component, with other brain regions, namely the thalamus, precuneus and frontal regions (Lordier et al., 2019b). Other studies, in adults, have also previously demonstrate an increase in rs-functional connectivity between the salience network and DMN, in response to passive music listening (Sridharan et al., 2008) and that music training could lead to a significant reorganization of insula-based networks, potentially facilitating high-level cognitive and affective functions (Zamorano et al., 2017).

All these brain regions undergoing significant maturational changes in relation to the early music intervention have been shown to be elicited by music listening, to be implicated in emotional processing and to be impaired by premature birth. Since preterm birth has been shown to be frequently associated with an atypical socio-emotional development (Bhutta et al., 2002; Hille et al., 2001; Hughes et al., 2002; Montagna and Nosarti, 2016; Spittle et al., 2009), an early postnatal music intervention, by enriching the environmental input during a critical period of brain activity-dependent plasticity, might lead to the maturation of brain regions important for emotional processing, what might help preterm infants to achieve their full potential, namely regarding behavior and social-emotional cognition capacities. In fact, our first cohort has participated in a clinical follow-up until 24 months of corrected age and infants that received the music intervention during NICU stay presented fear-reactivity scores at 12-months and anger-reactivity scores at 24-months of age that were closer to full-term newborns, when compared to preterm infants from the control group (Lejeune et al., 2019b), what supports a positive long-term impact of the early music intervention in premature infants' socio-emotional development.

3.4. Limitations and future perspectives

One limitation of our studies is the modest sample size for randomized clinical trials. Such is related to the specificity of our population and thus difficulty of recruitment of families into a research project during a stressful moment of their lives.

The number of times of music exposure during NICU stay can also be considered as limited. However, there are still no guidelines regarding the most adequate dosage to be used in music therapy. From our first cohort to the second, we have doubled the number of plays and the results obtained are complementary and encouraging. Indeed, among two cohorts of recruited infants, using two different diffusion protocols and different types of analysis, we find that music has enhanced the maturation of similar neural pathways. More studies concerning this point and correlating the obtained results with a quantification of music exposure should be ideally performed to better define dose effects.

The data acquisition process is also particularly difficult in this population, due to the possibility of unpredictable motion, since no sedation is used during the scanning. Although a motion correction neonatal specific algorithm has been used for dMRI data, there is still no optimised solution for T2-weighted images motion correction, what can compromise volumetric data analysis, such as the one performed for amygdala, where some data had to be discarded due to motion. Our team is developing therefore a super-resolution algorithm in order to try to diminish the scanning time of the T2-weighted image, dividing the whole acquisition in 3 shorter acquisitions alongside the 3 plans, to reconstruct posteriorly the final image, avoiding therefore a long acquisition time which is more prone to motion problems.

It is also important to point out that the clinical significance behind brain structural alterations following this music intervention, in particular dMRI metrics change, such as DTI, FBA and NODDI parameters, remains to be evaluated by investigating neurodevelopmental and cognitive outcomes in childhood, which are planned for future follow-up studies. Indeed, all the infants recruited undergo a complete neurodevelopment assessment at 12 and 24 months of corrected age in our child development center. This detailed assessment comprises a clinical neurologic evaluation, the Bayley III test and the LabTab test (to evaluate their socio-emotional development), accompanied by questionnaires, filled by the parents, aiming to better evaluate their clinical competences: the IBQ (Infant Behaviour Questionnaire) and ECBQ (Early Childhood Behavior Questionnaire). At 3 years of age we also aim to further evaluate their language competences and by 6 years of

age these infants will be re-contacted and invited to pass clinical evaluations and a new MRI protocol, aiming to study their performance in attentional, auditory and multisensory integration tasks. Therefore, in a nearby future, we hope to be able to respond to the question regarding the long-term clinical impact of this early music intervention on premature infants' long-term neurodevelopment.

In parallel to the MRI acquisition, we have also acquired physiologic data when the infants were being exposed to the intervention, including heart rate, respiratory rate and oxygen saturation level, and we have as well filmed the infant's facial expressions during the intervention, in order to address the physiological and behavioral changes accompanying music listening. These analyses are still in process.

Noise exposure during NICU stay was not quantified in this study and assumed to be equally distributed among groups, given the random allocation process and the similar topology of infants' single rooms in neonatology. This would be an interesting feature to address in future studies.

This study has compared a recorded instrumental music intervention to standard-of-care in the NICU. However, parental presence and exposure to speech (namely maternal singing), were considered to be equally distributed between groups, given the process of random allocation, and were not individually quantified. These factors might also hold an impact on preterm infant's brain development. In general, more research is needed to compare instrumental music interventions to other sound interventions, such as maternal singing, either recorded or life. Caregivers involvement in infants' care is believed to hold an extreme importance on the infant's development. In this study, we have also acquired fMRI task data aiming to evaluate specifically how the brain of premature and full-term infants processes the singing mother voice, in comparison to instrumental music and further analysis regarding this point are in process. Studies aiming to evaluate the impact of an intervention using singing mother voice on premature infant's brain development during NICU stay, which are still lacking in the literature, are also planned in a near future.

4.   CONCLUSION

In this thesis project, using MRI and multiple and novel analysis frameworks, we have studied, first, the microstructural maturational changes occurring longitudinally in early preterm brain development, from the 33th week GA to TEA, second, how preterm birth impacts brain structural maturation and connectivity at TEA in comparison to full-term birth, and third, the effects of an early postnatal music intervention on preterm infants' brain structural maturation, both longitudinally and at TEA.

We demonstrate that important brain maturational changes take place during early brain development in both WM and cortical GM. In particular, there is a significant increase in fiber density and specially in fiber cross-section of all major WM fibers, most likely in relation to pre-myelination and myelination processes. In cortical GM, on the other hand, there is an increase in fiber cross-section and decrease in fiber density, probably related to increased cortical complexity, subsequently to an increase in dendrite growth and arborisation, which was proven to occur during this period of development. These results support that fixel-based metrics may be used as potential biomarkers of, not only, WM, but also GM maturation during early brain development.

Furthermore, we show that preterm birth leads to an impaired microstructural maturation of several WM fibers by TEA, what might be at the origin of the observed decreased connectivity strength of diverse connections and decreased rich-club network connectivity, leading, consequently, to a decreased capacity to integrate information across disparate brain regions and an immature brain network topology at TEA, in comparison to full-term birth. In particular, our results reveal that preterm birth leads to an impaired maturation and connectivity of diverse brain regions known to be implied in emotional processing, namely the orbitofrontal-temporal pole circuitry and amygdala, what may underlie the observed difficulties in socio-emotional development observed in premature infants later in life.

By studying two different cohorts of premature infants participating in randomised clinical trials to evaluate the impact of an early music intervention on early brain development, we show that music impacts the maturation of brain neural correlates of sensory, cognitive and emotional processing, that were shown to undergo significant maturational changes during the third trimester of pregnancy

and/or to be impaired at TEA by premature birth, including the orbitofrontal cortex, the temporal pole, the uncinate fasciculus and the amygdala.

This is the first neuroimaging clinical study using MRI demonstrating a structural impact of an early music intervention on the maturation of brain regions known to be altered by prematurity and holding a key role in emotional processing. Future research aiming to evaluate the clinical long-term impact of such non-invasive early interventions are of major interest for ameliorating developmental care and thus prevent later developmental deficits associated with prematurity.

5. REFERENCES

Ackerman, S., 1992. Discovering the Brain, Vol., National Academies Press (US), Washington (DC).

Aeby, A., et al., 2009. Maturation of thalamic radiations between 34 and 41 weeks' gestation: a combined voxel-based study and probabilistic tractography with diffusion tensor imaging. AJNR Am J Neuroradiol. 30, 1780-6.

Aeby, A., et al., 2013. Language development at 2 years is correlated to brain microstructure in the left superior temporal gyrus at term equivalent age: a diffusion tensor imaging study. Neuroimage. 78, 145-51.

Aggleton, J.P., Saunders, C., 2000. The amygdala - what's happened in the last decade. In: The Amygdala: a Functional Analysis. Vol., ed.^eds. Oxford University Press, Oxford, pp. 1-30.

Akazawa, K., et al., 2016. Probabilistic maps of the white matter tracts with known associated functions on the neonatal brain atlas: Application to evaluate longitudinal developmental trajectories in term-born and preterm-born infants. Neuroimage. 128, 167-179.

Alexander, A.L., et al., 2007. Diffusion tensor imaging of the brain. Neurotherapeutics. 4, 316-29.

Als, H., et al., 2004. Early experience alters brain function and structure. Pediatrics. 113, 846-857.

Anderson, D.E., Patel, A.D., 2018. Infants born preterm, stress, and neurodevelopment in the neonatal intensive care unit: might music have an impact? Developmental Medicine and Child Neurology. 60, 256-266.

Anderson, P., Doyle, L.W., 2003. Neurobehavioral outcomes of school-age children born extremely low birth weight or very preterm in the 1990s. Jama-Journal of the American Medical Association. 289, 3264-3272.

Andiman, S.E., et al., 2010. The Cerebral Cortex Overlying Periventricular Leukomalacia: Analysis of Pyramidal Neurons. Brain Pathology. 20, 803-814.

Anjari, M., et al., 2007. Diffusion tensor imaging with tract-based spatial statistics reveals local white matter abnormalities in preterm infants. Neuroimage. 35, 1021-7.

Arpi, E., Ferrari, F., 2013. Preterm birth and behaviour problems in infants and preschool-age children: a review of the recent literature. Developmental Medicine and Child Neurology. 55, 788-796.

Arzoumanian, Y., et al., 2003. Diffusion tensor brain imaging findings at term-equivalent age may predict neurologic abnormalities in low birth weight preterm infants. AJNR Am J Neuroradiol. 24, 1646-53.

Assaf, Y., Basser, P.J., 2005. Composite hindered and restricted model of diffusion (CHARMED) MR imaging of the human brain. Neuroimage. 27, 48-58.

Assaf, Y., Pasternak, O., 2008. Diffusion tensor imaging (DTI)-based white matter mapping in brain research: a review. J Mol Neurosci. 34, 51-61.

Back, S.A., Miller, S.P., 2014. Brain Injury in Premature Neonates: A Primary Cerebral Dysmaturation Disorder? Annals of Neurology. 75, 469-486.

Ball, G., et al., 2010. An optimised tract-based spatial statistics protocol for neonates: Applications to prematurity and chronic lung disease. Neuroimage. 53, 94-102.

Ball, G., et al., 2013a. The influence of preterm birth on the developing thalamocortical connectome. Cortex; a journal devoted to the study of the nervous system and behavior. 49, 1711-1721.

Ball, G., et al., 2013b. Development of cortical microstructure in the preterm human brain. Proceedings of the National Academy of Sciences of the United States of America. 110, 9541-9546.

Ball, G., et al., 2014. Rich-club organization of the newborn human brain. Proceedings of the National Academy of Sciences of the United States of America. 111, 7456-7461.

Ball, G., et al., 2015. Thalamocortical Connectivity Predicts Cognition in Children Born Preterm. Cerebral Cortex. 25, 4310-4318.

Ball, T., et al., 2007. Response Properties of Human Amygdala Subregions: Evidence Based on Functional MRI Combined with Probabilistic Anatomical Maps. Plos One. 2.

Bammer, R., 2003. Basic principles of diffusion-weighted imaging. Eur J Radiol. 45, 169-84.

Barazany, D., Basser, P.J., Assaf, Y., 2009. In vivo measurement of axon diameter distribution in the corpus callosum of rat brain. Brain. 132, 1210-1220.

Baroncelli, L., et al., 2010. Nurturing brain plasticity: impact of environmental enrichment. Cell Death and Differentiation. 17, 1092-1103.

Basser, P.J., Mattiello, J., LeBihan, D., 1994a. MR diffusion tensor spectroscopy and imaging. Biophys J. 66, 259-67.

Basser, P.J., Mattiello, J., LeBihan, D., 1994b. Estimation of the effective self-diffusion tensor from the NMR spin echo. J Magn Reson B. 103, 247-54.

Basser, P.J., Pierpaoli, C., 1996. Microstructural and physiological features of tissues elucidated by quantitative-diffusion-tensor MRI. J Magn Reson B. 111, 209-19.

Bassett, D.S., et al., 2011. Dynamic reconfiguration of human brain networks during learning. Proc Natl Acad Sci U S A. 108, 7641-6.

Bassett, D.S., et al., 2015. Learning-induced autonomy of sensorimotor systems. Nat Neurosci. 18, 744-51.

Bassettt, D.S., et al., 2006. Adaptive reconfiguration of fractal small-world human brain functional networks. Proceedings of the National Academy of Sciences of the United States of America. 103, 19518-19523.

Bassi, L., et al., 2008. Probabilistic diffusion tractography of the optic radiations and visual function in preterm infants at term equivalent age. Brain. 131, 573-582.

Bastiani, M., Roebroeck, A., 2015. Unraveling the multiscale structural organization and connectivity of the human brain: the role of diffusion MRI. Frontiers in Neuroanatomy. 9.

Batalle, D., et al., 2017. Early development of structural networks and the impact of prematurity on brain connectivity. Neuroimage. 149, 379-392.

Batalle, D., et al., 2019. Different patterns of cortical maturation before and after 38 weeks gestational age demonstrated by diffusion MRI in vivo. Neuroimage. 185, 764-775.

Baumann, N., Pham-Dinh, D., 2001. Biology of oligodendrocyte and myelin in the mammalian central nervous system. Physiological Reviews. 81, 871-927.

Bax, M., Tydeman, C., Flodmark, O., 2006. Clinical and MRI correlates of cerebral palsy - The European Cerebral Palsy Study. Jama-Journal of the American Medical Association. 296, 1602-1608.

Beaino, G., et al., 2010. Predictors of cerebral palsy in very preterm infants: the EPIPAGE prospective population-based cohort study. Developmental Medicine and Child Neurology. 52, E119-E125.

Beaulieu, C., 2002. The basis of anisotropic water diffusion in the nervous system - a technical review. Nmr in Biomedicine. 15, 435-455.

Beaulieu, C., et al., 2005. Imaging brain connectivity in children with diverse reading ability. Neuroimage. 25, 1266-1271.

Behrens, T.E.J., et al., 2003. Characterization and propagation of uncertainty in diffusion-weighted MR imaging. Magnetic Resonance in Medicine. 50, 1077-1088.

Behrens, T.E.J., Sotiropoulos, S.N., Jbabdi, S., 2014. Diffusion MRI, From Quantitative Measurement to In vivo Neuroanatomy, Vol. Chapter 19 - MR Diffusion Tractography, Academic Press.

Benfield, R.D., 2004. Maternal, fetal, & neonatal physiology: A clinical perspective, 2nd Edition. Journal of Midwifery & Womens Health. 49, 164-165.

Benjamini, Y., Hochberg, Y., 1995. Controlling the False Discovery Rate - a Practical and Powerful Approach to Multiple Testing. Journal of the Royal Statistical Society Series B-Statistical Methodology. 57, 289-300.

Berman, J.I., et al., 2009. Quantitative fiber tracking analysis of the optic radiation correlated with visual performance in premature newborns. AJNR Am J Neuroradiol. 30, 120-4.

Bhutta, A.T., et al., 2002. Cognitive and behavioral outcomes of school-aged children who were born preterm - A meta-analysis. Jama-Journal of the American Medical Association. 288, 728-737.

Bieleninik, Ł., Ghetti, C., Gold, C., 2016. Music Therapy for Preterm Infants and Their Parents: A Meta-analysis. Pediatrics.

Birnholz, J.C., Benacerraf, B.R., 1983. The Development of Human-Fetal Hearing. Science. 222, 516-518.

Black, J.E., Sirevaag, A.M., Greenough, W.T., 1987. Complex Experience Promotes Capillary Formation in Young-Rat Visual-Cortex. Neuroscience Letters. 83, 351-355.

Blackman, J.A., 2002. Early intervention: A global perspective. Infants and Young Children. 15, 11-19.

Blankenship, A.G., Feller, M.B., 2010. Mechanisms underlying spontaneous patterned activity in developing neural circuits. Nature Reviews Neuroscience. 11, 18-29.

Blencowe, H., et al., 2013. Born too soon: the global epidemiology of 15 million preterm births. Reproductive health. 10 Suppl 1, S2-S2.

Blood, A.J., Zatorre, R.J., 2001. Intensely pleasurable responses to music correlate with activity in brain regions implicated in reward and emotion. Proc Natl Acad Sci U S A. 98, 11818-23.

Bock, A.S., et al., 2010. Diffusion tensor imaging detects early cerebral cortex abnormalities in neuronal architecture induced by bilateral neonatal enucleation: an experimental model in the ferret. Frontiers in systems neuroscience. 4, 149-149.

Bourgeois, J.P., Rakic, P., 1993. Changes of Synaptic Density in the Primary Visual-Cortex of the Macaque Monkey from Fetal to Adult Stage. Journal of Neuroscience. 13, 2801-2820.

Bregman, J., 1998. Developmental outcome in very low birthweight infants - Current status and future trends. Pediatric Clinics of North America. 45, 673-+.

Brody, B.A., et al., 1987. Sequence of central nervous system myelination in human infancy. I. An autopsy study of myelination. J Neuropathol Exp Neurol. 46, 283-301.

Brown, C.J., et al., 2014. Structural network analysis of brain development in young preterm neonates. Neuroimage. 101, 667-680.

Brummelte, S., et al., 2012. Procedural Pain and Brain Development in Premature Newborns. Annals of Neurology. 71, 385-396.

Bullmore, E.T., Sporns, O., 2009. Complex brain networks: graph theoretical analysis of structural and functional systems. Nature Reviews Neuroscience. 10, 186-198.

Bullmore, E.T., Bassett, D.S., 2011. Brain Graphs: Graphical Models of the Human Brain Connectome. Annual Review of Clinical Psychology. 7, 113-140.

Bystron, I., Blakemore, C., Rakic, P., 2008. Development of the human cerebral cortex: Boulder Committee revisited. Nat Rev Neurosci. 9, 110-22.

Cavanna, A.E., Trimble, M.R., 2006. The precuneus: a review of its functional anatomy and behavioural correlates. Brain. 129, 564-583.

Chan, W.Y., Yew, D.T., 1998. Apoptosis and Bcl-2 oncoprotein expression in the human fetal central nervous system. Anatomical Record. 252, 165-175.

Chang, E.F., Merzenich, M.M., 2003. Environmental noise retards auditory cortical development. Science. 300, 498-502.

Chang, L.J., et al., 2013. Decoding the Role of the Insula in Human Cognition: Functional Parcellation and Large-Scale Reverse Inference. Cerebral Cortex. 23, 739-749.

Chen, Z., et al., 2013. Graph theoretical analysis of developmental patterns of the white matter network. Frontiers in Human Neuroscience. 7.

Cheung, M.M., et al., 2009. Does diffusion kurtosis imaging lead to better neural tissue characterization? A rodent brain maturation study. Neuroimage. 45, 386-392.

Chilla, G.S., et al., 2015. Diffusion weighted magnetic resonance imaging and its recent trend- a survey. Quant Imaging Med Surg. 5, 407-22.

Chorna, O.D., et al., 2018. Feasibility of event-related potential (ERP) biomarker use to study effects of mother's voice exposure on speech sound differentiation of preterm infants. Developmental Neuropsychology. 43, 123-134.

Chun, S.K., et al., 2013. Thalamocortical Long-Term Potentiation Becomes Gated after the Early Critical Period in the Auditory Cortex. Journal of Neuroscience. 33, 7345-7357.

Cismaru, A.L., et al., 2016. Altered Amygdala Development and Fear Processing in Prematurely Born Infants. Front Neuroanat. 10, 55.

Conde-Agudelo, A., Belizan, J.M., Diaz-Rossello, J., 2011. Kangaroo mother care to reduce morbidity and mortality in low birthweight infants. Cochrane Database Syst Rev. CD002771.

Constable, R.T., et al., 2008. Prematurely born children demonstrate white matter microstructural differences at 12 years of age, relative to term control subjects: An investigation of group and gender effects. Pediatrics. 121, 306-316.

Counsell, S.J., et al., 2002. MR imaging assessment of myelination in the very preterm brain. American Journal of Neuroradiology. 23, 872-881.

Counsell, S.J., et al., 2006. Axial and radial diffusivity in preterm infants who have diffuse white matter changes on magnetic resonance imaging at term-equivalent age. Pediatrics. 117, 376-386.

Counsell, S.J., et al., 2008. Specific relations between neurodevelopmental abilities and white matter microstructure in children born preterm. Brain. 131, 3201-3208.

de Kieviet, J.F., et al., 2012. Brain development of very preterm and very low-birthweight children in childhood and adolescence: a meta-analysis. Developmental Medicine and Child Neurology. 54, 313-323.

Dean, D.C., 3rd, et al., 2017. Mapping White Matter Microstructure in the One Month Human Brain. Sci Rep. 7**,** 9759.

Dean, J.M., et al., 2013. Prenatal Cerebral Ischemia Disrupts MRI-Defined Cortical Microstructure Through Disturbances in Neuronal Arborization. Science Translational Medicine. 5.

deIpolyi, A.R., et al., 2005. Comparing microstructural and macrostructural development of the cerebral cortex in premature newborns: Diffusion tensor imaging versus cortical gyration. Neuroimage. 27**,** 579-586.

Demerens, C., et al., 1996. Induction of myelination in the central nervous system by electrical activity. Proceedings of the National Academy of Sciences of the United States of America. 93**,** 9887-9892.

Dennis, E.L., et al., 2013. DEVELOPMENT OF THE "RICH CLUB" IN BRAIN CONNECTIVITY NETWORKS FROM 438 ADOLESCENTS & ADULTS AGED 12 TO 30. Proceedings. IEEE International Symposium on Biomedical Imaging. 624-627.

Deutsch, G.K., et al., 2005. Children's reading performance is correlated with white matter structure measured by diffusion tensor imaging. Cortex. 41**,** 354-363.

Dimond, D., et al., 2020. Early childhood development of white matter fiber density and morphology. Neuroimage. 210:116552.

Draganova, R., et al., 2007. Serial magnetoencephalographic study of fetal and newborn auditory discriminative evoked responses. Early Hum Dev. 83**,** 199-207.

Drobyshevsky, A., et al., 2005. Developmental changes in diffusion anisotropy coincide with immature oligodendrocyte progression and maturation of compound action potential. J Neurosci. 25**,** 5988-97.

Drobyshevsky, A., et al., 2007. Serial diffusion tensor imaging detects white matter changes that correlate with motor outcome in premature infants. Developmental Neuroscience. 29**,** 289-301.

Dubois, J., et al., 2006. Assessment of the early organization and maturation of infants' cerebral white matter fiber bundles: a feasibility study using quantitative diffusion tensor imaging and tractography. Neuroimage. 30**,** 1121-32.

Dubois, J., et al., 2008. Asynchrony of the early maturation of white matter bundles in healthy infants: quantitative landmarks revealed noninvasively by diffusion tensor imaging. Human brain mapping. 29**,** 14-27.

Dubois, J., et al., 2014. The early development of brain white matter: A review of imaging studies in fetuses, newborns and infants. Neuroscience. 276**,** 48-71.

Dubois, J., Dehaene-Lambertz, G., 2015. Fetal and postnatal development of the cortex: insights from MRI and genetics. Brain Mapping: An Encyclopedic Reference. 2**,** 11-19.

Dudink, J., 2010. Diffusion weighted imaging of the neonatal brain. Vol. Doctor, ed.^eds. Erasmus Universiteit Rotterdam, Nederland.

Duerden, E.G., et al., 2013. Alterations in frontostriatal pathways in children born very preterm. Developmental Medicine and Child Neurology. 55**,** 952-958.

Dunn, O.J., 1961. Multiple Comparisons among Means. Journal of the American Statistical Association. 56**,** 52-&.

Duvanel, C.B., et al., 1999. Long-term effects of neonatal hypoglycemia on brain growth and psychomotor development in small-for-gestational-age preterm infants. Journal of Pediatrics. 134**,** 492-498.

Dyet, L.E., et al., 2006. Natural history of brain lesions in extremely preterm infants studied with serial magnetic resonance imaging from birth and neurodevelopmental assessment. Pediatrics. 118, 536-548.

Eaton-Rosen, Z., et al., 2015. Longitudinal measurement of the developing grey matter in preterm subjects using multi-modal MRI. Neuroimage. 111, 580-589.

Eaton-Rosen, Z., et al., 2017. Investigating the maturation of microstructure and radial orientation in the preterm human cortex with diffusion MRI. Neuroimage. 162, 65-72.

Engel, A., et al., 2014. Inter-individual differences in audio-motor learning of piano melodies and white matter fiber tract architecture. Human Brain Mapping. 35, 2483-2497.

Engvig, A., et al., 2012. Memory training impacts short-term changes in aging white matter: A Longitudinal Diffusion Tensor Imaging Study. Human Brain Mapping. 33, 2390-2406.

Erzurumlu, R.S., Gaspar, P., 2012. Development and critical period plasticity of the barrel cortex. Eur J Neurosci. 35, 1540-53.

Fair, D.A., et al., 2008. The maturing architecture of the brain's default network. Proceedings of the National Academy of Sciences of the United States of America. 105, 4028-4032.

Farquharson, S., et al., 2013. White matter fiber tractography: why we need to move beyond DTI Clinical article. Journal of Neurosurgery. 118, 1367-1377.

Feldman, H.M., Scher, M.S., Kemp, S.S., 1990. Neurodevelopmental Outcome of Children with Evidence of Periventricular Leukomalacia on Late Mri. Pediatric Neurology. 6, 296-302.

Fischi-Gomez, E., et al., 2015. Structural Brain Connectivity in School-Age Preterm Infants Provides Evidence for Impaired Networks Relevant for Higher Order Cognitive Skills and Social Cognition. Cereb Cortex. 25, 2793-805.

Fischi-Gomez, E., et al., 2016. Brain network characterization of high-risk preterm-born school-age children. NeuroImage: Clinical. 11, 195-209.

Forbes, K.P.N., Pipe, J.G., Bird, C.R., 2002. Changes in brain water diffusion during the 1st year of life. Radiology. 222, 405-409.

Fransson, P., Marrelec, G., 2008. The precuneus/posterior cingulate cortex plays a pivotal role in the default mode network: Evidence from a partial correlation network analysis. Neuroimage. 42, 1178-1184.

Freedman, N.S., et al., 2001. Abnormal sleep/wake cycles and the effect of environmental noise on sleep disruption in the intensive care unit. Am J Respir Crit Care Med.

Friederici, A.D., Gierhan, S.M.E., 2013. The language network. Current Opinion in Neurobiology. 23, 250-254.

Frye, R.E., et al., 2010. Preterm birth and maternal responsiveness during childhood are associated with brain morphology in adolescence. Journal of the International Neuropsychological Society. 16, 784-794.

Gajamange, S., et al., 2018. Fibre-specific white matter changes in multiple sclerosis patients with optic neuritis. Neuroimage-Clinical. 17, 60-68.

Ganella, E.P., et al., 2015. Abnormalities in Orbitofrontal Cortex Gyrification and Mental Health Outcomes in Adolescents Born Extremely Preterm and/or At an Extremely Low Birth Weight. Human Brain Mapping. 36, 1138-1150.

Genc, S., et al., 2018. Development of white matter fibre density and morphology over childhood: A longitudinal fixel-based analysis. Neuroimage. 183, 666-676.

Ghashghaei, H.T., Barbas, H., 2002. Pathways for emotion: Interactions of prefrontal and anterior temporal pathways in the amygdala of the rhesus monkey. Neuroscience. 115, 1261-1279.

Gimenez, M., et al., 2008. Accelerated cerebral white matter development in preterm infants: A voxel-based morphometry study with diffusion tensor MR imaging. Neuroimage. 41**,** 728-734.

Goldson, E., 1999. Nurturing the Premature Infant: Developmental Intervention in the Neonatal Intensive Care Nursery Vol., Oxford University Press, New York.

Goodman, C.S., Shatz, C.J., 1993. Developmental mechanisms that generate precise patterns of neuronal connectivity. Cell. 72 Suppl**,** 77-98.

Graven, S.N., Browne, J.V., 2008. Auditory Development in the Fetus and Infant. Newborn and Infant Nursing Reviews. 8**,** 187-193.

Greenough, W.T., Black, J.E., Wallace, C.S., 1987. Experience and Brain-Development. Child Development. 58**,** 539-559.

Gui, L., et al., 2019. Longitudinal study of neonatal brain tissue volumes in preterm infants and their ability to predict neurodevelopmental outcome. Neuroimage. 185**,** 728-741.

Guillery, R.W., 2005. Is postnatal neocortical maturation hierarchical? Trends in Neurosciences. 28**,** 512-517.

Hack, M., Breslau, N., 1986. Very-Low-Birth-Weight Infants - Effects of Brain Growth during Infancy on Intelligence Quotient at 3 Years of Age. Pediatrics. 77**,** 196-202.

Hagmann, P., et al., 2006. Understanding diffusion MR imaging techniques: from scalar diffusion-weighted imaging to diffusion tensor imaging and beyond. Radiographics. 26 Suppl 1**,** S205-23.

Hagmann, P., et al., 2010. White matter maturation reshapes structural connectivity in the late developing human brain. Proceedings of the National Academy of Sciences of the United States of America. 107**,** 19067-19072.

Hall, J.W., 3rd, 2000. Development of the ear and hearing. J Perinatol. 20**,** S12-20.

Haslbeck, F., Stegemann, T., 2018. The effect of music therapy on infants born preterm. Developmental Medicine and Child Neurology. 60**,** 217-217.

Haslbeck, F.B., et al., 2020. Creative music therapy to promote brain function and brain structure in preterm infants: A randomized controlled pilot study. Neuroimage Clin. 25**,** 102171.

He, Y., Evans, A., 2010. Graph theoretical modeling of brain connectivity. Curr Opin Neurol. 23**,** 341-50.

Hensch, T.K., 2005. Critical period plasticity in local cortical circuits. Nat Rev Neurosci. 6**,** 877-88.

Hermoye, L., et al., 2006. Pediatric diffusion tensor imaging: normal database and observation of the white matter maturation in early childhood. Neuroimage. 29**,** 493-504.

Hille, E.T.M., et al., 2001. Behavioural problems in children who weigh 1000 g or less at birth in four countries. Lancet. 357**,** 1641-1643.

Hofman, M.A., 2019. Progress in Brain Research, Vol. Evolution of the Human Brain: From Matter to Mind, volume 250, Academic Press.

Hoon, A.H., et al., 2009. Sensory and motor deficits in children with cerebral palsy born preterm correlate with diffusion tensor imaging abnormalities in thalamocortical pathways (vol 51, pg 697, 2009). Developmental Medicine and Child Neurology. 51**,** 1004-1004.

Hu, Y.Z., et al., 2011. Enhanced White Matter Tracts Integrity in Children With Abacus Training. Human Brain Mapping. 32**,** 10-21.

Huang, H., et al., 2006. White and gray matter development in human fetal, newborn and pediatric brains. Neuroimage. 33**,** 27-38.

Huang, H., et al., 2015. Development of Human Brain Structural Networks Through Infancy and Childhood. Cerebral Cortex. 25**,** 1389-1404.

Hubel, D.H., Freeman, D.C., 1977. Projection into Visual-Field of Ocular Dominance Columns in Macaque Monkey. Brain Research. 122**,** 336-343.

Hubel, D.H., Wiesel, T.N., 1977. Functional Architecture of Macaque Monkey Visual-Cortex. Proceedings of the Royal Society Series B-Biological Sciences. 198**,** 1-+.

Hughes, M.B., et al., 2002. Temperament characteristics of premature infants in the first year of life. Journal of Developmental and Behavioral Pediatrics. 23**,** 430-435.

Huppi, P.S., et al., 1996. Structural and neurobehavioral delay in postnatal brain development of preterm infants. Pediatric Research. 39**,** 895-901.

Huppi, P.S., et al., 1998a. Microstructural development of human newborn cerebral white matter assessed in vivo by diffusion tensor magnetic resonance imaging. Pediatric research. 44**,** 584-590.

Huppi, P.S., et al., 1998b. Quantitative magnetic resonance imaging of brain development in premature and mature newborns. Annals of Neurology. 43**,** 224-235.

Huppi, P.S., et al., 2001. Microstructural brain development after perinatal cerebral white matter injury assessed by diffusion tensor magnetic resonance imaging. Pediatrics. 107**,** 455-60.

Huppi, P.S., Dubois, J., 2006. Diffusion tensor imaging of brain development. Seminars in fetal & neonatal medicine. 11**,** 489-497.

Huttenlocher, P.R., 1990. Morphometric Study of Human Cerebral-Cortex Development. Neuropsychologia. 28**,** 517-527.

Huttenlocher, P.R., Dabholkar, A.S., 1997a. Regional differences in synaptogenesis in human cerebral cortex. The Journal of Comparative Neurology. 387**,** 167-178.

Huttenlocher, P.R., Dabholkar, A.S., 1997b. Regional differences in synaptogenesis in human cerebral cortex. Journal of Comparative Neurology. 387**,** 167-178.

Inder, T., et al., 1999a. Early detection of periventricular leukomalacia by diffusion-weighted magnetic resonance imaging techniques. J Pediatr. 134**,** 631-4.

Inder, T.E., et al., 1999b. Periventricular white matter injury in the premature infant is followed by reduced cerebral cortical gray matter volume at term. Annals of Neurology. 46**,** 755-760.

Inder, T.E., et al., 2003. Defining the nature of the cerebral abnormalities in the premature infant: a qualitative magnetic resonance imaging study. J Pediatr. 143**,** 171-9.

Inder, T.E., et al., 2005. Abnormal cerebral structure is present at term in premature infants. Pediatrics. 115**,** 286-94.

Innocenti, G.M., Price, D.J., 2005. Exuberance in the development of cortical networks. Nature Reviews Neuroscience. 6**,** 955-965.

Isaac, J.T.R., et al., 1997. Silent synapses during development of thalamocortical inputs. Neuron. 18**,** 269-280.

Ishibashi, T., et al., 2006. Astrocytes promote myelination in response to electrical impulses. Neuron. 49**,** 823-832.

Jbabdi, S., et al., 2012. Model-based analysis of multishell diffusion MR data for tractography: How to get over fitting problems. Magnetic Resonance in Medicine. 68**,** 1846-1855.

Jelescu, I.O., et al., 2015. One diffusion acquisition and different white matter models: How does microstructure change in human early development based on WMTI and NODDI? Neuroimage. 107**,** 242-256.

Jelescu, I.O., Budde, M.D., 2017. Design and validation of diffusion MRI models of white matter. Front Phys. 28.

Jensen, J.H., et al., 2005. Diffusional kurtosis imaging: The quantification of non-Gaussian water diffusion by means of magnetic resonance imaging. Magnetic Resonance in Medicine. 53**,** 1432-1440.

Jespersen, S.N., et al., 2010. Neurite density from magnetic resonance diffusion measurements at ultrahigh field: Comparison with light microscopy and electron microscopy. Neuroimage. 49**,** 205-216.

Jespersen, S.N., et al., 2012. Determination of Axonal and Dendritic Orientation Distributions Within the Developing Cerebral Cortex by Diffusion Tensor Imaging. Ieee Transactions on Medical Imaging. 31**,** 16-32.

Johnson, S., Marlow, N., 2011. Preterm birth and childhood psychiatric disorders. Pediatr Res. 69**,** 11R-8R.

Katz, L.C., Shatz, C.J., 1996. Synaptic activity and the construction of cortical circuits. Science. 274**,** 1133-8.

Keller, T.A., Just, M.A., 2009. Altering Cortical Connectivity: Remediation-induced Changes in the White Matter of Poor Readers. Neuron. 64**,** 624-631.

Kelly, C.E., et al., 2016. Axon Density and Axon Orientation Dispersion in Children Born Preterm. Human Brain Mapping. 37**,** 3080-3102.

Kelly, C.E., et al., 2020. Long-term development of white matter fibre density and morphology up to 13 years after preterm birth. medRxiv. 2020.04.01.20049585.

Kesler, S.R., et al., 2008. Brain volume reductions within multiple cognitive systems in male preterm children at age twelve. Journal of Pediatrics. 152**,** 513-520.

Kettenmann, H., Ransom, B.R., 2004. Neuroglia, Vol., Oxford University Press Inc., New York.

Keunen, K., et al., 2017. White matter maturation in the neonatal brain is predictive of school age cognitive capacities in children born very preterm. Developmental Medicine and Child Neurology. 59**,** 939-946.

Kim, J.H., et al., 2014. Comparison of statistical tests for group differences in brain functional networks. Neuroimage. 101**,** 681-694.

Kinney, H.C., et al., 1988. Sequence of central nervous system myelination in human infancy. II. Patterns of myelination in autopsied infants. J Neuropathol Exp Neurol. 47**,** 217-34.

Kinney, H.C., et al., 2012. Neuron Deficit in the White Matter and Subplate in Periventricular Leukomalacia. Annals of Neurology. 71**,** 397-406.

Kiss, J.Z., Vasung, L., Petrenko, V., 2014. Process of cortical network formation and impact of early brain damage. Current Opinion in Neurology. 27**,** 133-141.

Klingberg, T., et al., 1999. Myelination and organization of the frontal white matter in children: a diffusion tensor MRI study. Neuroreport. 10**,** 2817-21.

Klingberg, T., et al., 2000. Microstructure of temporo-parietal white matter as a basis for reading ability: Evidence from diffusion tensor magnetic resonance imaging. Neuron. 25**,** 493-500.

Knickmeyer, R.C., et al., 2008. A Structural MRI Study of Human Brain Development from Birth to 2 Years. Journal of Neuroscience. 28**,** 12176-12182.

Koelsch, S., et al., 2004. Music, language and meaning: brain signatures of semantic processing. Nature neuroscience. 7**,** 302-307.

Koelsch, S., 2010. Towards a neural basis of music-evoked emotions. Trends in cognitive sciences. 14**,** 131-137.

Koelsch, S., et al., 2013. The roles of superficial amygdala and auditory cortex in music-evoked fear and joy. Neuroimage. 81**,** 49-60.

Koelsch, S., 2014. Brain correlates of music-evoked emotions. Nat Rev Neurosci. 15**,** 170-80.

Koelsch, S., Skouras, S., Lohmann, G., 2018. The auditory cortex hosts network nodes influential for emotion processing: An fMRI study on music-evoked fear and joy. Plos One. 13.

Kostovic, I., Rakic, P., 1990. Developmental History of the Transient Subplate Zone in the Visual and Somatosensory Cortex of the Macaque Monkey and Human Brain. Journal of Comparative Neurology. 297**,** 441-470.

Kostovic, I., Jovanov-Milosevic, N., 2006. The development of cerebral connections during the first 20-45 weeks' gestation. Seminars in fetal & neonatal medicine. 11**,** 415-422.

Kostovic, I., Judas, M., 2007. Transient patterns of cortical lamination during prenatal life: Do they have implications for treatment? Neuroscience and Biobehavioral Reviews. 31**,** 1157-1168.

Kostovic, I., Judas, M., 2010. The development of the subplate and thalamocortical connections in the human foetal brain. Acta paediatrica (Oslo, Norway : 1992). 99**,** 1119-1127.

Kostovic, I., et al., 2014. Perinatal and early postnatal reorganization of the subplate and related cellular compartments in the human cerebral wall as revealed by histological and MRI approaches. Brain Struct Funct. 219**,** 231-53.

Kostović, I., Sedmak, G., Judaš, M., 2019. Neural histology and neurogenesis of the human fetal and infant brain. Neuroimage. 188**,** 743-773.

Kringelbach, M.L., 2005. The human orbitofrontal cortex: Linking reward to hedonic experience. Nature Reviews Neuroscience. 6**,** 691-702.

Krsnik, Z., et al., 2017. Growth of Thalamocortical Fibers to the Somatosensory Cortex in the Human Fetal Brain. Front Neurosci. 11**,** 233.

Kunz, N., et al., 2014. Assessing white matter microstructure of the newborn with multi-shell diffusion MRI and biophysical compartment models. Neuroimage. 96**,** 288-99.

Lagercrantz, H., et al., 1986. Plasma-Catecholamines Following Nursing Procedures in a Neonatal Ward. Early Human Development. 14**,** 61-65.

Lasky, R.E., Williams, A.L., 2005. The Development of the Auditory System from Conception to Term. NeoReviews. 6**,** e141-e152.

Latora, V., Marchiori, M., 2001. Efficient behavior of small-world networks. Physical Review Letters. 87.

Lawrence, A.J., et al., 2014. Structural network efficiency is associated with cognitive impairment in small-vessel disease. Neurology. 83**,** 304-311.

Le Bihan, D., et al., 1986. MR imaging of intravoxel incoherent motions: application to diffusion and perfusion in neurologic disorders. Radiology. 161**,** 401-7.

Le Bihan, D., 1991. Molecular diffusion nuclear magnetic resonance imaging. Magn Reson Q. 7**,** 1-30.

Le Bihan, D., et al., 2001. Diffusion tensor imaging: Concepts and applications. Journal of Magnetic Resonance Imaging. 13**,** 534-546.

Lebel, C., et al., 2008. Microstructural maturation of the human brain from childhood to adulthood. Neuroimage. 40**,** 1044-55.

Lee, J.Y., Park, H.K., Lee, H.J., 2019. Accelerated Small-World Property of Structural Brain Networks in Preterm Infants at Term-Equivalent Age. Neonatology. 115(2):99-107.

Leech, R., Sharp, D.J., 2014. The role of the posterior cingulate cortex in cognition and disease. Brain. 137, 12-32.

Lejeune, F., et al., 2015. Emotion, attention, and effortful control in 24-month-old very preterm and full-term children. Annee Psychologique. 115, 241-264.

Lejeune, F., et al., 2019. Effects of an Early Postnatal Music Intervention on Cognitive and Emotional Development in Preterm Children at 12 and 24 Months: Preliminary Findings. Frontiers in Psychology. 10.

Lewis, J.D., et al., 2014. Network inefficiencies in autism spectrum disorder at 24 months. Translational Psychiatry. 4.

Limperopoulos, C., 2010. Advanced Neuroimaging Techniques: Their Role in the Development of Future Fetal and Neonatal Neuroprotection. Seminars in Perinatology. 34, 93-101.

Lind, A., et al., 2011. Associations between regional brain volumes at term-equivalent age and development at 2 years of age in preterm children. Pediatric Radiology. 41, 953-961.

Lo, C.Y., et al., 2010. Diffusion Tensor Tractography Reveals Abnormal Topological Organization in Structural Cortical Networks in Alzheimer's Disease. Journal of Neuroscience. 30, 16876-16885.

Loe, I.M., Lee, E.S., Feldman, H.M., 2013. Attention and Internalizing Behaviors in Relation to White Matter in Children Born Preterm. Journal of Developmental and Behavioral Pediatrics. 34, 156-164.

Lordier, L., et al., 2018. Music processing in preterm and full-term newborns: A psychophysiological interaction (PPI) approach in neonatal fMRI. Neuroimage.

Lordier, L., et al., 2019. Music in premature infants enhances high-level cognitive brain networks. Proceedings of the National Academy of Sciences of the United States of America. 116, 12103-12108.

Lossi, L., Merighi, A., 2003. In vivo cellular and molecular mechanisms of neuronal apoptosis in the mammalian CNS. Progress in Neurobiology. 69, 287-312.

Maas, L.C., et al., 2004. Early laminar organization of the human cerebrum demonstrated with diffusion tensor imaging in extremely premature infants. Neuroimage. 22, 1134-40.

Mackes, N.K., et al., 2018. Tracking emotions in the brain - Revisiting the Empathic Accuracy Task. Neuroimage. 178, 677-686.

Malhotra, A., et al., 2019. Advanced MRI analysis to detect white matter brain injury in growth restricted newborn lambs. Neuroimage-Clinical. 24.

Malik, S., et al., 2013. Neurogenesis Continues in the Third Trimester of Pregnancy and Is Suppressed by Premature Birth. Journal of Neuroscience. 33, 411-+.

Markham, J.A., Greenough, W.T., 2004. Experience-driven brain plasticity: beyond the synapse. Neuron Glia Biology. 1, 351-363.

Marlow, N., 2004. Neurocognitive outcome after very preterm birth. Archives of disease in childhood. Fetal and neonatal edition. 89, F224-8.

Mars, R.B., et al., 2012. On the relationship between the "default mode network" and the "social brain". Front Hum Neurosci. 6, 189.

Maschke, C., Rupp, T., Hecht, K., 2000. The influence of stressors on biochemical reactions - a review of present scientific findings with noise. International Journal of Hygiene and Environmental Health. 203, 45-53.

McAnulty, G., et al., 2009. Individualized developmental care for a large sample of very preterm infants: health, neurobehaviour and neurophysiology. Acta Paediatr. 98, 1920-6.

McKiernan, K.A., et al., 2003. A parametric manipulation of factors affecting task-induced deactivation in functional neuroimaging. J Cogn Neurosci. 15, 394-408.

McKinstry, R.C., et al., 2002. Radial organization of developing preterm human cerebral cortex revealed by non-invasive water diffusion anisotropy MRI. Cerebral Cortex. 12, 1237-1243.

McQuillen, P.S., et al., 2003. Selective vulnerability of subplate neurons after early neonatal hypoxia-ischemia. Journal of Neuroscience. 23, 3308-3315.

Meng, H., et al., 2012. Development of the subcortical brain structures in the second trimester: assessment with 7.0-T MRI. Neuroradiology. 54, 1153-9.

Ment, L.R., Hirtz, D., Huppi, P.S., 2009. Imaging biomarkers of outcome in the developing preterm brain. Lancet Neurol. 8, 1042-55.

Meskaldji, D.E., et al., 2013. Comparing connectomes across subjects and populations at different scales. Neuroimage. 80, 416-425.

Meskaldji, D.E., et al., 2015. Improved statistical evaluation of group differences in connectomes by screening-filtering strategy with application to study maturation of brain connections between childhood and adolescence. Neuroimage. 108, 251-64.

Meunier, D., Lambiotte, R., Bullmore, E.T., 2010. Modular and hierarchically modular organization of brain networks. Front Neurosci. 4, 200.

Mewes, A.U.J., et al., 2006. Regional brain development in serial magnetic resonance imaging of low-risk preterm infants. Pediatrics. 118, 23-33.

Mewes, A.U.J., et al., 2007. Displacement of brain regions in preterm infants with non-synostotic dolichocephaly investigated by MRI. Neuroimage. 36, 1074-1085.

Milh, M., et al., 2007. Rapid cortical oscillations and early motor activity in premature human neonate. Cerebral Cortex. 17, 1582-1594.

Miller, S.P., et al., 2005. Early brain injury in premature newborns detected with magnetic resonance imaging is associated with adverse early neurodevelopmental outcome. Journal of Pediatrics. 147, 609-616.

Mire, E., et al., 2012. Spontaneous activity regulates Robo1 transcription to mediate a switch in thalamocortical axon growth. Nat Neurosci. 15, 1134-43.

Mizuno, H., Hirano, T., Tagawa, Y., 2010. Pre-synaptic and post-synaptic neuronal activity supports the axon development of callosal projection neurons during different post-natal periods in the mouse cerebral cortex. Eur J Neurosci. 31, 410-24.

Montagna, A., Nosarti, C., 2016. Socio-Emotional Development Following Very Preterm Birth: Pathways to Psychopathology. Frontiers in Psychology. 7.

Moore, E., et al., 2017. Diffusion tensor MRI tractography reveals increased fractional anisotropy (FA) in arcuate fasciculus following music-cued motor training. Brain Cogn. 116, 40-46.

Moore, J.K., Linthicum, F.H., 2007. The human auditory system: A timeline of development. International Journal of Audiology. 46, 460-478.

Mrzljak, L., et al., 1992. Prenatal Development of Neurons in the Human Prefrontal Cortex .2. A Quantitative Golgi-Study. Journal of Comparative Neurology. 316, 485-496.

Mukherjee, P., et al., 2001. Normal brain maturation during childhood: developmental trends characterized with diffusion-tensor MR imaging. Radiology. 221, 349-58.

Mukherjee, P., et al., 2002. Diffusion-tensor MR imaging of gray and white matter development during normal human brain maturation. AJNR Am J Neuroradiol. 23, 1445-56.

Mullen, K.M., et al., 2011. Preterm birth results in alterations in neural connectivity at age 16 years. Neuroimage. 54, 2563-2570.

Nagy, Z., et al., 2003. Preterm children have disturbances of white matter at 11 years of age as shown by diffusion tensor imaging. Pediatric Research. 54, 672-679.

Nagy, Z., Westerberg, H., Klingberg, T., 2004. Maturation of white matter is associated with the development of cognitive functions during childhood. J Cogn Neurosci. 16, 1227-33.

Nagy, Z., Lagercrantz, H., Hutton, C., 2011. Effects of Preterm Birth on Cortical Thickness Measured in Adolescence. Cerebral Cortex. 21, 300-306.

Neil, J., et al., 2002. Diffusion tensor imaging of normal and injured developing human brain - a technical review. NMR Biomed. 15, 543-52.

Neil, J.J., et al., 1998. Normal brain in human newborns: apparent diffusion coefficient and diffusion anisotropy measured by using diffusion tensor MR imaging. Radiology. 209, 57-66.

Newman, M.E.J., 2004. Fast algorithm for detecting community structure in networks. Physical Review E. 69.

Nomura, Y., et al., 1994. Diffusional anisotropy of the human brain assessed with diffusion-weighted MR: relation with normal brain development and aging. AJNR Am J Neuroradiol. 15, 231-8.

Nosarti, C., et al., 2012. Preterm Birth and Psychiatric Disorders in Young Adult Life. Archives of General Psychiatry. 69, 610-617.

Nosarti, C., 2013. Structural and functional brain correlates of behavioral outcomes during adolescence. Early human development. 89, 221-227.

Nossin-Manor, R., et al., 2013. Quantitative MRI in the very preterm brain: Assessing tissue organization and myelination using magnetization transfer, diffusion tensor and T-1 imaging. Neuroimage. 64, 505-516.

O'Donnell, L.J., Westin, C.F., 2011. An introduction to diffusion tensor image analysis. Neurosurg Clin N Am. 22, 185-96, viii.

Ohnishi, T., et al., 2001. Functional anatomy of musical perception in musicians. Cerebral Cortex. 11, 754-760.

Oishi, K., et al., 2011. Multi-contrast human neonatal brain atlas: application to normal neonate development analysis. Neuroimage. 56, 8-20.

Oishi, K., et al., 2015. Critical Role of the Right Uncinate Fasciculus in Emotional Empathy. Annals of Neurology. 77, 68-74.

Oldham, S., Fornito, A., 2019. The development of brain network hubs. Developmental Cognitive Neuroscience. 36.

Olson, I.R., Ploaker, A., Ezzyat, Y., 2007. The Enigmatic temporal pole: a review of findings on social and emotional processing. Brain. 130, 1718-1731.

Olson, I.R., et al., 2015. Development of the uncinate fasciculus: Implications for theory and developmental disorders. Developmental Cognitive Neuroscience. 14, 50-61.

Opsahl, T., et al., 2008. Prominence and Control: The Weighted Rich-Club Effect. Physical Review Letters. 101.

Otte, W.M., et al., 2015. Aging alterations in whole-brain networks during adulthood mapped with the minimum spanning tree indices: The interplay of density, connectivity cost and life-time trajectory. Neuroimage. 109, 171-189.

Ouyang, M.H., et al., 2019a. Delineation of early brain development from fetuses to infants with diffusion MRI and beyond. Neuroimage. 185, 836-850.

Ouyang, M.H., et al., 2019b. Differential cortical microstructural maturation in the preterm human brain with diffusion kurtosis and tensor imaging. Proceedings of the National Academy of Sciences of the United States of America. 116, 4681-4688.

Owen, J.P., et al., 2013. Test-retest reliability of computational network measurements derived from the structural connectome of the human brain. Brain Connect. 3, 160-76.

Padilla, N., et al., 2015. Brain Growth Gains and Losses in Extremely Preterm Infants at Term. Cerebral cortex (New York, N.Y. : 1991). 25, 1897-1905.

Panagiotaki, E., et al., 2012. Compartment models of the diffusion MR signal in brain white matter: A taxonomy and comparison. Neuroimage. 59, 2241-2254.

Pannek, K., et al., 2013. Assessment of Structural Connectivity in the Preterm Brain at Term Equivalent Age Using Diffusion MRI and T(2) Relaxometry: A Network-Based Analysis. PLoS ONE. 8, e68593-e68593.

Pannek, K., et al., 2018. Fixel-based analysis reveals alterations is brain microstructure and macrostructure of preterm-born infants at term equivalent age. Neuroimage-Clinical. 18, 51-59.

Papile, L.A., Munsickbruno, G., Schaefer, A., 1983. Relationship of Cerebral Intraventricular Hemorrhage and Early-Childhood Neurologic Handicaps. Journal of Pediatrics. 103, 273-277.

Partanen, E., et al., 2013. Prenatal Music Exposure Induces Long-Term Neural Effects. Plos One. 8.

Partridge, S.C., et al., 2004. Diffusion tensor imaging: serial quantitation of white matter tract maturity in premature newborns. Neuroimage. 22, 1302-1314.

Partridge, S.C., et al., 2005. Tractography-based quantitation of diffusion tensor imaging parameters in white matter tracts of preterm newborns. Journal of Magnetic Resonance Imaging. 22, 467-474.

Paus, T., et al., 1999. Structural maturation of neural pathways in children and adolescents: in vivo study. Science. 283, 1908-11.

Paydar, A., et al., 2014. Diffusional Kurtosis Imaging of the Developing Brain. American Journal of Neuroradiology. 35, 808-814.

Pecheva, D., et al., 2018. Recent advances in diffusion neuroimaging: applications in the developing preterm brain. F1000Res. 7.

Pecheva, D., et al., 2019. Fixel-based analysis of the preterm brain: Disentangling bundle-specific white matter microstructural and macrostructural changes in relation to clinical risk factors. Neuroimage-Clinical. 23.

Pereda, A.E., 2014. Electrical synapses and their functional interactions with chemical synapses. Nature Reviews Neuroscience. 15, 250-263.

Perlman, J.M., 2001. Neurobehavioral deficits in premature graduates of intensive care - Potential medical and neonatal environmental risk factors. Pediatrics. 108, 1339-1348.

Pessoa, L., 2012. Beyond brain regions: Network perspective of cognition-emotion interactions. Behavioral and Brain Sciences. 35, 158-159.

Peterson, B.S., et al., 2000. Regional brain volume abnormalities and long-term cognitive outcome in preterm infants. Jama-Journal of the American Medical Association. 284, 1939-1947.

Peterson, B.S., et al., 2003. Regional brain volumes and their later neurodevelopmental correlates in term and preterm infants. Pediatrics. 111, 939-948.

Petruska, J.C., Mendell, L.M., 2009. Encyclopedia of Neuroscience, Vol. Nerve Growth Factor, Academinc Press.

Phillips-Silver, J., Trainor, L.J., 2005. Feeling the beat: movement influences infant rhythm perception. Science (New York, N.Y.). 308**,** 1430-1430.

Pierpaoli, C., Basser, P.J., 1996. Toward a quantitative assessment of diffusion anisotropy. Magn Reson Med. 36**,** 893-906.

Pierpaoli, C., et al., 1996. Diffusion tensor MR imaging of the human brain. Radiology. 201**,** 637-48.

Pineda, R.G., et al., 2014. Alterations in brain structure and neurodevelopmental outcome in preterm infants hospitalized in different neonatal intensive care unit environments. J Pediatr. 164**,** 52-60 e2.

Polin, R.A., Fox, W.W., Abman, S.H., 2011. Fetal and neonatal physiology Vol., Philadelphia, Pa. : W.B. Saunders Co.

Ponton, C.W., Eggermont, J.J., 2001. Of kittens and kids: Altered cortical maturation following profound deafness and cochlear implant use. Audiology and Neuro-Otology. 6**,** 363-380.

Popescu, M., Otsuka, A., Ioannides, A.A., 2004. Dynamics of brain activity in motor and frontal cortical areas during music listening: a magnetoencephalographic study. NeuroImage. 21**,** 1622-1638.

Pouchelon, G., Jabaudon, D., 2014. Nurturing the cortex's thalamic nature. Current Opinion in Neurology. 27**,** 142-148.

Power, J.D., Petersen, S.E., 2013. Control-related systems in the human brain. Current Opinion in Neurobiology. 23**,** 223-228.

Provenzale, J.M., et al., 2007. Diffusion tensor imaging assessment of brain white matter maturation during the first postnatal year. AJR Am J Roentgenol. 189**,** 476-86.

Qiu, A., Mori, S., Miller, M.I., 2015. Diffusion tensor imaging for understanding brain development in early life. Annu Rev Psychol. 66**,** 853-76.

Qiu, D.Q., et al., 2008. Diffusion tensor imaging of normal white matter maturation from late childhood to young adulthood: Voxel-wise evaluation of mean diffusivity, fractional anisotropy, radial and axial diffusivities, and correlation with reading development. Neuroimage. 41**,** 223-232.

Radley, J.J., Morrison, J.H., 2005. Repeated stress and structural plasticity in the brain. Ageing Research Reviews. 4**,** 271-287.

Raffelt, D., et al., 2012. Apparent Fibre Density: A novel measure for the analysis of diffusion-weighted magnetic resonance images. Neuroimage. 59**,** 3976-3994.

Raffelt, D.A., et al., 2015. Connectivity-based fixel enhancement: Whole-brain statistical analysis of diffusion MRI measures in the presence of crossing fibres. Neuroimage. 117**,** 40-55.

Raffelt, D.A., et al., 2017. Investigating white matter fibre density and morphology using fixel-based analysis. Neuroimage. 144**,** 58-73.

Ramón y Cajal, S., 1899. Textura del Sistema Nervioso del Hombre y de los vertebrados. New York: Springer. 1.

Rathi, Y., et al., 2011. Sparse multi-shell diffusion imaging. Med Image Comput Comput Assist Interv. 14(0 2)**,** 58–65.

Richardson, D.K., et al., 1998. Declining severity adjusted mortality: Evidence of improving neonatal intensive care. Pediatrics. 102**,** 893-899.

Rimol, L.M., et al., 2019. Reduced white matter fractional anisotropy mediates cortical thickening in adults born preterm with very low birthweight. Neuroimage. 188, 217-227.

Rogers, C.E., et al., 2012. Regional cerebral development at term relates to school-age social-emotional development in very preterm children. Journal of the American Academy of Child and Adolescent Psychiatry. 51, 181-191.

Rose, J., et al., 2007. Neonatal microstructural development of the internal capsule on diffusion tensor imaging correlates with severity of gait and motor deficits. Dev Med Child Neurol. 49, 745-50.

Rose, J., et al., 2009. Neonatal brain structure on MRI and diffusion tensor imaging, sex, and neurodevelopment in very-low-birthweight preterm children. Dev Med Child Neurol. 51, 526-35.

Rose, J., et al., 2014. Brain microstructural development at near-term age in very-low-birth-weight preterm infants: an atlas-based diffusion imaging study. Neuroimage. 86, 244-56.

Rose, S.E., et al., 2008. Altered white matter diffusion anisotropy in normal and preterm infants at term-equivalent age. Magnetic Resonance in Medicine. 60, 761-767.

Rowley, C.D., et al., 2017. Age-Related Mapping of Intracortical Myelin from Late Adolescence to Middle Adulthood Using T-1-Weighted MRI. Human Brain Mapping. 38, 3691-3703.

Ruber, T., Lindenberg, R., Schlaug, G., 2015. Differential Adaptation of Descending Motor Tracts in Musicians. Cerebral Cortex. 25, 1490-1498.

Rubinov, M., Sporns, O., 2010. Complex network measures of brain connectivity: Uses and interpretations. Neuroimage. 52, 1059-1069.

Rutherford, M.A., et al., 1991. MR imaging of anisotropically restricted diffusion in the brain of neonates and infants. J Comput Assist Tomogr. 15, 188-98.

Sadeghi, N., et al., 2013. Regional characterization of longitudinal DT-MRI to study white the early developing brain. Neuroimage. 68, 236-247.

Sakuma, H., et al., 1991. Adult and neonatal human brain: diffusional anisotropy and myelination with diffusion-weighted MR imaging. Radiology. 180, 229-33.

Salami, M., et al., 2003. Change of conduction velocity by regional myelination yields constant latency irrespective of distance between thalamus and cortex. Proceedings of the National Academy of Sciences of the United States of America. 100, 6174-6179.

Sameroff, A., 2010. A Unified Theory of Development: A Dialectic Integration of Nature and Nurture. Child Development. 81, 6-22.

Sarkamo, T., Tervaniemi, M., Huotilainen, M., 2013. Music perception and cognition: development, neural basis, and rehabilitative use of music. Wiley Interdisciplinary Reviews-Cognitive Science. 4, 441-451.

Scheinost, D., et al., 2016. Preterm birth alters neonatal, functional rich club organization. Brain Structure & Function. 221, 3211-3222.

Scherrer, B., et al., 2016. Characterizing Brain Tissue by Assessment of the Distribution of Anisotropic Microstructural Environments in Diffusion-Compartment Imaging (DIAMOND). Magnetic Resonance in Medicine. 76, 963-977.

Schmithorst, V.J., et al., 2005. Cognitive functions correlate with white matter architecture in a normal pediatric population: A diffusion tensor MRI study. Human Brain Mapping. 26, 139-147.

Shim, S.Y., et al., 2012. Altered Microstructure of White Matter Except the Corpus Callosum Is Independent of Prematurity. Neonatology. 102, 309-315.

Shonkoff, J.P., 2010. Building a New Biodevelopmental Framework to Guide the Future of Early Childhood Policy. Child Development. 81**,** 357-367.

Short, S.J., et al., 2013. Associations between white matter microstructure and infants' working memory. Neuroimage. 64**,** 156-166.

Shu, N., et al., 2011. Diffusion tensor tractography reveals disrupted topological efficiency in white matter structural networks in multiple sclerosis. Cereb Cortex. 21**,** 2565-77.

Shu, N., et al., 2012. Disrupted Topological Organization in White Matter Structural Networks in Amnestic Mild Cognitive Impairment: Relationship to Subtype. Radiology. 265**,** 518-527.

Sie, L.T.L., et al., 1997. MRI assessment of myelination of motor and sensory pathways in the brain of preterm and term-born infants. Neuropediatrics. 28**,** 97-105.

Singh, K.K., et al., 2008. Developmental axon pruning mediated by BDNF-p75NTR-dependent axon degeneration. Nat Neurosci. 11**,** 649-58.

Sizonenko, S.P.V., et al., 2007. Developmental changes and injury induced disruption of the radial organization of the cortex in the immature rat brain revealed by in vivo diffusion tensor MRI. Cerebral Cortex. 17**,** 2609-2617.

Skranes, J., et al., 2007. Clinical findings and white matter abnormalities seen on diffusion tensor imaging in adolescents with very low birth weight. Brain. 130**,** 654-666.

Smith, G.C., et al., 2011. Neonatal intensive care unit stress is associated with brain development in preterm infants. Ann Neurol. 70**,** 541-9.

Snook, L., Plewes, C., Beaulieu, C., 2007. Voxel based versus region of interest analysis in diffusion tensor imaging of neurodevelopment. Neuroimage. 34**,** 243-52.

Soares, J.M., et al., 2013. A hitchhiker's guide to diffusion tensor imaging. Front Neurosci. 7**,** 31.

Soleimani, F., et al., 2020. Do NICU developmental care improve cognitive and motor outcomes for preterm infants? A systematic review and meta-analysis. Bmc Pediatrics. 20.

Song, L.M., et al., 2017. Human Fetal Brain Connectome: Structural Network Development from Middle Fetal Stage to Birth. Frontiers in Neuroscience. 11.

Song, S.K., et al., 2002. Dysmyelination revealed through MRI as increased radial (but unchanged axial) diffusion of water. Neuroimage. 17**,** 1429-1436.

Soria-Pastor, S., et al., 2009. Decreased Regional Brain Volume and Cognitive Impairment in Preterm Children at Low Risk. Pediatrics. 124**,** E1161-E1170.

Spittle, A., et al., 2015. Early developmental intervention programmes provided post hospital discharge to prevent motor and cognitive impairment in preterm infants. Cochrane Database of Systematic Reviews.

Spittle, A.J., et al., 2009. Early Emergence of Behavior and Social-Emotional Problems in Very Preterm Infants. Journal of the American Academy of Child and Adolescent Psychiatry. 48**,** 909-918.

Spittle, A.J., et al., 2011. Neonatal white matter abnormality predicts childhood motor impairment in very preterm children. Dev Med Child Neurol. 53**,** 1000-6.

Spittle, A.J., et al., 2016. School-Age Outcomes of Early Intervention for Preterm Infants and Their Parents: A Randomized Trial. Pediatrics. 138.

Sporns, O., Tononi, G., Kotter, R., 2005. The human connectome: A structural description of the human brain. Plos Computational Biology. 1**,** 245-251.

Sporns, O., 2012. From simple graphs to the connectome: Networks in neuroimaging. Neuroimage. 62**,** 881-886.

Sporns, O., Betzel, R.F., 2016. Modular Brain Networks. Annual Review of Psychology, Vol 67. 67, 613-640.

Sridharan, D., Levitin, D.J., Menon, V., 2008. A critical role for the right fronto-insular cortex in switching between central-executive and default-mode networks. Proc Natl Acad Sci U S A. 105, 12569-74.

Srinivasan, L., et al., 2007. Quantification of deep gray matter in preterm infants at term-equivalent age using manual volumetry of 3-tesla magnetic resonance images. Pediatrics. 119, 759-765.

Standley, J.M., 2003. Music therapy with premature infants: Research and developmental interventions. American Music Therapy Association, Silver Spring, MD.

Stejskal, E.O., Tanner, J.E., 1965. Spin Diffusion Measurements: Spin Echoes in the Presence of a Time-Dependent Field Gradient. Journal of Chemical Physics. 42, 288-+.

Stiles, J., Jernigan, T.L., 2010. The Basics of Brain Development. Neuropsychology Review. 20, 327-348.

Suzuki, Y., et al., 2003. Absolute eigenvalue diffusion tensor analysis for human brain maturation. Nmr in Biomedicine. 16, 257-260.

Swingler, M.M., Perry, N.B., Calkins, S.D., 2015. Neural plasticity and the development of attention: Intrinsic and extrinsic influences. Development and Psychopathology. 27, 443-457.

Takeda, K., et al., 1997. MR assessment of normal brain development in neonates and infants: comparative study of T1- and diffusion-weighted images. J Comput Assist Tomogr. 21, 1-7.

Tang, Y.Y., et al., 2012. Mechanisms of white matter changes induced by meditation. Proceedings of the National Academy of Sciences of the United States of America. 109, 10570-10574.

Taubert, M., Villringer, A., Ragert, P., 2012. Learning-Related Gray and White Matter Changes in Humans: An Update. Neuroscientist. 18, 320-325.

Thomas, J.L., et al., 2000. Spatiotemporal development of oligodendrocytes in the embryonic brain. Journal of Neuroscience Research. 59, 471-476.

Thompson, D.K., et al., 2007. Perinatal risk factors altering regional brain structure in the preterm infant. Brain. 130, 667-77.

Thompson, D.K., et al., 2008. Neonate hippocampal volumes: Prematurity, perinatal predictors, and 2-year outcome. Annals of Neurology. 63, 642-651.

Thompson, D.K., et al., 2011. Characterization of the corpus callosum in very preterm and full-term infants utilizing MRI. Neuroimage. 55, 479-490.

Thompson, D.K., et al., 2016. Structural connectivity relates to perinatal factors and functional impairment at 7years in children born very preterm. NeuroImage. 134.

Tournier, J.D., Calamante, F., Connelly, A., 2007. Robust determination of the fibre orientation distribution in diffusion MRI: non-negativity constrained super-resolved spherical deconvolution. Neuroimage. 35, 1459-72.

Treyvaud, K., et al., 2013. Psychiatric outcomes at age seven for very preterm children: rates and predictors. Journal of Child Psychology and Psychiatry. 54, 772-779.

Tuch, D.S., et al., 2003. Diffusion MRI of complex neural architecture. Neuron. 40, 885-95.

Tymofiyeva, O., et al., 2013. A DTI-Based Template-Free Cortical Connectome Study of Brain Maturation. Plos One. 8.

Ullman, H., et al., 2015. Neonatal MRI is associated with future cognition and academic achievement in preterm children. Brain. 138.

Ulug, A.M., et al., 1997. Absolute quantitation of diffusion constants in human stroke. Stroke. 28**,** 483-90.

van den Heuvel, M.P., Sporns, O., 2011. Rich-Club Organization of the Human Connectome. Journal of Neuroscience. 31**,** 15775-15786.

van den Heuvel, M.P., et al., 2012. High-cost, high-capacity backbone for global brain communication. Proc Natl Acad Sci U S A. 109**,** 11372-7.

van den Heuvel, M.P., Sporns, O., 2013. Network hubs in the human brain. Trends Cogn Sci. 17**,** 683-96.

van den Heuvel, M.P., et al., 2015. The Neonatal Connectome During Preterm Brain Development. Cerebral Cortex. 25**,** 3000-3013.

van der Heijden, M.J., et al., 2016. Do Hospitalized Premature Infants Benefit from Music Interventions? A Systematic Review of Randomized Controlled Trials. PLoS One. 11**,** e0161848.

van Kooij, B.J.M., et al., 2012. Neonatal Tract-Based Spatial Statistics Findings and Outcome in Preterm Infants. American Journal of Neuroradiology. 33**,** 188-194.

van't Hooft, J., et al., 2015. Predicting developmental outcomes in premature infants by term equivalent MRI: systematic review and meta-analysis. Systematic Reviews. 4.

Vangberg, T.R., et al., 2006. Changes in white matter diffusion anisotropy in adolescents born prematurely. Neuroimage. 32**,** 1538-1548.

Vinall, J., et al., 2012. Neonatal pain in relation to postnatal growth in infants born very preterm. Pain. 153**,** 1374-1381.

Vohr, B.R., 2014. Neurodevelopmental Outcomes of Extremely Preterm Infants. Clinics in Perinatology. 41**,** 241-+.

Volpe, J.J., 2001a. Neurology of the newborn (4th ed.), Vol., W.B. Saunders, Philadelphia.

Volpe, J.J., 2001b. Neurobiology of periventricular leukomalacia in the premature infant. Pediatr Res. 50**,** 553-62.

Volpe, J.J., 2009. Brain injury in premature infants: a complex amalgam of destructive and developmental disturbances. Lancet Neurology. 8**,** 110-124.

Von Der Heide, R.J., et al., 2013. Dissecting the uncinate fasciculus: disorders, controversies and a hypothesis. Brain. 136**,** 1692-1707.

Watts, D.J., Strogatz, S.H., 1998. Collective dynamics of 'small-world' networks. Nature. 393**,** 440-442.

Webb, A.R., et al., 2015. Mother's voice and heartbeat sounds elicit auditory plasticity in the human brain before full gestation. Proceedings of the National Academy of Sciences of the United States of America. 112**,** 3152-3157.

Wedeen, V.J., et al., 2005. Mapping complex tissue architecture with diffusion spectrum magnetic resonance imaging. Magnetic Resonance in Medicine. 54**,** 1377-1386.

Wee, C.Y., et al., 2017. Neonatal Neural Networks Predict Children Behavioral Profiles Later in Life. Human Brain Mapping. 38**,** 1362-1373.

Whitfield-Gabrieli, S., Ford, J.M., 2012. Default Mode Network Activity and Connectivity in Psychopathology. Annual Review of Clinical Psychology, Vol 8. 8**,** 49-+.

Wildgruber, D., et al., 2005. Identification of emotional intonation evaluated by fMRI. Neuroimage. 24**,** 1233-1241.

Williams, J., Lee, K.J., Anderson, P.J., 2010. Prevalence of motor-skill impairment in preterm children who do not develop cerebral palsy: a systematic review. Dev Med Child Neurol. 52**,** 232-7.

Wimberger, D.M., et al., 1995. Identification of "premyelination" by diffusion-weighted MRI. J Comput Assist Tomogr. 19, 28-33.

Witt, A., et al., 2014. Emotional and effortful control abilities in 42-month-old very preterm and full-term children. Early Hum Dev. 90, 565-9.

Woodward, L.J., et al., 2005. Object working memory deficits predicted by early brain injury and development in the preterm infant. Brain. 128, 2578-2587.

Woodward, L.J., et al., 2006. Neonatal MRI to predict neurodevelopmental outcomes in preterm infants. N Engl J Med. 355, 685-94.

Wu, F.X., et al., 2018. Biomolecular Networks for Complex Diseases. Complexity.

Yap, P.T., et al., 2011. Development Trends of White Matter Connectivity in the First Years of Life. Plos One. 6.

Yoshida, S., et al., 2013. Diffusion tensor imaging of normal brain development. Pediatr Radiol. 43, 15-27.

Young, J.M., et al., 2019. White matter microstructural differences identified using multi-shell diffusion imaging in six-year-old children born very preterm. Neuroimage Clin. 23, 101855.

Yu, Q.W., et al., 2016. Structural Development of Human Fetal and Preterm Brain Cortical Plate Based on Population-Averaged Templates. Cerebral Cortex. 26, 4381-4391.

Yung, A., et al., 2007. White matter volume and anisotropy in preterm children: A pilot study of neurocognitive correlates. Pediatric Research. 61, 732-736.

Zalesky, A., Fornito, A., Bullmore, E.T., 2010. Network-based statistic: Identifying differences in brain networks. Neuroimage. 53, 1197-1207.

Zamorano, A.M., et al., 2017. Insula-Based Networks in Professional Musicians: evidence for Increased Functional Connectivity during Resting State fMRI. Human Brain Mapping. 38, 4834-4849.

Zanin, E., et al., 2011. White matter maturation of normal human fetal brain. An in vivo diffusion tensor tractography study. Brain and Behavior. 1, 95-108.

Zatorre, R.J., Peretz, I., Penhune, V., 2009. Neuroscience and Music ("Neuromusic") III: disorders and plasticity. . Annals of the New York Academy of Sciences. 1169, 1-2.

Zatorre, R.J., Fields, R.D., Johansen-Berg, H., 2012. Plasticity in gray and white: neuroimaging changes in brain structure during learning. Nature Neuroscience. 15, 528-536.

Zhai, G., et al., 2003. Comparisons of regional white matter diffusion in healthy neonates and adults performed with a 3.0-T head-only MR imaging unit. Radiology. 229, 673-81.

Zhang, H., et al., 2011. Axon diameter mapping in the presence of orientation dispersion with diffusion MRI. Neuroimage. 56, 1301-1315.

Zhang, H., et al., 2012. NODDI: Practical in vivo neurite orientation dispersion and density imaging of the human brain. Neuroimage. 61, 1000-1016.

Zhang, L.I., Bao, S.W., Merzenich, M.M., 2002. Disruption of primary auditory cortex by synchronous auditory inputs during a critical period. Proceedings of the National Academy of Sciences of the United States of America. 99, 2309-2314.

Zhao, T.D., et al., 2019. Structural network maturation of the preterm human brain. Neuroimage. 185, 699-710.

Zubiaurre-Elorza, L., et al., 2012. Cortical Thickness and Behavior Abnormalities in Children Born Preterm. Plos One. 7.

6. ARTICLES

Study 1

Preterm birth leads to impaired rich-club organization and fronto paralimbic/limbic structural connectivity in newborns

Preterm birth leads to impaired rich-club organization and fronto-paralimbic/limbic structural connectivity in newborns

Joana Sa de Almeida[1]; Djalel-Eddine Meskaldji[1,2]; Serafeim Loukas[1,3]; Lara Lordier[1]; Laura Gui[4]; François Lazeyras[4]; Petra S. Hüppi[1]*

[1] Division of Development and Growth, Department of Woman, Child and Adolescent, University Hospitals of Geneva, Geneva, Switzerland

[2] Institute of Mathematics, Ecole Polytechnique Fédérale de Lausanne, Switzerland

[3] Institute of Bioengineering, Ecole Polytechnique Fédérale de Lausanne, Lausanne, Switzerland

[4] Department of Radiology and Medical Informatics; Center of BioMedical Imaging (CIBM), University of Geneva, Geneva, Switzerland

*Corresponding author address:

Hôpitaux Universitaires de Genève; Département de la femme, de l'enfant et de l'adolescent, Service de développement et croissance, Hôpital des enfants, Rue Willy-Donzé 6, CH-1211 Genève 14, Suisse; petra.huppi@hcuge.ch

Abstract

Prematurity disrupts brain development during a critical period of brain growth and organization and is known to be associated with an increased risk of neurodevelopmental impairments. Investigating whole-brain structural connectivity alterations accompanying preterm birth may provide a better comprehension of the neurobiological mechanisms related to the later neurocognitive deficits observed in this population.

Using a connectome approach, we aimed to study the impact of prematurity on neonatal whole-brain structural network organization at term-equivalent age. In this cohort study, twenty-four very preterm infants at term-equivalent age (VPT-TEA) and fourteen full-term (FT) newborns underwent a brain MRI exam at term age, comprising T2-weighted imaging and diffusion MRI, used to reconstruct brain connectomes by applying probabilistic constrained spherical deconvolution whole-brain tractography. The topological properties of brain networks were quantified through a graph-theoretical approach. Furthermore, edge-wise connectivity strength was compared between groups.

Overall, VPT-TEA infants' brain networks evidenced increased segregation and decreased integration capacity, revealed by an increased clustering coefficient, increased modularity, increased characteristic path length, decreased global efficiency and diminished rich-club coefficient. Furthermore, in comparison to FT, VPT-TEA infants had decreased connectivity strength in various cortico-cortical, cortico-subcortical and intra-subcortical networks, the majority of them being intra-hemispheric fronto-paralimbic and fronto-limbic. Inter-hemispheric connectivity was also decreased in VPT-TEA infants, namely through connections linking to the left precuneus or left dorsal cingulate gyrus – two regions that were found to be hubs in FT but not in VPT-TEA infants. Moreover, posterior regions from Default-Mode-Network (DMN), namely precuneus and posterior cingulate gyrus, had decreased structural connectivity in VPT-TEA group.

Our finding that VPT-TEA infants' brain networks displayed increased modularity, weakened rich-club connectivity and diminished global efficiency compared to FT infants suggests a delayed transition from a local architecture, focused on short-range connections, to a more distributed architecture with efficient long-range connections in those infants. The disruption of connectivity in fronto-paralimbic/limbic and posterior DMN regions might underlie the behavioral and social cognition difficulties previously reported in the preterm population.

100

Keywords

Diffusion magnetic resonance imaging, connectomics, graph-theory, human brain development, preterm birth

Abbreviations

CSD = constrained spherical deconvolution; DCG = dorsal cingulate gyrus; DGM = deep grey-matter; dMRI = Diffusion magnetic resonance imaging; FA = fractional anisotropy; fMRI = functional magnetic resonance imaging; FT = full-term; GM = grey-matter; OFC = orbito-frontal cortex; PCG = posterior cingulate gyrus; PCUN = precuneus; RC = rich-club; SC = streamline counting; SW = small-world index, TEA = term-equivalent age; TPO = temporal pole; VPT-TEA = very preterm infants at term-equivalent age; WM = white matter

1. Introduction

Dynamic macrostructural and microstructural changes take place from the mid-fetal stage to birth. Indeed, the third trimester of gestation is characterized by rapid brain growth, with grey-matter (GM) and white matter (WM) volume expansion driven by increasing density, diameter and myelination of both dendritic and axonal structures (Dubois et al., 2008; Innocenti and Price, 2005; Kiss et al., 2014a; Mills et al., 2016; Nickel and Gu, 2018; Nossin-Manor et al., 2013), as well as the establishment of functional thalamocortical and other long-range brain connections (Batalle et al., 2017; Kostovic and Jovanov-Milosevic, 2006; Kostovic and Judas, 2010b; Kostovic et al., 2014; van den Heuvel et al., 2015).

Preterm birth disrupts brain maturation during a critical period of fetal brain growth (Kiss et al., 2014a; Radley and Morrison, 2005). It impacts typical brain developmental processes, as a result of complex environmental factors (Simmons et al., 2010), leading consequently to structural brain alterations. These alterations might be at the origin of the later neurodevelopmental impairments observed in preterm infants, comprising motor, cognitive, behavioral and socio-emotional deficits (Anjari et al., 2007; Ball et al., 2012; Cismaru et al., 2016; Huppi et al., 1998a; Inder et al., 2005; Montagna and Nosarti, 2016; Thompson et al., 2007; Thompson et al., 2013).

Magnetic resonance imaging (MRI) has been employed to study the early brain developmental anomalies observed in preterm infants. Such anomalies have been shown to be associated with specific neuropsychological deficits after preterm birth and include regional cortical and subcortical volumetric changes (Ball et al., 2017; Cismaru et al., 2016; Huppi and

Dubois, 2006; Ment et al., 2009; Nosarti, 2013; Padilla et al., 2015; Peterson et al., 2000), as well as alterations of brain WM networks and their microstructural characteristics (Ball et al., 2014; Batalle et al., 2017; Fischi-Gomez et al., 2015; Mullen et al., 2011; Pannek et al., 2018; Pecheva et al., 2018; Rogers et al., 2012; Sa de Almeida et al., 2019).

Previous studies have focused mostly on regional brain structural differences between very preterm infants at term-equivalent age (VPT-TEA) and full-term born infants (FT). To date, there is still limited knowledge regarding whole-brain structural alterations at term-equivalent age (TEA) following preterm birth.

The macroscopic whole-brain structural network organization can be investigated using a connectomic analysis, where brain networks are derived by whole-brain tractography, through reconstruction of WM connections between brain regions using brain diffusion MRI (dMRI). In the resulting connectome, brain regions are represented by nodes and the structural connections between brain regions by edges. The edge weights can be either the number of streamlines connecting two regions (SC) or can be defined by measures of microstructural organization, such as fractional anisotropy (FA).

Graph-based measures allow us to study brain network topology, revealing meaningful information regarding small-worldness, integration, segregation, modular organization, the presence of hubs and rich-club connectivity (Bullmore and Sporns, 2009; He and Evans, 2010; Meunier et al., 2010; van den Heuvel and Sporns, 2013). These network measures have been shown to be reliable biomarkers for discriminating normal and abnormal brain networks (Lo et al., 2010; Owen et al., 2013; Shu et al., 2011). Moreover, alterations in structural connectivity have been related to a range of developmental disorders (Crossley et al., 2015; van den Heuvel et al., 2013).

To date, only three studies have used a connectomic analysis to reconstruct whole-brain networks of VPT-TEA and FT infants and compare their topological organization at term age using graph-analysis. In particular, Ball et al., using unweighted brain connectomes, have focused mainly on rich-club connectivity and have found that, although it was intact following preterm birth, VPT-TEA had a greater proportion of direct cortico-cortical connections within the rich-club than FT infants, what was interpreted as a measure of altered deep grey-matter (DGM) connectivity. In addition, brain networks of VPT-TEA infants evidenced increased local connectivity between peripheral nodes, correlating with increased network segregation (Ball et al., 2014). Lee et al. and Brown et al., using weighted brain connectomes, have also addressed this question using graph theoretical measures (Brown et al., 2014; Lee et al., 2019). Lee et al. have found a decreased network global efficiency in VPT-TEA infants in comparison

to FT newborns (Lee et al., 2019). On the other hand, Brown et al. have found an increased global network efficiency and modularity in VPT-TEA infants. However, they have compared their own cohort of VPT-TEA infants to an external cohort of FT infants from a previously published study (Yap et al., 2011) and have stated that their findings were resulting from differences in image acquisition and connectome construction pipelines (Brown et al., 2014). Therefore, literature is still not completely clear regarding this matter and lacking a more complete graph-based analysis between the brain networks of VPT-TEA and FT infants. Additionally, there are no reports regarding hub differences and there is only one study evaluating whole-brain edge-wise connectivity strength differences between these groups at term age (Pannek et al., 2013). Further information on this topic would thus be of great importance for understanding the impact of preterm birth on global brain network organization and connectivity at TEA.

In this study, we constructed weighted structural connectomes of a cohort of VPT-TEA and FT infants using dMRI whole-brain probabilistic constrained spherical deconvolution (CSD)-based tractography. We aimed to study whole-brain network topological alterations related to prematurity by employing graph-based analysis on weighted structural networks and comparison of brain network hubs and edge-wise connectivity differences between these two groups of infants. Capitalizing on the latest methodological advances, we intended to contribute to the described gap in the literature regarding this subject.

We hypothesize that, in comparison to FT neonates, VPT-TEA infants' structural connectomes will reveal macroscale brain network differences related to the disruption of early brain development by preterm birth.

2. Materials and Methods

2.1. Subjects

A cohort of thirty-nine very preterm (VPT) infants (gestational age (GA) at birth <32 weeks) and twenty-four FT infants was recruited at the neonatal unit of the University Hospitals of Geneva (HUG), Switzerland, from 2013 to 2016, in order to evaluate the impact of prematurity on brain development and clinical neurodevelopment. The study was approved by the local Research Ethics Committee and written parental consent was obtained before the infants' participation to the study. All subjects underwent an MRI examination at TEA (37-42 weeks GA). Infants whose MRI protocol acquisition was incomplete, not comprising a T2-

weighted image and/or dMRI sequence, or that presented major focal brain lesions were excluded from the analysis.

The final sample used in this case-control study was of 24 VPT and 14 FT infants. As expected, VPT infants' GA at birth, weight, height and head circumference at birth, as well as APGAR scores were significantly inferior to those of FT newborns. Additionally, presence of bronchopulmonary dysplasia was significantly superior in VPT infants. No significant differences between VPT and FT groups were found in the following demographic and perinatal variables: sex, intrauterine growth restriction, intraventricular hemorrhage (grade I-IV), neonatal asphyxia, blood culture positive sepsis, gestational age at MRI and socio-economic parental status (Largo et al., 1989) (Table 1).

Table 1

Clinical characteristics of the infants

Clinical Characteristics	FT n=14	VPT-TEA n=24	p-value* FT vs VPT-TEA
Gestational age at birth, weeks, mean (SD)	39.2 ($\pm$1.3)	28.3 ($\pm$2.5)	0.0001*
Gestational age at birth, weeks, range	$37^{2/7} - 41^{5/7}$	$23^{6/7} - 32^{0/7}$	
Sex: female (%)/male (%)	6(15.8)/8(21.1)	10(26.3)/14(36.8)	0.943
Birth weight, gram, mean (SD)	3223.6 ($\pm$440.5)	1077.5 ($\pm$328.7)	0.0001*
Birth height, centimetre, mean (SD)	49.8 ($\pm$1.7)	36.2 ($\pm$3.6)	0.0001*
Birth head circumference (cm), mean (SD)	34.3 ($\pm$1.1)	25.8 ($\pm$2.6)	0.0001*
APGAR score, 1 min (SD)	8.9 ($\pm$0.5)	4.8 ($\pm$3.1)	0.0001*
APGAR score, 5 min (SD)	9.5 ($\pm$0.9)	7.1 ($\pm$1.9)	0.0001*
Intrauterine Growth Restriction, n (%)	1 (2.6)	3 (7.9)	0.604
Bronchopulmonary dysplasia (%)	0 (0.0)	7 (18.4)	0.025*
Intraventricular Hemorrhage grade I-II (%)	0 (0.0)	5 (13.2)	0.067
Intraventricular Hemorrhage grade III-IV (%)	0 (0.0)	0 (0.0)	
Neonatal asphyxia, n (%)	0 (0.0)	0 (0.0)	
Blood culture positive Sepsis (%)	0 (0.0)	5 (13.2)	0.067
Gestational age at MRI scan, weeks, mean (SD)	39.6 ($\pm$1.2)	40.3 ($\pm$0.6)	0.073
Gestational age at MRI scan, weeks, range	$37^{2/7} - 42^{0/7}$	$39^{1/7} - 41^{1/7}$	
Socio-economic score (range 2-12), mean (SD)	4.10 ($\pm$2.5)	5.67 ($\pm$3.1)	0.169

* Group-characteristics were compared using independent samples T-test for continuous variables and chi-squared test for categorical variables.

2.2. MRI acquisition

All infants were scanned after receiving breast or formula feeding, during natural sleep (no sedation used) and using a vacuum mattress for immobilization. MR-compatible headphones were used (MR confon, Magdeburg, Germany) to protect infants from the

scanner's noise. All infants were monitored for heart rate and oxygen saturation during the entire scanning time.

MRI acquisition was performed on 3.0T Siemens MR scanners (Siemens, Erlangen, Germany): Siemens TIM Trio with a 32-channel head coil and Siemens Prisma with a 64-channel head coil. Chi-squared test revealed no significant difference regarding the distribution of scanner/coils between groups, $\chi^2(1) = 1.057$, $p = 0.304$ (TIMTrio-32channel: FT=11, VPT=15; Prisma-64channel: FT=3, VPT=9).

T2-weighted images were acquired using the following parameters: 113 coronal slices, TR= 4990ms, TE=151ms, flip angle=150°, matrix size=256x164; voxel size=0.4x0.4x1.2mm^3, total scan time of 6:01 minutes.

dMRI was acquired with a single-shot spin echo echo-planar imaging (SE-EPI) Stejksal-Tanner sequence (TE=84ms, TR= 7400ms, acquisition matrix 128x128 mm, reconstruction matrix 128x128mm, 60 slices, voxel size 2x2x2mm^3). Images were acquired in the axial plane, in anterior-posterior (AP) phase encoding (PE) direction, with diffusion gradients applied in 30 non-collinear directions with a b-value of 1000 s/mm^2 and one non-diffusion weighted image (b=0), with a total scan time of 4:12 minutes.

dMRI motion metrics estimates per subject, including percentage of outliers, as well as relative and absolute between volumes motion, were calculated using EDDY QC tools from diffusion toolbox of the FMRIB Software Library, FSL v6.0.3, https://fsl.fmrib.ox.ac.uk/fsl/fslwiki/ (Behrens et al., 2003; Smith et al., 2004). No statistically significant differences between groups were found for any of the motion metrics (Table 2, Supplementary Figure S1).

Table 2

Group-wise comparison of dMRI motion metrics

Motion metrics	FT n=14	VPT-TEA n=24	p-value* FT vs VPT-TEA
Number of outliers, mean percentage (SD)	3.24 (±1.68)	3.05 (±2.33)	0.789
Number of outliers, percentage, range	0.87 – 6.22	0.22 – 9.67	
Absolute between volumes motion, mm (SD)	1.40 (0.46)	1.39 (0.49)	0.950
Absolute between volumes motion, mm, range	0.60 – 2.30	0.64 – 2.41	
Relative between volumes motion, mm (SD)	0.66 (±0.30)	0.76 (±0.38)	0.375
Relative between volumes motion, mm, range	0.16 – 1.21	0.25 – 1.88	

* Motion metrics were compared between groups using independent samples T-test

2.3. Pre-processing

T2-weighted brain volumes were bias-corrected, skull-striped and tissue-segmented into WM, GM, DGM, cerebrospinal fluid (CSF) and cerebellum using an automatic neonatal-specific segmentation algorithm (Gui et al., 2012).

dMRI data were preprocessed using the diffusion toolbox of the FMRIB Software Library, FSL v5.0.10, https://fsl.fmrib.ox.ac.uk/fsl/fslwiki/ (Behrens et al., 2003; Smith et al., 2004). Brain extraction was performed using "BET". Eddy current-induced distortions and gross subject movement were corrected using the FSL "EDDY" tool (Andersson and Sotiropoulos, 2016) optimized for neonatal dMRI data. This command is part of the neonatal dMRI automated pipeline from the developing Human Connectome Project and corrects distortions caused by motion-induced signal dropout and intra-volume subject movement (Andersson et al., 2016; Andersson et al., 2017; Bastiani et al., 2019).

2.4. Network nodes definition: brain parcellation

Parcellation into cortical and subcortical regions was based on the UNC neonatal brain atlas (Shi et al., 2011), consisting of 90 regions, which represented the nodes used in the network analysis.

The T2 UNC neonatal brain atlas (Shi et al., 2011) was registered to each subject's T2-weighted structural image by means of a non-linear registration using the advanced normalization tools (ANTs) package (Avants et al., 2011) adapted for neonatal data (Bastiani et al., 2018). Subject's dMRI data was registered to the T2-weighted structural image by means of FSL FLIRT (Jenkinson et al., 2002). All the registrations were individually visually inspected in order to guarantee the quality of the process.

We then combined the linear transformation (subject's dMRI to T2 structural) with the non-linear warp registration (subject's T2 structural to T2 atlas) to obtain the transformations needed to bring the T2 atlas to subjects' dMRI space. Therefore, the anatomical regions (labels) from the UNC atlas were propagated to each subject's dMRI space by applying this combined transformation using nearest neighbour interpolation, and used as nodes for network analysis.

2.5. Network edges definition: tractography

In order to reconstruct WM fibers to define network edges, whole-brain tractography was performed in native diffusion space using probabilistic single-shell, single tissue constrained spherical deconvolution (SSST-CSD) tracking. It was performed by means of

MRtrix3 (Tournier et al., 2019), using iFOD2, anatomically constrained tractography (ACT) and backtrack re-tracking algorithms, with streamlines seeded dynamically throughout the WM, producing 100 million streamlines per subject. The reconstructed data was then further processed using spherical-deconvolution informed filtering of tractograms (SIFT) algorithm, producing 10 million streamlines for each subject, which were used as brain network edges.

2.6. Network construction and global network analysis

In order to construct the individual WM structural brain networks, the reconstructed set of streamlines were combined with each subject's anatomical parcellation. This resulted in a 90x90 interregional connectivity matrix, where each anatomical region is considered as a node (Supplementary Table S1), and each pair of nodes is connected by an edge, representing the strength of connectivity between the corresponding regions. Self-connections were excluded. For each pair of nodes/regions, we computed the number of filtered streamlines (SC) connecting both regions, as well as the mean fractional anisotropy (FA) along streamlines connecting the regions. In order to remove spurious connections in the SC-weighted (SCw) connectomes, all connections where FA was inferior or equal to 0.1 were considered as noise floor and therefore removed, according to (Jones and Basser, 2004). This threshold was chosen due to the low anisotropy of the preterm infant's brain and has been applied in previous studies performing structural network analysis in the preterm and neonatal brain (Brown et al., 2014; van den Heuvel et al., 2015; Zhao et al., 2019).

For analysing results from graph network measures, first, for each subject, network weights were normalized by the maximum weight value of that network, in order to normalise all edge weights per subject. The edge weights in SCw networks will represent therefore relative connectivity.

Graph theoretical analysis of SCw connective matrices was performed by using the Brain Connectivity Toolbox (BCT) for Matlab (Rubinov and Sporns, 2010). The metrics evaluated included:

1. Density (d): computes the observed connections as a percentage of all possible connections.
2. Total strength (S): computed as the sum of the strength (sum of weights) across all the nodes in the network.
3. Characteristic path length (L): computed as the average of shortest path lengths between all pairs of nodes in the network (Watts and Strogatz, 1998).

4. Global efficiency (GEff): computed as the average inverse of the shortest path lengths (Rubinov and Sporns, 2010).

5. Average clustering coefficient (C): clustering coefficient was first computed as the fraction of a node's neighbors that are also connected to each other. These fractions at each node were averaged over all the nodes of the network to give the overall network C (Watts and Strogatz, 1998).

6. Local efficiency (LEff): computed as the average of the global efficiency of each node's neighborhood sub-graph, averaged over all the nodes of the network (Latora and Marchiori, 2001; Wu et al., 2018).

7. Small-world index (SW): computed as the ratio of the normalized C and the normalized L (which were obtained as the ratio between the metrics derived from each subject network and its matched randomized network metrics).

8. Modularity index (Q): Louvain algorithm for community detection was used to identify modules in the network (Blondel et al., 2008). Q was calculated by computing the ratio between the number of connections (sum of edge weights) within the modules and the number of connections exiting the same modules, and taking the maximum of these ratios across all possible modules (Newman, 2004).

9. Rich-club (RC) coefficient ($\phi(\kappa)$): computed as proposed by Opsahl et al. for weighted networks (Opsahl et al., 2008). Given a nodal strength κ, we identified the subset of nodes $E_{>\kappa}$ with a nodal strength $> \kappa$. The weighted $\phi(\kappa)$ was computed as the ratio between the sum of weights of the connections between the nodes present in $E_{>\kappa}$, and the maximal possible weighted connectedness within $E_{>\kappa}$. The chosen κ corresponded to the 9th highest nodal strength per subject, in order to include the top 10% nodes.

In order to remove bias related to the fraction of measure's value that may arrive by chance, we generated 10 matched random equivalent networks for each subject (where each edge was rewired 1000 times), preserving the same number of nodes and degree distributions as in the SCw networks. The network measures of each of the 10 random networks were then averaged per subject and used for normalisation.

Normalized (calibrated) C (nC), LEff (nLEff), L (nL), GEff (nGEff) and Q (nQ) were estimated as the ratio between the metrics derived from each subject network and its matched randomized network metrics. The normalized $\phi(\kappa)$ (ϕ_{norm}) was obtaining by multiplying $\phi(\kappa)$ by the ratio between the number of nodes included into the RC pool $E>\kappa$ (varying as a function of RC strength κ) and the total number of network nodes. This computation is

motivated by the fact that $\phi(\kappa)$ is inversely proportional to the number of nodes included in the RC pool (Karolis et al., 2016).

Group-average weighted structural connectomes and matched randomized network structural connectomes were computed for both VPT-TEA and FT infants' groups. $\phi(\kappa)$ was computed as a function of κ per group for both networks. $\phi(\kappa)_{norm}$ was computed has the ratio between the $\phi(\kappa)$, for the different levels of κ, of the group-average weighted structural connectome and the $\phi(\kappa)$, for the same levels of κ, of the matched randomized network structural connectomes.

For the detection of hubs within each group's brain networks, group-average binary structural connectomes were computed for both VPT-TEA and FT infants' groups, by including the structural connections that were present in at least 70% of the total group. We used the nodal degree (the number of connections of a node) as a measure to define the hubs. Using BCT, nodal degree was calculated for all nodes of each binary group network. Hubs were identified for each group as the nodes with a nodal degree superior to the average nodal degree plus 1 standard deviation.

2.7. Edge-wise connectivity strength analysis

To evaluate edge-wise connectivity strength differences between groups based on SCw structural networks, we performed t-tests at the connection level with false discovery rate (FDR) control (significance value of 0.05 and 100.000 random permutations). To this end, we used the NBS toolbox implemented in Matlab by Zalesky et al. (Benjamini and Hochberg, 1995; Zalesky et al., 2010).

Connectomic data was visualized using the Circos software (Krzywinski et al., 2009). Statistically significantly different connections between groups were categorized into: (1) cortico-cortical; (2) cortico-subcortical and (3) subcortico-subcortical.

2.8. Statistical analysis

Neonatal and demographic data, categorical variables (sex, intrauterine growth restriction, bronchopulmonary dysplasia, intraventricular hemorrhage (grade I-IV), blood culture positive sepsis and neonatal asphyxia) were analysed using chi-squared test, whereas continuous variables were compared using independent samples t-test, with group as independent variable and the following dependent variables: GA at birth, GA at MRI, birth

weight, birth height, birth head circumference, APGAR score at 1 and 5 minutes after birth and socio-economic parental status.

dMRI motion metrics were compared between groups using independent samples t-test, with group as independent variable and the following dependent variables: percentage of number of outliers, absolute between volumes motion, relative between volumes motion.

Group-wise differences in network graph-theoretical metrics and number of thalamic connections were investigated with one-way between-subjects ANCOVA, controlling for GA at MRI and sex, using IBM SPSS Statistics version 25 (IBM Corp., Armonk, N.Y., USA). One-way between-subjects MANCOVA, controlling for GA at MRI and sex, was performed first, comprising all graph-theoretical metrics analysed, namely network strength, network density, nC, nLEff, nL, nGEff, nQ and ϕ_{norm}, to correct for the multiplicity of global tests.

Independent-samples t-test was used to compare Q from SCw networks to Q from its matched random networks.

P-values that resulted from edge-wise comparison of connectivity matrices statistics were corrected using Benjamini-Hochberg FDR control procedure at level alpha of 5%, implemented in the NBS toolbox (Benjamini and Hochberg, 1995; Zalesky et al., 2010).

2.9.   Data and code availability

All data were acquired in the context of the research project approved by the ethical committee in 2011. The patient consent form did not include any clause for reuse or share of data. It stated explicitly that all data (clinic, biologic and imaging) would not be used with any other aim apart from the present research study and would not be shared with third parties.

Software and code used in this study are publicly available as part of FSL v5.0.10 (https://fsl.fmrib.ox.ac.uk/fsl/fslwiki/), MRtrix3 (Tournier et al., 2019), ANTs (Avants et al., 2011), BCT (Rubinov and Sporns, 2010) and NBS (Benjamini and Hochberg, 1995; Zalesky et al., 2010) software packages. dMRI data were pre-processed using EDDY command adapted for neonatal motion, which is part from the neonatal dMRI automated pipeline from developing Human Connectome Project (dHCP, http://www.developingconnectome.org), and can   be   found   at   this   link: https://git.fmrib.ox.ac.uk/matteob/dHCP_neo_dMRI_pipeline_release (Bastiani et al. 2019).

3. Results

3.1. Preterm neonatal structural brain network topological organization

3.1.1. Integration, segregation and small-world properties

Structural network topology was compared at TEA between VPT-TEA infants and FT newborns using metrics derived from graph-analysis. One-way MANCOVA multivariate test yielded a significant difference between the group contrasts, [Wilks'λ = 0.362, F(8,26)=4.182, p=0.005], when considering all graph metrics. Given the significance of the overall test, the univariate main effects of each metric were examined.

No significant differences were found in mean network density (p=0.135) or total network strength (p=0.892) between FT newborns and VPT-TEA infants' SCw networks (Table 3).

We explored the differences in brain networks integration capacity between FT and VPT-TEA infants using characteristic path length and global efficiency. In comparison to FT newborns, VPT-TEA infants showed a significantly higher normalized characteristic path length (p=0.049) and significantly diminished normalized global efficiency (p=0.045) (Fig. 1A, 1B, Table 3). Although a similar tendency was observed in networks before normalisation with matched random networks, the differences were not statistically significant, p>0.05 (Supplementary Table S2).

Network segregation was measured by means of average cluster coefficient, local efficiency and modularity. In comparison to FT newborns, VPT-TEA infants showed a significantly higher normalized average clustering coefficient, (p=0.001) and significantly higher normalized local efficiency (Fig. 1C, 1D, Table 3). A similar tendency was observed in networks before normalisation with matched random networks, but the differences were not statistically significant, p>0.05 (Supplementary Table S2).

Both FT and VPT-TEA infants presented a modular architecture in their brain networks. This is reflected by Q > 0.3 in both groups (Supplementary Table S2), which is indicative of a non-random modular structure (Newman and Girvan, 2004). VPT-TEA infants had a significantly higher nQ (p=0.006) and Q (p=0.007) compared to FT infants (Fig. 1D, Table 3, Supplementary Table S2).

The balance between segregation and integration was quantified by the small-world network topology. Both FT and VPT-TEA infants brain networks had a SW>1, without statistically significant differences between groups (Table 3), proving the small-world organization of the neonatal brain in both groups.
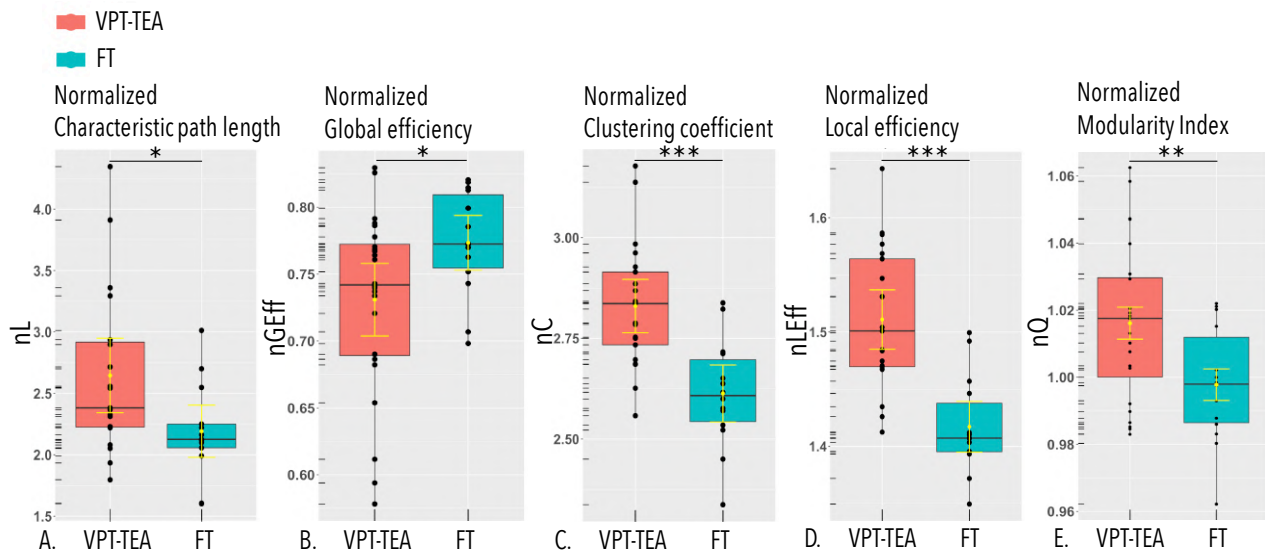
Fig. 1. **Global network measures differences between VPT-TEA and FT infants.** Boxplots of global network measures in VPT-TEA (in red) and FT infants (in green): normalized characteristic path length, nL (A), normalized global efficiency, nGEff (B), normalized cluster coefficient, nC (C), normalized local efficiency, nLEff (D), and normalized modularity index, nQ (E). One-way ANCOVA, controlling for GA at MRI and sex, was performed to determine differences between groups. Mean and standard deviation are illustrated in yellow on each boxplot. Lines indicate significant differences between groups ($*p < 0.05$, $**p < 0.01$, $***p < 0.001$).

Table 3

Global network measures comparison between groups.

Global Network measures	VPT-TEA	FT	p-value
d	0.435 (±0.031)	0.452 (±0.026)	0.135
S	1.158 (±0.231)	1.170 (±0.251)	0.892
nL	2.657 (±0.675)	2.175 (±0.391)	**0.049**
nGEff	0.701 (±0.068)	0.775 (±0.039)	**0.045**
nC	2.827 (±0.155)	2.618 (±0.135)	**0.001**
nLEff	1.522 (±0.076)	1.416 (±0.042)	**0.0001**
SW	1.117 (±0.232)	1.157 (±0.115)	0.677
nQ	1.017 (±0.023)	0.998 (±0.018)	**0.006**

One-way ANCOVA, controlling for GA at MRI and sex, was performed to determine differences between groups. Numbers in bold indicate significant results between groups ($p<0.05$).

3.1.2. Hubs and Rich-Club organization

Both FT and VPT-TEA infants' structural brain networks revealed a right-tailed distribution of nodal degree, suggestive of the existence of densely connected nodes, hubs (Fig. 2A, 2B).

We found 9 hubs in FT infants with an average nodal degree of 51.67, whereas VPT-TEA infants presented a higher number of hubs, namely 16, but with an inferior average number of connections (average nodal degree of 45.38). The hub regions in both groups consisted of mainly subcortical (thalamus, caudate and putamen) and limbic (dorsal cingulate gyrus, insula and hippocampus) nodes. Noticeably, FT newborns had a parietal hub (left precuneus) not present in VPT-TEA infants, whereas VPT-TEA infants had temporal hubs not present in FT newborns (bilateral superior temporal gyrus and left Heschl gyrus), as well as both amygdalae as hubs (Fig. 3, Supplementary Table S3). The following hubs were discovered in VPT-TEA infants: bilateral thalamus, bilateral caudate, bilateral putamen, bilateral hippocampus, bilateral insula, bilateral amygdala, right dorsal cingulate gyrus, left Heschl gyrus and bilateral superior temporal gyrus. The following hubs were present in FT newborns: bilateral thalamus, left caudate, right putamen, right insula, right hippocampus, bilateral dorsal cingulate gyrus and left precuneus (Supplementary Table S3).

For both groups, left and right thalamus were the two regions with highest nodal degree (Supplementary Table S3). When comparing the number of connections of these two regions, combined, between VPT-TEA and FT infants, the VPT-TEA showed a statistically significantly lower number of connections of the left and right thalamus in comparison to FT infants (p=0.025) (Fig. 2C).

Normalized rich-club curves, representative of both FT and VPT-TEA groups, show an increasing ϕ_{norm} with the increase of κ for both groups. This increase is superior for FT infants, in comparison to VPT-TEA infants, at the strongest network nodes (from κ=45 to κ=60) (Fig. 2E). Both the FT and VPT-TEA infants' brain networks displayed RC organization, with $\phi_{norm}(\kappa) > 1$ for $\kappa \geq 9$. Considering the top 10% strongest network nodes, FT infants presented both a statistically significantly higher ϕ_{norm} (p=0.007) and ϕ (p=0.003) in comparison to VPT-TEA infants (Fig. 2D, Supplementary Table S2).
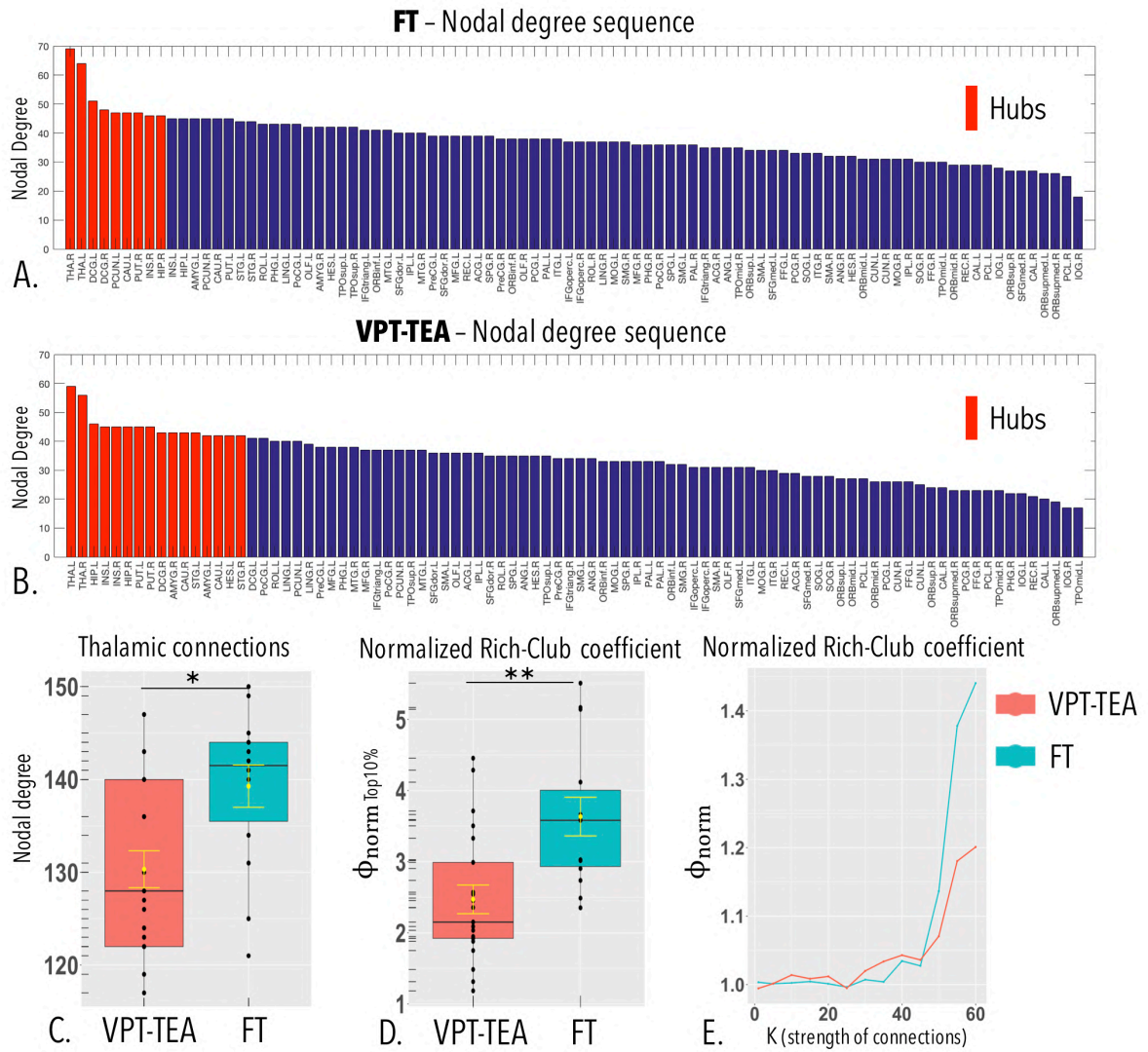
Fig. 2. **Hubs, thalamic connectivity and rich-club organization.** A and B: Structural brain hubs of FT (A) and VPT-TEA (B) infants. Hubs (in red) were defined as nodes whose degree was ≥ 1 standard deviation above the average nodal degree. C and D: Boxplots of mean thalamic connections (C) and normalized rich-club coefficient of the top 10% strongest network nodes ($\phi_{norm\ Top\ 10\%}$) (D) in VPT-TEA and FT infants. One-way ANCOVA, controlling for GA at MRI and sex, was performed to determine differences between groups. Mean and standard deviation are illustrated in yellow on each boxplot. Lines indicate statistically significant differences between groups (*p < 0.05, **p < 0.01). E: Normalized rich-club curves (ϕ_{norm}) of FT and VPT-TEA infant's representative weighted networks.

3.2. Prematurity and the connectivity strength of structural networks

In comparison to FT, the VPT-TEA infants brain networks presented 90 connections (out of the total 4005 unique possible connections) with a statistically significant decreased structural connectivity strength (p<0.05, FDR corrected). These included both intra-hemispheric (88%, out of which 51% in the left and 37% in right hemisphere) and inter-hemispheric (12%) connections (Fig. 3A). A complete description of all connections with decreased structural connectivity strength in VPT-TEA can be found in Supplementary Table S4.

In both cortico-cortical and cortico-subcortical connections, the cortical nodes participating in the connections with decreased connectivity strength in VPT-TEA infants belonged mostly to the frontal cortex. In cortico-cortical connections, these were followed by temporal, limbic, parietal and occipital cortices, and in cortico-subcortical connections, by the temporal, occipital and limbic cortices (Fig. 3B).

Among the fronto-cortical and fronto-subcortical connections with decreased connectivity strength in VPT-TEA infants, the orbito-frontal cortex (OFC) was the frontal node the most frequently involved (participating in 44% of all fronto-cortical/subcortical connections) (Supplementary Table S6).

Fronto-temporal connections were the most frequently affected, not only among fronto-cortical, but among all cortico-cortical connections (Fig. 3C, Supplementary Table S5). Out of those, 93% were connecting to the temporal pole (TPO). Indeed, connections from the OFC to the TPO were the most frequent (50%) among all frontal-temporal connections with decreased connectivity strength in VPT-TEA, as well as among all fronto-cortical connections (almost 20% of these) (Supplementary Tables S4 and S5). Noticeably, the TPO was the region most frequently involved in all connections with decreased connectivity strength in VPT-TEA infants, followed by the OFC (Supplementary Table S7).

The fronto-limbic connections were the second most affected cortico-cortical connections after fronto-temporal connections. The cingulate gyrus was the limbic region most frequently present, not only in the affected fronto-limbic connections, but among all limbic connections with decreased connectivity strength in VPT-TEA infants, in particular the posterior cingulate gyrus (PCG) (Fig. 3C, Supplementary Tables S4, S5, S6 and S7). Indeed, the PCG was the third most frequent region among all connections with decreased connectivity strength in VPT-TEA infants, after the TPO and OFC (Supplementary Table S7).

Of notice, the precuneus (PCUN), the fourth most frequent region among all connections with decreased connectivity strength in VPT-TEA infants, was the most frequent region participating in all parieto-cortical affected connections (Supplementary Tables S6 and S7). Furthermore, the left PCUN was the node the most frequently involved in inter-hemispheric connections with decreased connectivity strength in VPT-TEA infants, followed by the left dorsal cingulate gyrus (DCG) (Supplementary Tables S4).
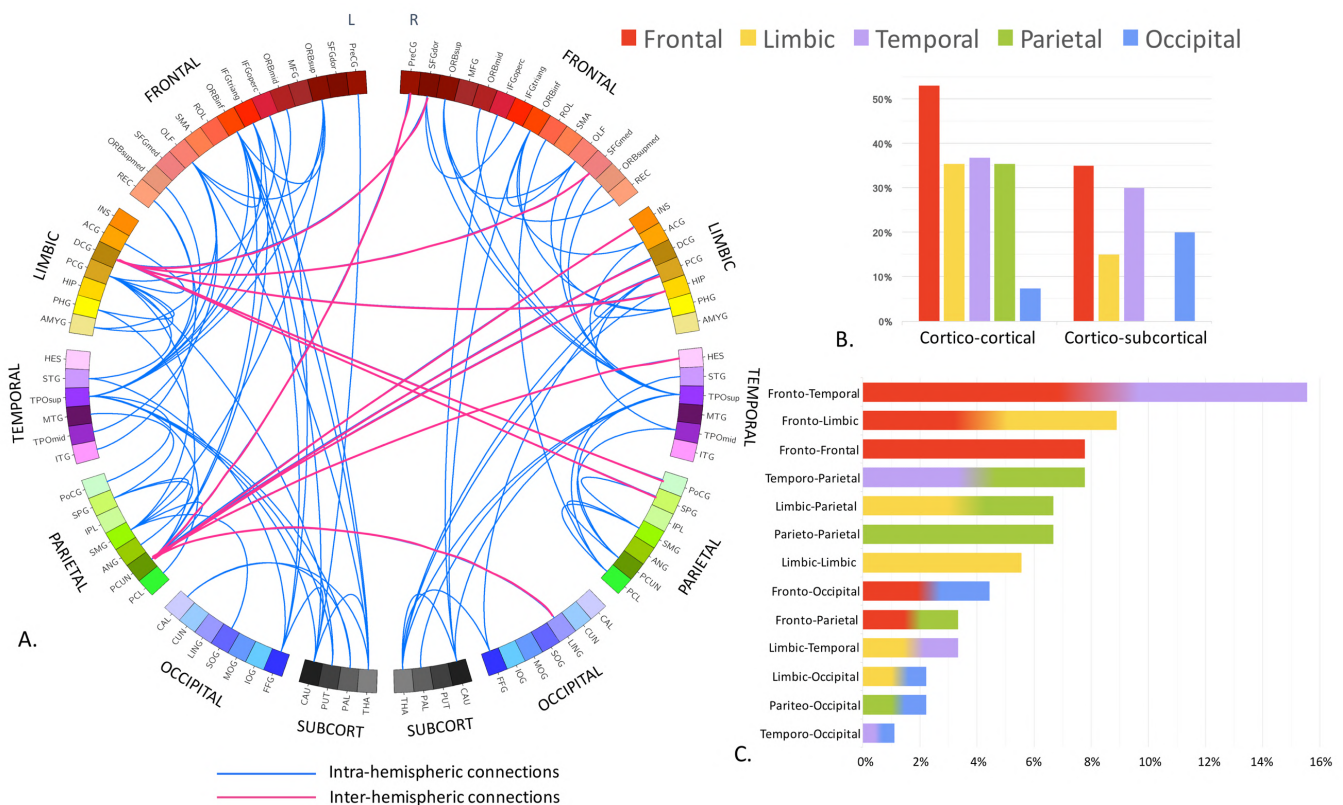
Fig. 3. **Brain network connections with significant diminished structural connectivity in prematurely born neonates.** A. Representation of brain network connections with a statistically significantly decreased structural connectivity strength in VPT-TEA in comparison to FT infants. Intra-hemispheric connections are represented in blue while inter-hemispheric in pink. Visualization made using the Circos software (Krzywinski et al., 2009). B. Bar graph representation of the relative percentual distribution of cortical nodes participating in the cortico-cortical and cortico-subcortical connections with a diminished connectivity strength in VPT-TEA in comparison to FT infants. C. Bar graph representing the relative percentual distribution of cortico-cortical connections with a diminished connectivity strength in VPT-TEA in comparison to FT infants.

4. Discussion

In this study, using a connectome approach, we explored whole-brain network topological alterations using graph-based analysis and edge-wise connectivity strength in order to compare brain structural connectivity alterations on VPT-TEA infants and FT newborns and thus assess the impact of prematurity on whole-brain structural organization at TEA.

The major findings from this study are: 1) VPT-TEA infants' brain networks presented an increased characteristic path length, decreased global efficiency, increased clustering coefficient and increased modularity index, reflecting increased segregation and decreased integration in comparison to FT newborns; 2) Altered connectivity of typical neonatal network hubs, in particular the thalamus, left PCUN and left DCG, as well as a diminished rich-club coefficient in VPT-TEA infants' brain networks; 3) Decreased connectivity of fronto-paralimbic and fronto-limbic connections, in particular of the orbitofrontal-temporal pole circuitry, as well as of DMN posterior regions, such as the PCUN and PCG, in VPT-TEA infants' brain networks in comparison to FT infants.

4.1. Prematurity is associated with an immature brain structural network topological organization at TEA

4.1.1. Increased segregation and decreased integration of brain networks in prematurely born neonates

The topological organization of the brain structural network has been investigated in fetal and preterm infants throughout development. From the second trimester to TEA, various studies have shown an increase in network strength and integration capacity, with a decrease of characteristic path length and increase of network global efficiency, both during normal fetal (Song et al., 2017) as well as preterm brain development (Ball et al., 2014; Batalle et al., 2017; Brown et al., 2014; van den Heuvel et al., 2015; Zhao et al., 2019). Characteristic path length and network global efficiency refer to the ability of communication between distributed nodes and thus reflect the global information transfer efficiency (Rubinov and Sporns, 2010). Indeed, during fetal brain development, there is a dramatic growth of major long association WM fibers from 20 to 40 weeks GA, which is thought to underlie the dramatic increases of network strength and efficiency (Song et al., 2017). Since preterm birth occurs during this critical period of brain development, it might impact normal topological network organization, namely by disrupting the establishment of long-range structural connections. This could explain the significantly higher characteristic path length and significantly diminished global efficiency

that we found at term age in the brain networks of VPT-TEA infants in comparison to FT newborns, what is in line with previous literature findings (Ball et al., 2014; Fischi-Gomez et al., 2015; Lee et al., 2019; Thompson et al., 2016b).

Literature has suggested that the typical developmental course of the brain structural network is characterized by a progressive maturational shift from short-range to long-distance connections, with a continuously increasing integration and decreasing segregation with age, favouring thus an integrative topology (Hagmann et al., 2010; Huang et al., 2015; Tymofiyeva et al., 2013; Yap et al., 2011). Network segregation relates to its organization into a collection of sub-networks and can be measured by means of average clustering coefficient, local efficiency and modularity. During early development, a decreasing clustering coefficient has been observed both in fetal development, from 20 to 35 weeks GA (Song et al., 2017), as well as in preterm development between 30 and 40 weeks GA (Ball et al., 2014). In this study, we found that VPT-TEA infants showed a significantly higher clustering coefficient and local efficiency in comparison to FT newborns, which confirms previous reported findings (Ball et al., 2014) and suggests that the expected decrease in brain network segregation described during normal development is affected by preterm birth. In non-normalised networks, a tendency for an increased characteristic path length, diminished global efficiency and increased clustering coefficient and local efficiency was also observed in FT newborns, in comparison to VPT-TEA infants, although not statistically significant, what can be related to the reduced study sample size.

Additionally, modularity index revealed that both VPT-TEA and FT groups had a modular network organization, in which nodes are highly connected to one another within the same community and sparsely connected to nodes in other communities (Newman, 2004). However, we found an increased modularity index in VPT-TEA infants compared to FT newborns. Modularity has been shown to decrease along development, with an increase of communications between different modules from birth to adolescence (Huang et al., 2015). Our results indicate for the first time that prematurity leads to an increase of structural brain network modularity at TEA, with network nodes holding more connections within nodes from the same module than with nodes from other modules, what supports the increased segregation and decreased integration observed in VPT-TEA infants' brain networks.

An optimal balance between segregation and integration is ideal to allow high capacity for local and global information transfer. This aspect was quantified by the small-world network topology. No differences were found between VPT-TEA and FT infants regarding the

SW index, which was >1 in both cases, suggesting a generally efficient local and global organization in both groups.

Summing up, our data reveals that the brain of a VPT infant at TEA, in comparison to a FT newborn, evidences a topological organization corresponding to a typical earlier stage of development, with decreased integration and increased segregation properties. Integration of distributed neuronal activity across specialized brain systems is required for higher brain function and supports diverse cognitive processes, such as language (Friederici and Gierhan, 2013), emotion (Pessoa, 2012), cognitive control (Power and Petersen, 2013) and learning (Bassett et al., 2011; Bassett et al., 2015), skills known to be impaired in infants that were born preterm (Anderson and Doyle, 2003; Bhutta et al., 2002; Marlow, 2004; Montagna and Nosarti, 2016; Spittle et al., 2009; Spittle et al., 2011; Witt et al., 2014). The fact that VPT-TEA infants' structural brain networks were found to be more modular and less globally efficient than in FT newborns might result from different factors potentially associated with preterm birth, such as a disruption of the activity-dependent synaptic pruning, of the growth and maturation of major long-range association WM fibers, or an impaired reinforcement of the maturation of WM connections. Such factors could explain the observed delayed shift from a local emphasis, based on short-range connections, to a more distributed brain network architecture, based on long-range connections.

Topological characteristics of structural brain networks observed early in development, including network integration and segregation measures, such as global efficiency and clustering coefficient, have been found, respectively, to be significantly correlated with cognitive performance (Keunen et al., 2017) and internalizing and externalizing behaviours assessed in early childhood (Wee et al., 2017). These findings support the hypothesis that the altered global brain network organization observed in VPT-TEA infants might underlie the neurodevelopmental impairments reported in preterm-born infants at later ages.

4.1.2. Brain network hubs differences and impaired rich-club organization in prematurely born neonates

Connections within the connectome can be distributed unevenly, such that certain nodes possess a larger number of connections than others, which makes them network hubs (van den Heuvel and Sporns, 2013). Brain network hubs play a central role in facilitating the integration of disparate neural systems, namely by forming long-range connections (van den Heuvel and Sporns, 2011; van den Heuvel et al., 2012). Structural hubs have been shown to be present

already during the prenatal period and to have a consistent spatial topography throughout development (Ball et al., 2014; Chen et al., 2013; Hagmann et al., 2010).

Our results confirm that by term age, both FT and VPT-TEA infants' brain networks demonstrate the presence of network hubs, comprising mainly subcortical (thalamus, caudate and putamen) and limbic (dorsal cingulate gyrus, insula and hippocampus) regions in both groups. Interestingly, the left PCUN was detected as a hub only in FT infants, whereas the bilateral superior temporal gyrus, left Heschl gyrus and both amygdalae were identified as hubs only in VPT-TEA infants. Most of these regions have already been reported as network hubs in neonates and many of them have been shown to persist throughout development (Ball et al., 2014; Chen et al., 2013; Huang et al., 2015; Pandit et al., 2014; van den Heuvel and Sporns, 2011; van den Heuvel et al., 2015).

From all detected network hubs, the left and right thalamus were the two regions with the highest nodal degree in both VPT-TEA and FT newborns. Of notice, VPT-TEA infants presented a significantly diminished number of thalamic connections in comparison to FT infants, which is in agreement with previous literature evidencing diminished thalamocortical connectivity and reduced network capacity of DGM following preterm birth (Ball et al., 2013a; Ball et al., 2014; Ball et al., 2015). Moreover, this diminished connectivity might contribute to the reduced integration capacity observed in VPT-TEA infants' brain networks. Thalamocortical connections are established during the late second and third trimester of development, when preterm birth occurs (Kostovic et al., 2002; Kostovic et al., 2014), and therefore prematurity and its associated events, such as inflammation, hypoxia/ischemia, stress and important environmental changes, may affect the establishment of these connections. The thalamus, as a subcortical hub, has been shown to present a rich-club connectivity pattern, to be involved in large-scale integration of neural signals (Alexander et al., 1986; van den Heuvel and Sporns, 2011) and in important higher-order cognitive functions (Bressler, 1995; Bressler and Menon, 2010). In particular, an impaired thalamocortical structural connectivity at TEA, following preterm birth, has been shown to correlate with impaired cognitive performance in premature infants at two years of age (Ball et al., 2015). Additionally, at school age, alterations in the cortico-basal ganglia-thalamo-cortical loop (namely prefrontal-subcortical circuits), following preterm birth, were associated with poorer social behavior, recognition of social context and simultaneous information processing at school age (Fischi-Gomez et al., 2015).

The left PCUN, a hub that we observed in FT but not in VPT-TEA infants, has already been shown to be a network hub in the newborn brain (Huang et al., 2015; Yap et al., 2011). The PCUN is a brain region situated in a strategic location with wide-spread connections and

is suggested to be a major association area, supporting a variety of behavioural functions (Cavanna and Trimble, 2006), including memory retrieval (Lundstrom et al., 2005), reward monitoring (Hayden et al., 2008), emotional processing (Maddock et al., 2003) and mediation between task and rest states (Li et al., 2019; Utevsky et al., 2014). It also plays an important role in "default mode network" (DMN), functionally linked to self-consciousness (Cavanna and Trimble, 2006; Fransson and Marrelec, 2008), social cognitive functions (Mars et al., 2012), regulation of attentional states and cognition (Leech and Sharp, 2014; McKiernan et al., 2003), and which is known to appear later in the development of preterm infants (Smyser et al., 2010). Interestingly, resting-state functional MRI (rs-fMRI) has shown that the left PCUN plays a central role in integration in newborns and also belongs to the nodes hierarchically more important for the propagation of neural activity to other brain regions in FT but not in VPT infants, when at 10 years old (Padilla et al., 2020). Additionally, at TEA, rs-functional connectivity between the salience network and the PCUN has been shown to be significantly decreased in VPT-TEA infants in comparison to FT newborns (Lordier et al., 2019b). Structural brain network studies have shown that the PCUN has an increased efficiency associated with longer gestational age, when evaluated at preadolescent age (Kim et al., 2014a), what supports also the impact of prematurity in this node efficiency, and presents a consistently high and increasing centrality from early infancy to adulthood (Chen et al., 2013; Hagmann et al., 2010; Huang et al., 2015). On the other hand, the superior temporal gyrus and the Heschl gyrus, which were detected as hubs in VPT-TEA but not in FT infants, have been shown to have a decreased centrality with age, from neonatal to pre-adolescence period (Huang et al., 2015). Such findings are thought to be related to a selective strengthening of the growing structural networks, through both microstructural enhancement of major WM tracts and axon pruning, based on a genetics and epigenetics background (Huang et al., 2015). Our results support the hypothesis of a delayed structural maturation in VPT-TEA structural brain networks, since the PCUN, a hub with increased centrality during development from term birth to adulthood, was found in FT newborns but not in VPT-TEA infants, while temporal regions that tend to have a decreased centrality during normal brain development were still identified as hubs in VPT-TEA, but not in FT infants. Another important reflection is that VPT infants are known to be exposed to many new different acoustic solicitations from the external world, in comparison to FT newborns that remain inside their mother's womb until term age. The differences in the acoustic environment might lead to changes in activity-dependent synaptic plasticity and could justify the fact that temporal regions important for sound processing, such

as the Heschl gyrus and the superior temporal gyrus (Fulford et al., 2004; Jardri et al., 2008), were found as hubs only in VPT-TEA infants.

Remarkably, VPT-TEA presented a superior number of hubs, with an inferior average number of connections, in comparison to FT newborns. This finding was confirmed and complemented by the reduced "rich-club" coefficient observed in VPT-TEA infants. A "rich-club" organization refers to the presence of some hub regions that are particularly densely connected to each other (more than what would be expected by chance) and is thought to be an important characteristic for efficient global information integration (van den Heuvel and Sporns, 2011; van den Heuvel et al., 2012). Literature has shown that the developmental window between 30 and 40 weeks GA, when preterm birth occurs, corresponds to an essential period for the establishment of connections between RC regions and the rest of the cortex, contributing to an increase in RC connectivity (Ball et al., 2014). Our data demonstrates, for the first time in literature, that VPT-TEA infants' structural brain networks have a higher number of hubs, but present a diminished weighted RC coefficient in comparison to FT infants, revealing thus a significantly diminished connectivity of highly connected and highly central brain regions in VPT-TEA vs FT infants, in agreement with our finding that in VPT-TEA brain networks are more segregated and less integrated than in FT infants. Ball et al. had found no difference between VPT-TEA and FT infants in the nodal degree within the RC domain, when considering only the connections among the RC nodes (Ball et al., 2014), but they have evaluated unweighted structural brain networks. Using fMRI, it has also been shown that VPT-TEA infants exhibit a significantly reduced functional connectivity within RC nodes in comparison to FT infants (Scheinost et al., 2016). Literature has also shown that longer gestation preferentially enhances RC connections and increases global network efficiency in the pre-adolescent brain (Kim et al., 2014a). Additionally, an atypical RC organization has been found in various clinical disorders of neuronal connectivity, comprising attention-deficit/hyperactivity disorder (ADHD) and autism spectrum disorders (ASD), frequently observed in the preterm population (Ray et al., 2014). Our findings support thus not only the hypothesis that VPT-TEA infants' brain might present a delay in early development, with an organization which is typical of an earlier developmental stage in comparison to FT infants, but also that prematurity and its associated events might disrupt early structural connectivity and network organization.

4.2. Prematurity is associated with decreased connectivity strength in structural brain networks at TEA

In our study, VPT-TEA infants evidenced decreased connectivity strength in a set of inter and intra-hemispheric cortico-cortical connections, as well as in a set of intra-hemispheric cortico-subcortical and subcortico-subcortical connections in comparison to FT newborns. These findings are in agreement with other structural connectivity investigations in preterm infants (Ball et al., 2014; Batalle et al., 2017).

Among all cortical regions, the frontal cortex was the one exhibiting the majority of connections with decreased connectivity strength in VPT-TEA infants, with the OFC being the frontal region the most frequently involved. Decreased connectivity of the orbitofrontal network has already been shown in extremely preterm infants at 6 years of age (Fischi-Gomez et al., 2015). Literature has also shown that VPT infants present volumetric reductions, cortical immaturity and cortical gyrification abnormalities in the OFC in comparison to FT infants (Ganella et al., 2015; Rogers et al., 2012; Thompson et al., 2007). These could be a consequence of the altered WM connectivity, to and from the OFC, that we find in VPT infants at TEA, and might be at the origin of the orbitofrontal specific cognitive and executive functioning deficits reported in preterm population (Luu et al., 2011; Mulder et al., 2009; Taylor and Clark, 2016).

From all the affected connections, the majority were intra-hemispheric cortico-cortical and, from these, the fronto-temporal connections were the most frequent, in particular those connecting the OFC to the TPO. These two regions were also the ones participating the most frequently in the connections with decreased connectivity strength in VPT-TEA. Both the OFC and the TPO have been considered as paralimbic regions, based on their anatomical location and connectivity (Duvernoy, 1999; Hof et al., 1995; Mesulam, 2000). One of the most important WM connections between the OFC and the TPO is the uncinate fasciculus (Oishi et al., 2015; Von Der Heide et al., 2013), which has been proven to be involved in behavioral and socio-emotional processing (Ghashghaei and Barbas, 2002; Kringelbach, 2005; Wildgruber et al., 2005) and to present a decreased maturation in prematurely born neonates, adolescents and adults (Constable et al., 2008; Mullen et al., 2011; Rimol et al., 2019; Sa de Almeida et al., 2019). After fronto-temporal connections, the fronto-limbic connections were the second most affected cortico-cortical connections. Indeed, these results are in agreement with previous studies, which have identified an immaturity of cortical fronto-temporal connectivity between VPT-TEA and FT infants (Pannek et al., 2013), as well as alterations in frontal-basal-ganglia-

thalamocortical and limbic networks in 6 year-old infants born extremely prematurely, correlating with behaviour and socio-emotional evaluation scores (Fischi-Gomez et al., 2016). Thus, our findings support the hypothesis that the diminished connectivity strength of frontal, paralimbic and limbic networks is already present in preterm infants by term-age and might be associated with the behavioral socio-emotional difficulties observed in prematurely born infants later in development (Bhutta et al., 2002; Fischi-Gomez et al., 2015; Hille et al., 2001; Hughes et al., 2002; Lejeune et al., 2015; Montagna and Nosarti, 2016; Spittle et al., 2009; Witt et al., 2014).

After the OFC and TPO, the PCG gyrus was the region the most frequently involved in the connections with decreased connectivity strength in VPT-TEA, as well as the most frequent among all limbic nodes participating in such connections. It was followed by the PCUN, which was also the most frequent among all parietal nodes participating in the connections with decreased connectivity strength in VPT-TEA infants. These two regions are part of DMN, which is associated with cognitive development (Palacios et al., 2013; Raichle et al., 2001) and is involved in a variety of high-level functions, such as attention and inhibitory control (Fair et al., 2008; Whitfield-Gabrieli and Ford, 2012), social cognition (Iacoboni et al., 2004), episodic memory (Greicius and Menon, 2004), and self-related processes (Gusnard et al., 2001). An altered DMN connectivity has been found to be associated with developmental disorders, such as ADHD (Castellanos et al., 2009; Fair et al., 2010) and ASD (Assaf et al., 2010; Nielsen et al., 2014), which are commonly reported in preterm population (Johnson and Marlow, 2011; Nosarti et al., 2012; Treyvaud et al., 2013). DMN is known to be incomplete/fragmented and with a posterior predominance in preterm infants, even at TEA, appearing later in their development (Doria et al., 2010; Fransson et al., 2007; Lordier et al., 2019b; Smyser et al., 2010). Our results reveal that components from posterior DMN, namely the PCG and PCUN, have a decreased structural connectivity strength in VPT-TEA infants, in comparison to FT infants. This diminished structural connectivity might underlie the diminished functional connectivity observed in DMN in preterm infants at TEA and later in life (Lordier et al., 2019b; Smyser et al., 2010; White et al., 2014), as well as the deficits in behavior and social cognition observed in this population (Anderson and Doyle, 2003; Arpi and Ferrari, 2013; Bhutta et al., 2002; Marlow, 2004; Montagna and Nosarti, 2016; Spittle et al., 2009; Witt et al., 2014).

Additionally, the left PCUN was the node the most frequently involved in inter-hemispheric connections with decreased connectivity strength in VPT-TEA infants, followed by the left DCG. Interestingly, these two regions were both detected as hubs in FT infants, evidencing thus a high centrality in this group, but not in VP-TEA infants. Inter-hemispheric

124

connections are known to play an important role in long-range integration. The fact that the inter-hemispheric connections that pass through the left PCUN and left DCG had a decreased connectivity strength in VPT-TEA infants, in comparison to FT infants, might explain why these two regions were detected as hubs only in FT infants, as well as the decreased integration capacity detected in VPT-TEA brain networks in comparison to FT infants.

4.3.   Limitations and future directions

This study has limitations that have to be considered. First, the sample size is modest. This limitation is related to the difficulty of recruitment of newborns and families into a research project during a stressful time in their life, in particular for healthy FT newborns, where an MRI has only a limited clinical role. We are now recruiting a new cohort of VPT and FT infants for a second longitudinal study, which will allow to further validate our results. Second, although chi-squared test revealed no significant difference regarding the distribution of scanner/coils between groups, this is still a limitation to be taken into account. Furthermore, topup correction for EPI distortions was not applied in the present dataset, given the acquisition protocol. Such is a limitation that should be considered when interpreting the results from ACT tractography algorithm. Nevertheless, as we are comparing two groups of infants with the same age at MRI, the possible errors arriving from tractography would be similar between groups and thus data would be comparable. Additionally, we have opted to use SIFT for streamlines filtering, instead of the new available SIFT2 algorithm, mainly for the following reasons: 1) SIFT has been considered as effective in achieving its goal and has been used in previous recent neonatal connectome studies (Batalle et al., 2017; Blesa et al., 2019); 2) SIFT offers more flexibility in streamlines visualisation; 3) SIFT allows more flexibility regarding subsequent analysis, since SIFT2 requires any following processing to be compatible with the definition of a cross-sectional multiplier for each streamline (Smith et al., 2015).

While our structural brain results support published data on specific neurocognitive and neurobehavioral deficits in preterm infants, the clinical significance of these specific brain structural alterations remains to be further evaluated by investigating neurodevelopmental and cognitive outcomes in this study population. These infants are currently being followed-up in our child development center with detailed neurodevelopmental assessments and the first results are expected within one year.

Given the specific alterations in network characteristics found in VPT infants at TEA, compared to FT infants, the question remains open as to the origin of these alterations. In our

current longitudinal design, we are investigating if these brain network alterations are present in VPT infants already at birth or if they develop through the first weeks of life during NICU (neonatal intensive care unit) stay. This information will be crucial for the development of potential interventions aiming to prevent brain network alterations in preterm infants.

5. Conclusion

A whole-brain connectome analysis was used to study brain networks' differences between FT and VPT-TEA infants.

Overall, our results suggest that, although both FT and VPT-TEA groups evidence a small-world, modular and rich-club organization, VPT-TEA infants' brain networks display a typically more immature topology, compared to the expected development at term age. In particular, they evidence increased segregation and decreased integration, and thus a delayed shift from a local emphasis to a more distributed network architecture. The impaired integration might be explained by the detected increased modularity index, diminished rich-club coefficient and, in particular, by the observed decreased connectivity of typical neonatal hubs, such as bilateral thalamus, left PCUN and left DCG. Fronto-paralimbic and fronto-limbic were the most frequently affected connections in VPT-TEA. The noticeable decreased connectivity strength of the OFC-TPO circuitry might be at the origin of the behaviour and socio-emotional difficulties associated with prematurity and thus early interventions aiming to promote this circuitry plasticity might hold a relevant clinical impact in this population. Additionally, posterior regions from DMN, namely the PCUN and PCG, were also found to have a decreased structural connectivity in VPT-TEA infants, which might underlie the diminished functional connectivity of this network and thus the impaired behavioral and social cognition reported in preterm infants.

Acknowledgments

Funding

Competing interests

The authors declare no competing interests.

References

Alexander, G.E., Delong, M.R., Strick, P.L., 1986. Parallel Organization of Functionally Segregated Circuits Linking Basal Ganglia and Cortex. Annual Review of Neuroscience. 9**,** 357-381.

Anderson, P., Doyle, L.W., 2003. Neurobehavioral outcomes of school-age children born extremely low birth weight or very preterm in the 1990s. Jama-Journal of the American Medical Association. 289**,** 3264-3272.

Andersson, J.L.R., et al., 2016. Incorporating outlier detection and replacement into a non-parametric framework for movement and distortion correction of diffusion MR images. Neuroimage. 141**,** 556-572.

Andersson, J.L.R., Sotiropoulos, S.N., 2016. An integrated approach to correction for off-resonance effects and subject movement in diffusion MR imaging. Neuroimage. 125**,** 1063-1078.

Andersson, J.L.R., et al., 2017. Towards a comprehensive framework for movement and distortion correction of diffusion MR images: Within volume movement. Neuroimage. 152**,** 450-466.

Anjari, M., et al., 2007. Diffusion tensor imaging with tract-based spatial statistics reveals local white matter abnormalities in preterm infants. Neuroimage. 35**,** 1021-7.

Arpi, E., Ferrari, F., 2013. Preterm birth and behaviour problems in infants and preschool-age children: a review of the recent literature. Developmental Medicine and Child Neurology. 55**,** 788-796.

Assaf, M., et al., 2010. Abnormal functional connectivity of default mode sub-networks in autism spectrum disorder patients. Neuroimage. 53**,** 247-256.

Avants, B.B., et al., 2011. A reproducible evaluation of ANTs similarity metric performance in brain image registration. Neuroimage. 54**,** 2033-2044.

Ball, G., et al., 2012. The effect of preterm birth on thalamic and cortical development. Cereb Cortex. 22**,** 1016-24.

Ball, G., et al., 2013. The influence of preterm birth on the developing thalamocortical connectome. Cortex; a journal devoted to the study of the nervous system and behavior. 49**,** 1711-1721.

Ball, G., et al., 2014. Rich-club organization of the newborn human brain. Proceedings of the National Academy of Sciences of the United States of America. 111**,** 7456-7461.

Ball, G., et al., 2015. Thalamocortical Connectivity Predicts Cognition in Children Born Preterm. Cerebral Cortex. 25**,** 4310-4318.

Ball, G., et al., 2017. Multimodal image analysis of clinical influences on preterm brain development. Ann Neurol. 82**,** 233-246.

Bassett, D.S., et al., 2011. Dynamic reconfiguration of human brain networks during learning. Proc Natl Acad Sci U S A. 108**,** 7641-6.

Bassett, D.S., et al., 2015. Learning-induced autonomy of sensorimotor systems. Nat Neurosci. 18**,** 744-51.

Bastiani, M., et al., 2019. Automated processing pipeline for neonatal diffusion MRI in the developing Human Connectome Project. Neuroimage. 185**,** 750-763.

Batalle, D., et al., 2017. Early development of structural networks and the impact of prematurity on brain connectivity. Neuroimage. 149**,** 379-392.

Behrens, T.E.J., et al., 2003. Characterization and propagation of uncertainty in diffusion-weighted MR imaging. Magnetic Resonance in Medicine. 50**,** 1077-1088.

Benjamini, Y., Hochberg, Y., 1995. Controlling the False Discovery Rate - a Practical and Powerful Approach to Multiple Testing. Journal of the Royal Statistical Society Series B-Statistical Methodology. 57**,** 289-300.

Bhutta, A.T., et al., 2002. Cognitive and behavioral outcomes of school-aged children who were born preterm - A meta-analysis. Jama-Journal of the American Medical Association. 288**,** 728-737.

Blondel, V.D., et al., 2008. Fast unfolding of communities in large networks. Journal of Statistical Mechanics-Theory and Experiment.

Bressler, S.L., 1995. Large-Scale Cortical Networks and Cognition. Brain Research Reviews. 20**,** 288-304.

Bressler, S.L., Menon, V., 2010. Large-scale brain networks in cognition: emerging methods and principles. Trends in Cognitive Sciences. 14**,** 277-290.

Brown, C.J., et al., 2014. Structural network analysis of brain development in young preterm neonates. Neuroimage. 101**,** 667-680.

Bullmore, E.T., Sporns, O., 2009. Complex brain networks: graph theoretical analysis of structural and functional systems. Nature Reviews Neuroscience. 10**,** 186-198.

Castellanos, F.X., Kelly, C., Milham, M.P., 2009. The Restless Brain: Attention-Deficit Hyperactivity Disorder, Resting-State Functional Connectivity, and Intrasubject Variability. Canadian Journal of Psychiatry-Revue Canadienne De Psychiatrie. 54**,** 665-672.

Cavanna, A.E., Trimble, M.R., 2006. The precuneus: a review of its functional anatomy and behavioural correlates. Brain. 129**,** 564-583.

Chen, Z., et al., 2013. Graph theoretical analysis of developmental patterns of the white matter network. Frontiers in Human Neuroscience. 7.

Cismaru, A.L., et al., 2016. Altered Amygdala Development and Fear Processing in Prematurely Born Infants. Front Neuroanat. 10**,** 55.

Constable, R.T., et al., 2008. Prematurely born children demonstrate white matter microstructural differences at 12 years of age, relative to term control subjects: An investigation of group and gender effects. Pediatrics. 121**,** 306-316.

Crossley, N.A., et al., 2015. The hubs of the human connectome are generally implicated in the anatomy of brain disorders (vol 137, 2382, 2014). Brain. 138, E374-E374.

Doria, V., et al., 2010. Emergence of resting state networks in the preterm human brain. Proc Natl Acad Sci U S A. 107**,** 20015-20.

Dubois, J., et al., 2008. Asynchrony of the early maturation of white matter bundles in healthy infants: quantitative landmarks revealed noninvasively by diffusion tensor imaging. Human brain mapping. 29, 14-27.

Duvernoy, H.M., 1999. The human brain. Surface, blood supply, and three-dimensional sectional anatomy, Vol., Springer Wien, New York.

Fair, D.A., et al., 2008. The maturing architecture of the brain's default network. Proceedings of the National Academy of Sciences of the United States of America. 105, 4028-4032.

Fair, D.A., et al., 2010. Atypical Default Network Connectivity in Youth with Attention-Deficit/Hyperactivity Disorder. Biological Psychiatry. 68, 1084-1091.

Fischi-Gomez, E., et al., 2015. Structural Brain Connectivity in School-Age Preterm Infants Provides Evidence for Impaired Networks Relevant for Higher Order Cognitive Skills and Social Cognition. Cereb Cortex. 25, 2793-805.

Fischi-Gomez, E., et al., 2016. Brain network characterization of high-risk preterm-born school-age children. NeuroImage: Clinical. 11, 195-209.

Fransson, P., et al., 2007. Resting-state networks in the infant brain. Proc Natl Acad Sci U S A. 104, 15531-6.

Fransson, P., Marrelec, G., 2008. The precuneus/posterior cingulate cortex plays a pivotal role in the default mode network: Evidence from a partial correlation network analysis. Neuroimage. 42, 1178-1184.

Friederici, A.D., Gierhan, S.M.E., 2013. The language network. Current Opinion in Neurobiology. 23, 250-254.

Fulford, J., et al., 2004. Fetal brain activity and hemodynamic response to a vibroacoustic stimulus. Human Brain Mapping. 22, 116-121.

Ganella, E.P., et al., 2015. Abnormalities in Orbitofrontal Cortex Gyrification and Mental Health Outcomes in Adolescents Born Extremely Preterm and/or At an Extremely Low Birth Weight. Human Brain Mapping. 36, 1138-1150.

Ghashghaei, H.T., Barbas, H., 2002. Pathways for emotion: Interactions of prefrontal and anterior temporal pathways in the amygdala of the rhesus monkey. Neuroscience. 115, 1261-1279.

Greicius, M.D., Menon, V., 2004. Default-mode activity during a passive sensory task: Uncoupled from deactivation but impacting activation. Journal of Cognitive Neuroscience. 16, 1484-1492.

Gui, L., et al., 2012. Morphology-driven automatic segmentation of MR images of the neonatal brain. Medical Image Analysis. 16, 1565-1579.

Gusnard, D.A., et al., 2001. Medial prefrontal cortex and self-referential mental activity: Relation to a default mode of brain function. Proceedings of the National Academy of Sciences of the United States of America. 98, 4259-4264.

Hagmann, P., et al., 2010. White matter maturation reshapes structural connectivity in the late developing human brain. Proceedings of the National Academy of Sciences of the United States of America. 107, 19067-19072.

Hayden, B.Y., et al., 2008. Posterior Cingulate Cortex Mediates Outcome-Contingent Allocation of Behavior. Neuron. 60, 19-25.

He, Y., Evans, A., 2010. Graph theoretical modeling of brain connectivity. Curr Opin Neurol. 23, 341-50.

Hille, E.T.M., et al., 2001. Behavioural problems in children who weigh 1000 g or less at birth in four countries. Lancet. 357, 1641-1643.

Hof, P.R., Mufson, E.J., Morrison, J.H., 1995. Human Orbitofrontal Cortex - Cytoarchitecture and Quantitative Immunohistochemical Parcellation. Journal of Comparative Neurology. 359**,** 48-68.

Huang, H., et al., 2015. Development of Human Brain Structural Networks Through Infancy and Childhood. Cerebral Cortex. 25**,** 1389-1404.

Hughes, M.B., et al., 2002. Temperament characteristics of premature infants in the first year of life. Journal of Developmental and Behavioral Pediatrics. 23**,** 430-435.

Huppi, P.S., et al., 1998. Microstructural development of human newborn cerebral white matter assessed in vivo by diffusion tensor magnetic resonance imaging. Pediatric research. 44**,** 584-590.

Huppi, P.S., Dubois, J., 2006. Diffusion tensor imaging of brain development. Seminars in fetal & neonatal medicine. 11**,** 489-497.

Iacoboni, M., et al., 2004. Watching social interactions produces dorsomedial prefrontal and medial parietal BOLD fMRI signal increases compared to a resting baseline. Neuroimage. 21**,** 1167-1173.

Inder, T.E., et al., 2005. Abnormal cerebral structure is present at term in premature infants. Pediatrics. 115**,** 286-94.

Innocenti, G.M., Price, D.J., 2005. Exuberance in the development of cortical networks. Nature Reviews Neuroscience. 6**,** 955-965.

Jardri, R., et al., 2008. Fetal cortical activation to sound at 33 weeks of gestation: a functional MRI study. Neuroimage. 42**,** 10-8.

Johnson, S., Marlow, N., 2011. Preterm birth and childhood psychiatric disorders. Pediatr Res. 69**,** 11R-8R.

Jones, D.K., Basser, P.J., 2004. "Squashing peanuts and smashing pumpkins": How noise distorts diffusion-weighted MR data. Magnetic Resonance in Medicine. 52**,** 979-993.

Karolis, V.R., et al., 2016. Reinforcement of the Brain's Rich-Club Architecture Following Early Neurodevelopmental Disruption Caused by Very Preterm Birth. Cerebral Cortex. 26**,** 1322-1335.

Keunen, K., et al., 2017. White matter maturation in the neonatal brain is predictive of school age cognitive capacities in children born very preterm. Developmental Medicine and Child Neurology. 59**,** 939-946.

Kim, D.J., et al., 2014. Longer gestation is associated with more efficient brain networks in preadolescent children. Neuroimage. 100**,** 619-627.

Kiss, J.Z., Vasung, L., Petrenko, V., 2014. Process of cortical network formation and impact of early brain damage. Curr Opin Neurol. 27**,** 133-41.

Kostovic, I., et al., 2002. Laminar organization of the human fetal cerebrum revealed by histochemical markers and magnetic resonance imaging. Cerebral Cortex. 12**,** 536-544.

Kostovic, I., Jovanov-Milosevic, N., 2006. The development of cerebral connections during the first 20-45 weeks' gestation. Seminars in Fetal & Neonatal Medicine. 11**,** 415-422.

Kostovic, I., Judas, M., 2010. The development of the subplate and thalamocortical connections in the human foetal brain. Acta Paediatrica. 99**,** 1119-1127.

Kostovic, I., et al., 2014. Perinatal and early postnatal reorganization of the subplate and related cellular compartments in the human cerebral wall as revealed by histological and MRI approaches. Brain Struct Funct. 219**,** 231-53.

Kringelbach, M.L., 2005. The human orbitofrontal cortex: Linking reward to hedonic experience. Nature Reviews Neuroscience. 6**,** 691-702.

Krzywinski, M., et al., 2009. Circos: an information aesthetic for comparative genomics. Genome Res. 19, 1639-45.

Largo, R., et al., 1989. Significance of prenatal, perinatal and postnatal factors in the development of AGA preterm infants at five to seven years. Developmental Medicine & Child Neurology. 31, 440-456.

Lee, J.Y., Park, H.K., Lee, H.J., 2019. Accelerated Small-World Property of Structural Brain Networks in Preterm Infants at Term-Equivalent Age. Neonatology. 115(2):99-107.

Leech, R., Sharp, D.J., 2014. The role of the posterior cingulate cortex in cognition and disease. Brain. 137, 12-32.

Lejeune, F., et al., 2015. Emotion, attention, and effortful control in 24-month-old very preterm and full-term children. Annee Psychologique. 115, 241-264.

Li, R., et al., 2019. Developmental Maturation of the Precuneus as a Functional Core of the Default Mode Network. Journal of Cognitive Neuroscience. 31, 1506-1519.

Lo, C.Y., et al., 2010. Diffusion Tensor Tractography Reveals Abnormal Topological Organization in Structural Cortical Networks in Alzheimer's Disease. Journal of Neuroscience. 30, 16876-16885.

Lordier, L., et al., 2019. Music in premature infants enhances high-level cognitive brain networks. Proceedings of the National Academy of Sciences of the United States of America. 116, 12103-12108.

Lundstrom, B.N., Ingvar, M., Petersson, K.M., 2005. The role of precuneus and left inferior frontal cortex during source memory episodic retrieval. Neuroimage. 27, 824-834.

Luu, T.M., et al., 2011. Executive and memory function in adolescents born very preterm. Pediatrics. 127, e639-46.

Maddock, R.J., Garrett, A.S., Buonocore, M.H., 2003. Posterior cingulate cortex activation by emotional words: fMRI evidence from a valence decision task. Human Brain Mapping. 18, 30-41.

Marlow, N., 2004. Neurocognitive outcome after very preterm birth. Archives of disease in childhood. Fetal and neonatal edition. 89, F224-8.

Mars, R.B., et al., 2012. On the relationship between the "default mode network" and the "social brain". Front Hum Neurosci. 6, 189.

McKiernan, K.A., et al., 2003. A parametric manipulation of factors affecting task-induced deactivation in functional neuroimaging. J Cogn Neurosci. 15, 394-408.

Ment, L.R., Hirtz, D., Huppi, P.S., 2009. Imaging biomarkers of outcome in the developing preterm brain. Lancet Neurol. 8, 1042-55.

Mesulam, M.M., 2000. Paralimbic (mesocortical) areas, Principles of behavioral and cognitive neurology, Vol., Oxford University Press, New York

Meunier, D., Lambiotte, R., Bullmore, E.T., 2010. Modular and hierarchically modular organization of brain networks. Front Neurosci. 4, 200.

Mills, K.L., et al., 2016. Structural brain development between childhood and adulthood: Convergence across four longitudinal samples. Neuroimage. 141, 273-281.

Montagna, A., Nosarti, C., 2016. Socio-Emotional Development Following Very Preterm Birth: Pathways to Psychopathology. Frontiers in Psychology. 7.

Mulder, H., et al., 2009. Development of executive function and attention in preterm children: a systematic review. Dev Neuropsychol. 34, 393-421.

Mullen, K.M., et al., 2011. Preterm birth results in alterations in neural connectivity at age 16 years. Neuroimage. 54, 2563-2570.

Newman, M.E., Girvan, M., 2004. Finding and evaluating community structure in networks. Phys Rev E Stat Nonlin Soft Matter Phys. 69**,** 026113.

Newman, M.E.J., 2004. Fast algorithm for detecting community structure in networks. Physical Review E. 69.

Nickel, M., Gu, C., 2018. Regulation of Central Nervous System Myelination in Higher Brain Functions. Neural Plasticity.

Nielsen, J.A., et al., 2014. Abnormal lateralization of functional connectivity between language and default mode regions in autism. Molecular Autism. 5.

Nosarti, C., et al., 2012. Preterm Birth and Psychiatric Disorders in Young Adult Life. Archives of General Psychiatry. 69**,** 610-617.

Nosarti, C., 2013. Structural and functional brain correlates of behavioral outcomes during adolescence. Early human development. 89**,** 221-227.

Nossin-Manor, R., et al., 2013. Quantitative MRI in the very preterm brain: Assessing tissue organization and myelination using magnetization transfer, diffusion tensor and T-1 imaging. Neuroimage. 64**,** 505-516.

Oishi, K., et al., 2015. Critical Role of the Right Uncinate Fasciculus in Emotional Empathy. Annals of Neurology. 77**,** 68-74.

Opsahl, T., et al., 2008. Prominence and Control: The Weighted Rich-Club Effect. Physical Review Letters. 101.

Owen, J.P., et al., 2013. Test-retest reliability of computational network measurements derived from the structural connectome of the human brain. Brain Connect. 3**,** 160-76.

Padilla, N., et al., 2015. Brain Growth Gains and Losses in Extremely Preterm Infants at Term. Cerebral cortex (New York, N.Y. : 1991). 25**,** 1897-1905.

Padilla, N., et al., 2020. Breakdown of Whole-brain Dynamics in Preterm-born Children. Cereb Cortex. 30**,** 1159-1170.

Palacios, E.M., et al., 2013. Resting-State Functional Magnetic Resonance Imaging Activity and Connectivity and Cognitive Outcome in Traumatic Brain Injury. Jama Neurology. 70**,** 845-851.

Pandit, A.S., et al., 2014. Whole-Brain Mapping of Structural Connectivity in Infants Reveals Altered Connection Strength Associated with Growth and Preterm Birth. Cerebral Cortex. 24**,** 2324-2333.

Pannek, K., et al., 2013. Assessment of Structural Connectivity in the Preterm Brain at Term Equivalent Age Using Diffusion MRI and T(2) Relaxometry: A Network-Based Analysis. PLoS ONE. 8**,** e68593-e68593.

Pannek, K., et al., 2018. Fixel-based analysis reveals alterations is brain microstructure and macrostructure of preterm-born infants at term equivalent age. Neuroimage-Clinical. 18**,** 51-59.

Pecheva, D., et al., 2018. Recent advances in diffusion neuroimaging: applications in the developing preterm brain. F1000Res. 7.

Pessoa, L., 2012. Beyond brain regions: Network perspective of cognition-emotion interactions. Behavioral and Brain Sciences. 35**,** 158-159.

Peterson, B.S., et al., 2000. Regional brain volume abnormalities and long-term cognitive outcome in preterm infants. Jama-Journal of the American Medical Association. 284**,** 1939-1947.

Power, J.D., Petersen, S.E., 2013. Control-related systems in the human brain. Current Opinion in Neurobiology. 23**,** 223-228.

Radley, J.J., Morrison, J.H., 2005. Repeated stress and structural plasticity in the brain. Ageing Research Reviews. 4, 271-287.

Raichle, M.E., et al., 2001. A default mode of brain function. Proceedings of the National Academy of Sciences of the United States of America. 98, 676-682.

Ray, S., et al., 2014. Structural and Functional Connectivity of the Human Brain in Autism Spectrum Disorders and Attention-Deficit/Hyperactivity Disorder: A Rich Club-Organization Study. Human Brain Mapping. 35, 6032-6048.

Rimol, L.M., et al., 2019. Reduced white matter fractional anisotropy mediates cortical thickening in adults born preterm with very low birthweight. Neuroimage. 188, 217-227.

Rogers, C.E., et al., 2012. Regional Cerebral Development at Term Relates to School-Age Social-Emotional Development in Very Preterm Children. Journal of the American Academy of Child and Adolescent Psychiatry. 51, 181-191.

Rubinov, M., Sporns, O., 2010. Complex network measures of brain connectivity: Uses and interpretations. Neuroimage. 52, 1059-1069.

Sa de Almeida, J., et al., 2019. Music enhances structural maturation of emotional processing neural pathways in very preterm infants. Neuroimage. 207, 116391.

Scheinost, D., et al., 2016. Preterm birth alters neonatal, functional rich club organization. Brain Structure & Function. 221, 3211-3222.

Shu, N., et al., 2011. Diffusion tensor tractography reveals disrupted topological efficiency in white matter structural networks in multiple sclerosis. Cereb Cortex. 21, 2565-77.

Simmons, L.E., et al., 2010. Preventing Preterm Birth and Neonatal Mortality: Exploring the Epidemiology, Causes, and Interventions. Seminars in Perinatology. 34, 408-415.

Smith, S.M., et al., 2004. Advances in functional and structural MR image analysis and implementation as FSL. Neuroimage. 23, S208-S219.

Smyser, C.D., et al., 2010. Longitudinal analysis of neural network development in preterm infants. Cereb Cortex. 20, 2852-62.

Song, L.M., et al., 2017. Human Fetal Brain Connectome: Structural Network Development from Middle Fetal Stage to Birth. Frontiers in Neuroscience. 11.

Spittle, A.J., et al., 2009. Early Emergence of Behavior and Social-Emotional Problems in Very Preterm Infants. Journal of the American Academy of Child and Adolescent Psychiatry. 48, 909-918.

Spittle, A.J., et al., 2011. Neonatal white matter abnormality predicts childhood motor impairment in very preterm children. Dev Med Child Neurol. 53, 1000-6.

Taylor, H.G., Clark, C.A.C., 2016. Executive function in children born preterm: Risk factors and implications for outcome. Seminars in Perinatology. 40, 520-529.

Thompson, D.K., et al., 2007. Perinatal risk factors altering regional brain structure in the preterm infant. Brain. 130, 667-77.

Thompson, D.K., et al., 2013. Hippocampal shape variations at term equivalent age in very preterm infants compared with term controls: perinatal predictors and functional significance at age 7. Neuroimage. 70, 278-87.

Thompson, D.K., et al., 2016. Structural connectivity relates to perinatal factors and functional impairment at 7 years in children born very preterm. Neuroimage. 134, 328-337.

Tournier, J.D., et al., 2019. MRtrix3: A fast, flexible and open software framework for medical image processing and visualisation. Neuroimage. 202, 116137.

Treyvaud, K., et al., 2013. Psychiatric outcomes at age seven for very preterm children: rates and predictors. Journal of Child Psychology and Psychiatry. 54, 772-779.

Tymofiyeva, O., et al., 2013. A DTI-Based Template-Free Cortical Connectome Study of Brain Maturation. Plos One. 8.

Utevsky, A.V., Smith, D.V., Huettel, S.A., 2014. Precuneus Is a Functional Core of the Default-Mode Network. Journal of Neuroscience. 34**,** 932-940.

van den Heuvel, M.P., Sporns, O., 2011. Rich-Club Organization of the Human Connectome. Journal of Neuroscience. 31**,** 15775-15786.

van den Heuvel, M.P., et al., 2012. High-cost, high-capacity backbone for global brain communication. Proc Natl Acad Sci U S A. 109**,** 11372-7.

van den Heuvel, M.P., Sporns, O., 2013. Network hubs in the human brain. Trends Cogn Sci. 17**,** 683-96.

van den Heuvel, M.P., et al., 2013. Abnormal Rich Club Organization and Functional Brain Dynamics in Schizophrenia. Jama Psychiatry. 70**,** 783-792.

van den Heuvel, M.P., et al., 2015. The Neonatal Connectome During Preterm Brain Development. Cerebral Cortex. 25**,** 3000-3013.

Von Der Heide, R.J., et al., 2013. Dissecting the uncinate fasciculus: disorders, controversies and a hypothesis. Brain. 136**,** 1692-1707.

Watts, D.J., Strogatz, S.H., 1998. Collective dynamics of 'small-world' networks. Nature. 393**,** 440-442.

Wee, C.Y., et al., 2017. Neonatal Neural Networks Predict Children Behavioral Profiles Later in Life. Human Brain Mapping. 38**,** 1362-1373.

White, T.P., et al., 2014. Dysconnectivity of neurocognitive networks at rest in very-preterm born adults. Neuroimage-Clinical. 4**,** 352-365.

Whitfield-Gabrieli, S., Ford, J.M., 2012. Default Mode Network Activity and Connectivity in Psychopathology. Annual Review of Clinical Psychology, Vol 8. 8**,** 49-+.

Wildgruber, D., et al., 2005. Identification of emotional intonation evaluated by fMRI. Neuroimage. 24**,** 1233-1241.

Witt, A., et al., 2014. Emotional and effortful control abilities in 42-month-old very preterm and full-term children. Early Hum Dev. 90**,** 565-9.

Yap, P.T., et al., 2011. Development Trends of White Matter Connectivity in the First Years of Life. Plos One. 6.

Zalesky, A., Fornito, A., Bullmore, E.T., 2010. Network-based statistic: Identifying differences in brain networks. Neuroimage. 53**,** 1197-1207.

Zhao, T.D., et al., 2019. Structural network maturation of the preterm human brain. Neuroimage. 185**,** 699-710.

Supplementary material

Supplementary Tables
Supplementary Table S1

List of nodes abbreviations, based on UNC atlas (Shi et al., 2011).

	Node	Abbreviation		Node	Abbreviation
1	Precentral gyrus left	PreCG.L	46	Cuneus right	CUN.R
2	Precentral gyrus right	PreCG.R	47	Lingual gyrus left	LING.L
3	Superior frontal gyrus (dorsal) left	SFGdor.L	48	Lingual gyrus right	LING.R
4	Superior frontal gyrus (dorsal) right	SFGdor.R	49	Superior occipital gyrus left	SOG.L
5	Orbitofrontal cortex (superior) left	ORBsup.L	50	Superior occipital gyrus right	SOG.R
6	Orbitofrontal cortex (superior) right	ORBsup.R	51	Middle occipital gyrus left	MOG.L
7	Middle frontal gyrus left	MFG.L	52	Middle occipital gyrus right	MOG.R
8	Middle frontal gyrus right	MFG.R	53	Inferior occipital gyrus left	IOG.L
9	Orbitofrontal cortex (middle) left	ORBmid.L	54	Inferior occipital gyrus right	IOG.R
10	Orbitofrontal cortex (middle) right	ORBmid.R	55	Fusiform gyrus left	FFG.L
11	Inferior frontal gyrus (opercular) left	IFGoperc.L	56	Fusiform gyrus right	FFG.R
12	Inferior frontal gyrus (opercular) right	IFGoperc.R	57	Postcentral gyrus left	PoCG.L
13	Inferior frontal gyrus (triangular) left	IFGtriang.L	58	Postcentral gyrus right	PoCG.R
14	Inferior frontal gyrus (triangular) right	IFGtriang.R	59	Superior parietal gyrus left	SPG.L
15	Orbitofrontal cortex (inferior) left	ORBinf.L	60	Superior parietal gyrus right	SPG.R
16	Orbitofrontal cortex (inferior) right	ORBinf.R	61	Inferior parietal lobule left	IPL.L
17	Rolandic operculum left	ROL.L	62	Inferior parietal lobule right	IPL.R
18	Rolandic operculum right	ROL.R	63	Supramarginal gyrus left	SMG.L
19	Supplementary motor area left	SMA.L	64	Supramarginal gyrus right	SMG.R
20	Supplementary motor area right	SMA.R	65	Angular gyrus left	ANG.L
21	Olfactory left	OLF.L	66	Angular gyrus right	ANG.R
22	Olfactory right	OLF.R	67	Precuneus left	PCUN.L
23	Superior frontal gyrus (medial) left	SFGmed.L	68	Precuneus right	PCUN.R
24	Superior frontal gyrus (medial) right	SFGmed.R	69	Paracentral lobule left	PCL.L
25	Orbitofrontal cortex (medial) left	ORBsupmed.L	70	Paracentral lobule right	PCL.R
26	Orbitofrontal cortex (medial) right	ORBsupmed.R	71	Caudate left	CAU.L
27	Rectus gyrus left	REC.L	72	Caudate right	CAU.R
28	Rectus gyrus right	REC.R	73	Putamen left	PUT.L
29	Insula left	INS.L	74	Putamen right	PUT.R
30	Insula right	INS.R	75	Pallidum left	PAL.L
31	Anterior cingulate gyrus left	ACG.L	76	Pallidum right	PAL.R
32	Anterior cingulate gyrus right	ACG.R	77	Thalamus left	THA.L
33	Dorsal (middle) cingulate gyrus left	DCG.L	78	Thalamus right	THA.R
34	Dorsal (middle) cingulate gyrus right	DCG.R	79	Heschl gyrus left	HES.L
35	Posterior cingulate gyrus left	PCG.L	80	Heschl gyrus right	HES.R
36	Dorsal/Middle cingulate gyrus right	PCG.R	81	Superior temporal gyrus left	STG.L
37	Hippocampus left	HIP.L	82	Superior temporal gyrus right	STG.R
38	Hippocampus right	HIP.R	83	Temporal pole (superior) left	TPOsup.L
39	ParaHippocampal gyrus left	PHG.L	84	Temporal pole (superior) right	TPOsup.R
40	ParaHippocampal gyrus right	PHG.R	85	Middle temporal gyrus left	MTG.L
41	Amygdala left	AMYG.L	86	Middle temporal gyrus right	MTG.R
42	Amygdala right	AMYG.R	87	Temporal pole (middle) left	TPOmid.L
43	Calcarine cortex left	CAL.L	88	Temporal pole (middle) right	TPOmid.R
44	Calcarine cortex right	CAL.R	89	Inferior temporal gyrus left	ITG.L
45	Cuneus left	CUN.L	90	Inferior temporal gyrus right	ITG.R

Supplementary Table S2

Global not normalised network measures comparison between groups.

Global not normalised Network measures	VPT-TEA	FT	p-value
L	56.95 (±14.42)	45.02 (±9.867)	0.368
GEff	5.458 (±1.292)	5.743 (±1.151)	0.524
C	7.109 (±1.724)	6.551 (±1.654)	0.358
LEff	0.913 (±0.210)	0.846 (±0.204)	0.365
Q	0.607 (±0.148)	0.594 (±0.008)	**0.007**
ϕ	2.343 (±0.786)	3.379 (±0.997)	**0.003**

One-way ANCOVA, controlling for GA at MRI and sex, was performed to determine differences between groups. Numbers in bold indicate significant results between groups (p<0.05).

Supplementary Table S3

Hub regions in VPT-TEA and FT infants. Color-code: grey – subcortical nodes; yellow – limbic nodes; purple – temporal nodes; green – parietal nodes.

VPT-TEA	Nodal degree	FT	Nodal degree
Thalamus right	59	Thalamus right	69
Thalamus left	56	Thalamus left	64
Hippocampus left	46	Dorsal cingulate gyrus left	51
Insula left	45	Dorsal cingulate gyrus right	48
Insula right	45	Precuneus left	47
Hippocampus right	45	Caudate left	47
Putamen left	45	Putamen right	47
Putamen right	45	Insula right	46
Dorsal cingulate gyrus right	43	Hippocampus right	46
Amygdala right	43		
Caudate right	43		
Superior temporal gyrus left	43		
Amygdala left	42		
Caudate left	42		
Heschl gyrus left	42		
Superior temporal gyrus right	42		
Average nodal degree	51.67	**Average nodal degree**	45.38

136

Supplementary Table S4

Description of cortico-cortical, cortico-subcortical and subcortico-subcortical connections (in the right hemisphere, left hemisphere and inter-hemispheric) with decreased connectivity strength in VPT-TEA in comparison to FT infants.

		RH	**LH**	**IH**
FRONTAL	**Fronto-Frontal**	SFGdor.R to IFGtriang.R. ORBsup.R to OLF.R. ORBinf.R to OLF.R. ORBsup.R to REC.R.	ORBsup.L to ORBinf.L. ORBsup.L to OLF.L. ORBinf.L to OLF.L.	
	Fronto-Temporal	SFGdor.R to TPOsup.R. ORBsup.R to TPOsup.R. ORBmid.R to TPOsup.R. SFGmed.R to TPOsup.R. ORBsupmed.R to TPOsup.R.	ORBsup.L to TPOsup.L. ORBmid.L to TPOsup.L. IFGtriang.L to TPOsup.L. ORBinf.L to TPOsup.L. OLF.L to TPOsup.L. ORBsupmed.L to TPOsup.L. REC.L to TPOsup.L. OLF.L to TPOmid.L. REC.L to ITG.L.	
	Fronto-Parietal	ROL.R to PCL.R.	ORBsup.L to SMG.L.	PreCG.R to PCUN.L.
	Fronto-Occipital		IFGtriang.L to CUN.L. ORBinf.L to CUN.L. IFGoperc.L to FFG.L. ORBinf.L to FFG.L.	
LIMBIC	**Limbic-Frontal**	OLF.R to INS.R. ORBinf.R to ACG.R. ORBinf.R to PHG.R. OLF.R to PHG.R.	IFGoperc.L to PCG.L. OLF.L to AMYG.L.	SFGdor.R to DCG.L. SFGmed.R to DCG.L.
	Limbic-Limbic	PCG.R to PHG.R.	ACG.L to PCG.L. PCG.L to PHG.L. PCG.L to AMYG.L.	DCG.L to HIP.R.
	Limbic-Temporal	ACG.R to TPOsup.R. PCG.R to TPOmid.R.	PCG.L to STG.L.	
	Limbic-Parietal		PCG.L to SMG.L.	DCG.L to PoCG.R. DCG.L to SPG.R. INS.R to PCUN.L. DCG.R to PCUN.L. PCG.R to PCUN.L.
	Limbic-Occipital	PCG.R to FFG.R.	PHG.L to CUN.L.	
OTHERS	**Parieto-Parietal**	SPG.R to SMG.R. SMG.R to PCUN.R. SMG.R to PCL.R.	SPG.L to SMG.L. SPG.L to ANG.L. SMG.L to PCUN.L.	
	Parieto-Temporal	PCL.R to STG.R. PCUN.R to TPOsup.R. PCUN.R to TPOmid.R.	PoCG.L to TPOsup.L. PCL.L to TPOsup.L. SPG.L to MTG.L.	PCUN.L to HES.R.
	Parieto-Occipital		SOG.L to SMG.L.	LING.R to PCUN.L.
	Temporo-Occipital		FFG.L to STG.L.	

Table header spanning: *Cortico-Cortical*

137

Cortico-Subcortical			
	RH	**LH**	**IH**
FRONTAL	IFGoperc.R to CAU.R. ORBinf.R to CAU.R.	PreCG.L to CAU.L. ORBinf.L to CAU.L. IFGtriang.L to THA.L. ORBinf.L to THA.L. OLF.L to THA.L.	
LIMBIC	PCG.R to THA.R. HIP.R to THA.R.	PCG.L to PUT.L.	
TEMPORAL	TPOsup.R. to CAU.R TPOsup.R. to PAL.R TPOsup.R. to THA.R	TPOsup.L. to CAU.L TPOsup.L. to PUT.L TPOsup.L. to PAL.L	
OCCIPITAL	FFG.R to THA.R.	CAL.L to PAL.L. CAL.L to THA.L. FFG.L to CAU.L.	
Subcortico-Subcortical			
	RH	**LH**	**IH**
	CAU.R to THA.R.	CAU.L to THA.L.	

Supplementary Table S5

Number and Frequency of cortico-cortical, cortico-subcortical and subcortico-subcortical connections with decreased connectivity strength in VPT-TEA in comparison to FT infants.

	Cortico-Cortical		
	Connections	**Number**	**Frequency**
Fronto-Temporal	ORB to TPO	7	0.077777778
	SFG to TPO	2	0.022222222
	OLF to TPO	2	0.022222222
	IFG to TPO	1	0.011111111
	REC to TPO	1	0.011111111
	REC to ITG	1	0.011111111
	sum	14	0.155555555
Fronto-Limbic	SFG to DCG	2	0.022222222
	ORB to ACG	1	0.011111111
	ORB to PHG	1	0.011111111
	OLF to INS	1	0.011111111
	OLF to PHG	1	0.011111111
	OLF to AMYG	1	0.011111111
	IFG to PCG	1	0.011111111
	sum	8	0.088888888
Fronto-Frontal	ORB to OLF	4	0.044444444
	ORB to ORB	1	0.011111111
	ORB to REC	1	0.011111111
	SFG to IFG	1	0.011111111
	sum	7	0.077777777
Temporo-Parietal	PCUN to TPO	2	0.022222222
	PoCG to TPO	1	0.011111111
	PCL to TPO	1	0.011111111
	PCL to STG	1	0.011111111
	SPG to MTG	1	0.011111111
	PCUN to HES	1	0.011111111
	sum	7	0.077777777
Limbic-Parietal	PCG to SMG	1	0.011111111
	DCG to PoCG	1	0.011111111
	DCG to SPG	1	0.011111111
	INS to PCUN	1	0.011111111
	DCG to PCUN	1	0.011111111
	PCG to PCUN	1	0.011111111
	sum	6	0.066666666
Parieto-Parietal	SPG to SMG	2	0.022222222
	SMG to PCUN	2	0.022222222
	SMG to PCL	1	0.011111111
	SPG to ANG	1	0.011111111
	sum	6	0.066666666
Limbic-Limbic	PCG to PHG	2	0.022222222
	ACG to PCG	1	0.011111111
	PCG to AMYG	1	0.011111111
	DCG to HIP	1	0.011111111
	sum	5	0.055555555
Fronto-Ocipital	ORB to CUN	1	0.011111111
	ORB to FFG	1	0.011111111
	IFG to FFG	1	0.011111111
	IFG to CUN	1	0.011111111
	sum	4	0.044444444

	Connections	Number	Frequency
Fronto-Parietal	ORB to SMG	1	0.011111111
	ROL to PCL	1	0.011111111
	PreCG to PCUN	1	0.011111111
	sum	3	0.033333333
Limbic-Temporal	ACG to TPO	1	0.011111111
	PCG to TPO	1	0.011111111
	PCG to STG	1	0.011111111
	sum	3	0.033333333
Limbic-Occipital	PCG to FFG	1	0.011111111
	PHG to CUN	1	0.011111111
	sum	2	0.022222222
Parieto-Occipital	SOG to SMG	1	0.011111111
	LING to PCUN	1	0.011111111
	sum	2	0.022222222
Temporo-Occipital	FFG.L to STG.L	1	0.011111111
	sum	1	0.011111111

Subcortico-Cortical			
	Connections	**Number**	**Frequency**
Frontal	ORB to CAU	2	0.022222222
	ORB to THA	1	0.011111111
	IFG to CAU	1	0.011111111
	IFG to THA	1	0.011111111
	PreCG to CAU	1	0.011111111
	OLF to THA	1	0.011111111
	sum	7	0.077777777
Temporal	TPO to CAU	2	0.022222222
	TPO to PAL	2	0.022222222
	TPO to THA	1	0.011111111
	TPO to PUT	1	0.011111111
	sum	6	0.066666666
Limbic	PCG to THA	1	0.011111111
	HIP to THA	1	0.011111111
	PCG to PUT	1	0.011111111
	sum	3	0.033333333
Occipital	FFG to THA	1	0.011111111
	CAL to PAL	1	0.011111111
	CAL to THA	1	0.011111111
	FFG to CAU	1	0.011111111
	sum	4	0.044444444
Subcortico-Subcortical			
	CAU to THA	2	0.022222222

Supplementary Table S6

Number and frequency of nodes participating in all connections with decreased connectivity strength in VPT-TEA in comparison to FT infants.

|	*Nodes*	*Number*	*Frequency*
Frontal	ORB (sup, supmed, mid, inf) L/R	22	0.244444444
	IFG (triang, operc) L/R	7	0.077777778
	SFG (dor, med) L/R	5	0.055555556
	OLF L/R	10	0.111111111
	REC L/R	3	0.033333333
	PreCG. L/R	2	0.022222222
	ROL R	1	0.011111111
	sum	50	0.555555556
Temporal	TPO (sup, mid) L/R	25	0.277777778
	STG L/R	3	0.033333333
	MTG L	1	0.011111111
	ITG L	1	0.011111111
	HES R	1	0.011111111
	sum	31	0.344444444
Limbic	PCG L/R	12	0.133333333
	DCG L/R	6	0.066666667
	PHG L/R	5	0.055555556
	ACG L/R	3	0.033333333
	HIP R	2	0.022222222
	AMYG L	2	0.022222222
	INS R	1	0.011111111
	sum	31	0.344444444
Parietal	PCUN L/R	10	0.111111111
	SMG L/R	8	0.088888889
	SPG L/R	5	0.055555556
	PCL L/R	4	0.044444444
	PoCG L/R	2	0.022222222
	ANG L	1	0.011111111
	sum	30	0.333333333
Occipital	FFG L/R	6	0.066666667
	CUN L	3	0.033333333
	CAL L	2	0.022222222
	LING.R	1	0.011111111
	SOG.L	1	0.011111111
	sum	13	0.144444444
Subcortical	THA L/R	10	0.111111111
	CAU L/R	9	0.1
	PAL L/R	3	0.033333333
	PUT.L	2	0.022222222
	sum	24	0.266666667

Supplementary Table S7

Nodes ordered by the number and frequency of connections with decreased connectivity strength in VPT-TEA, in which they participate.

Nodes	Number	Frequency
TPO (sup, mid) L/R	25	0.277777778
ORB (sup, supmed, mid, inf) L/R	*22*	*0.244444444*
PCG L/R	12	0.133333333
PCUN L/R	10	0.111111111
THA L/R	10	0.111111111
OLF L/R	10	0.111111111
CAU L/R	9	0.1
SMG L/R	8	0.088888889
IFG (triang, operc) L/R	7	0.077777778
DCG L/R	6	0.066666667
FFG L/R	6	0.066666667
PHG L/R	5	0.055555556
SFG (dor, med) L/R	5	0.055555556
SPG L/R	5	0.055555556
PCL L/R	4	0.044444444
PAL L/R	3	0.033333333
ACG L/R	3	0.033333333
REC L/R	3	0.033333333
STG L/R	3	0.033333333
CUN L	3	0.033333333
PreCG. L/R	2	0.022222222
HIP R	2	0.022222222
AMYG L	2	0.022222222
PoCG L/R	2	0.022222222
PUT.L	2	0.022222222
CAL L	2	0.022222222
ROL R	1	0.011111111
MTG L	1	0.011111111
ITG L	1	0.011111111
HES R	1	0.011111111
INS R	1	0.011111111
ANG L	1	0.011111111
LING.R	1	0.011111111
SOG.L	1	0.011111111

Supplementary Figures
Supplementary Figure S1
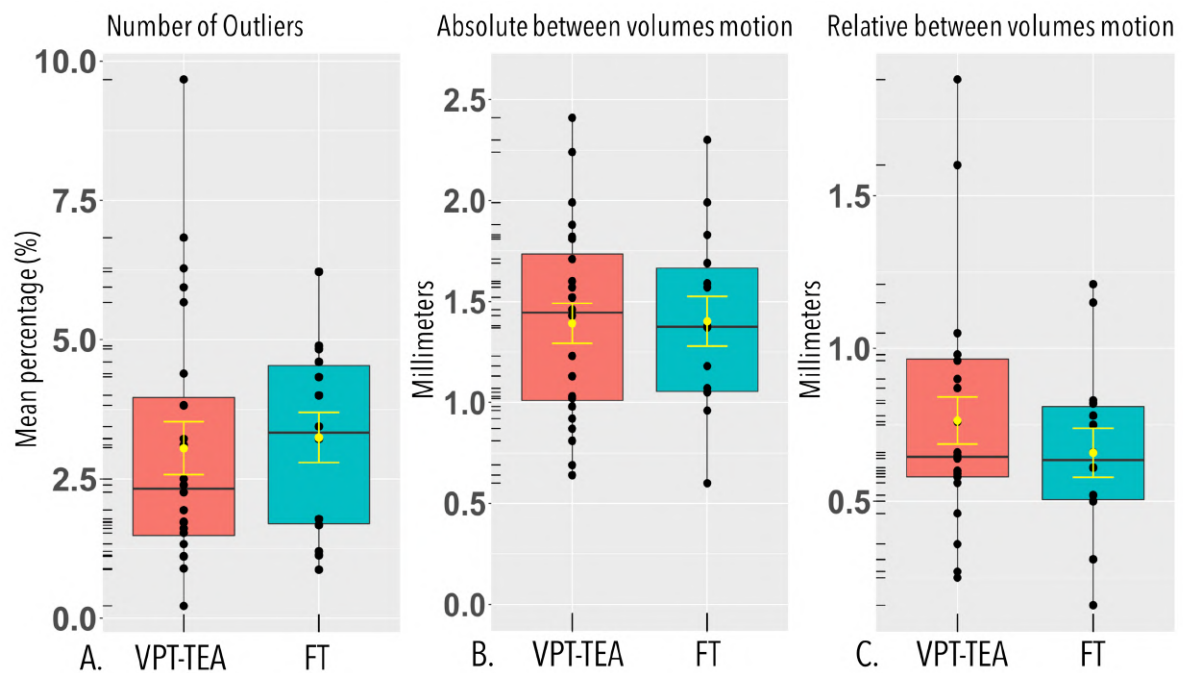
Boxplots of motion measures in VPT-TEA (in red) and FT infants (in green): Number of outliers, mean percentage (%) (A), Absolute between volumes motion, millimetres (B), Relative between volumes motion, millimetres (C). Independent samples T-test was performed to determine differences between groups. Mean and standard deviation are illustrated in yellow on each boxplot. No statistically significant differences were found between groups (p > 0.05).

Study 2

Music enhances structural maturation of emotional processing neural pathways in very preterm infants

Music enhances structural maturation of emotional processing neural pathways in very preterm infants

Joana Sa de Almeida[1]; Lara Lordier[1]; Benjamin Zollinger[2]; Nicolas Kunz[3]; Matteo Bastiani[4,5,6]; Laura Gui[7]; Alexandra Adam-Darque[1]; Cristina Borradori-Tolsa[1]; François Lazeyras[7]; Petra S. Hüppi[1*]

[1] Division of Development and Growth, Department of Woman, Child and Adolescent, University Hospitals of Geneva, Geneva, Switzerland

[2] Department of Psychology of Yale University, New Haven, Connecticut, USA

[3] Center of BioMedical Imaging (CIBM), Ecole Polytechnique Fédérale de Lausanne (EPFL), Lausanne, Switzerland

[4] Sir Peter Mansfield Imaging Centre, School of Medicine, University of Nottingham, UK

[5] NIHR Biomedical Research Centre, University of Nottingham, UK

[6] Wellcome Centre for Integrative Neuroimaging (WIN) - Centre for Functional Magnetic Resonance Imaging of the Brain (FMRIB), University of Oxford, UK

[7] Department of Radiology and Medical Informatics; Center of BioMedical Imaging (CIBM), University of Geneva, Geneva, Switzerland

*Corresponding author address:

Hôpitaux Universitaires de Genève; Département de la femme, de l'enfant et de l'adolescent, Service de développement et croissance, Hôpital des enfants, Rue Willy-Donzé 6, CH-1211 Genève 14, Suisse; petra.huppi@hcuge.ch

Abstract

Prematurity disrupts brain maturation by exposing the developing brain to different noxious stimuli present in the neonatal intensive care unit (NICU) and depriving it from meaningful sensory inputs during a critical period of brain development, leading to later neurodevelopmental impairments.

Musicotherapy in the NICU environment has been proposed to promote sensory stimulation, relevant for activity-dependent brain plasticity, but its impact on brain structural maturation is unknown. Neuroimaging studies have demonstrated that music listening triggers neural substrates implied in socio-emotional processing and, thus, it might influence networks formed early in development and known to be affected by prematurity.

Using multi-modal MRI, we aimed to evaluate the impact of a specially composed music intervention during NICU stay on preterm infant's brain structure maturation. 30 preterm newborns (out of which 15 were exposed to music during NICU stay and 15 without music intervention) and 15 full-term newborns underwent an MRI examination at term-equivalent age, comprising diffusion tensor imaging (DTI), used to evaluate white matter maturation using both region-of-interest and seed-based tractography approaches, as well as a T2-weighted image, used to perform amygdala volumetric analysis.

Overall, WM microstructural maturity measured through DTI metrics was reduced in preterm infants receiving the standard-of-care in comparison to full-term newborns, whereas preterm infants exposed to the music intervention demonstrated significantly improved white matter maturation in acoustic radiations, external capsule/claustrum/extreme capsule and uncinate fasciculus, as well as larger amygdala volumes, in comparison to preterm infants with standard-of-care. These results suggest a structural maturational effect of the proposed music intervention on premature infants' auditory and emotional processing neural pathways during a key period of brain development.

Keywords

1. Introduction

Preterm birth, accounting for approximately 15 million yearly cases worldwide, is associated with a range of long-term complications (Blencowe et al., 2013), in particular neurodevelopmental disorders. Such complications stem from the fact that preterm birth disrupts the normal brain maturation during a critical period of fetal brain growth (Brody et al., 1987; Dubois et al., 2008; Huang et al., 2006; Kiss et al., 2014a; Nossin-Manor et al., 2013; Volpe, 2009b), exposing the developing brain to different noxious events in the neonatal intensive care unit (NICU) and depriving it from meaningful sensory inputs relevant for activity-dependent plasticity (Kiss et al., 2014a; Radley and Morrison, 2005).

Although advances in neonatal medicine have improved preterm infants' outcome, dedicated brain-oriented care has not been established yet (Als and McAnulty, 2014; Chang, 2015; Sizun and Westrup, 2004). Up to 40%-50% of very preterm infants (VPT), those born before 32 weeks gestational age (GA), still experience neurodevelopmental impairments evident in childhood (Anderson and Doyle, 2003; Bhutta et al., 2002; Marlow, 2004; Montagna and Nosarti, 2016; Spittle et al., 2009; Spittle et al., 2011; Williams et al., 2010; Witt et al., 2014), and 25% of VPT infants evidence behavioral impairments, characterized by inattention, anxiety, internalizing and socio-emotional problems (Anderson and Doyle, 2003; Arpi and Ferrari, 2013; Bhutta et al., 2002; Marlow, 2004; Montagna and Nosarti, 2016; Spittle et al., 2009; Spittle et al., 2011; Williams et al., 2010; Witt et al., 2014). Moreover, VPT infants are at higher risk of developing psychiatric disorders, such as attention deficit and hyperactivity disorder (ADHD), autism spectrum disorder (ASD), anxiety and depression (Johnson and Marlow, 2011; Nosarti et al., 2012; Treyvaud et al., 2013).

By term-equivalent age (TEA) and also later in childhood and adulthood, the preterm brain has been found to be structurally different from that of a healthy full-term born individual. Magnetic resonance imaging (MRI) has evidenced early developmental brain anomalies in preterm infants, such as regional cortical and subcortical volumes changes (Ball et al., 2017; Cismaru et al., 2016; Huppi and Dubois, 2006; Ment et al., 2009; Nosarti, 2013; Padilla et al., 2015; Peterson et al., 2000) and alterations of brain networks and their microstructural characteristics (Fischi-Gomez et al., 2015; Pecheva et al., 2018; Rogers et al., 2012), which were shown to correlate with specific neuropsychological deficits after preterm birth. In particular, preterm infants were found to present structural brain alterations in regions thought to subserve emotional processing and which were related to later socio-emotional deficits.

These alterations include reduced volumes of amygdala, hippocampus, orbito-frontal cortex (OFC), insula and posterior cingulate cortex (Aanes et al., 2015; Anjari et al., 2007; Ball et al., 2012; Cismaru et al., 2016; Gimenez et al., 2006; Huppi et al., 1998a; Inder et al., 2005; Nosarti et al., 2014; Peterson et al., 2000; Rogers et al., 2012; Thompson et al., 2007; Thompson et al., 2013), white matter (WM) immaturity of the OFC regions (Rogers et al., 2012), prefrontal and medial orbito-frontal-cortico-striatal networks (Fischi-Gomez et al., 2016), and of several WM tracts, namely forceps minor, forceps major, inferior fronto-occipital fasciculus/inferior longitudinal fasciculus, superior longitudinal fasciculus and external capsule (Loe et al., 2013; Skranes et al., 2007).

Recently, NICUs have been searching for developmentally oriented care to modulate preterm infants' sensory input during this critical period of development, with the aim of improving early brain maturation. Music has been an implemented approach for meaningful sensory stimulation during NICU stay, thought to be relevant for activity-dependent brain plasticity during a critical period of auditory maturation (Graven and Browne, 2008; Kiss et al., 2014a; Lasky and Williams, 2005). In adults, music listening is known to trigger neural substrates involved in socio-emotional functions, comprising amygdala, hippocampal formation, ventral striatum (including nucleus accumbens), pre-supplementary motor area, cingulate cortex, insula and OFC (Koelsch et al., 2004; Koelsch, 2010; Popescu et al., 2004; Zatorre et al., 2009). Thus, music listening might hold the potential to modulate neural networks known to be affected by prematurity early in development and in particular involved in socio-emotional processing.

However, to date, there is little evidence of the effect of music on preterm infants' brain development. An ultrasound study has shown that the enrichment of preterm infants' early postnatal environment with audio recordings of maternal sounds (heartbeat, speech, reading and singing voice) increases cortical thickness in the primary auditory cortex (Webb et al., 2015). In a fMRI study, preterm infants exposed to a specific music intervention during NICU stay, when at term-age, had an increased functional connectivity between the primary auditory cortex and the thalamus, middle cingulate cortex and striatum when listening to the known music, regions linked to familiarity, pleasant and arousing music processing (Lordier et al., 2018). Additionally, the effect of this music intervention was explored by means of its impact on preterm infants' resting-state functional connectivity. When compared to full-term infants, premature infants in the control group evidenced a decreased functional connectivity of the salience network (comprising bilateral insula and anterior cingulate) with other networks involved both in sensory and high level cognitive networks (auditory, sensorimotor, superior

frontal, thalamus and precuneus networks). Conversely, preterm infants receiving the music intervention evidenced a higher functional connectivity in these same regions when compared to preterm infants control (Lordier et al., 2019a). However, the extent to which music listening during the early postnatal period in preterm infants can influence brain macrostructure and microstructural network maturation remains to be explored and is the primary aim of this study.

Diffusion tensor imaging (DTI) is a non-invasive MRI method that uses the diffusion anisotropy of water molecules within the tissues to allow *in vivo* visualization and quantification of WM microstructure and connectivity (Huppi and Dubois, 2006; Pierpaoli and Basser, 1996b). It characterises water diffusion using a mathematical tensor model, allowing the calculation of several DTI-derived scalar indices, including: fractional anisotropy (FA), quantifying the degree of tissue anisotropy and which has been used to assess WM integrity (Kamagata et al., 2012; Kochunov et al., 2009; Onu et al., 2012); and mean diffusivity (MD) providing the overall magnitude of water diffusion. Rapid changes in FA and MD take place early in development: in preterm infants from 27 to 42 weeks GA, WM FA increases while the MD decreases (Aeby et al., 2009; Neil et al., 2002; Partridge et al., 2004), accompanying an increased WM-fiber organization, increased axonal density and coherence, decreased water content and preliminary myelination occurring during early brain development (Aeby et al., 2009; Beaulieu, 2002; Dubois et al., 2008; Mukherjee et al., 2002; Shim et al., 2012). To better characterize the mechanisms underlying FA modifications, studies investigate radial diffusivity (RD) and axial diffusivity (AD), indices also derived from the diffusion tensor. RD may be sensitive to myelination and correlates positively with mean axon diameter (Beaulieu, 2002), whereas AD alterations have been associated with axon morphologic changes, such as axonal density or calibre (Jones, 2011). Increased FA and decreased MD and RD in WM of preterm infants at TEA have been shown to be related to subsequent improved neurodevelopmental performance, namely motor, cognitive and language performance in early childhood (Counsell et al., 2008; Duerden et al., 2015; Krishnan et al., 2007), as well as improved visual function (Bassi et al., 2008; Groppo et al., 2014).

In this study, we used DTI to characterize the WM microstructural maturation in VPT infants exposed to music during NICU stay, in comparison to VPT infants receiving the standard-of-care and to full-term infants, all at term age. For that purpose, we used a template-based region-of-interest (ROI) analysis method comprising 20 WM ROI and subsequently a seed-based tractography analysis of three selected tracts involved in auditory or socio-emotional processing: acoustic radiations, interhemispheric temporal callosal fibers and uncinate fasciculus. Additionally, at a macrostructural level, we aimed to assess if a music

intervention in VPT infants during NICU stay could have an impact on amygdala volume, given amygdala's central role in emotion modulation during music processing and evidence of its volumetric reduction in preterm infants at both TEA and in adulthood, according to previous studies (Cismaru et al., 2016; Peterson et al., 2000).

We hypothesize that an early postnatal music intervention, during NICU hospitalization, can improve preterm infants' macro and microstructural brain maturation, falling in line with the expected developmental trajectory, in particular in the cortico-limbic networks.

2. Materials and Methods

2.1. Subjects

39 VPT infants (GA at birth <32 weeks) were recruited at the neonatal unit of the University Hospitals of Geneva (HUG), Switzerland, from 2013 to 2016, as part of a prospective randomized clinical trial entitled 'The effect of music on preterm infant's development' (NCT03689725), registered at register.clinicaltrials.gov. Out of these, 20 received a music intervention during NICU stay (PTM), whereas 19 did not listen to music and received the standard-of-care during NICU stay (PTC).

Additionally, 40 full-term (FT) infants were recruited at the maternity of HUG, from 2011 to 2016 as part of clinical trials studying the impact of prematurity on neonatal preterm brain development.

Research Ethics Committee approval was granted for the studies and written parental consent was obtained prior to infant's participation to the studies.

Six preterm infants were excluded from the study before the MRI due to: parental refusal (2 PTM, 1 PTC), transfer to another hospital (1 PTM) and insufficient number of music intervention sessions (less than 15 intervention sessions: 2 PTM).

All subjects underwent an MRI examination at TEA (37-42 weeks GA). Infants whose MRI protocol acquisition was incomplete, not comprising a T2-weighted image and DTI sequence, or that presented major focal brain lesions or major movement on MRI images were excluded from the analysis. The final sample of infants used for DTI analysis consisted of: 15 PTM (7 females/8 males, mean GA at birth: 28.58 ± 2.30 weeks, mean GA at MRI: 40.15 ± 0.61 weeks), 15 PTC (10 females/5 males, mean GA at birth: 28.30 ± 2.34 weeks, mean GA at MRI: 40.48 ± 0.61 weeks) and 15 FT infants (9 females/6 males, mean GA at birth: 39.32 ± 1.03 weeks, mean GA at MRI: 39.63 ± 1.02 weeks). The flow chart of the participant selection process is provided in Supplementary Fig. S1. No significant difference between the PTM and PTC

152

groups was found in demographic and perinatal variables: GA at birth, weight, sex, height, head circumference at birth, neonatal asphyxia, bronchopulmonary dysplasia, intraventricular hemorrhages, sepsis (positive blood culture), GA at MRI and socio-economic parental status (Largo et al., 1989) (Table 1). Regarding T2-weighted images used for amygdala volumetric analysis, from the 45 infants retained for DTI analysis, 11 were excluded due to movement artifacts preventing correct amygdala segmentation. The remaining 34 infants included in this analysis were distributed as follow: 10 PTC, 11 PTM and 13 FT infants.

Table 1

Clinical characteristics of the infants

Clinical Characteristics	Full-term (FT) n=15	Preterm Music (PTM) n=15	Preterm Control (PTC) n=15	p-value* PTM vs PTC
Gestational age at birth, weeks, mean (SD)	39.2 (±1.3)	28.58 (±2.3)	28.30 (±2.3)	0.74
Extremely Premature, n (%)		4 (26.7%)	8 (53.3%)	0.14
Sex: female (%)/male (%)	6(40.0)/9(60.0)	8(53.3)/7(46.7)	5(33.3)/10(66.7)	0.27
Birth weight, gram, mean (SD)	3275.3 (±440.5)	1129.7 (±328.5)	1101 (±411.9)	0.84
Birth height, centimetre, mean (SD)	50.0 (±1.8)	36.8 (±3.2)	36.5 (±4.7)	0.88
Birth head circumference (cm), mean (SD)	34.4 (±1.3)	26.5 (±3.1)	25.7 (±2.6)	0.45
APGAR score, 1 min (SD)	8.87 (±0.5)	4.93 (±3.4)	5.13 (±2.8)	0.86
APGAR score, 5 min (SD)	9.53 (±0.9)	6.73 (±2.2)	7.87 (±1.2)	0.09
Intrauterine Growth Restriction, n (%)	1 (6.7)	1 (6.7)	4 (66.7)	0.14
Neonatal asphyxia, n (%)	0	0	0	
Bronchopulmonary dysplasia, n (%)	1 (6.7)	5 (33.3)	4 (26.7)	0.69
Intraventricular Haemorrhage (grade 1-2), n (%)	0	4 (26.7%)	1 (6.7%)	0.14
Gestational age at MRI scan, weeks, mean (SD)	39.54 (±1.2)	40.15 (±0.6)	40.48 (±0.6)	0.16
Socio-economic score (range 2-12), mean (SD)	4.10 (±2.5)	6.07 (±3.5)	6.00 (±3.4)	0.96

* Group-characteristics were compared using one-way between-subjects ANOVA for continuous variables and chi-squared test for categorical variables.

2.2. Music Intervention

During NICU stay, from 33 weeks GA until discharge, the PTC group received standard-of-care, while the PTM group listened approximately five times per week (mean: 4.84 ± 1.18), through headphones, to an 8 minutes musical piece created for the project by the composer Andreas Vollenweider (http://vollenweider.com/en). The musical piece was selected among three different music tracks of 8 minutes duration, according to the waking state of the child (waking up, falling asleep, being active). All tracts were composed of sounds of harp, punji (charming snake flute) and bells, that interactively create a melody. The 8 minutes duration was chosen to suit the duration of the sleep-wake state transitions of the infant. The musical

instruments and melody were chosen based on the behavioral and physiological responses of preterm newborns (for more details consult Appendix B of Lordier et al., 2018).

2.3. MRI acquisition

All infants were scanned after receiving breast or formula feeding, during natural sleep and using a vacuum mattress for immobilization. No sedation was used. MR-compatible headphones were used (MR confon, Magdeburg, Germany) to protect infants from scanner's noise. All infants were monitored for heart rate and oxygen saturation during the entire scanning time.

MRI acquisition was performed on 3.0T Siemens MR scanners (Siemens, Erlangen, Germany): Siemens TIM Trio with a 32-channel head coil and Siemens Prisma with a 64-channel head coil. Chi-squared test revealed no significant difference regarding the distribution of scanner/coils between groups, $\chi(2) = 3.462$, p = 0.177 (TIMTrio-32channel: FT=12, PTM=8, PTC=12; Prisma-64channel: FT=3, PTM=7, PTC=3).

T2-weighted images for anatomical reference were acquired using the following parameters: 113 coronal slices, TR= 4990ms, TE=151ms, flip angle=150°, matrix size=256x164; voxel size=0.4x0.4x1.2mm^3, total scan time of 6:01 minutes.

DTI protocol was acquired with a single-shot spin echo echo-planar imaging (SE-EPI) Stejksal-Tanner sequence (TE=84ms, TR= 7400ms, acquisition matrix 128x128 mm, reconstruction matrix 128x128mm, 60 slices, voxel size 2x2x2mm^3). Images were acquired in the axial plane, in anterior-posterior (AP) phase encoding (PE) direction, with diffusion gradients applied in 30 non-collinear directions with a b-value of 1000 s/mm^2 and one non-diffusion weighted image (b=0), with a total scan time of 4:12 minutes.

2.4. Pre-processing

DTI data were preprocessed using the diffusion toolbox of the FMRIB Software Library, FSL v5.0.10, https://fsl.fmrib.ox.ac.uk/fsl/fslwiki/ (Behrens et al., 2003; Smith et al., 2004). Eddy current-induced distortions and gross subject movement were corrected using the FSL "eddy" tool (Andersson and Sotiropoulos, 2016), which included a function optimized for neonatal diffusion data regarding correction of distortions caused by motion-induced signal dropout and intra-volume subject movement (Andersson et al., 2016; Andersson et al., 2017; Bastiani et al., 2019).

2.5. Data analysis

2.5.1. ROI analysis

20 ROI situated in the WM were manually drawn on a study-specific template. This template was generated using DTI-TK (http://www.nitrc.org/projects/dtitk), a toolkit used for tensor-based spatial normalization of diffusion MRI data to an iteratively optimized study-specific template (Zhang et al., 2006). First, we created a study-specific template by choosing one subject and registering all the subjects to that particular one. Then, we re-registered all subjects to this newly generated template in order to obtain our final study-specific template where we drew the 20 ROI. The study-specific template and details regarding its construction can be found in Supplementary Material Fig. S2. The 20 ROI drawn on this template were back transformed to each subject's space in order to compute ROI-average estimates of DTI measures (FA, MD, AD, RD) per subject using FSL DTIFIT. Besides the ROI-average DTI estimates per subject, global DTI average measures (FA, MD, AD, RD) were obtained for each subject by averaging the mean DTI measures of all 20 ROI. The 20 ROI were the following: splenium of corpus callosum (cc-sp), body of corpus callosum (cc-bd), genu of corpus callosum (cc-ge), superior corona radiata (scr), forceps minor (fmin), anterior commissure (ac), forceps major (fmaj), posterior limb of the internal capsule (plic), anterior limb of the internal capsule (alic), inferior longitudinal fasciculus (ilf), external capsule/claustrum/extreme capsule (ec), superior longitudinal fasciculus (slf), optic radiation (or), acoustic radiation (ar), frontal gyrus white matter (fg-wm), arcuate fasciculus (af), superior temporal gyrus white matter (stg-wm), medial temporal gyrus white matter (mtg-wm), cingulum (cg) and fornix (fx), (Supplementary Fig. S3).

2.5.2. Tractography analysis

In the context of this study, a hypothesis-based tractography approach was chosen and three tracts were reconstructed using seed-based probabilistic tractography performed with FSL v5.0.10 (Behrens et al., 2003; Smith et al., 2004): acoustic radiations, interhemispheric temporal callosal fibers (both involved in the processing of auditory information) and the uncinate fasciculus (known to be implicated in socio-emotional processing) (Supplementary Fig. S4). Fiber orientation distributions (FOD) were estimated using the model-based approach available in FSL's Bedpostx (Behrens et al., 2007). This method runs Markov Chain Monte Carlo sampling to build up distributions on FOD parameters at each voxel, with up to three fiber compartments estimated in each voxel, allowing the automatic detection of the number

of crossing fibres per voxel. Following Bedpostx, seed-based probabilistic tractography was performed using Probtrackx2 (Behrens et al., 2007), computing 5000 streamlines from each seed voxel.

Given the specificity of our population and of the tracts we aimed to reconstruct, we performed tractography in the subject's native diffusion space using manually-placed masks. Therefore, sets of "seed" (regions where the tract starts), "waypoint" (regions through which tracts should go through), "stop" (regions where tracts terminate) and "exclusion" (regions that tracts should avoid) masks were drawn manually directly in the subject diffusion space, always by the same operator, blinded for the groups, and in the same manner for all subjects (the same masks were selected per tract for each subject). Tractography results obtained for each subject were thresholded at 0.01 and binarized to obtain tract-specific masks. DTI metrics (FA, MD, AD and RD) were calculated in each subject's diffusion space for each tract using the obtained masks.

Masks for each tract were drawn according to published literature and atlases (Adibpour et al., 2018; Akazawa et al., 2016; Oishi et al., 2010) and were designed as follows. For the left and right acoustic radiations, a seed mask was placed in primary auditory cortex (either left or right) in the temporal lobe and a waypoint mask was placed in the ipsilateral thalamus medial geniculate nucleus; an exclusion mask was generated to restrict the pathway to the hemisphere ipsilateral to the seed mask and exclude ipsilateral optic radiations fibers. For the interhemispheric temporal callosal fibers, two seeds were used, comprising the left and right primary auditory cortex and a waypoint in the splenium of corpus callosum; an exclusion mask was generated to exclude ipsilateral optic radiations and fibers of the posterior limb of internal capsule. For the left and right uncinate fasciculus, a first seed was placed in the temporal lobe (either right or left) and a second seed was placed in the ipsilateral inferior part of the frontal lobe; the seed masks were also used as waypoint masks; an exclusion mask was generated to restrict the pathway to the hemisphere ipsilateral to the seed mask and exclude fibers from the posterior limb of internal capsule (Supplementary Fig. S5).

2.5.3. Amygdala Volumetric analysis

To evaluate differences regarding amygdala volumes between PTM, PTC and FT newborns, amygdala was segmented on T2-weighted images. Segmentation was manually performed by a single rater using the manual contour editing function of ITK-SNAP visualization software (Yushkevich et al., 2006), based on anatomical guidelines for the localization of amygdala, according to published literature and to a neonatal atlas describing a protocol for amygdala

manual segmentation (Cismaru et al., 2016; Gousias et al., 2012). All segmentations were validated by a neurosurgeon with expertise in neuroanatomy. With the 0.4x0.4x1.2mm^3 voxel size resolution, amygdala delineation ran through approximately 8 coronal slices, 28 sagittal slices and 28 axial slices, which was deemed to enable a good visualization of the structure by the expert neurosurgeon. Additionally, intracranial cavity (ICC) volumes were obtained from the T2-weighted images of each subject with an automatic neonatal brain segmentation method (Gui et al., 2012). Out of the 45 patients, only 34 could be used for the analysis, due to movement in T2-weighted images, preventing correct delineation of amygdala limits (Supplementary Fig. S6).

2.6. Statistical analysis

All statistical analyses were performed with IBM SPSS Statistics version 25 (IBM Corp., Armonk, N.Y., USA).

Regarding neonatal and demographic data, categorical variables (sex, cases of extremely premature, intrauterine growth restriction, bronco-pulmonary dysplasia and intraventricular haemorrhage grade 1 and 2) were analysed using chi-squared test, whereas continuous variables were compared using one-way between-subjects ANOVA, with group (FT, PTC, PTM) as independent variable and the following dependent variables: GA at birth, GA at MRI, birth weight, birth height, birth head circumference, APGAR score at 1 and 5 minutes after birth and socio-economic parental status.

The global mean DTI metrics, obtained by averaging the 20 ROI per subject, were analysed by means of one-way between-subjects ANCOVA to investigate differences in global DTI metrics (FA, MD, RD and AD) between FT, PTM and PTC groups, controlling for GA at MRI. Additionally, DTI metrics per ROI were analysed by means of one-way between-subjects MANCOVA to study significant differences between FT, PTM and PTC groups on the mean FA, MD, RD and AD of each ROI, controlling for GA at MRI. Sex was not a significant predictor for any of the dependent variables, which is why it was not included as a co-variable in the final analysis.

Regarding tractography results of interhemispheric temporal callosal fibers, one-way between-subjects ANCOVA, controlling for GA at MRI, was conducted to determine the statistically significant differences between FT, PTM and PTC groups on mean FA, MD, RD and AD. For acoustic radiations and uncinate fasciculus tractography results, a two-way between-subjects ANCOVA, controlling for GA at MRI, was conducted to investigate statistically significant

differences in mean DTI metrics (FA, MD, RD and AD) between FT, PTM and PTC groups, as well as between left and right hemisphere. Sex was not a significant predictor for any of the dependent variables, which is why it was not included as a co-variable in the final analysis. Additionally, hemispheric asymmetries within each group were investigated by conducting paired-samples t-tests comparing mean DTI metrics of the left- and right-hemisphere fiber tracts per group.

Group differences in amygdala volumes were analysed using two-way between-subjects ANCOVA, with amygdala volume as dependent variable, ICC volume, GA at MRI and sex as covariates, and group (FT, PTM and PTC) and hemisphere (right and left) as independent variables. Hemispheric asymmetries were investigated with paired-samples t-tests, comparing left- and right-hemisphere amygdala volumes within each group.

One-way and two-way between-subjects ANOVA, ANCOVA and MANCOVA results were corrected for multiple comparisons, using Bonferroni post hoc test correction.

2.7. Data and code availability

All data were acquired in the context of the research project approved by the ethical committee in 2011.

Patient consent form did not include any clause for reuse or share of data. It stated explicitly that all data (clinic, biologic and imaging) would not be used with any other aim apart from the present research study and would not be shared with third parties.

Software and code used in this study are publically available as part of: FSL v5.0.10 (https://fsl.fmrib.ox.ac.uk/fsl/fslwiki/) and DTI-TK (http://www.nitrc.org/projects/dtitk) toolkits. Diffusion MRI data was processed using the developing Human Connectome Project (dHCP, http://www.developingconnectome.org) neonatal diffusion MRI automated pipeline, which can be found at this link: https://git.fmrib.ox.ac.uk/matteob/dHCP_neo_dMRI_pipeline_release (Bastiani et al. 2019).

3. Results

3.1. ROI analysis

First, whole-brain WM maturation per group was investigated using global DTI metrics (FA, MD, RD and AD averaged between all 20 ROI per subject). Our analysis revealed a statistically significant difference between FT, PTM and PTC on the global mean FA, $[F_{(2,41)}=9.285, p=0.0001]$, global mean MD, $[F_{(2,41)}=5.157, p=0.01]$ and global mean RD $[F_{(2,41)}=6.706,$

p=0.003]. After Bonferroni post hoc correction, PTC had a significantly lower global FA (p=0.0001) and a significantly higher global MD (p=0.008) and RD (p=0.002) than FT newborns, while PTM showed no significant difference in any of DTI metrics in comparison to FT infants (Fig. 1A, Fig. 1B, Tables 2 and 3).

Second, we analysed group differences in WM maturation in each ROI. Considering all the regions at the same time, one-way MANCOVA multivariate test yielded a significant difference between the group contrasts, [Wilks'λ = 0.147, F(40,44)=1.770, p=0.033]. Given the significance of the overall test, the univariate main effects were examined. There was a statistically significant difference between FT, PTM and PTC on mean FA in 11 of the 20 ROI: "cc-sp", "cc-bd", "cc-ge", "scr", "fmin", "ac", "plic", "ilf", "ec", "mtg-wm" and "fg-wm". Bonferroni post hoc test showed that mean FA was significantly reduced in PTC vs FT newborns in 11 ROI: "cc-sp" (p=0.0001), "cc-bd" (p=0.001), "cc-ge" (p=0.003), "scr" (p=0.043), "fmin" (p=0.011), "ac" (p=0.01), "plic" (p=0.045), "ilf" (p=0.024), "ec" (p=0.019), "fg-wm" (p=0.006) and "mtg-wm" (p=0.02). In contrast, mean FA was significantly reduced in PTM vs FT newborns in only 3 ROI: "cc-sp" (p=0.016), "cc-bd" (p=0.011) and "fg-wm" (p=0.027), and no significant difference was detected between PTM and FT infants in the other ROI. Moreover, in the "ec" ROI, FA was significantly higher in PTM vs PTC (p=0.01) (Fig.1C, Table 2).

In order to further explore the reduction of FA in preterm newborns vs full-term infants, we analysed the MD, RD and AD of those 11 ROI. In comparison to FT infants, PTC had a significantly higher MD in "cc-sp", "cc-bd", "ilf" and "fg-wm"; as well as a significantly higher RD in "cc-sp", "cc-bd", "cc-ge", "fmin", "ac", "ilf" and "fg-wm", and a significantly lower AD in "plic". PTM, in comparison to FT newborns, presented a significantly higher MD only in "cc-sp", a significantly higher RD in "cc-sp" and "cc-bd" and a significantly higher AD in "fg-wm". In the ROI "scr", "ec" and "mtg-wm" there were no significant differences regarding MD, RD or AD between groups (Table 3).

Effect size between groups in each region were calculated by means of Cohen's d, revealing a high practical significance (d > 0.8) between groups in all the regions where p≤0.05 (Supplementary Tables S1 and S2).
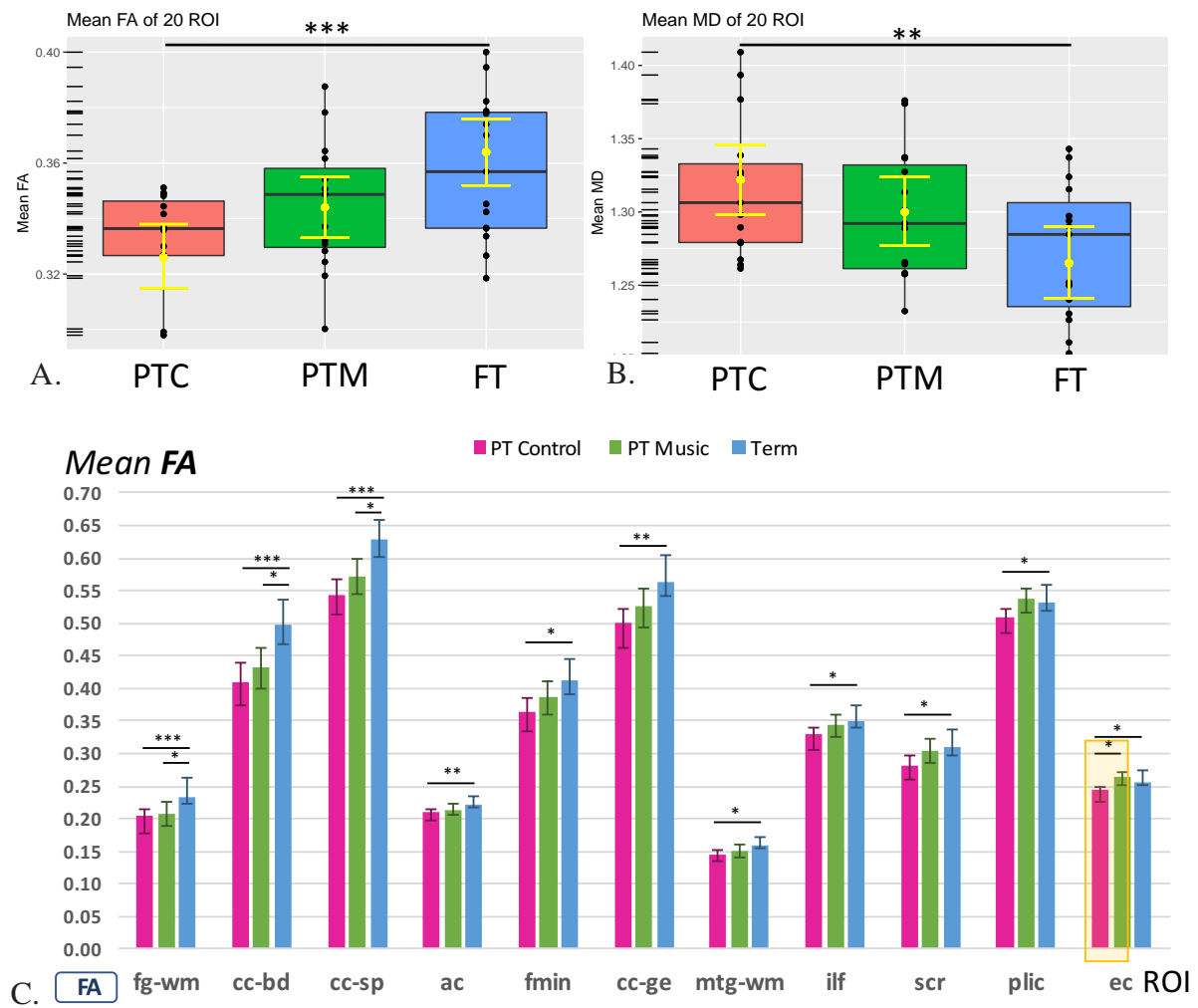
Fig. 1. Illustration of results from the statistical analysis of ROI-based DTI metrics. A - Boxplot of global mean FA over all ROI with mean and 95% confidence intervals (in yellow); B - Boxplot of global mean MD over all ROI with mean and 95% confidence intervals (in yellow); One-way between-subjects ANCOVA with correction for gestational age at MRI was performed with Bonferroni post hoc test. C - Bar graph of mean FA per ROI (mean and 95% confidence intervals) in 11 of the 20 ROI where statistical differences between groups were found. One-way between-subjects MANCOVA with correction for gestational age at MRI was performed with Bonferroni post hoc test. Lines indicate significant differences between groups (*p < 0.05, **p < 0.01, ***p < 0.001). ROI abbreviations: fg-wm - frontal gyrus white matter, cc-bd - body of corpus callosum, cc-sp - splenium of corpus callosum, ac - anterior commissure, fmin - forceps minor, cc-ge - genu of corpus callosum, mtg-wm - medial temporal gyrus white matter, ilf - inferior longitudinal fasciculus, scr - superior corona radiata, plic - posterior limb of the internal capsule, ec - external capsule/claustrum/extreme capsule.

Table 2

Corrected global mean FA (of the averaged 20 ROI) with differences between groups calculated using one-way between-subjects ANCOVA and corrected mean FA of each ROI with differences between groups calculated using one-way between-subjects MANCOVA. Numbers in bold indicate significant results between groups (p<0.05) and pairwise comparisons that survived Bonferroni post hoc test (p≤0.05).

ROI	Mean FA (95% CI)			Statistical Results			
	Full-term	Preterm Music	Preterm Control	Group effect (p)	Pairwise comparison (p)		
					FT vs PTC	FT vs PTM	PTM vs PTC
Average all 20 ROI	0.364 (0.352-0.376)	0.344 (0.333-0.355)	0.326 (0.315-0.338)	**0.0001**	**0.0001**	0.058	0.106
cc-sp	0.630 (0.602-0.659)	0.573 (0.546-0.600)	0.540 (0.513-0.568)	**0.0001**	**0.0001**	**0.016**	0.282
cc-bd	0.503 (0.469-0.536)	0.432 (0.400-0.463)	0.406 (0.373-0.439)	**0.001**	**0.001**	**0.011**	0.781
cc-ge	0.573 (0.542-0.605)	0.523 (0.494-0.553)	0.492 (0.461-0.523)	**0.004**	**0.003**	0.76	0.434
scr	0.316 (0.296-0.336)	0.303 (0.285-0.322)	0.279 (0.260-0.298)	**0.041**	**0.043**	1	0.223
fmin	0.419 (0.392-0.445)	0.385 (0.360-0.410)	0.359 (0.333-0.385)	**0.014**	**0.011**	0.224	0.454
ac	0.226 (0.217-0.235)	0.214 (0.205-0.222)	0.206 (0.197-0.215)	**0.013**	**0.01**	0.153	0.597
fmaj	0.508 (0.479-0.538)	0.489 (0.461-0.517)	0.468 (0.439-0.497)	0.186	0.206	1	0.914
plic	0.539 (0.519-0.558)	0.535 (0.517-0.554)	0.503 (0.484-0.522)	**0.022**	**0.045**	1	0.051
alic	0.344 (0.324-0.363)	0.337 (0.319-0.355)	0.325 (0.306-0.344)	0.404	0.569	1	1
ilf	0.358 (0.340-0.375)	0.342 (0.325-0.359)	0.322 (0.305-0.340)	**0.028**	**0.024**	0.588	0.303
ec	0.262 (0.251-0.274)	0.262 (0.252-0.273)	0.238 (0.227-0.250)	**0.005**	**0.019**	1	**0.01**
slf	0.301 (0.285-0.318)	0.299 (0.283-0.314)	0.287 (0.271-0.303)	0.420	0.694	1	0.842
or	0.321 (0.299-0.344)	0.300 (0.279-0.320)	0.288 (0.266-0.309)	0.117	0.125	0.472	1
ar	0.265 (0.252-0.277)	0.277 (0.265-0.289)	0.265 (0.253-0.277)	0.252	1	0.484	0.483
fg-wm	0.243 (0.223-0.262)	0.206 (0.188-0.225)	0.197 (0.178-0.216)	**0.005**	**0.006**	**0.027**	1
af	0.271 (0.251-0.292)	0.251 (0.232-0.271)	0.240 (0.220-0.261)	0.123	0.132	0.493	1
stg-wm	0.214 (0.204-0.223)	0.206 (0.197-0.215)	0.199 (0.190-0.208)	0.113	0.113	0.697	0.851
mtg-wm	0.163 (0.154-0.172)	0.151 (0.142-0.160)	0.144 (0.135-0.153)	**0.023**	**0.02**	0.188	0.795
cg	0.344 (0.330-0.359)	0.331 (0.317-0.345)	0.329 (0.314-0.343)	0.284	0.434	0.561	1
fx	0.475 (0.434-0.516)	0.460 (0.421-0.499)	0.441 (0.401-0.482)	0.529	0.794	1	1

cc-sp - splenium of corpus callosum, cc-bd - body of corpus callosum, cc-ge - genu of corpus callosum, scr - superior corona radiata, fmin - forceps minor, ac – anterior commissure, fmaj - forceps major, plic - posterior limb of the internal capsule, alic - anterior limb of the internal capsule, ilf - inferior longitudinal fasciculus, ec - external capsule/claustrum/extreme capsule, slf - superior longitudinal fasciculus, or - optic radiation, ar - acoustic radiation, fg-wm - frontal gyrus white matter, af - arcuate fasciculus, stg-wm - superior temporal gyrus white matter, mtg-wm - medial temporal gyrus white matter, cg - cingulum, fx - fornix; CI - confidence interval; (p) - p-value.

Table 3

Corrected global mean MD, RD and AD (of the averaged 20 ROI) with differences between groups calculated using one-way between-subjects ANCOVA, and corrected mean MD, RD and AD of the 11 ROI where FA was statistically different between groups, with differences between groups calculated using one-way between-subjects MANCOVA. Numbers in bold indicate significant results between groups (p<0.05) and pairwise comparisons that survived Bonferroni post hoc test (p≤0.05).

ROI		Mean DTI measurements (95% CI)			Statistical Results			
		Full-term	Preterm Music	Preterm Control	Group effect (p)	Pairwise comparison (p)		
						FT vs PTC	FT vs PTM	PTM vs PTC
Mean MD of all 20 ROI		1.265 (1.241-1.290)	1.300 (1.277-1.324)	1.322 (1.298-1.346)	**0.01**	**0.008**	0.134	0.566
Mean RD of all 20 ROI		1.000 (0.970-1.029)	1.045 (1.018-1.073)	1.078 (1.049-1.107)	**0.003**	**0.002**	0.089	0.319
Mean AD of all 20 ROI		1.796 (1.777-1.816)	1.810 (1.792-1.829)	1.811 (1.792-1.831)	0.513			
cc-sp	MD	1.199 (1.154-1.245)	1.283 (1.288-1.375)	1.346 (1.301-1.390)	**0.0001**	**0.0001**	**0.033**	0.140
	RD	0.693 (0.638-0.748)	0.807 (0.755-0.859)	0.886 (0.832-0.940)	**0.0001**	**0.0001**	**0.014**	0.109
	AD	2.212 (2.157-2.266)	2.236 (2.185-2.287)	2.264 (2.211-2.318)	0.414			
cc-bd	MD	1.255 (1.209-1.301)	1.331 (1.288-1.375)	1.382 (1.337-1.427)	**0.002**	**0.001**	0.06	0.317
	RD	0.863 (0.804-0.921)	0.987 (0.932-1.042)	1.050 (0.993-1.107)	**0.0001**	**0.0001**	**0.010**	0.339
	AD	2.039 (1.967-2.111)	2.020 (1.952-2.088)	2.047 (1.976-2.117)	0.850			
cc-ge	MD	1.244 (1.190-1.298)	1.287 (1.236-1.337)	1.336 (1.284-1.389)	0.072			
	RD	0.782 (0.715-0.849)	0.862 (0.798-0.925)	0.929 (0.864-0.995)	**0.016**	**0.013**	0.279	0.419
	AD	2.168 (2.123-2.213)	2.136 (2.094-2.179)	2.150 (2.106-2.195)	0.605			
scr	MD	1.200 (1.154-1.246)	1.219 (1.175-1.262)	1.268 (1.223-1.313)	0.110			
	RD	0.982 (0.932-1.031)	1.007 (0.960-1.053)	1.065 (1.017-1.114)	0.064			
	AD	1.636 (1.589-1.683)	1.642 (1.598-1.687)	1.674 (1.628-1.720)	0.472			
fmin	MD	1.366 (1.321-1.411)	1.407 (1.365-1.450)	1.444 (1.399-1.488)	0.073			
	RD	1.020 (0.962-1.079)	1.084 (1.029-1.140)	1.136 (1.078-1.193)	**0.034**	**0.029**	0.360	0.588
	AD	2.059 (2.025-2.092)	2.053 (2.022-2.084)	2.059 (2.026-2.091)	0.956			
ac	MD	1.100 (1.070-1.129)	1.141 (1.114-1.169)	1.156 (1.127-1.185)	0.033			
	RD	0.967 (0.939-0.995)	1.010 (0.984-1.036)	1.027 (0.999-1.055)	**0.016**	**0.016**	0.097	1
	AD	1.365 (1.328-1.401)	1.404 (1.370-1.438)	1.413 (1.378-1.449)	0.159			
plic	MD	1.021 (1.005-1.037)	1.006 (0.990-1.021)	1.018 (1.002-1.034)	0.313			
	RD	0.670 (0.646-0.694)	0.664 (0.642-0.686)	0.698 (0.675-0.721)	0.097			
	AD	1.723 (1.695-1.751)	1.688 (1.662-1.715)	1.659 (1.631-1.686)	**0.011**	**0.009**	0.234	0.364
ilf	MD	1.361 (1.320-1.402)	1.387 (1.348-1.426)	1.439 (1.399-1.479)	**0.037**	**0.039**	1	0.197
	RD	1.077 (1.032-1.122)	1.113 (1.071-1.155)	1.174 (1.130-1.218)	**0.015**	**0.014**	0.748	0.137
	AD	1.930 (1.883-1.977)	1.936 (1.891-1.980)	1.969 (1.923-2.015)	0.455			
ec	MD	1.188 (1.165-1.211)	1.203 (1.182-1.225)	1.200 (1.177-1.223)	0.614			
	RD	1.033 (1.008-1.058)	1.048 (1.024-1.071)	1.062 (1.037-1.086)	0.296			
	AD	1.498 (1.471-1.524)	1.515 (1.490-1.540)	1.477 (1.451-1.503)	0.112			
fg-wm	MD	1.356 (1.302-1.410)	1.464 (1.414-1.515)	1.458 (1.405-1.511)	**0.011**	**0.037**	**0.017**	1
	RD	1.208 (1.147-1.270)	1.329 (1.271-1.387)	1.331 (1.271-1.391)	**0.011**	**0.026**	**0.020**	1
	AD	1.651 (1.609-1.693)	1.735 (1.696-1.774)	1.712 (1.671-1.753)	**0.018**	0.146	**0.016**	1
mtg-wm	MD	1.402 (1.366-1.439)	1.435 (1.400-1.469)	1.427 (1.391-1.463)	0.431			
	RD	1.296 (1.257-1.334)	1.334 (1.298-1.370)	1.329 (1.292-1.367)	0.321			

| | *AD* | 1.616 (1.580-1.652) | 1.638 (1.604-1.671) | 1.622 (1.587-1.657) | 0.657 | | | |

cc-sp - splenium of corpus callosum, cc-bd - body of corpus callosum, cc-ge - genu of corpus callosum, scr - superior corona radiata, fmin - forceps minor, ac - anterior commissure, plic - posterior limb of the internal capsule, ilf– inferior longitudinal fasciculus, ec - external capsule/claustrum/extreme capsule, fg-wm - frontal gyrus white matter, mtg-wm - medial temporal gyrus white matter; CI - confidence interval; (p) - p-value.

3.2. Tractography analysis

The analysis of the left and right acoustic radiations tractography data resulted in a statistically significant difference between FT, PTM and PTC on mean FA, $[F_{(2,82)}=4.216, p=0.018]$. Bonferroni post hoc test showed that mean FA was significantly higher in PTM vs PTC newborns (p=0.023). There was no statistically significant difference between the three groups in mean MD, $[F_{(2,82)}=0.619, p=0.481]$, mean RD $[F_{(2,82)}=0.942, p=0.394]$ and mean AD $[F_{(2,82)}=1.341, p=0.267]$ (Fig. 2A, Fig. 2B, Table 4). Moreover, there was no significant difference regarding mean FA, MD, RD and AD between left and right acoustic radiations, neither when considering the three groups together, nor when evaluating per group (Table 4 and Supplementary Table S3).

Regarding interhemispheric temporal callosal fibers, our analysis revealed a statistically significant difference between FT, PTM and PTC in mean FA $[F_{(2,40)}=5.879, p=0.006]$, as well as in mean MD $[F_{(2,41)}=9.248, p=0.001]$, mean RD $[F_{(2,41)}=5.681, p=0.007]$ and mean AD $[F_{(2,41)}=12.450, p=0.0001]$. Bonferroni post hoc test showed that, in comparison to FT newborns, PTC evidenced a significantly lower FA (p=0.004), higher MD (p=0.001), higher RD (p=0.008) and higher AD (p=0.04); while PTM presented no significant difference in FA or AD compared to FT infants, but a significantly higher mean MD (p=0.018) and RD (p=0.033). Additionally, in comparison to PTC, PTM exhibited a lower AD (p=0.0001) (Fig. 2C, Fig. 2D, Table 4).

Tractography analysis of the left and right uncinate fasciculus revealed a statistically significant difference between FT, PTM and PTC on mean FA $[F_{(2,82)}=6.802, p=0.001]$, mean MD $[F_{(2,82)}=8.311, p=0.001]$, mean RD $[F_{(2,82)}=5.133, p=0.008]$ and mean AD $[F_{(2,82)}=10.391, p=0.0001]$. Bonferroni post hoc test showed that, in comparison to FT newborns, PTC had a significantly lower FA (p=0.004), while PTM presented a significantly lower MD (p=0.001), RD (p=0.018) and AD (p=0.0001). Additionally, in comparison to PTC, PTM had a significantly higher FA (p=0.03) and a significantly lower MD (p=0.01), RD (p=0.037) and AD (p=0.05) (Fig. 2E, Fig. 2F, Table 4). There was no significant difference in mean FA, MD,

RD and AD between the left and right uncinate fasciculi, neither when considering the three groups together, nor when evaluating per group (Table 4 and Supplementary Table S3). Effect size between groups in each region were calculated by means of Cohen's, revealing a moderate to high practical significance (0.592 ≤ d ≤ 1.482) in all the regions where p≤0.05 (Supplementary Table S4).

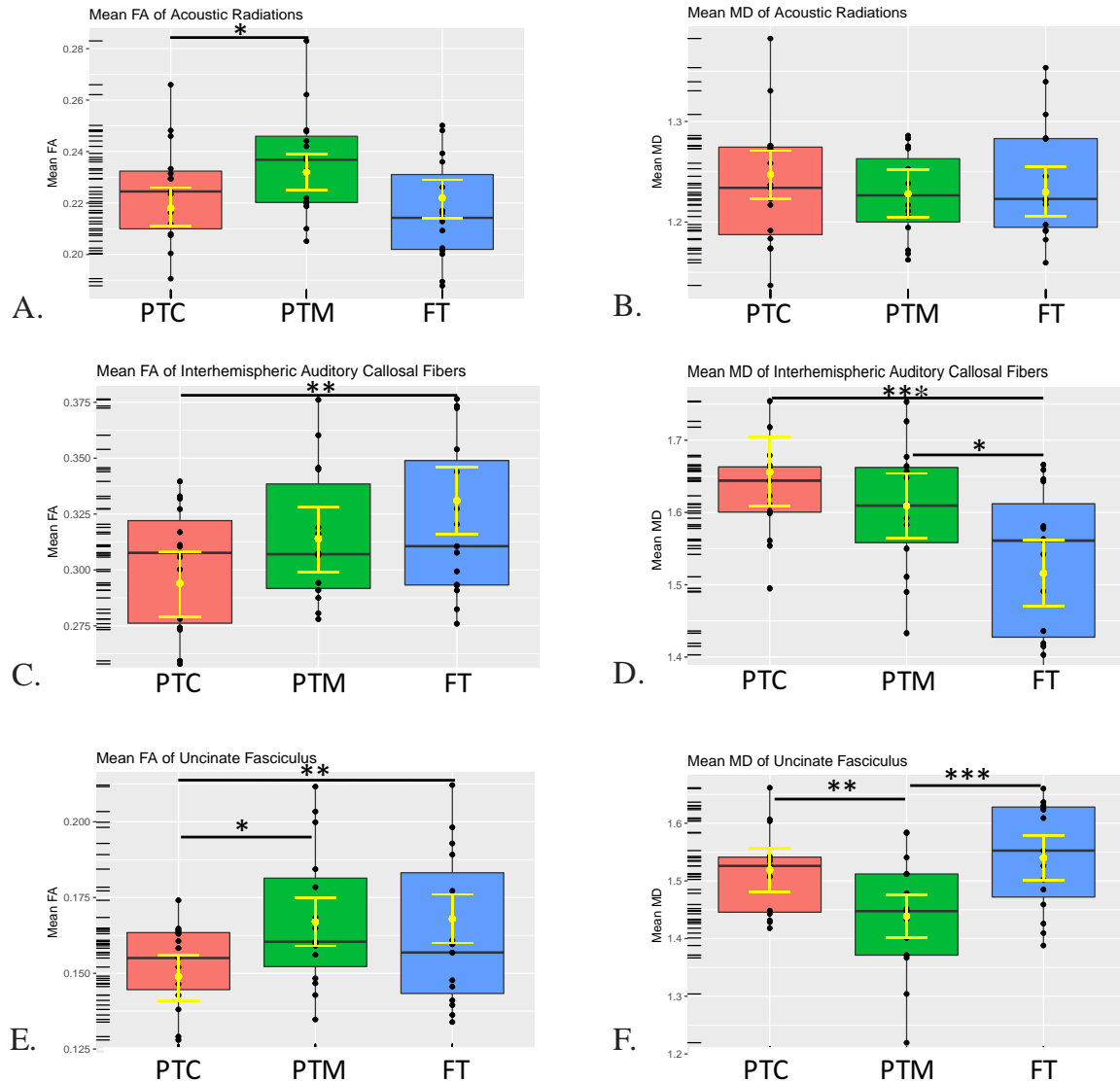Fig. 2. Analysis of DTI metrics of tracts obtained via tractography. A - Boxplot of mean FA for acoustic radiations; Two-way between-subjects ANCOVA with correction for gestational age at MRI was performed. Left and right fasciculi differences are not shown. B- Boxplot of mean MD for acoustic radiations; Two-way between-subjects ANCOVA with correction for gestational age at MRI was performed. Left and right fasciculi differences are not shown. C - Boxplot of mean FA for interhemispheric temporal callosal fibers; One-way between-subjects ANCOVA with correction for gestational age at MRI was performed. D - Boxplot of mean MD for interhemispheric temporal callosal fibers; One-way between-subjects ANCOVA with correction for gestational age at MRI was performed. E - Boxplot of mean FA for uncinate fasciculus; Two-way between-subjects ANCOVA with correction for gestational age at MRI

was performed. Left and right fasciculi differences are not shown. F- Boxplot of mean MD for uncinate fasciculus; Two-way between-subjects ANCOVA with correction for gestational age at MRI was performed. Left and right fasciculi differences are not shown. All analyses were performed with Bonferroni post hoc test. Mean and 95% confidence intervals are illustrated in yellow on each boxplot. Lines indicate significant differences between groups (*$p < 0.05$, **$p < 0.01$, ***$p < 0.001$).

Table 4

Corrected mean FA, MD, RD and AD for acoustic radiations, interhemispheric temporal callosal fibers and uncinate fasciculus, with groups differences calculated using one-way and two-way between-subjects ANCOVA. Numbers in bold indicate significant results between groups ($p<0.05$) and pairwise comparisons that survived Bonferroni post hoc test ($p\leq0.05$).

ROI	Mean FA (95% CI)			Statistical Results			
	Full-term	Preterm Music	Preterm Control	Group effect (p)	Pairwise comparison (p)		
					FT vs PTC	FT vs PTM	PTM vs PTC
Ac. Rad. average	0.222 (0.214-0.229)	0.232 (0.225-0.239)	0.218 (0.211-0.226)	**0.018**	1	0.133	**0.023**
Left	0.221 (0.211-0.231)	0.231 (0.221-0.241)	0.219 (0.209-0.230)	0.845			
Right	0.222 (0.212-0.233)	0.234 (0.224-0.244)	0.217 (0.207-0.228)				
Interhemispheric Temp. Call. Fib.	0.331 (0.316-0.346)	0.314 (0.299-0.328)	0.294 (0.279-0.308)	**0.006**	**0.004**	0.323	0.170
Unc. F. average	0.168 (0.160-0.176)	0.167 (0.159-0.175)	0.149 (0.141-0.156)	**0.001**	**0.004**	1	**0.03**
Left	0.168 (0.157-0.179)	0.166 (0.155-0.177)	0.149 (0.138-0.160)	0.908			
Right	0.168 (0.157-0.179)	0.168 (0.157-0.179)	0.148 (0.137-0.159)				
Mean MD (95% CI)							
Ac. Rad. average	1.230 (1.206-1.255)	1.228 (1.205-1.252)	1.247 (1.223-1.271)	0.481			
Left	1.217 (1.183-1.250)	1.241 (1.208-1.273)	1.249 (1.216-1.282)	0.978			
Right	1.244 (1.210-1.277)	1.216 (1.183-1.249)	1.246 (1.212-1.279)				
Interhemispheric Temp. Call. Fib.	1.516 (1.470-1.562)	1.609 (1.564-1.654)	1.656 (1.609-1.704)	**0.001**	**0.001**	**0.018**	0.441
Unc. F. average	1.540 (1.501-1.579)	1.439 (1.402-1.476)	1.519 (1.481-1.557)	**0.001**	1	**0.001**	**0.01**
Left	1.554 (1.501-1.608)	1.449 (1.397-1.501)	1.534 (1.481-1.587)	0.229			
Right	1.526 (1.472-1.579)	1.429 (1.377-1.482)	1.504 (1.451-1.557)				
Mean RD (95% CI)							
Ac. Rad. average	1.091 (1.066-1.116)	1.083 (1.059-1.106)	1.106 (1.081-1.131)	0.394			
Left	1.078 (1.044-1.113)	1.090 (1.057-1.124)	1.104 (1.070-1.139)	0.712			
Right	1.105 (1.070-1.139)	1.075 (1.042-1.109)	1.108 (1.073-1.143)				
Interhemispheric Temp. Call. Fib.	1.245 (1.188-1.302)	1.349 (1.296-1.403)	1.377 (1.321-1.433)	**0.007**	**0.008**	**0.033**	1
Unc. F. average	1.418 (1.375-1.461)	1.333 (1.293-1.374)	1.408 (1.366-1.451)	**0.008**	1	**0.018**	**0.037**
Left	1.424 (1.365-1.482)	1.341 (1.284-1.398)	1.414 (1.356-1.473)	0.584			
Right	1.412 (1.353-1.471)	1.326 (1.269-1.383)	1.402 (1.342-1.462)				
Mean AD (95% CI)							
Ac. Rad. average	1.511 (1.483-1.538)	1.540 (1.515-1.566)	1.536 (1.509-1.563)	0.267			
Left	1.496 (1.459-1.534)	1.549 (1.513-1.585)	1.538 (1.502-1.575)	0.908			
Right	1.525 (1.459-1.534)	1.531 (1.495-1.568)	1.533 (1.495-1.571)				
Interhemispheric Temp. Call. Fib.	2.057 (2.001-2.113)	1.976 (1.923-2.029)	2.162 (2.107-2.216)	**0.0001**	**0.04**	0.124	**0.0001**
Unc. F. average	1.811 (1.773-1.850)	1.690 (1.654-1.726)	1.754 (1.716-1.792)	**0.0001**	0.143	**0.0001**	**0.050**
Left	1.824 (1.771-1.876)	1.696 (1.645-1.748)	1.767 (1.715-1.819)	0.315			
Right	1.799 (1.746-1.852)	1.683 (1.632-1.735)	1.741 (1.687-1.795)				

Ac. Rad. – acoustic radiations, Interhemispheric Temp. Call. Fib. – Interhemispheric temporal callosal fibers, Unc. F. – uncinate fasciculus; CI - confidence interval; (p) - p-value.

3.3. Amygdala volumetric analysis

Amygdala volumetric statistical analysis showed a statistically significant difference between FT, PTM and PTC, [$F_{(2,59)}=8.833$, $p=0.0001$], correcting for GA at MRI, sex and ICC volumes. Bonferroni post hoc test showed that amygdala volumes were significantly smaller in PTC vs FT ($p=0.001$), whereas PTM had significantly larger amygdala volumes vs PTC ($p=0.006$), and not significantly different from FT newborns (Fig. 3, Table 5). There were no significant differences between left and right amygdala volumes, neither when considering the three groups together, nor when evaluating per group (Table 5 and Supplementary Table S5). Effect size between groups regarding amygdala volumes were calculated by means of Cohen's d, revealing a moderate to high practical significance ($0.718 \leq d \leq 1.285$) where $p \leq 0.05$ (Supplementary Table S6).

Table 5

Mean amygdala volumes corrected for GA at MRI, sex and ICC volumes and difference between groups

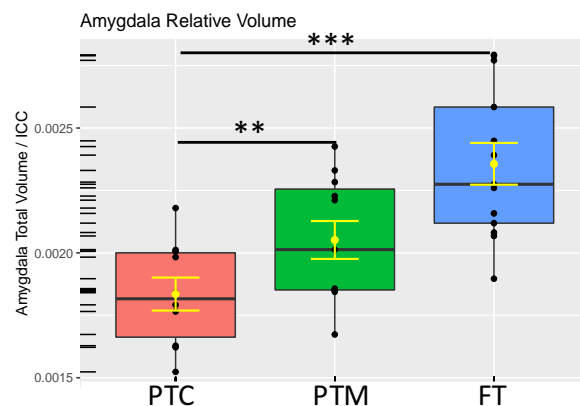|	Amygdala Volumes (95% CI)			Statistical Results			
	Full-term	Preterm Music	Preterm Control	Group effect (p-value)	Pairwise comparison (p)		
					FT vs PTC	FT vs PTM	PTM vs PTC
Amygdala	514.9 (484.0-545.8)	492.2 (461.5-522.9)	422.9 (391.4-454.4)	**0.0001**	**0.001**	1	**0.006**
Left	521.3 (481.6-561.0)	496.4 (455.4-537.3)	422.4 (380.0-464.9)	0.665			
Right	508.4 (468.7-548.1)	488.0 (447.0-529.0)	423.4 (381.0-465.8)				

Fig. 3. Boxplot representing the distribution of total amygdala volume (left and right) relative to the ICC volume per group. Mean and 95% confidence intervals are illustrated in yellow. Lines indicate significant differences between groups that survived two-way between-subjects ANCOVA analysis with Bonferroni post hoc test correction; (*$p < 0.05$, **$p < 0.01$, ***$p < 0.001$). The analysis was performed using as covariates: gestational age at MRI, ICC volumes and sex.

4. Discussion

The aim of the present study was to evaluate the effect of an early postnatal music intervention during NICU stay on VPT infants' brain structural maturation. Music has been proven to elicit changes in limbic and paralimbic brain functional networks that are involved in socio-emotional processing in both adults (Blood and Zatorre, 2001; Koelsch, 2014) and in newborn infants (Lordier et al., 2018; Perani et al., 2010)

We therefore hypothesized that an early music intervention in VPT infants could have an effect on VPT infants' macro and microstructural brain development, in particular regarding cortico-limbic networks.

To study these structural brain effects of an early music intervention, we assessed brain WM maturation, using DTI, in 20 different regions defined across the whole-brain WM and specifically in tracts involved in auditory and socio-emotional processing (acoustic radiations, interhemispheric temporal callosal fibers and uncinate fasciculus). Furthermore, we investigated the effect of the music intervention on the amygdala volume – an integral part of the limbic system which plays a central role in emotion modulation during music processing (Ball et al., 2007; Blood and Zatorre, 2001; Koelsch et al., 2013; Koelsch, 2014).

4.1.   Regional effects of prematurity and music intervention on WM maturation

Our ROI-based analysis revealed that VPT infants who received standard-of-care and without signs of brain lesions on conventional MRI, when at TEA, show an overall decreased WM maturation in comparison to FT newborns, with several regions of diminished FA and/or higher diffusivity when compared to FT newborns.

The brain areas that we found to be affected by prematurity are similar to the ones described in the existing literature, comprising "fg-wm", "cc-sp", "cc-bd", "cc-ge", "plic", "ilf", "ec" and "scr" (Akazawa et al., 2016; Anjari et al., 2007; Dyet et al., 2006; Huppi et al., 1998a; Rose et al., 2008; Thompson et al., 2011). Besides these regions, we show, to the best of our knowledge, for the first time, that PTC at TEA also present a diminished FA and/or higher diffusivity in "ac", "fmin" and "mtg-wm", in comparison to FT infants. Furthermore, we show that the lower FA in most of these regions is due to a significantly increased RD, and no changes in AD. Indeed, maturational changes in anisotropy during development are predominantly attributable to a decrease in RD reflecting myelination and pre-myelination events, such as increased axonal calibre, decreased membrane permeability and development of functioning ionic channels (Partridge et al., 2004; Qiu et al., 2008; Suzuki et al., 2003;

Wimberger et al., 1995). Since the regions with an increased RD in PTC vs FT infants are not myelinated at TEA, these increases cannot be attributed to myelin deficits per se, but could be due to a delayed or deficient wrapping of the oligodendrocytes around the axons before myelination, resulting in increased membrane permeability and a decreased axonal diameter, or to a greater spacing between axons constituting a WM fascicle (Counsell et al., 2006; Huppi et al., 1998a). Our findings therefore confirm a decreased overall maturation of the WM in preterm control infants at TEA compared to the FT control group.

As for the PTM group, the mean FA, MD, RD and AD values, when averaging all the 20 ROI together, were not significantly different from FT newborns, suggesting overall similar maturity of the two groups. When evaluating mean diffusivities per ROI, mean FA was significantly reduced in PTM vs FT newborns only in "cc-sp", "cc-bd" and "fg-wm", regions where RD was increased. But, more importantly, in the "ec" region PTM had a higher mean FA compared to PTC infants. The small sample size might be hiding significant differences that are not evident in other regions, given these data. Indeed, other regions might be affected, as suggested by the tendency of PTM mean FA values to be superior to PTC and closer to FT infants in some of the regions, although we have not found a statistically significant difference. The "ec" ROI comprises, due to our spatial resolution of 2x2x2mm^3, the external capsule, claustrum and extreme capsule. Through the extreme capsule pass bidirectional fibers providing communication between the claustrum and insular cortex, as well as between Broca's area and Wernicke's area (Makris and Pandya, 2009). The insula is a multimodal area involved in music and emotion processing (Pouladi et al., 2010) and lesions in this area have been proven to alter emotional responses to music (Gosselin et al., 2005; Griffiths et al., 2004). Furthermore it is an integrant part of the salience network, which recently has been shown to present a decreased functional connectivity in PTC newborns in comparison to FT infants, but an enhanced functional connectivity in PTM (Lordier et al., 2019a). The claustrum projects to and receives projections from several cortical areas, such as the auditory cortex, prefrontal cortex and cingulate cortex, as well as subcortical areas such as the hippocampus, amygdala and caudate nucleus (Amaral and Insausti, 1992; Crick and Koch, 2005) and has been shown to be involved in the processing of emotional faces in children (Pagliaccio et al., 2013). The external capsule is composed of claustro-cortical fibres dorsally, along with the combined mass of the uncinate fasciculus (connecting the amygdala to the OFC) and inferior frontal occipital fasciculus (IFOF) ventrally (connecting the occipital, posterior temporal and the orbito-frontal areas), and the anterior limb of the anterior commissure, which interconnects the amygdalae

and the temporal lobes (Catani and Thiebaut de Schotten, 2008; Dejerine, 1985; Standring, 2015). Therefore, the improved structural maturation of this WM region provides evidence for a structural effect of the early preterm music intervention in these areas transited by WM fibers connecting areas involved in emotion and music processing.

4.2. Effects of prematurity and music on WM connectivity: tractography results

To deepen the study of the structural effect that the musical intervention could have on the VPT infants' brain, we performed tractography of two tracts involved in the processing of auditory information: the acoustic radiations, which relay the auditory information from the thalamus to primary auditory cortex; and the interhemispheric temporal callosal fibers, which transmit the auditory information between the two hemispheres.

Tractography analysis of acoustic radiations revealed, first, that the auditory thalamic route is structurally present already at TEA in both full-term and preterm infants, suggesting therefore that the sophisticated auditory behavior shown by infants early in life might well be cortical. Our findings are consistent with previous histochemical studies that have found evidence of thalamo-cortical afferents reaching the cortical plate after the 24th postconceptional week (Kostovic et al., 2002; Kostovic and Judas, 2010a) and refute the model stating that the brainstem reticular-auditory pathway is the only existing path to the auditory cortex at birth (Eggermont and Moore, 2012). Second, analysis of acoustic radiations revealed that PTM presented a significantly higher mean FA than PTC group. In fact, training, including musical training, has been found to result in changes in WM microstructure measured by a higher FA, a finding that has been related to improved performance (Engel et al., 2014; Ruber et al., 2015; Taubert et al., 2012). Thus, our findings suggest an effect of the musical training in the maturation of acoustic radiations in preterm infants.

Regarding the interhemispheric temporal callosal fibers, our results suggest that PTC, who are exposed to an auditory environment very different from the mother's womb during early brain development, present a reduced maturation of these pathways at TEA, in comparison to FT newborns, as suggested by the reduced FA and increased MD, RD and AD. While the increased RD could be explained by possible deficits in pre-myelination, mean AD changes are more difficult to explain, but a decrease in mean AD has been reported in early development (Brouwer et al., 2012; Krogsrud et al., 2016; Mukherjee et al., 2002; Partridge et al., 2004; Qiu et al., 2008; Snook et al., 2005). A possible explanation for the diminished AD in early development might be related to the growth of neurofibrils, such as neurofilaments and

microtubules, as well as glial cells during brain development, increasing axonal density or calibre, but also the tortuosity of extra-axonal space and diminishing the extra-axonal water content (Qiu et al., 2008; Takahashi et al., 2000). In contrast to the PTC, PTM presented an overall mean FA and AD closer to and not significantly different from FT newborns, again suggesting an improved WM tract maturation with the early activity induced by the music intervention.

We also performed tractography of the uncinate fasciculus, known to be implicated in socio-emotional processing and constituting the ventral part of the external capsule, which presented an increased FA in PTM vs PTC in our ROI-based analysis.

Tractography analysis of the uncinate fasciculus revealed that PTC had a decreased FA of this tract in comparison to FT newborns, while PTM presented a higher FA and diminished MD, RD and AD, suggesting an increased maturation of this tract after the music intervention.

Training, as well as experience during development, might influence myelination, promoted by neural firing across axons, and subsequently alter WM diffusion parameters (Demerens et al., 1996; Ishibashi et al., 2006; Zatorre et al., 2012), with typical diminished RD and increased FA – changes described after training in reading, working memory, music playing and meditation (Engvig et al., 2012; Hu et al., 2011; Keller and Just, 2009; Moore et al., 2017; Tang et al., 2012). Interestingly, it has been previously shown that musicians with absolute pitch ability have an increased FA in the uncinate fasciculus, in comparison to non-musicians.

The uncinate fasciculus is a WM association tract that connects parts of the limbic system in the temporal lobe, comprising the hippocampus and amygdala, with frontal regions, such as the OFC, which is involved in sensory integration and processing of affective stimuli (Kringelbach, 2005), evaluation of emotional association (Wildgruber et al., 2005) and top-down modulation of behavior (Ghashghaei and Barbas, 2002; Mcdonald, 1987). Neuroimaging studies of affective control in adults suggest prefrontal/orbitofrontal modulation of subcortical regions during emotion processing (Hariri et al., 2003; Keightley et al., 2003; Ochsner et al., 2002; Ochsner et al., 2004). Given the protracted development of the prefrontal cortex (Casey et al., 2000; Sowell et al., 1999), prefrontal-amygdala interactions are likely to play an important role in developmental changes in emotion processing. Connectivity analysis of 6 years-old infants born extremely preterm had revealed alterations in prefrontal cortico-basal ganglia-thalamocortical and limbic networks in these infants (Fischi-Gomez et al., 2016).

Our results suggest thus a decreased maturation of the uncinate fasciculus in PTC vs FT infants, in agreement with previous literature reporting a decreased FA in the uncinate fasciculus in adolescents (Constable et al., 2008; Mullen et al., 2011) and adults (Rimol et al., 2019) that

were born prematurely. This finding may contribute to the behavioral socio-emotional difficulties present in prematurely born infants later in development (Bhutta et al., 2002; Hille et al., 2001; Hughes et al., 2002; Lejeune et al., 2015; Montagna and Nosarti, 2016; Spittle et al., 2009; Witt et al., 2014). Multisensory stimulation as provided by the early music intervention in preterm infants might therefore induce specific WM tract maturation and improve brain connectivity in these networks, whose maturation was shown to be delayed in preterm newborns (Fischi-Gomez et al., 2015; Spittle et al., 2009) and which are key pathways for emotional processing (Koelsch, 2014).

4.3.   Effects of prematurity and music on brain amygdala volume

The volumetric analysis of the brain amygdala showed that PTC infants, when at TEA, have a significantly smaller amygdala volume in comparison to FT infants, which is in agreement with the literature (Cismaru et al., 2016; Peterson et al., 2000).

It has been widely accepted that the amygdala, which is a primary structure of the brain limbic network, constitutes a central component of emotional processing and can regulate and modulate this network (Aggleton and Saunders, 2000). The amygdala processes emotions such as happiness, humour, anxiety, anger, fear and annoyance. It is involved in the assessment of emotional content of facial expressions and plays an important role in the recognition of and response to emotionally relevant social stimuli, thus participating in communication, social behavior and memory (Kraus and Canlon, 2012; Phan et al., 2002).

Studies on amygdala lesions in primates during the neonatal period have demonstrated exaggerated fear responses during social interactions (Bauman et al., 2004; Prather et al., 2001), which was interpreted as resulting from an incapacity to learn and recognize social cues that signal safety. Human studies have also suggested that amygdala lesions early in life dramatically impair processing of facial expressions (Adolphs et al., 1994; Adolphs et al., 1995).

Literature shows that premature newborns present an atypical socio-emotional development, comprising diminished social competences and self-esteem, emotional dysregulation, shyness and timidity (Bhutta et al., 2002; Hille et al., 2001; Hughes et al., 2002; Montagna and Nosarti, 2016; Spittle et al., 2009). In particular, VPT infants have been shown to present increased difficulties with regulating fear at 12 and 42-months-old (Langerock et al., 2013; Witt et al., 2014), as well as anger at 12 months (Langerock et al., 2013), frustration at 42 months accompanied by difficulties with decoding facial expressions of emotions (Witt et al., 2014),

171

an immature sustained attention and inhibitory control at 24 months (Lejeune et al., 2015) and increased difficulties with recognizing emotional content and regulating social behavior at 5-7 years-old (Lejeune et al., 2016).

Biological and environmental factors associated with VPT birth are thus thought to lead to structural and functional alterations in brain areas involved in processing emotion and social stimuli. These alterations comprise, among others, a reduced amygdala volume (Cismaru et al., 2016; Peterson et al., 2000) and altered connectivity in prefrontal cortico-basal ganglia-thalamo-cortical and limbic networks (Fischi-Gomez et al., 2016; Witt et al., 2014).

Music has long been shown to be capable of evoking emotions (Ferguson and Sheldon, 2013; Lamont, 2011). Meta-interpretive literature reviews including functional neuroimaging studies have indicated that emotional stimuli, both negative and positive, are more likely to activate amygdala than neutral stimuli (Costafreda et al., 2008; Phan et al., 2002) and that the amygdala holds a central role in emotion modulation during music processing (Ball et al., 2007; Blood and Zatorre, 2001; Koelsch et al., 2013; Koelsch, 2014). Neuropsychological studies have further suggested that the amygdala is necessary in the emotional processing of music (Gosselin et al., 2005; Gosselin et al., 2007; Griffiths et al., 2004).

Our results show that VPT infants exposed to music during NICU stay, when at TEA, present a significantly larger amygdala volume in comparison to those receiving standard-of-care. This suggests that the music intervention in preterm infants might modulate amygdala activity during a critical period of brain development and thus have a structural impact on its volume. Since this region is part of a complex neural circuit, such modulation might also influence other brain regions within the circuitry, namely the orbitofrontal/prefrontal cortex, which is connected to the amygdala via the uncinate fasciculus, as suggested by our results on the improved microstructural maturation of this fasciculus by the music intervention. Together these brain structural effects might have an impact on VPT infants' later socio-emotional development. Indeed, preliminary clinical findings regarding the effect of this early postnatal music intervention on VPT infants' long-term emotional development revealed significantly decreased scores for fear-reactivity at 12 months and for anger-reactivity at 24 months' age in comparison to FT infants, with less important differences between PTM vs FT, than between PTC and FT newborns (Lejeune et al., 2019a).

5. Conclusion

Overall brain microstructural maturation at TEA was decreased in VPT infants receiving the standard-of-care, when compared to FT newborns. Regions of significantly decreased maturation included the frontal white matter, genu, body and splenium of corpus callosum, anterior commissure, fornix minor, posterior limb of internal capsule, inferior longitudinal fasciculus, medial temporal gyrus white matter, external capsule/claustrum/extreme capsule, interhemispherical auditory callosal fibers and uncinate fasciculus.

VPT infants listening to music during NICU stay, in comparison to VPT infants receiving the standard-of-care, showed an increased WM microstructural maturation in acoustic radiations, external capsule/claustrum/extreme capsule and uncinate fasciculus, as well as larger amygdala volumes, all of which are brain structures involved in acoustic and/or emotion processing.

This is the first neuroimaging clinical study showing a structural impact of a music intervention created specifically for premature infants upon the maturation of brain regions known to be altered by prematurity and which hold key roles in emotional processing. In particular, the effect of music on the amygdala volume and on the maturation of the uncinate fasciculus, described by using two independent MRI techniques, supports the clinical use of such an intervention in mitigating later social-emotional difficulties associated with prematurity.

Limitations, technical considerations and future directions

One limitation of the study is the modest sample size for a randomized clinical trial and the limited number of times of music exposition.

The modest sample size and the specificity of our neonatal population imposes some technical considerations. For an overall evaluation of the impact of the intervention in the main WM tracts, we opted for a template-based region-of-interest (ROI) analysis method comprising 20 different WM ROI. Due to the diffusion imaging resolution ($2x2x2$ mm^3), this technique may be affected by the partial volume problem. However, automated whole-brain diffusion-based group analysis techniques such as TBSS and TSA were considered less suited to our study, since they are generally appropriate for larger cohorts and have been proven to be less suitable to neonatal population (Pecheva et al., 2017). In particular, robust medial tracts are difficult to compute from the premature infant's thin sheet-like tracts, making TSA less appropriate to study certain WM fibers of interest to our hypothesis.

We would also like to point out that mean DTI metrics, such as mean FA, depend on the number of crossings and microstructural complexity, which varies with age. For this reason, we have

scanned our population within at a narrow age range and we have controlled the data for the infant's age at the MRI.

Despite the relatively limited number of times of music exposition, our intervention results are encouraging. Thus, currently we are replicating this music intervention study on a second population in order to assess the reproducibility of the music effect. We have further increased the number of music expositions per day and included an MRI before, in addition to the one after the intervention, to decrease inter-subject variability bias, using a multi-shell diffusion protocol.

This study compared instrumental music intervention to standard-of-care in the NICU. We show that this early intervention in preterm newborns leads to an increased structural brain maturation specifically of some auditory and emotional processing pathways. However, parental presence and exposure to speech (namely maternal singing), considered to be equally distributed between groups given the process of random allocation, were not individually quantified and might also have an impact in infant's brain development. More research is needed to compare this instrumental music intervention to other sound interventions such as maternal singing.

The clinical significance of these brain structural effects of music remains to be evaluated by investigating neurodevelopmental and cognitive outcomes in childhood planned for future follow-up studies.

Acknowledgments

Funding

References

Aanes, S., et al., 2015. Memory function and hippocampal volumes in preterm born very-low-birth-weight (VLBW) young adults. Neuroimage. 105**,** 76-83.

Adibpour, P., Dubois, J., Dehaene-Lambertz, G., 2018. Right but not left hemispheric discrimination of faces in infancy. Nature Human Behaviour. 2**,** 67-79.

Adolphs, R., et al., 1994. Impaired Recognition of Emotion in Facial Expressions Following Bilateral Damage to the Human Amygdala. Nature. 372**,** 669-672.

Adolphs, R., et al., 1995. Fear and the Human Amygdala. Journal of Neuroscience. 15**,** 5879-5891.

Aeby, A., et al., 2009. Maturation of thalamic radiations between 34 and 41 weeks' gestation: a combined voxel-based study and probabilistic tractography with diffusion tensor imaging. AJNR Am J Neuroradiol. 30**,** 1780-6.

Aggleton, J.P., Saunders, C., 2000. The amygdala - what's happened in the last decade. In: The Amygdala: a Functional Analysis. Vol., ed.^eds. Oxford University Press, Oxford, pp. 1-30.

Akazawa, K., et al., 2016. Probabilistic maps of the white matter tracts with known associated functions on the neonatal brain atlas: Application to evaluate longitudinal developmental trajectories in term-born and preterm-born infants. Neuroimage. 128**,** 167-179.

Als, H., McAnulty, G., 2014. The Newborn Individualized Developmental Care and Assessment Program (NIDCAP) with Kangaroo Mother Care (KMC): Comprehensive Care for Preterm Infants.

Amaral, D.G., Insausti, R., 1992. Retrograde Transport of D-[H-3]-Aspartate Injected into the Monkey Amygdaloid Complex. Experimental Brain Research. 88**,** 375-388.

Anderson, P., Doyle, L.W., 2003. Neurobehavioral outcomes of school-age children born extremely low birth weight or very preterm in the 1990s. Jama-Journal of the American Medical Association. 289**,** 3264-3272.

Andersson, J.L.R., et al., 2016. Incorporating outlier detection and replacement into a non-parametric framework for movement and distortion correction of diffusion MR images. Neuroimage. 141**,** 556-572.

Andersson, J.L.R., Sotiropoulos, S.N., 2016. An integrated approach to correction for off-resonance effects and subject movement in diffusion MR imaging. Neuroimage. 125**,** 1063-1078.

Andersson, J.L.R., et al., 2017. Towards a comprehensive framework for movement and distortion correction of diffusion MR images: Within volume movement. Neuroimage. 152**,** 450-466.

Anjari, M., et al., 2007. Diffusion tensor imaging with tract-based spatial statistics reveals local white matter abnormalities in preterm infants. Neuroimage. 35**,** 1021-7.

Arpi, E., Ferrari, F., 2013. Preterm birth and behaviour problems in infants and preschool-age children: a review of the recent literature. Developmental Medicine and Child Neurology. 55**,** 788-796.

Ball, G., et al., 2012. The effect of preterm birth on thalamic and cortical development. Cereb Cortex. 22**,** 1016-24.

Ball, G., et al., 2017. Multimodal image analysis of clinical influences on preterm brain development. Ann Neurol. 82**,** 233-246.

Ball, T., et al., 2007. Response Properties of Human Amygdala Subregions: Evidence Based on Functional MRI Combined with Probabilistic Anatomical Maps. Plos One. 2.

Bassi, L., et al., 2008. Probabilistic diffusion tractography of the optic radiations and visual function in preterm infants at term equivalent age. Brain. 131, 573-582.

Bastiani, M., et al., 2019. Automated processing pipeline for neonatal diffusion MRI in the developing Human Connectome Project. Neuroimage. 185, 750-763.

Bauman, M.D., et al., 2004. The development of social behavior following neonatal amygdala lesions in rhesus monkeys. Journal of Cognitive Neuroscience. 16, 1388-1411.

Beaulieu, C., 2002. The basis of anisotropic water diffusion in the nervous system - a technical review. Nmr in Biomedicine. 15, 435-455.

Behrens, T.E.J., et al., 2003. Characterization and propagation of uncertainty in diffusion-weighted MR imaging. Magnetic Resonance in Medicine. 50, 1077-1088.

Behrens, T.E.J., et al., 2007. Probabilistic diffusion tractography with multiple fibre orientations: What can we gain? Neuroimage. 34, 144-155.

Bhutta, A.T., et al., 2002. Cognitive and behavioral outcomes of school-aged children who were born preterm - A meta-analysis. Jama-Journal of the American Medical Association. 288, 728-737.

Blencowe, H., et al., 2013. Born too soon: the global epidemiology of 15 million preterm births. Reproductive health. 10 Suppl 1, S2-S2.

Blood, A.J., Zatorre, R.J., 2001. Intensely pleasurable responses to music correlate with activity in brain regions implicated in reward and emotion. Proc Natl Acad Sci U S A. 98, 11818-23.

Brody, B.A., et al., 1987. Sequence of central nervous system myelination in human infancy. I. An autopsy study of myelination. J Neuropathol Exp Neurol. 46, 283-301.

Brouwer, R.M., et al., 2012. White Matter Development in Early Puberty: A Longitudinal Volumetric and Diffusion Tensor Imaging Twin Study. Plos One. 7.

Casey, B.J., Giedd, J.N., Thomas, K.M., 2000. Structural and functional brain development and its relation to cognitive development. Biol Psychol. 54, 241-57.

Catani, M., Thiebaut de Schotten, M., 2008. A diffusion tensor imaging tractography atlas for virtual in vivo dissections. Cortex; a journal devoted to the study of the nervous system and behavior. 44, 1105-1132.

Chang, E., 2015. Preterm birth and the role of neuroprotection. Bmj-British Medical Journal. 350.

Cismaru, A.L., et al., 2016. Altered Amygdala Development and Fear Processing in Prematurely Born Infants. Front Neuroanat. 10, 55.

Constable, R.T., et al., 2008. Prematurely born children demonstrate white matter microstructural differences at 12 years of age, relative to term control subjects: An investigation of group and gender effects. Pediatrics. 121, 306-316.

Costafreda, S.G., et al., 2008. Predictors of amygdala activation during the processing of emotional stimuli: A meta-analysis of 385 PET and fMRI studies. Brain Research Reviews. 58, 57-70.

Counsell, S.J., et al., 2006. Axial and radial diffusivity in preterm infants who have diffuse white matter changes on magnetic resonance imaging at term-equivalent age. Pediatrics. 117, 376-386.

Counsell, S.J., et al., 2008. Specific relations between neurodevelopmental abilities and white matter microstructure in children born preterm. Brain. 131, 3201-3208.

Crick, F.C., Koch, C., 2005. What is the function of the claustrum? Philosophical Transactions of the Royal Society B-Biological Sciences. 360, 1271-1279.

Dejerine, J., 1985. Classics in Neurology - Intermittent Claudication of the Spinal-Cord (Reprinted from Semiologie Des Affections Du Systeme Nerveux, P9 267-269, 1914). Neurology. 35, 860-860.

Demerens, C., et al., 1996. Induction of myelination in the central nervous system by electrical activity. Proceedings of the National Academy of Sciences of the United States of America. 93, 9887-9892.

Dubois, J., et al., 2008. Asynchrony of the early maturation of white matter bundles in healthy infants: quantitative landmarks revealed noninvasively by diffusion tensor imaging. Human brain mapping. 29, 14-27.

Duerden, E.G., et al., 2015. Tract-Based Spatial Statistics in Preterm-Born Neonates Predicts Cognitive and Motor Outcomes at 18 Months. American Journal of Neuroradiology. 36, 1565-1571.

Dyet, L.E., et al., 2006. Natural history of brain lesions in extremely preterm infants studied with serial magnetic resonance imaging from birth and neurodevelopmental assessment. Pediatrics. 118, 536-548.

Eggermont, J.J., Moore, J.K., 2012. Morphological and Functional Development of the Auditory Nervous System. In: Human Auditory Development. Vol., L.a.F. Werner, Richard R. and Popper, Arthur N., ed.^eds., pp. 61-105.

Engel, A., et al., 2014. Inter-individual differences in audio-motor learning of piano melodies and white matter fiber tract architecture. Human Brain Mapping. 35, 2483-2497.

Engvig, A., et al., 2012. Memory training impacts short-term changes in aging white matter: A Longitudinal Diffusion Tensor Imaging Study. Human Brain Mapping. 33, 2390-2406.

Ferguson, Y.L., Sheldon, K.M., 2013. Trying to be happier really can work: Two experimental studies. Journal of Positive Psychology. 8, 23-33.

Fischi-Gomez, E., et al., 2015. Structural Brain Connectivity in School-Age Preterm Infants Provides Evidence for Impaired Networks Relevant for Higher Order Cognitive Skills and Social Cognition. Cereb Cortex. 25, 2793-805.

Fischi-Gomez, E., et al., 2016. Brain network characterization of high-risk preterm-born school-age children. NeuroImage: Clinical. 11, 195-209.

Ghashghaei, H.T., Barbas, H., 2002. Pathways for emotion: Interactions of prefrontal and anterior temporal pathways in the amygdala of the rhesus monkey. Neuroscience. 115, 1261-1279.

Gimenez, M., et al., 2006. Abnormal orbitofrontal development due to prematurity. Neurology. 67, 1818-1822.

Gosselin, N., et al., 2005. Impaired recognition of scary music following unilateral temporal lobe excision. Brain. 128, 628-640.

Gosselin, N., et al., 2007. Amygdala damage impairs emotion recognition from music. Neuropsychologia. 45, 236-244.

Gousias, I.S., et al., 2012. Magnetic resonance imaging of the newborn brain: Manual segmentation of labelled atlases in term-born and preterm infants. Neuroimage. 62, 1499-1509.

Graven, S.N., Browne, J.V., 2008. Auditory Development in the Fetus and Infant. Newborn and Infant Nursing Reviews. 8, 187-193.

Griffiths, T.D., et al., 2004. "When the feeling's gone": a selective loss of musical emotion. Journal of Neurology Neurosurgery and Psychiatry. 75, 344-345.

Groppo, M., et al., 2014. Development of the optic radiations and visual function after premature birth. Cortex. 56, 30-37.

Gui, L., et al., 2012. Morphology-driven automatic segmentation of MR images of the neonatal brain. Medical Image Analysis. 16, 1565-1579.

Hariri, A.R., et al., 2003. Neocortical modulation of the amygdala response to fearful stimuli. Biological Psychiatry. 53, 494-501.

Hille, E.T.M., et al., 2001. Behavioural problems in children who weigh 1000 g or less at birth in four countries. Lancet. 357, 1641-1643.

Hu, Y.Z., et al., 2011. Enhanced White Matter Tracts Integrity in Children With Abacus Training. Human Brain Mapping. 32, 10-21.

Huang, H., et al., 2006. White and gray matter development in human fetal, newborn and pediatric brains. Neuroimage. 33, 27-38.

Hughes, M.B., et al., 2002. Temperament characteristics of premature infants in the first year of life. Journal of Developmental and Behavioral Pediatrics. 23, 430-435.

Huppi, P.S., et al., 1998. Microstructural development of human newborn cerebral white matter assessed in vivo by diffusion tensor magnetic resonance imaging. Pediatric Research. 44, 584-590.

Huppi, P.S., Dubois, J., 2006. Diffusion tensor imaging of brain development. Seminars in fetal & neonatal medicine. 11, 489-497.

Inder, T.E., et al., 2005. Abnormal cerebral structure is present at term in premature infants. Pediatrics. 115, 286-94.

Ishibashi, T., et al., 2006. Astrocytes promote myelination in response to electrical impulses. Neuron. 49, 823-832.

Johnson, S., Marlow, N., 2011. Preterm birth and childhood psychiatric disorders. Pediatr Res. 69, 11R-8R.

Jones, D.K., 2011. Diffusion MRI — theory, methods and applications, Vol., Oxford University Press USA, New York.

Kamagata, K., et al., 2012. White Matter Alteration of the Cingulum in Parkinson Disease with and without Dementia: Evaluation by Diffusion Tensor Tract-Specific Analysis. American Journal of Neuroradiology. 33, 890-895.

Keightley, M.L., et al., 2003. An fMRI study investigating cognitive modulation of brain regions associated with emotional processing of visual stimuli. Neuropsychologia. 41, 585-596.

Keller, T.A., Just, M.A., 2009. Altering Cortical Connectivity: Remediation-induced Changes in the White Matter of Poor Readers. Neuron. 64, 624-631.

Kiss, J.Z., Vasung, L., Petrenko, V., 2014. Process of cortical network formation and impact of early brain damage. Curr Opin Neurol. 27, 133-41.

Kochunov, P., et al., 2009. Analysis of Genetic Variability and Whole Genome Linkage of Whole-Brain, Subcortical, and Ependymal Hyperintense White Matter Volume. Stroke. 40, 3685-3690.

Koelsch, S., et al., 2004. Music, language and meaning: brain signatures of semantic processing. Nature neuroscience. 7, 302-307.

Koelsch, S., 2010. Towards a neural basis of music-evoked emotions. Trends in cognitive sciences. 14, 131-137.

Koelsch, S., et al., 2013. The roles of superficial amygdala and auditory cortex in music-evoked fear and joy. Neuroimage. 81, 49-60.

Koelsch, S., 2014. Brain correlates of music-evoked emotions. Nat Rev Neurosci. 15, 170-80.

Kostovic, I., et al., 2002. Laminar organization of the human fetal cerebrum revealed by histochemical markers and magnetic resonance imaging. Cerebral Cortex. 12, 536-544.

Kostovic, I., Judas, M., 2010. The development of the subplate and thalamocortical connections in the human foetal brain. Acta paediatrica (Oslo, Norway : 1992). 99, 1119-1127.

Kraus, K.S., Canlon, B., 2012. Neuronal connectivity and interactions between the auditory and limbic systems. Effects of noise and tinnitus. Hearing Research. 288, 34-46.

Kringelbach, M.L., 2005. The human orbitofrontal cortex: Linking reward to hedonic experience. Nature Reviews Neuroscience. 6, 691-702.

Krishnan, M.L., et al., 2007. Relationship between white matter apparent diffusion coefficients in preterm infants at term-equivalent age and developmental outcome at 2 years. Pediatrics. 120, E604-E609.

Krogsrud, S.K., et al., 2016. Changes in white matter microstructure in the developing brain-A longitudinal diffusion tensor imaging study of children from 4 to 11 years of age. Neuroimage. 124, 473-486.

Lamont, A., 2011. University students' strong experiences of music: Pleasure, engagement, and meaning. Musicae Scientiae. 15, 229-249.

Langerock, N., et al., 2013. Emotional reactivity at 12 months in very preterm infants born at <29 weeks of gestation. Infant Behav Dev. 36, 289-97.

Largo, R., et al., 1989. Significance of prenatal, perinatal and postnatal factors in the development of AGA preterm infants at five to seven years. Developmental Medicine & Child Neurology. 31, 440-456.

Lasky, R.E., Williams, A.L., 2005. The Development of the Auditory System from Conception to Term. NeoReviews. 6, e141-e152.

Lejeune, F., et al., 2015. Emotion, attention, and effortful control in 24-month-old very preterm and full-term children. Annee Psychologique. 115, 241-264.

Lejeune, F., et al., 2016. Social reasoning abilities in preterm and full-term children aged 5-7years. Early Hum Dev. 103, 49-54.

Lejeune, F., et al., 2019. Effects of an Early Postnatal Music Intervention on Cognitive and Emotional Development in Preterm Children at 12 and 24 Months: Preliminary Findings. Front Psychol. 10, 494.

Loe, I.M., Lee, E.S., Feldman, H.M., 2013. Attention and Internalizing Behaviors in Relation to White Matter in Children Born Preterm. Journal of Developmental and Behavioral Pediatrics. 34, 156-164.

Lordier, L., et al., 2018. Music processing in preterm and full-term newborns: A psychophysiological interaction (PPI) approach in neonatal fMRI. Neuroimage.

Lordier, L., et al., 2019. Music in premature infants enhances high-level cognitive brain networks. Proceedings of the National Academy of Sciences of the United States of America.

Makris, N., Pandya, D.N., 2009. The extreme capsule in humans and rethinking of the language circuitry. Brain Structure & Function. 213, 343-358.

Marlow, N., 2004. Neurocognitive outcome after very preterm birth. Archives of disease in childhood. Fetal and neonatal edition. 89, F224-8.

Mcdonald, A.J., 1987. Somatostatinergic Projections from the Amygdala to the Bed Nucleus of the Stria Terminalis and Medial Preoptic-Hypothalamic Region. Neuroscience Letters. 75, 271-277.

Ment, L.R., Hirtz, D., Huppi, P.S., 2009. Imaging biomarkers of outcome in the developing preterm brain. Lancet Neurol. 8, 1042-55.

Montagna, A., Nosarti, C., 2016. Socio-Emotional Development Following Very Preterm Birth: Pathways to Psychopathology. Frontiers in Psychology. 7.

Moore, E., et al., 2017. Diffusion tensor MRI tractography reveals increased fractional anisotropy (FA) in arcuate fasciculus following music-cued motor training. Brain Cogn. 116, 40-46.

Mukherjee, P., et al., 2002. Diffusion-tensor MR imaging of gray and white matter development during normal human brain maturation. AJNR Am J Neuroradiol. 23, 1445-56.

Mullen, K.M., et al., 2011. Preterm birth results in alterations in neural connectivity at age 16 years. Neuroimage. 54, 2563-2570.

Neil, J., et al., 2002. Diffusion tensor imaging of normal and injured developing human brain - a technical review. NMR Biomed. 15, 543-52.

Nosarti, C., et al., 2012. Preterm Birth and Psychiatric Disorders in Young Adult Life. Archives of General Psychiatry. 69, 610-617.

Nosarti, C., 2013. Structural and functional brain correlates of behavioral outcomes during adolescence. Early human development. 89, 221-227.

Nosarti, C., et al., 2014. Preterm birth and structural brain alterations in early adulthood. Neuroimage-Clinical. 6, 180-191.

Nossin-Manor, R., et al., 2013. Quantitative MRI in the very preterm brain: Assessing tissue organization and myelination using magnetization transfer, diffusion tensor and T-1 imaging. Neuroimage. 64, 505-516.

Ochsner, K.N., et al., 2002. Rethinking feelings: An fMRI study of the cognitive regulation of emotion. Journal of Cognitive Neuroscience. 14, 1215-1229.

Ochsner, K.N., et al., 2004. For better or for worse: neural systems supporting the cognitive down- and up-regulation of negative emotion. Neuroimage. 23, 483-499.

Oishi, K., et al., 2010. MRI Atlas of Human White Matter Vol., Academic Press

Onu, M., et al., 2012. Diffusion abnormality maps in demyelinating disease: Correlations with clinical scores. European Journal of Radiology. 81, E386-E391.

Padilla, N., et al., 2015. Brain Growth Gains and Losses in Extremely Preterm Infants at Term. Cerebral cortex (New York, N.Y. : 1991). 25, 1897-1905.

Pagliaccio, D., et al., 2013. Functional brain activation to emotional and nonemotional faces in healthy children: evidence for developmentally undifferentiated amygdala function during the school-age period. Cogn Affect Behav Neurosci. 13, 771-89.

Partridge, S.C., et al., 2004. Diffusion tensor imaging: serial quantitation of white matter tract maturity in premature newborns. Neuroimage. 22, 1302-1314.

Pecheva, D., et al., 2017. A tract-specific approach to assessing white matter in preterm infants. Neuroimage. 157, 675-694.

Pecheva, D., et al., 2018. Recent advances in diffusion neuroimaging: applications in the developing preterm brain. F1000Res. 7.

Perani, D., et al., 2010. Functional specializations for music processing in the human newborn brain. Proceedings of the National Academy of Sciences of the United States of America. 107, 4758-4763.

Peterson, B.S., et al., 2000. Regional brain volume abnormalities and long-term cognitive outcome in preterm infants. Jama-Journal of the American Medical Association. 284, 1939-1947.

Phan, K.L., et al., 2002. Functional neuroanatomy of emotion: A meta-analysis of emotion activation studies in PET and fMRI. Neuroimage. 16, 331-348.

Pierpaoli, C., Basser, P.J., 1996. Toward a quantitative assessment of diffusion anisotropy. Magnetic Resonance in Medicine. 36, 893-906.

Popescu, M., Otsuka, A., Ioannides, A.A., 2004. Dynamics of brain activity in motor and frontal cortical areas during music listening: a magnetoencephalographic study. NeuroImage. 21, 1622-1638.

Pouladi, F., et al., 2010. Involved brain areas in processing of Persian classical music: an fMRI study. Procedia - Social and Behavioral Sciences. 5, 1124-1128.

Prather, M.D., et al., 2001. Increased social fear and decreased fear of objects in monkeys with neonatal amygdala lesions. Neuroscience. 106, 653-658.

Qiu, D.Q., et al., 2008. Diffusion tensor imaging of normal white matter maturation from late childhood to young adulthood: Voxel-wise evaluation of mean diffusivity, fractional anisotropy, radial and axial diffusivities, and correlation with reading development. Neuroimage. 41, 223-232.

Radley, J.J., Morrison, J.H., 2005. Repeated stress and structural plasticity in the brain. Ageing Research Reviews. 4, 271-287.

Rimol, L.M., et al., 2019. Reduced white matter fractional anisotropy mediates cortical thickening in adults born preterm with very low birthweight. Neuroimage. 188, 217-227.

Rogers, C.E., et al., 2012. Regional Cerebral Development at Term Relates to School-Age Social-Emotional Development in Very Preterm Children. Journal of the American Academy of Child and Adolescent Psychiatry. 51, 181-191.

Rose, S.E., et al., 2008. Altered white matter diffusion anisotropy in normal and preterm infants at term-equivalent age. Magnetic Resonance in Medicine. 60, 761-767.

Ruber, T., Lindenberg, R., Schlaug, G., 2015. Differential Adaptation of Descending Motor Tracts in Musicians. Cerebral Cortex. 25, 1490-1498.

Shim, S.Y., et al., 2012. Altered Microstructure of White Matter Except the Corpus Callosum Is Independent of Prematurity. Neonatology. 102, 309-315.

Sizun, J., Westrup, B., 2004. Early developmental care for preterm neonates: a call for more research. Arch Dis Child Fetal Neonatal Ed. 89, F384-8.

Skranes, J., et al., 2007. Clinical findings and white matter abnormalities seen on diffusion tensor imaging in adolescents with very low birth weight. Brain. 130, 654-666.

Smith, S.M., et al., 2004. Advances in functional and structural MR image analysis and implementation as FSL. Neuroimage. 23, S208-S219.

Snook, L., et al., 2005. Diffusion tensor imaging of neuro development in children and young adults. Neuroimage. 26, 1164-1173.

Sowell, E.R., et al., 1999. In vivo evidence for post-adolescent brain maturation in frontal and striatal regions. Nat Neurosci. 2, 859-61.

Spittle, A.J., et al., 2009. Early Emergence of Behavior and Social-Emotional Problems in Very Preterm Infants. Journal of the American Academy of Child and Adolescent Psychiatry. 48, 909-918.

Spittle, A.J., et al., 2011. Neonatal white matter abnormality predicts childhood motor impairment in very preterm children. Dev Med Child Neurol. 53, 1000-6.

Standring, S., 2015. Gray's Anatomy: The anatomical Basis of Clinical Practice, Vol., Elsevier, Edinburgh: Churchill Livingstone.

Suzuki, Y., et al., 2003. Absolute eigenvalue diffusion tensor analysis for human brain maturation. Nmr in Biomedicine. 16, 257-260.

Takahashi, M., et al., 2000. Diffusional anisotropy in cranial nerves with maturation: Quantitative evaluation with diffusion MR imaging in rats. Radiology. 216, 881-885.

Tang, Y.Y., et al., 2012. Mechanisms of white matter changes induced by meditation. Proceedings of the National Academy of Sciences of the United States of America. 109, 10570-10574.

Taubert, M., Villringer, A., Ragert, P., 2012. Learning-Related Gray and White Matter Changes in Humans: An Update. Neuroscientist. 18, 320-325.

Thompson, D.K., et al., 2007. Perinatal risk factors altering regional brain structure in the preterm infant. Brain. 130, 667-77.

Thompson, D.K., et al., 2011. Characterization of the corpus callosum in very preterm and full-term infants utilizing MRI. Neuroimage. 55, 479-490.

Thompson, D.K., et al., 2013. Hippocampal shape variations at term equivalent age in very preterm infants compared with term controls: perinatal predictors and functional significance at age 7. Neuroimage. 70, 278-87.

Treyvaud, K., et al., 2013. Psychiatric outcomes at age seven for very preterm children: rates and predictors. Journal of Child Psychology and Psychiatry. 54, 772-779.

Volpe, J.J., 2009. The encephalopathy of prematurity--brain injury and impaired brain development inextricably intertwined. Semin Pediatr Neurol. 16, 167-78.

Webb, A.R., et al., 2015. Mother's voice and heartbeat sounds elicit auditory plasticity in the human brain before full gestation. Proceedings of the National Academy of Sciences of the United States of America. 112, 3152-3157.

Wildgruber, D., et al., 2005. Identification of emotional intonation evaluated by fMRI. Neuroimage. 24, 1233-1241.

Williams, J., Lee, K.J., Anderson, P.J., 2010. Prevalence of motor-skill impairment in preterm children who do not develop cerebral palsy: a systematic review. Dev Med Child Neurol. 52, 232-7.

Wimberger, D.M., et al., 1995. Identification of "premyelination" by diffusion-weighted MRI. J Comput Assist Tomogr. 19, 28-33.

Witt, A., et al., 2014. Emotional and effortful control abilities in 42-month-old very preterm and full-term children. Early Hum Dev. 90, 565-9.

Yushkevich, P.A., et al., 2006. User-guided 3D active contour segmentation of anatomical structures: Significantly improved efficiency and reliability. Neuroimage. 31, 1116-1128.

Zatorre, R.J., Peretz, I., Penhune, V., 2009. Neuroscience and Music ("Neuromusic") III: disorders and plasticity. . Annals of the New York Academy of Sciences. 1169, 1-2.

Zatorre, R.J., Fields, R.D., Johansen-Berg, H., 2012. Plasticity in gray and white: neuroimaging changes in brain structure during learning. Nature Neuroscience. 15, 528-536.

Zhang, H., et al., 2006. Deformable registration of diffusion tensor MR images with explicit orientation optimization. Med Image Anal. 10, 764-85.

Supplementary material

Supplementary Figures

Supplementary Fig. S1
Flow chart of the participant selection process
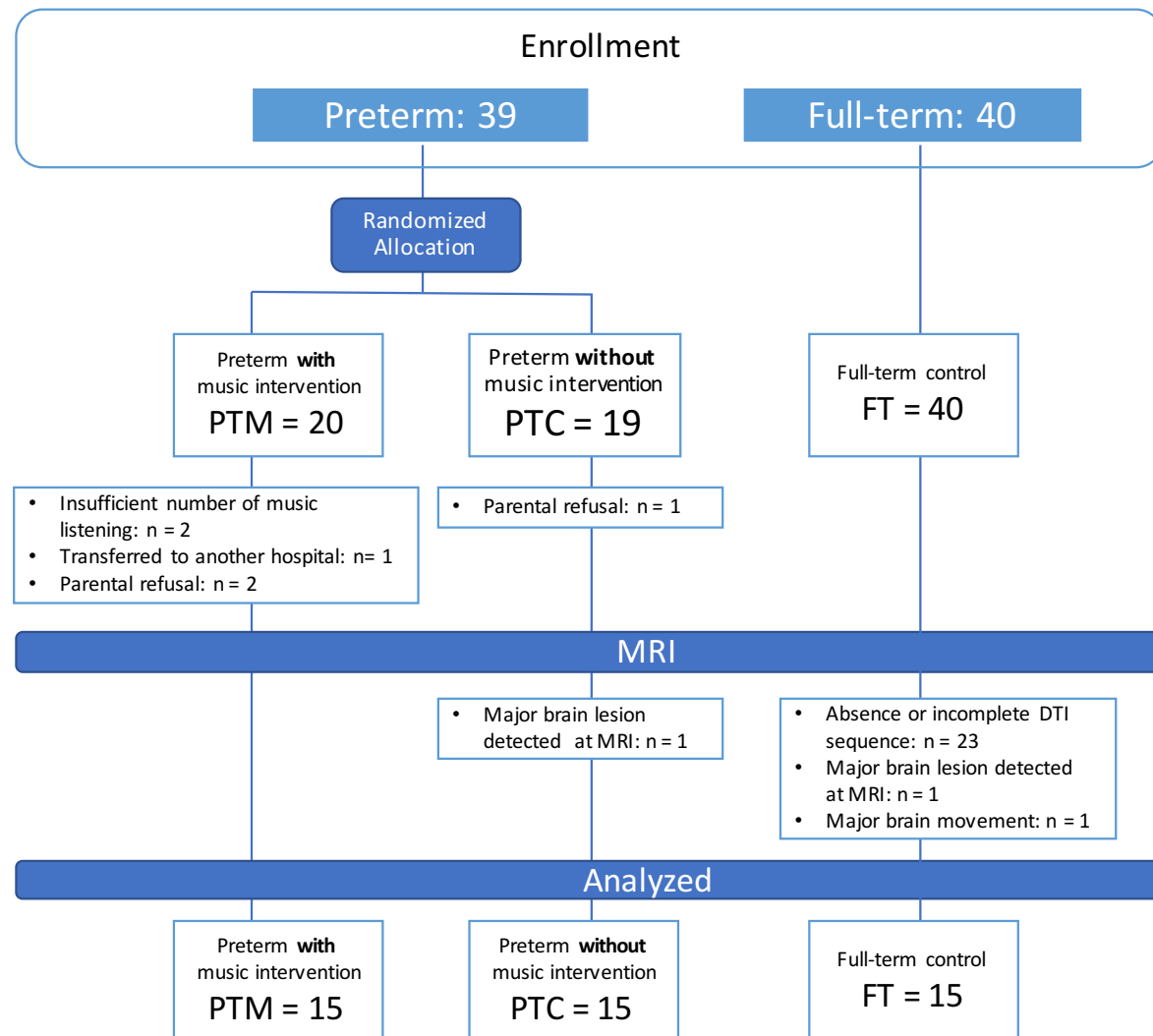
Supplementary Fig. S1: 39 preterm infants (GA at birth <32 weeks) were recruited at the neonatal unit of the University Hospitals of Geneva (HUG), Switzerland, from 2013 to 2016, as part of a prospective randomized clinical trial entitled 'The effect of music on preterm infant's development' (NCT03689725). The eligibility criteria for preterm infant's recruitment included GA at birth < 32 weeks and presence of CPAP pauses. Exclusion criteria comprised detection of severe brain lesions on MRI, such as intraventricular haemorrhage stage III-IV, hydrocephaly or leukomalacia, microcephaly or macrocephaly and presence of congenital syndrome.

The 39 preterm infants were randomized into two groups, 20 received a music intervention during NICU stay (PTM) and 19 received standard-of-care during NICU stay (PTC). Randomization was performed using an aleatory function for an unpredictable allocation sequence with concealment of that sequence until assignment occurred. The random allocation, enrolment of patients and assignment of patients to intervention was performed by the research assistant. Parents, music intervention providers, and caregivers were blinded to the group assignment.

Additionally, 40 full-term (FT) infants were recruited at the maternity of HUG, from 2010 to 2016 as part of clinical trials studying the impact of prematurity on neonatal preterm brain development. Inclusion criteria for
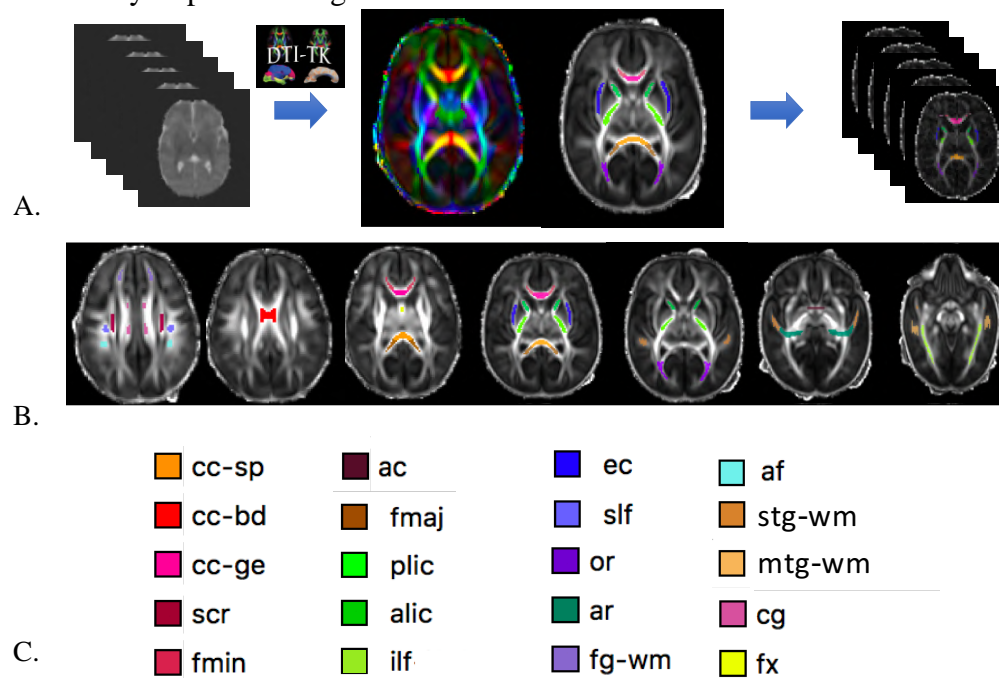
full-term newborns included: birth after 37 weeks GA and an appropriate height, weight or head circumference (above the 5th and below the 95th percentiles). Exclusion criteria were similar to those used for preterm infants. Six preterm infants were excluded from the study before the MRI due to: parental refusal (2 PTM, 1 PTC), transfer to another hospital (1 PTM) and insufficient number of music intervention sessions (less than 15 intervention sessions: 2 PTM). All subjects underwent an MRI examination at TEA (37-42 weeks GA). Infants whose MRI protocol acquisition was incomplete, not comprising a T2-weighted image and DTI sequence, or that presented major focal brain lesions or major movement on MRI images were excluded from the analysis. The final sample of infants used for DTI analysis consisted of: 15 PTM, 15 PTC and 15 FT infants.

Supplementary Fig. S2
Study-specific template
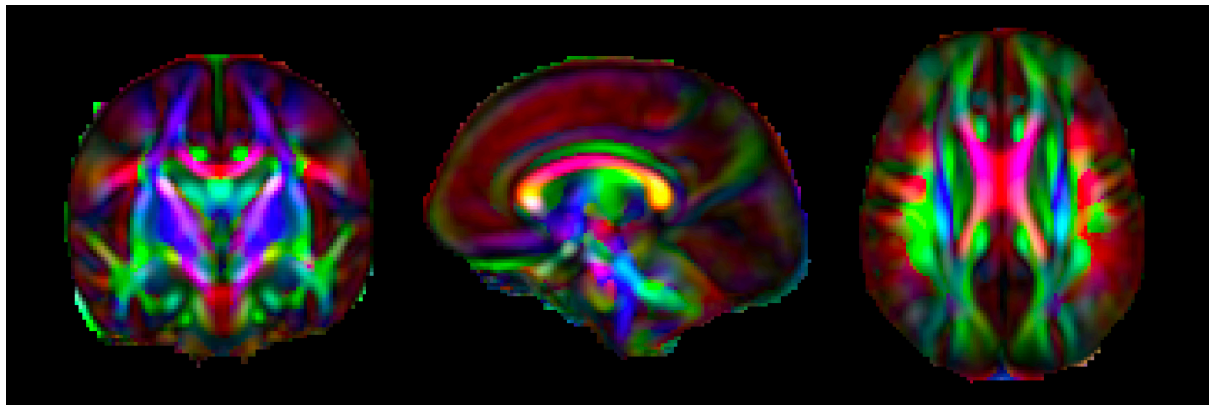
Supplementary Fig. S2: Coronal, sagittal and axial views (from left to right) of the final study-specific template (principal diffusion direction mapped into an RGB image). The final study-specific template was generated using DTI-TK (http://www.nitrc.org/projects/dtitk), a toolkit used for tensor-based spatial normalization of diffusion MRI data (Zhang et al., 2006). All the diffusion MRI data were first pre-processed as described in the materials and methods section 2.4. The volumes were transformed into DTI-TK compatible format (including adjustment to DTI-TK diffusivity units) and a first study-specific template was created by choosing one subject and registering all the subjects to that one. The steps for creating this template comprise: bootstrapping an initial study-specific template from the input DTI volumes using one subject tensor image as existing template, resampling to isotropic 1.0x1.0x1.0mm3 voxels, rigid alignment with the bootstrapped template, affine alignment with refined template estimated from rigid alignment, identification and removal via masking of outlier voxels by binary thresholding of the trace map (lower 0.01, upper 100) and deformable alignment of DTI volumes (number of iterations = 6, optimization stopping condition = 0.002). After creating this first study-specific template, we re-registered all subjects to this newly generated template, by repeating all the previous enumerated steps, and we obtained our final study-specific template where we drew the 20 ROI. The resulting study-specific final template was visually assessed and compared to white matter brain atlas of (Oishi et al., 2010). Each subject's FA map was overlaid on the top of the template in order to assess correspondence.

Supplementary Fig. S3
ROI analysis process diag

A.

B.

C. ROIs legend:

cc-sp		ac		ec		af
cc-bd		fmaj		slf		stg-wm
cc-ge		plic		or		mtg-wm
scr		alic		ar		cg
fmin		ilf		fg-wm		fx

...ata processing diagram: diffusion tensors of all subjects were used to generate a ... means of DTI-TK) where ROIs were drawn manually and then back transformed to ... n FA map with ROIs overlaid; C. ROIs legend: cc-sp - splenium part of corpus callosum, ...us callosum, cc-ge - genu part of corpus callosum, scr - superior corona radiata, fmin - ...ior commissure, fmaj - forceps major, plic - posterior limb of the internal capsule, alic - ...nternal capsule, ilf– inferior longitudinal fasciculus, ec– external capsule/claustrum/extreme ...r longitudinal fasciculus, or– optic radiation, ar– acoustic radiation, fg-wm–frontal gyrus ...arcuate fasciculus, stg-wm– superior temporal gyrus white matter, mtg-wm– medial temporal ...atter, cg– cingulum, fx– fornix.

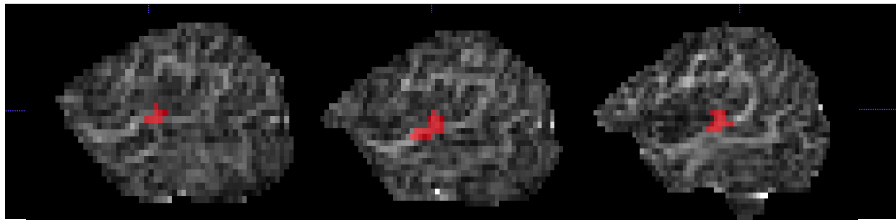## Supplementary Fig. S4

A.　　　　　　　　B.　　　　　　　　C.
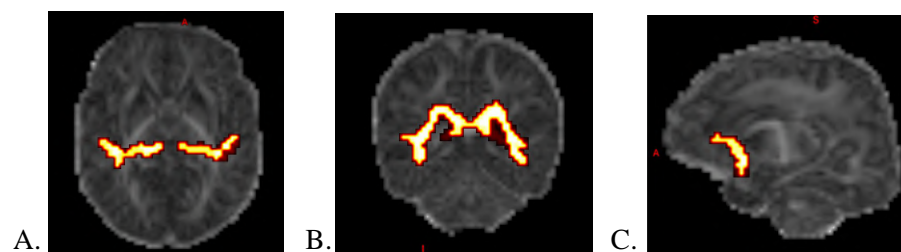
Supplementary Fig. S4: Tractography examples illustrating the following fibers: A. Acoustic radiations, axial plane; B. Interhemispheric temporal callosal fibers, coronal plane; C. Uncinate fasciculus, sagittal plane.
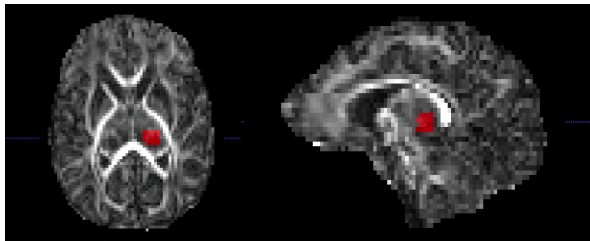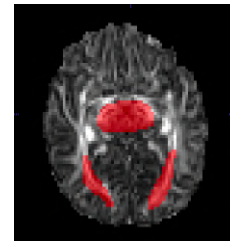
Supplementary Fig. S5

A. Acoustic radiations
a) Heschl's gyrus (seed)

b) Thalamus (waypoint)

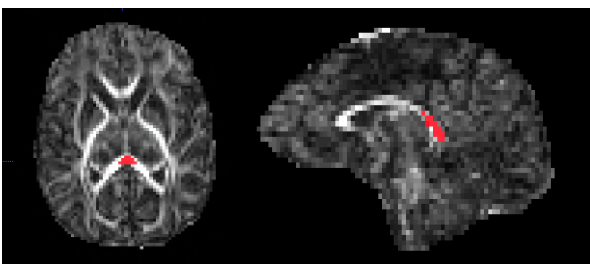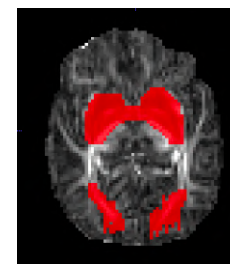c) Exclusion mask

B. Interhemispheric temporal callosal fibers
b) Splenium of corpus callosum (waypoint)

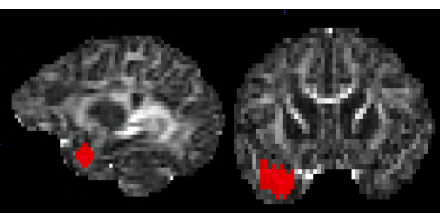c) Exclusion mask
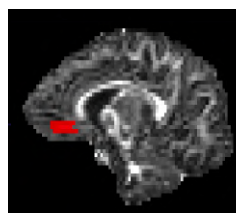

C. Uncinate fasciculus
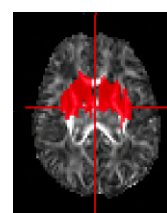a) Temporal lobe (seed 1)

b) OFC (seed 2)   c) Exclusion mask

Supplementary Fig. S5: Illustration of the masks used for the tractography. A. Acoustic Radiations masks: a seed mask was placed in either left or right Heschl's gyrus (a; sagittal slices, from the more lateral to the more medial one), a waypoint mask was placed in the ipsilateral posterior thalamus to comprise medial geniculate nucleus (b; axial and sagittal views) and an exclusion mask was generated to restrict the pathway to the hemisphere ipsilateral to the seed mask and exclude ipsilateral optic radiations fibers (c; axial view). B. Interhemispheric temporal callosal fibers masks: two seeds were used, comprising the left and right primary auditory cortex (A, a), a waypoint in the splenium of corpus callosum (b; axial and sagittal views); and an exclusion mask to exclude ipsilateral optic radiations and fibers of the posterior limb of internal capsule (c; axial view). C. Uncinate fasciculus masks: a first seed was placed in the left or right temporal lobe (a; sagittal and coronal views) and a second seed was placed in the ipsilateral inferior part of the frontal lobe (b; sagittal view; OFC- orbito-fronto-cortex); the seed masks were also used as waypoint masks; an exclusion mask was used to restrict the pathway to the hemisphere ipsilateral to the seed mask and exclude fibers from the posterior limb of internal capsule (c; axial view).

Supplementary Fig. S6
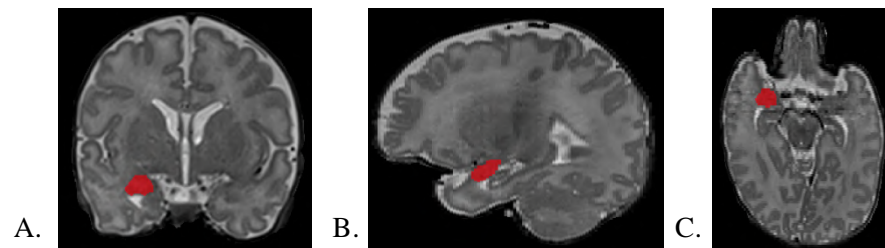
Supplementary Fig. S6: Segmentation example of right amygdala on T2-weighted image: (A) coronal view; (B) sagittal view; (C) axial view.

Supplementary Tables

Supplementary Table S1
Mean FA per ROI (corrected for GA at MRI) and effect size (Cohen's d) between groups. In orange, we select regions where effect size between groups was large (Cohen's d>0.8). Numbers in bold represent the pairwise comparisons that survived Bonferroni post hoc test.

ROI	Mean FA (95% CI)			Pairwise comparison		
				Effect Size (Cohen's d)		
	Full-term	Preterm Music	Preterm Control	FT vs PTC	FT vs PTM	PTM vs PTC
cc-sp	0.630 (0.602-0.659)	0.573 (0.546-0.600)	0.540 (0.513-0.568)	**1.471**	**0.940**	0.531
cc-bd	0.503 (0.469-0.536)	0.432 (0.400-0.463)	0.406 (0.373-0.439)	**1.380**	**1.016**	0.364
cc-ge	0.573 (0.542-0.605)	0.523 (0.494-0.553)	0.492 (0.461-0.523)	**1.296**	0.799	0.497
scr	0.316 (0.296-0.336)	0.303 (0.285-0.322)	0.279 (0.260-0.298)	**0.984**	0.336	0.648
fmin	0.419 (0.392-0.445)	0.385 (0.360-0.410)	0.359 (0.333-0.385)	**1.156**	0.652	0.504
ac	0.226 (0.217-0.235)	0.214 (0.205-0.222)	0.206 (0.197-0.215)	**1.139**	0.699	0.440
fmaj	0.508 (0.479-0.538)	0.489 (0.461-0.517)	0.468 (0.439-0.497)	0.748	0.366	0.382
plic	0.539 (0.519-0.558)	0.535 (0.517-0.554)	0.503 (0.484-0.522)	**0.949**	0.094	0.855
alic	0.344 (0.324-0.363)	0.337 (0.319-0.355)	0.325 (0.306-0.344)	0.538	0.197	0.341
ilf	0.358 (0.340-0.375)	0.342 (0.325-0.359)	0.322 (0.305-0.340)	**1.017**	0.455	0.562
ec	0.262 (0.251-0.274)	0.262 (0.252-0.273)	0.238 (0.227-0.250)	**0.994**	0.002	**0.991**
slf	0.301 (0.285-0.318)	0.299 (0.283-0.314)	0.287 (0.271-0.303)	0.482	0.083	0.398
or	0.321 (0.299-0.344)	0.300 (0.279-0.320)	0.288 (0.266-0.309)	0.829	0.539	0.290
ar	0.265 (0.252-0.277)	0.277 (0.265-0.289)	0.265 (0.253-0.277)	0.016	0.521	0.505
fg-wm	0.243 (0.223-0.262)	0.206 (0.188-0.225)	0.197 (0.178-0.216)	**1.192**	**0.940**	0.251
af	0.271 (0.251-0.292)	0.251 (0.232-0.271)	0.240 (0.220-0.261)	0.806	0.521	285
stg-wm	0.214 (0.204-0.223)	0.206 (0.197-0.215)	0.199 (0.190-0.208)	0.845	0.452	0.393
mtg-wm	0.163 (0.154-0.172)	0.151 (0.142-0.160)	0.144 (0.135-0.153)	**1.083**	0.689	0.394
cg	0.344 (0.330-0.359)	0.331 (0.317-0.345)	0.329 (0.314-0.343)	0.591	0.505	0.086
fx	0.475 (0.434-0.516)	0.460 (0.421-0.499)	0.441 (0.401-0.482)	0.444	0.200	0.245

cc-bd - body part of corpus callosum, cc-ge - genu part of corpus callosum, scr - superior corona radiata, fmin - forceps minor, ac - anterior commissure, fmaj - forceps major, plic - posterior limb of the internal capsule, alic - anterior limb of the internal capsule, ilf - inferior longitudinal fasciculus, ec - external capsule/claustrum/extreme capsule, slf - superior longitudinal fasciculus, or - optic radiation, ar - acoustic radiation, fg-wm - frontal gyrus white matter, af - arcuate fasciculus, stg-wm - superior temporal gyrus white matter, mtg-wm - medial temporal gyrus white matter, cg - cingulum, fx - fornix; CI - confidence interval; FT - full-term, PTC - preterm control, PTM - preterm music; (p) - p-value.

Supplementary Table S2
Mean MD, RD and AD (corrected for GA at MRI) of the 11 ROI where FA was statistically different between groups and effect size (Cohen's d) between groups. In orange, we select regions where effect size between groups was large (Cohen's d>0.8). Numbers in bold represent the pairwise comparisons that survived Bonferroni post hoc test.

ROI		Mean DTI measurements (95% CI)			Pairwise comparison		
		Full-term	Preterm Music	Preterm Control	Effect Size (Cohen's d)		
					FT vs PTC	FT vs PTM	PTM vs PTC
cc-sp	MD	1.199 (1.154-1.245)	1.283 (1.288-1.375)	1.346 (1.301-1.390)	**1.459**	**0.836**	0.623
	RD	0.693 (0.638-0.748)	0.807 (0.755-0.859)	0.886 (0.832-0.940)	**1.553**	**0.913**	0.641
	AD	2.212 (2.157-2.266)	2.236 (2.185-2.287)	2.264 (2.211-2.318)	0.537	0.250	0.287
cc-bd	MD	1.255 (1.209-1.301)	1.331 (1.288-1.375)	1.382 (1.337-1.427)	**1.364**	0.821	0.543
	RD	0.863 (0.804-0.921)	0.987 (0.932-1.042)	1.050 (0.993-1.107)	**1.500**	**0.996**	0.504
	AD	2.039 (1.967-2.111)	2.020 (1.952-2.088)	2.047 (1.976-2.117)	0.059	0.148	0.207
cc-ge	MD	1.244 (1.190-1.298)	1.287 (1.236-1.337)	1.336 (1.284-1.389)	0.921	0.425	0.495
	RD	0.782 (0.715-0.849)	0.862 (0.798-0.925)	0.929 (0.864-0.995)	**1.137**	0.615	0.522
	AD	2.168 (2.123-2.213)	2.136 (2.094-2.179)	2.150 (2.106-2.195)	0.220	0.387	0.167
scr	MD	1.200 (1.154-1.246)	1.219 (1.175-1.262)	1.268 (1.223-1.313)	0.813	0.223	0.590
	RD	0.982 (0.932-1.031)	1.007 (0.960-1.053)	1.065 (1.017-1.114)	0.908	0.271	0.637
	AD	1.636 (1.589-1.683)	1.642 (1.598-1.687)	1.674 (1.628-1.720)	0.461	0.078	0.383
fmin	MD	1.366 (1.321-1.411)	1.407 (1.365-1.450)	1.444 (1.399-1.488)	0.908	0.481	0.427
	RD	1.020 (0.962-1.079)	1.084 (1.029-1.140)	1.136 (1.078-1.193)	**1.034**	0.574	0.460
	AD	2.059 (2.025-2.092)	2.053 (2.022-2.084)	2.059 (2.026-2.091)	0.006	0.090	0.095
ac	MD	1.100 (1.070-1.129)	1.141 (1.114-1.169)	1.156 (1.127-1.185)	1.004	0.744	0.259
	RD	0.967 (0.939-0.995)	1.010 (0.984-1.036)	1.027 (0.999-1.055)	**1.094**	0.783	0.311
	AD	1.365 (1.328-1.401)	1.404 (1.370-1.438)	1.413 (1.378-1.449)	0.736	0.593	0.143
plic	MD	1.021 (1.005-1.037)	1.006 (0.990-1.021)	1.018 (1.002-1.034)	0.091	0.507	0.416
	RD	0.670 (0.646-0.694)	0.664 (0.642-0.686)	0.698 (0.675-0.721)	0.613	0.129	0.742
	AD	1.723 (1.695-1.751)	1.688 (1.662-1.715)	1.659 (1.631-1.686)	**1.178**	0.637	0.541
ilf	MD	1.361 (1.320-1.402)	1.387 (1.348-1.426)	1.439 (1.399-1.479)	**1.000**	0.333	0.668
	RD	1.077 (1.032-1.122)	1.113 (1.071-1.155)	1.174 (1.130-1.218)	**1.121**	0.414	0.707
	AD	1.930 (1.883-1.977)	1.936 (1.891-1.980)	1.969 (1.923-2.015)	0.462	0.069	0.392
ec	MD	1.188 (1.165-1.211)	1.203 (1.182-1.225)	1.200 (1.177-1.223)	0.263	0.333	0.070
	RD	1.033 (1.008-1.058)	1.048 (1.024-1.071)	1.062 (1.037-1.086)	0.566	0.289	0.277
	AD	1.498 (1.471-1.524)	1.515 (1.490-1.540)	1.477 (1.451-1.503)	0.408	0.325	0.733
fg-wm	MD	1.356 (1.302-1.410)	1.464 (1.414-1.515)	1.458 (1.405-1.511)	**0.977**	**1.038**	0.061
	RD	1.208 (1.147-1.270)	1.329 (1.271-1.387)	1.331 (1.271-1.391)	**1.026**	**1.011**	0.015
	AD	1.651 (1.609-1.693)	1.735 (1.696-1.774)	1.712 (1.671-1.753)	0.762	**1.045**	0.283
mtg-wm	MD	1.402 (1.366-1.439)	1.435 (1.400-1.469)	1.427 (1.391-1.463)	0.363	0.485	0.122
	RD	1.296 (1.257-1.334)	1.334 (1.298-1.370)	1.329 (1.292-1.367)	0.479	0.541	0.062
	AD	1.616 (1.580-1.652)	1.638 (1.604-1.671)	1.622 (1.587-1.657)	0.086	0.326	0.242

cc-bd - body part of corpus callosum, cc-ge - genu part of corpus callosum, scr - superior corona radiata, fmin - forceps minor, ac - anterior commissure, plic - posterior limb of the internal capsule, ilf– inferior longitudinal fasciculus, ec - external capsule/claustrum/extreme capsule, fg-wm - frontal gyrus white matter, mtg-wm - medial temporal gyrus white matter; CI - confidence interval; FT - full-term, PTC - preterm control, PTM - preterm music; (p) - p-value.

Supplementary Table S3

Paired sample t-test: differences within-group (PTM, PTC and FT) regarding mean FA, MD, AD and RD of left and right acoustic radiations, as well as left and right uncinated fasciculus

		Preterm Music		
Tract	*DTI metric*	*Left*	*Right*	*Paired Sample T-test*
Acoustic Radiations	FA (SD)	0.232 (0.016)	0.235 (0.026)	0.648
	MD (SD)	1.239 (0.047)	1.214 (0.062)	0.202
	AD (SD)	1.548 (0.068)	1.530 (0.064)	0.425
	RD (SD)	1.088 (0.045)	1.073 (0.056)	0.426
Uncinate Fasciculus	FA (SD)	0.167 (0.023)	0.024 (0.024)	0.509
	MD (SD)	1.448 (0.115)	1.429 (0.104)	0.355
	AD (SD)	1.697 (0.101)	1.683 (0.111)	0.615
	RD (SD)	1.339 (0.126)	1.324 (0.131)	0.493
		Preterm Control		
Tract	*DTI metric*	*Left*	*Right*	*Paired Sample T-test*
Acoustic Radiations	FA (SD)	0.224 (0.014)	0.219 (0.021)	0.187
	MD (SD)	1.239 (0.063)	1.236 (0.074)	0.794
	AD (SD)	1.533 (0.061)	1.526 (0.065)	0.669
	RD (SD)	1.094 (0.065)	1.097 (0.086)	0.847
Uncinate Fasciculus	FA (SD)	0.153 (0.015)	0.152 (0.013)	0.769
	MD (SD)	1.530 (0.084)	1.501 (0.082)	0.175
	AD (SD)	1.767 (0.077)	1.733 (0.083)	0.163
	RD (SD)	1.405 (0.094)	1.385 (0.083)	0.339
		Full-term		
Tract	*DTI metric*	*Left*	*Right*	*Paired Sample T-test*
Acoustic Radiations	FA (SD)	0.216 (0.025)	0.217 (0.018)	0.827
	MD (SD)	1.228 (0.062)	1.255 (0.082)	0.235
	AD (SD)	1.503 (0.077)	1.531 (0.083)	0.357
	RD (SD)	1.091 (0.062)	1.117 (0.083)	0.189
Uncinate Fasciculus	FA (SD)	1.163 (0.025)	1.163 (0.279)	0.966
	MD (SD)	1.559 (0.110)	1.530 (0.105)	0.315
	AD (SD)	1.824 (0.113)	1.799 (0.104)	0.196
	RD (SD)	1.434 (0.110)	1.423 (0.117)	0.502

Supplementary Table S4

Mean FA, MD, RD and AD (corrected for GA at MRI) of acoustic radiations, interhemispheric callosal fibers and uncinate fasciculus per group, accompanied of effect size (Cohen's d) between groups. In orange, we select regions where effect size between groups was large (Cohen's d>0.8). Numbers in bold represent the pairwise comparisons that survived Bonferroni post hoc test.

| ROI | Mean FA (95% CI) | | | Pairwise comparison | | |
| | | | | Effect Size (Cohen's d) | | |
	Full-term	Preterm Music	Preterm Control	FT vs PTC	FT vs PTM	PTM vs PTC
Ac. Rad. average	0.22 (0.214-0.229)	0.232 (0.225-0.239)	0.218 (0.211-0.226)	0.495	0.155	**0.650**
Interhemispheric Temp. Call. Fib.	0.331 (0.316-0.346)	0.314 (0.299-0.328)	0.294 (0.279-0.308)	**1.179**	0.545	0.633
Unc. F. average	0.168 (0.160-0.176)	0.167 (0.159-0.175)	0.149 (0.141-0.156)	**0.878**	0.048	**0.831**
Mean MD (95% CI)						
Ac. Rad. average	1.230 (1.206-1.255)	1.228 (1.205-1.252)	1.247 (1.223-1.271)	0.264	0.025	0.289
Interhemispheric Temp. Call. Fib.	1.516 (0.147-1.56)	1.604 (1.56-1.65)	1.656 (1.61-1.70)	**1.463**	**0.969**	0.494
Unc. F. average	1.540 (1.501-1.579)	1.439 (1.402-1.476)	1.519 (1.481-1.557)	0.194	**0.928**	**0.735**
Mean RD (95% CI)						
Ac. Rad. average	1.091 (1.066-1.116)	1.083 (1.059-1.106)	1.106 (1.081-1.131)	0.214	0.128	0.342
Interhemispheric Temp. Call. Fib.	1.245 (1.188-1.302)	1.349 (1.296-1.403)	1.377 (1.321-1.433)	**1.179**	**0.934**	0.245
Unc. F. average	1.418 (1.375-1.461)	1.333 (1.293-1.374)	1.408 (1.366-1.451)	0.117	**0.726**	**0.609**
Mean AD (95% CI)						
Ac. Rad. average	1.511 (1.483-1.538)	1.540 (1.515-1.566)	1.536 (1.509-1.563)	0.364	0.428	0.064
Interhemispheric Temp. Call. Fib.	2.057 (2.001-2.113)	1.976 (1.923-2.029)	2.162 (2.107-2.216)	**0.837**	0.644	**1.482**
Unc. F. average	1.811 (1.773-1.850)	1.690 (1.654-1.726)	1.754 (1.716-1.792)	0.522	**1.115**	**0.592**

Ac. Rad. – acoustic radiations, Interhemispheric Temp. Call. Fib. – Interhemispheric temporal callosal fibers, Unc. F. – uncinate fasciculus, CI - confidence interval; FT - full-term, PTC - preterm control, PTM - preterm music; (p) - p-value.

Supplementary Table S5

Paired sample t-test: differences within-group (PTM, PTC and FT) regarding mean left and right amygdala corrected volumes.

Region Volume	Group	Left	Right	(p) Paired Sample T-test
Amygdala	PTM	496.9 (39.73)	488.55 (64.94)	0.655
	PTC	443.97 (64.04)	444.95 (71.42)	0.954
	FT	504.29 (61.68)	491.39 (91.47)	0.598

(p) - p-value.

Supplementary Table S6

Corrected mean amygdala volumes and effect size (Cohen's d) between groups. In orange, we select regions where effect size between groups was large (Cohen's d>0.8). Numbers in bold represent the pairwise comparisons that survived Bonferroni post hoc test.

| | Amygdala Volumes (95% CI) | | | Pairwise comparison | | |
| | | | | Effect Size (Cohen's d) | | |
	Full-term	Preterm Music	Preterm Control	FT vs PTC	FT vs PTM	PTM vs PTC
Amygdala	514.9 (484.0-545.8)	492.2 (461.5-522.9)	422.9 (391.4-454.4)	**1.285**	0.567	**0.718**

Study 3

Music impacts brain cortical maturation in very preterm infants: a longitudinal fixel-based and NODDI analysis

In preparation

Music impacts brain cortical maturation in very preterm infants: a longitudinal fixel-based and NODDI analysis

Joana Sa de Almeida[1]; Olivier Baud[2], Sebastien Fau[2], Francsica Barcos[2], Sebastien Courvoisier[3]; Lara Lordier[1]; François Lazeyras[3]; Petra S. Hüppi[1]*

[1] Division of Development and Growth, Department of Woman, Child and Adolescent, University Hospitals of Geneva, Geneva, Switzerland

[2] Division of Neonatal and Intensive Care, Department of Woman, Child and Adolescent, University Hospitals of Geneva, Geneva, Switzerland

[3] Department of Radiology and Medical Informatics; Center of BioMedical Imaging (CIBM), University of Geneva, Geneva, Switzerland

*Corresponding author address:

Hôpitaux Universitaires de Genève; Département de la femme, de l'enfant et de l'adolescent, Service de développement et croissance, Hôpital des enfants, Rue Willy-Donzé 6, CH-1211

Abstract

Dynamic micro and macrostructural changes take place from mid-fetal stage to birth, comprising increasing axon density and myelination in white matter (WM), as well as dendritic growth and arborisation in grey-matter (GM), leading to a significant expansion of brain volumes during the third trimester of brain development.

Preterm birth interrupts abruptly the normal brain maturation, exposing preterm infants to multiple pathological events and noxious stimuli, as well as depriving them from meaningful sensory inputs during a critical period of activity-dependent plasticity.

Musicotherapy has been used in neonatal intensive care units (NICU) as a relevant approach for activity-dependent brain plasticity that may influence brain networks formed early in development and affected by prematurity.

Multi-shell diffusion imaging data was acquired in 24 full-term (FT) newborns and 54 very preterm infants (VPT), 26 without music exposure and 28 exposed daily to a musicotherapy protocol during neonatal stay, from the 33th week gestational age (GA) to term-equivalent age (TEA). FT newborns underwent the MRI at TEA whereas the VPT underwent an MRI at two-time points: the first during the 33th week GA before starting the intervention and the second at TEA, at the end of the intervention.

Using a whole-brain fixel-based analysis (FBA) complemented by NODDI, we aimed to study: the longitudinal whole-brain micro and macroscopic changes occurring in preterm infants from the 33th week GA to TEA; the impact of preterm birth on brain maturation at TEA, in comparison to FT birth; and the longitudinal effect of an early music intervention during neonatal stay on preterm infants' brain maturation, from the 33th week GA to TEA.

Overall, during preterm infants' early brain development, from the 33th week GA to TEA, there is a significant longitudinal increase of fiber density (FD), fiber cross-section (FC) and fiber density cross-section (FDC) in all major cerebral WM fibers, as well as in the thalamus, brainstem, cerebellum and cerebellar peduncles, whereas in cortical GM there is an increase of FC accompanied by a decrease of FD and FDC. Preterm birth led to a diminished FD in commissural and projection WM fibers at TEA, in comparison to FT birth. An early music intervention from the 33th week GA to TEA has resulted in a significant longitudinal increase of cortical FC in the right middle temporal gyrus, the left insulo-orbito-temporopolar complex, and the right precuneus and posterior cingulate gyrus, which was accompanied by an increase of ODI, reflecting an increase in dendrite arborisation and cortical geometrical

complexity of these regions, undergoing important maturation changes during the third trimester and known to be impaired by prematurity.

Our findings support therefore that: important micro and macroscopic changes are taking place in human brain WM and GM during the third trimester; that preterm birth impairs microscopic WM maturation by TEA in comparison to FT birth; and that an early music intervention can enhance maturation of diverse cortical regions undergoing significant maturational changes during the third trimester and implied in auditory, cognitive and specially socio-emotional processing.

Keywords

Diffusion MRI, Fixel-based analysis, Human brain development, Longitudinal, Music intervention, Preterm birth

1. Introduction

During early brain development, important macrostructural and microstructural maturational changes take place. The third trimester, in particular, is characterized by a rapid brain growth with expansion of grey-matter (GM) and white matter (WM) volumes and a linear increase of the total brain tissue volume. During this period, important processes such as axonal and dendritic growth and arborisation, synaptogenesis, myelination, cortical gyration and sulcation take place (Knickmeyer et al., 2008; Volpe, 2001a), leading to a fourfold increase of the cortical GM (Huppi et al., 1998b) and an important organization and maturation of the axonal pathways (Kostovic and Jovanov-Milosevic, 2006; Volpe, 2009a). These maturational processes, at this developmental phase, are known to be activity-dependent driven and regulated by the early cortical synaptic activity (Kiss et al., 2014b).

Preterm birth, by predisposing to pathological events that might injure directly the brain and exposing the infants to complex environmental factors (Back and Miller, 2014; Duvanel et al., 1999; Simmons et al., 2010), interferes abruptly with the normal brain maturation during a critical period of brain growth (Kiss et al., 2014a; Radley and Morrison, 2005). Furthermore, during neonatal intensive care unit (NICU) stay, preterm infants are exposed routinely to multiple noxious stimuli (Vinall et al., 2012) and denied meaningful sensory inputs relevant for activity-dependent plasticity (Kiss et al., 2014b; Radley and Morrison, 2005). Prematurity has been thus associated with various structural brain alterations, which might be at the origin of the later neurodevelopmental impairments observed in preterm infants, comprising motor, cognitive, behavioral and socio-emotional deficits (Anjari et al., 2007; Ball et al., 2012; Cismaru et al., 2016; Huppi et al., 1998a; Inder et al., 2005; Montagna and Nosarti, 2016; Thompson et al., 2007; Thompson et al., 2013).

On the other hand, preterm birth constitutes a window of opportunity to study early brain development and setting-up early postnatal interventions aiming to modulate preterm infants' sensory input and thus enhance brain activity-dependent plasticity and maturation. Musicotherapy, in particular, has been implemented in the past years as a meaningful sensory stimulation approach during NICU stay. Indeed, music listening triggers a rich brain processing comprising both cognitive and emotional components with distinct neural substrates (Koelsch, 2014; Sarkamo et al., 2013; Zatorre et al., 2009). Musicotherapy is thought to be relevant for activity-dependent brain plasticity during a critical period of auditory and related brain networks maturation (Graven and Browne, 2008; Kiss et al., 2014b; Lasky and Williams, 2005). Although the rational is clear, there is still little literature regarding the effects of music

interventions on the brain during early development, namely its effects on brain structure (Sa de Almeida et al., 2019; Webb et al., 2015).

Magnetic Resonance Imaging (MRI) has revolutionised the study of early brain development, through in-vivo and non-invasive imaging of the human brain with high contrast and resolution. Diffusion MRI (dMRI), in particular, provides unique information about the WM fibers, which are not yet myelinated in the premature brain and for which relaxation-based contrast is still inadequate (Hermoye et al., 2006; Huppi et al., 1998a; Neil et al., 1998), allowing thus the study of WM fibers architecture, as well as quantification of WM and GM maturation.

Diffusion tensor imaging (DTI) has been the most widely used dMRI analysis approach in the developing brain. DTI has proven that, during early brain development, with increasing gestational age (GA), there is an increase of fractional anisotropy (FA) accompanied by a decrease of mean diffusivity (MD) in the WM fibers, due to the increasing axonal structural coherence and myelination (Dubois et al., 2008; Neil et al., 1998; Nossin-Manor et al., 2013), whereas in the cortex is observed a decrease of FA and MD related to the elaboration of the radial glial cells, increased dendritic density and general increase in complexity in the cortical plate (Ball et al., 2013b; Batalle et al., 2019; McKinstry et al., 2002). DTI has also proven that very preterm infants (VPT) at term-equivalent age (TEA) present an immaturity of several WM tracts (with decreased FA and increased MD) in comparison to full-term (FT) newborns (Akazawa et al., 2016; Anjari et al., 2007; Huppi et al., 1998a; Rose et al., 2008; Sa de Almeida et al., 2019) and that an early music intervention could enhance the maturation, in particular, of the acoustic radiations and uncinate fasciculus (Sa de Almeida et al., 2019). Recently, new higher-order dMRI models capable of resolving multiple fiber orientations within a voxel have been proposed in order to overpass some limitations of DTI, that doesn't resolve the crossing fibers issue and provides voxel-based metrics, which are not fiber-specific. Indeed, is important to take in account that the diffusion-weighted (DW) signal in each voxel combines different microstructural environments, including multiple cell types and extra-cellular space.

Fixel-based analysis (FBA) is a recent technique that allows to characterize multiple fiber orientations within the voxel and perform whole-brain comparisons of fiber-specific properties. FBA metrics are represented within "fixels", which refer to single fiber populations within voxels, and comprise: fiber density (FD), reflecting fiber's microstructural changes in intra-axonal volume/packing; fiber cross-section (FC), referring to macrostructural changes in the cross-sectional area of the fiber bundle; and fiber density cross-section (FDC), combining both micro and macrostructural changes (Raffelt et al., 2017). Additionally, multi-

compartment dMRI models, such as neurite orientation dispersion and density imaging (NODDI) allow to characterize the DW signal in three compartments (intra-neurite, extra-neurite and free water), providing parameters such as intra-cellular volume fraction (v_{ic}, relating to neurite density index, NDI) and orientation dispersion index (ODI; describing the degree of incoherence in fiber orientations) (Zhang et al., 2012). NODDI offers thus additional information about tissue microstructure that correlates with histological measures of neurite geometrical complexity and density in both WM and GM (Grussu et al., 2017).

In this study, we used FBA to characterize, 1) longitudinally, whole-brain structural maturational changes occurring in VPT infants from the 33th week GA to TEA 2) at TEA, the differences regarding brain maturation in VPT in comparison to full-term (FT) newborns. 3) the longitudinal effects of an early music intervention in brain FBA metrics changes between VPT infants exposed to a music intervention and VPT infants in the control group. Moreover, using NODDI model we aimed to evaluate 4) the microstructural modifications underlying the FBA metrics changes in brain regions where the music intervention had a structural maturational effect. To the best of our knowledge, FBA had not been applied yet to a longitudinal analysis of preterm infants' early brain development, but only in preterm infants at TEA (Pannek et al., 2018; Pecheva et al., 2019), neither to study the longitudinal impact of a specially designed music intervention on preterm infants' structural early brain maturation.

We hypothesize that: 1) important micro and macrostructural brain maturational changes occur in VPT infants brain during early development; 2) preterm birth will impact brain maturation at TEA, in comparison to full-term birth and; 3) an early postnatal music intervention, during NICU hospitalization, will enhance important structural brain maturational changes occurring during VPT infants' early brain development.

2. Materials and Methods

2.1. Subjects

54 VPT infants (GA at birth <32 weeks) and 24 full-term (FT) infants were recruited at the neonatal and maternity units of the University Hospitals of Geneva (HUG), Switzerland, from 2017 to 2020, as part of a prospective randomized clinical trial entitled "The effect of music on preterm infant's brain development" (NCT03689725), registered at register.clinicaltrials.gov. Out of 54 recruited VPT infants, 28 received a music intervention during NICU stay (PTM), whereas 26 were allocated to the control group without the music intervention (PTC). For FT newborns, inclusion criteria included birth after 37 weeks GA, height, weight and head circumference above the 5th and below the 95th percentiles, APGAR score > 8 at the 5th minute and absence of reanimation, infection or hospitalisation in neonatology unit. Exclusion criteria for all babies included major brain lesions detected on the MRI, such as high-grade intraventricular hemorrhage, as well as micro or macrocephaly and congenital syndromes.

Research Ethics Committee approval was granted for the studies and written parental consent was obtained prior to infant's participation to the studies.

Six preterm infants were excluded from the study due to parental refusal (1 PTM, 4 PTC) or genetic problems (1 PTM), and two full-term infants were excluded due to parental refusal.

VPT infants underwent an MRI examination at two time-points, during the 33th week of GA (time point 1) and at TEA (time point 2). FT newborns underwent a single MRI examination few days after being born, at term age (time point 2). Infants whose MRI protocol acquisition was incomplete (not comprising a T2-weighted image and/or complete multi-shell diffusion imaging (MSDI) sequence), without both longitudinal time-points (in preterm infants' case) or whose images presented registration issues during pre-processing, were excluded from the analysis. The final sample of infants used for the analysis consisted of: 40 VPT infants, from which 21 PTM and 19 PTC, and 19 FT infants. The flow chart of the participant selection process is provided in Supplementary Figure S1. No significant difference between the PTM and PTC groups was found in demographic and perinatal variables: GA at birth, weight, sex, extremely premature birth, birth weight, birth height, birth head circumference, APGAR at 1 and 5 minutes, intrauterine growth restriction, neonatal asphyxia, bronchopulmonary dysplasia, intraventricular hemorrhage, sepsis (positive blood culture), GA

at MRI scan 1 (33th week), FA at MRI scan 2 (TEA), number of music/no music plays and socio-economic parental status score (Largo et al., 1989) (Table 1).

Table 1

Clinical characteristics of the infants

Clinical Characteristics	Preterm Music (PTM) n=21	Preterm Control (PTC) n=19	Full-term (FT) n=19	p-value* PTM vs PTC	p-value* PTC vs FT
Gestational age at birth, weeks, mean (SD)	29.40 ($\pm$1.7)	28.83 ($\pm$2.6)	39.4 ($\pm$1.2)	0.404	0.0001
Gestational age at birth, weeks, range	$27^{2/7} - 32^{4/7}$	$24^{1/7} - 31^{6/7}$	$37^{0/7} - 41^{1/7}$		
Sex: female (%)/male (%)	9(42.8)/12(57.2)	13(68.4)/6(31.6)	11(57.9)/8(42.1)	0.125	0.501
Extremely Premature (<27 weeks GA), n (%)	1 (4.8)	2 (10.5)	0 (0)	0.596	0.146
Birth weight, gram, mean (SD)	1241.5 ($\pm$450.6)	1129.7 ($\pm$328.5)	3316.8 ($\pm$380.4)	0.633	0.0001
Birth height, centimetre, mean (SD)	38.2 ($\pm$4.2)	36.8 ($\pm$3.2)	50.2 ($\pm$2.0)	0.461	0.0001
Birth head circumference (cm), mean (SD)	26.3 ($\pm$2.6)	26.5 ($\pm$3.1)	34.9 ($\pm$1.2)	0.404	0.0001
APGAR score, 1 min (SD)	5.14 ($\pm$3.0)	4.93 ($\pm$3.4)	8.68 ($\pm$1.6)	0.900	0.0001
APGAR score, 5 min (SD)	7.86 ($\pm$1.8)	6.73 ($\pm$2.2)	9.58 ($\pm$0.8)	0.625	0.001
Intrauterine Growth Restriction, n (%)	3 (14.3)	2 (10.5)	0 (0)	1.000	0.146
Neonatal asphyxia, n (%)	0	0	0		
Bronchopulmonary dysplasia, n (%)	8 (38.1)	7 (36.8)	0 (0)	1.000	0.003
Sepsis, n (%)	3 (14.3)	6 (31.6)	0 (0)	0.265	0.008
Intraventricular Haemorrhage (grade 1), n (%)	4 (19.0)	3 (15.8)	0 (0)	1.000	0.071
Gestational age at MRI scan1, weeks, mean (SD)	33.6 ($\pm$0.44)	33.7 ($\pm$0.43)		0.512	
Gestational age at MRI scan1, weeks, range	$33^{0/7} - 34^{3/7}$	$32^{6/7} - 34^{3/7}$			
Gestational age at MRI scan2, weeks, mean (SD)	40.1 ($\pm$0.58)	40.3 ($\pm$0.44)	40.14 ($\pm$0.8)	0.416	0.478
Gestational age at MRI scan2, weeks, range	$38^{5/7} - 41^{1/7}$	$39^{3/7} - 40^{6/7}$	$39^{0/7} - 41^{3/7}$		
Number of music/no music plays	60.52 ($\pm$24.2)	55.11 ($\pm$28.8)		0.528	
Socio-economic score, mean (SD)	3.67 ($\pm$2.0)	5.42 ($\pm$3.4)	3.89 ($\pm$3.1)	0.051	0.153

* Group-characteristics were compared using independent samples T-test for continuous variables and chi-squared test for categorical variables.

2.2. Music Intervention

VPT infants were randomly allocated to either the PTM or the PTC group. Research assistant, clinical staff and parents were blind to the group assignment.

The musical pieces used in this intervention were produced by A.V. (http://vollenweider.com/en), specifically for this project, and composed of a calming background, bells, harp, and punji (charming snake flute) interactively creating a melody. The musical instruments and melody were chosen based on the behavioral and physiological responses of preterm newborns (for more details consult Appendix B of Lordier et al., 2018). Three different music tracks of 8 minutes' duration were to be daily selected according to the waking state of the child (waking up, falling asleep, being active). Readiness for the

intervention as well as choice of music track (waking up, falling asleep, be active) was determined by the nurse based on a neonatal behavioral assessment scale (Martinet et al., 2013). The 8 minutes' duration was chosen to suit the duration of the sleep-wake state transitions of the infant.

The musical pieces were played daily during the infant's hospitalization, approximately two times per day, through headphones specifically designed for the project and adapted to preterm infants' head size (Supplementary Fig. S2), from the 33th week GA, after the MRI at time point 1, until TEA or hospital discharge, before MRI at time point 2. The control group had the same handling as the intervention group (same headphones and equivalent number of interventions) but the headphones were not functional.

2.3.   MRI acquisition

All infants were scanned after receiving breast or formula feeding, during natural sleep (no sedation used). At time-point 1 preterm infants were scanned using an MR compatible incubator built by Lammers Medical Technology (Lübeck, Germany) and monitored using Philips MR patient monitor Expression MR400 and Philips quadtrode MRI neonatal ECG electrodes. At time-point 2 infants were scanned using a vacuum mattress for immobilization. All infants, at both time points, were monitored for heart rate and oxygen saturation during the entire scanning time. MR-compatible headphones were used (MR confon, Magdeburg, Germany) to protect infants from the scanner's noise.

MRI acquisition at both time points was performed on 3.0T Siemens MR scanners (Siemens, Erlangen, Germany) Siemens Magnetom, using a 16-channel neonatal head coil.

T2-weighted images were acquired using the following parameters: 113 coronal slices, TR= 4990ms, TE=160ms, flip angle=150°, matrix size=256x164; voxel size=0.8x0.8x1.2mm^3.

Multi-shell diffusion imaging (MSDI) was acquired with a single-shot spin echo echo-planar imaging (SE-EPI) Stejksal-Tanner sequence (TE=85ms, TR= 3170ms, voxel size 1.8x1.8x1.8mm^3, multi-band acceleration factor of 2, GRAPPA 2. Images were acquired in the axial plane, in anterior-posterior (AP) phase encoding (PE) direction, with 4 volumes without diffusion-weighting (b0); 10 non-collinear directions with b=200 s/mm^2, 30 non-collinear directions with b=1000 s/mm^2; 50 non-collinear directions with b=2000 s/mm^2. Additionally, the b0 images were collected with reversed phase-encode blips (AP and PA), resulting in pairs of images with distortions going in opposite directions

2.4. Pre-processing

MSDI data were preprocessed using MRtrix3 (version 3.0rc3, https://www.mrtrix.org) (Tournier et al., 2019) for denoising, Gibbs ringing removal, bias field corrections and intensity normalization. FSL diffusion toolbox (v5.0.11, https://fsl.fmrib.ox.ac.uk/fsl/fslwiki/) (Behrens et al., 2003; Smith et al., 2004) was used for estimation of the off-resonance field and correction of susceptibility- and eddy current-induced distortions, as well as subject movement (Andersson and Sotiropoulos, 2016). FSL's TOPUP (Andersson et al., 2003; Smith et al., 2004) (Andersson et al., 2003; Smith et al., 2004) was used to estimate the off-resonance field, which was then used as input for FSL's EDDY function optimized for neonatal diffusion data, which corrects distortions caused by susceptibility and eddy currents, as well as by motion-induced signal dropout and intra-volume subject movement (Andersson et al., 2016; Andersson et al., 2017; Bastiani et al., 2019). Data were visually inspected to assure quality of motion artifacts correction.

2.5. Fixel-based analysis

After the pre-processing, dMRI images were analyzed using the recommended multi-tissue FBA analysis pipeline from Mrtrix3 (version 3.0rc3).

Each subject data was up-sampled to 1.3 mm^3 isotropic voxel size and fiber orientation distribution (FOD) was estimated in each voxel using 3-tissue constrained spherical deconvolution (CSD), with group averaged response functions for WM, GM and CSF. FOD maps were computed for each subject using a group-average response function (Dhollander et al., 2016).

Two FBA protocols were performed in order to evaluate: 1) the longitudinal brain maturational changes occurring during early development in preterm infants, by using the longitudinal data at time point 1 and time point 2 of the recruited preterm babies; 2) the impact of prematurity in brain maturation at TEA brain, by using the data from PTC at TEA and FT newborns.

In case 1, an unbiased study-specific FOD template was computed using 40 intra-subject templates (19 PTC and 21 PTM). In order to generate the intra-subject templates, time-point 1 and time-point 2 subjects' FOD maps were first rigidly transformed to midway space and then averaged. These intra-subject templates served as input to create the final study-specific population template used for the longitudinal analyses. Each subject FOD map, at each time-point, was registered to this template.

In case 2, an unbiased study-specific FOD template was computed using FOD images from the 19 PTC infants and 19 FT newborns. Each subject FOD map was registered to this template. We restricted the analysis to PTC infants (PTM were not included), in order to avoid biases related to the intervention and evaluate the differences regarding whole-brain maturation at TEA between FT newborns and VPT infants receiving standard-of-care, that is the standard condition in the NICU.

For both cases, the transformed FOD were segmented to produce discrete fixels, whose directions were re-oriented, and was established correspondence to template space with calculation of FBA metrics (FD, log(FC), and FDC), as previously described (Raffelt et al., 2017). FD is a microstructural metric that serves as a representation of axonal density or packing; FC is a macrostructural metric that aims to calculate the approximate relative fiber bundle diameter. Measures of FC were log-transformed prior to statistical analysis (Log(FC)), to ensure data are center around zero and normally distributed, as described previously. FDC is the product of FD and FC, combining changes of both micro and macrostructure (Raffelt et al., 2017).

Whole-brain tractography was performed in template space, using Mrtrix3 iFOD2 algorithm (Tournier et al., 2010) and generating 20 million tracts, that were subsequently filtered to 2 million tracts using spherical-deconvolution informed filtering of tractograms (SIFT) (Smith et al., 2013).

2.6. NODDI analysis

After the pre-processing, MSDI data were also analyzed using neurite orientation dispersion and density imaging (NODDI) model (Zhang et al., 2012). NODDI describes the dMRI signal as a summation of three different compartments: intra-cellular (neurites, restricted), extra-cellular (space around neurites, hindered) and CSF (isotropic). It estimates, as parameters, a neurite density index (NDI) as the intra-cellular volume fraction (v_{ic}), an orientation dispersion index (ODI) to account for fiber bending and fanning and also the isotropic volume fraction (v_{iso}). We used Watson distribution to model the distribution of fiber orientations using a GPU-based library for accelerated nonlinear optimization, cuDIMOT (Hernandez Fernandez et al., 2017, www.fmrib.ox.ac.uk/~moisesf/cudimot) and generate subjects' ODI and v_{ic} maps.

2.7.   Statistical analysis

2.7.1. Whole brain fixel-based analysis

Statistical analysis to evaluate whole-brain maturational changes occurring in the preterm brain from the 33th week GA to TEA (case 1) and to evaluate the impact of prematurity on whole-brain brain maturation at TEA (case 2) were performed using connectivity-based fixel enhancement (CFE) method (Raffelt et al., 2015) with 5000 permutations and family-wise error (FWE) for multiple comparisons correction performed for each FBA output metric (FD, log(FC), and FDC). All comparisons were adjusted: in case 1, for GA at MRI at time-point 1, delta of the GA at MRI between the two time-points and sex; and in case 2, for GA at MRI and sex.

Significant fixels (FWE-corrected P-value < 0.05) were displayed using the *mrview* tool in MRtrix3 on the template-derived tractogram, in which streamlines were cropped to display only significant fixels. Significant streamlines were colour-coded either by streamline orientation (left-right: red, inferior-superior: blue, anterior-posterior: green) or by the relative effect size (expressed as a percentage relative to the first time-point in case 1 or as a percentage relative to FT newborn control group in case 2). Both whole-brain fixel-based statistical analyses and visualizations were performed in MRtrix3.

2.7.2. ROI fixel-based analysis

In order to evaluate the effect of music on brain regions undergoing important maturational changes or at risk during early brain development, brain regions containing the fixels where FBA output metrics were statistically significantly different ($p_{FWE} < 0.05$) between the two time-points in preterm infants (case 1) or between PTC-TEA and FT newborns (case 2) were anatomically identified and segmented into ROI, according to DTI atlases (Akazawa et al., 2016; Oishi et al., 2010). The ROI were subsequently converted to fixel maps and the FBA output metrics were calculated using these masks for each participant at each time-point.

Repeated measures ANCOVA, controlling for GA at MRI at time-point 1, delta of the GA at MRI between the two time-points and sex, was conducted to determine the statistically significant differences between PTM and PTC groups on FBA metrics from the 33th week GA to TEA in the selected brain ROI, using IBM SPSS Statistics version 25 (IBM Corp., Armonk, N.Y., USA).

2.7.3. ROI NODDI analysis

For better understanding the microstructural alterations underlying the effect of music observed in the FBA ROI analysis on certain brain regions during early brain development, the ROI with a statistically significant difference on FBA metrics evolution (from the 33th week GA to TEA) between PTM and PTC groups were selected and warped to the subject space, using the warps derived from the FBA pipeline. The warped ROI were used to calculate NODDI metrics in the subjects' ODI and v_{ic} maps. Repeated measures ANCOVA, controlling for GA at MRI time-point 1, delta of the GA at MRI between the two time-points and sex, was conducted to determine the statistically significant differences between PTM and PTC groups on NODDI metrics from the 33th week GA to TEA in the selected brain ROI, using IBM SPSS Statistics version 25 (IBM Corp., Armonk, N.Y., USA).

2.7.4. Neonatal and demographic data

Regarding neonatal and demographic data, categorical variables (sex, intrauterine growth restriction, bronchopulmonary dysplasia, intraventricular hemorrhage, blood culture positive sepsis and extremely premature birth) were analysed between groups using chi-squared test, whereas continuous variables were compared between groups using independent samples t-test, with group as independent variable and the following dependent variables: GA at birth, GA at MRI time point 1, GA at MRI time point 2, birth weight, birth height, birth head circumference, APGAR score at 1 and 5 minutes after birth and socio-economic parental status). The groups compared were PTC vs PTM, as well as PTC vs FT newborns.

2.8. Data and code availability

All data were acquired in the context of the research project approved by the ethical committee in 2016. The patient consent form did not include any clause for reuse or share of data. Software and code used in this study are publicly available as part of FSL v5.0.10 (https://fsl.fmrib.ox.ac.uk/fsl/fslwiki/), MRtrix3 (Tournier et al., 2019) and cuDIMOT (Hernandez Fernandez et al., 2017, www.fmrib.ox.ac.uk/~moisesf/cudimot) software packages. dMRI data were pre-processed using EDDY command adapted for neonatal motion, which is part from the neonatal dMRI automated pipeline from developing Human Connectome Project (dHCP, http://www.developingconnectome.org), and can be found at this link: https://git.fmrib.ox.ac.uk/matteob/dHCP_neo_dMRI_pipeline_release (Bastiani et al. 2019).

3. Results

3.1. Longitudinal whole-brain maturational changes during early development

3.1.1. Preterm brain WM maturational changes from the 33th week GA to TEA

Longitudinally, in the preterm brain, from the 33th week GA to TEA there is a statistically significant ($p_{FWE} < 0.05$) increase of FD, FC and FDC in all major brain WM fibers in preterm infants, comprising commissural fibers: body, splenium and genu of corpus callosum, forceps majors, forceps minor, anterior commissure; association fibers bilaterally: cingulum, superior longitudinal fasciculus, arcuate fasciculus, inferior fronto-occipital fasciculus, inferior longitudinal fasciculus, uncinate fasciculus; and projection fibers bilaterally: superior corona radiata, fibers passing in the internal capsule (such as the cortico-spinal tract) and in the external capsule, as well as the fornix, optic and acoustic radiations. Additionally, there was also a significant increase of FD, FC and FDC in the thalamus (from where the main ascending projection fibres originate), in the brainstem (where projection fibers pass), cerebellum and cerebellar peduncles (where also pass projection fibers) (Fig. 1).

Whole-brain macrostructural increases of FC were generally more pronounced (until 50% of increase) than FD increases (until 20% of increase). The WM fibers with the highest FD, FC and FDC increase from the 33th week GA to TEA were the projection fibers (Fig. 1).
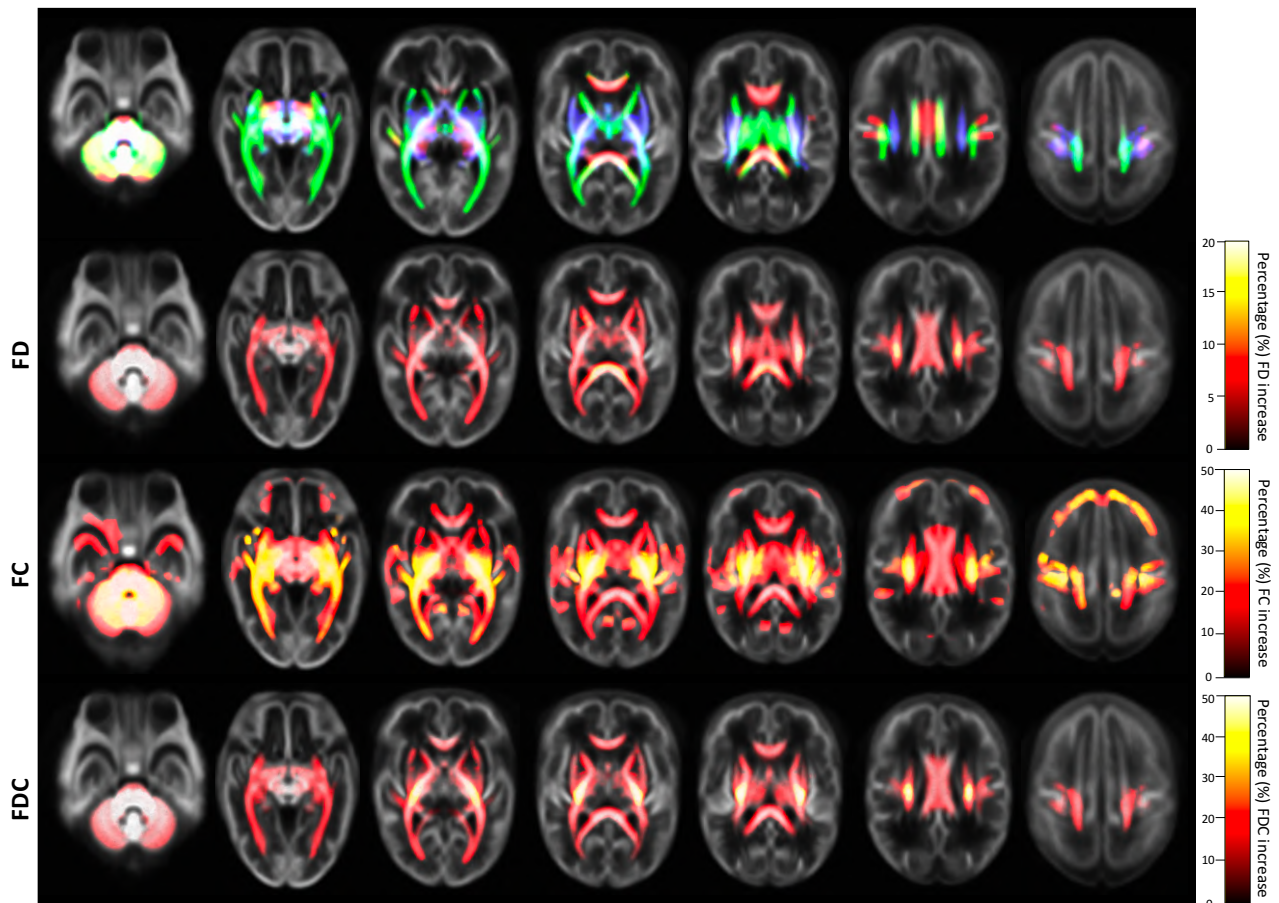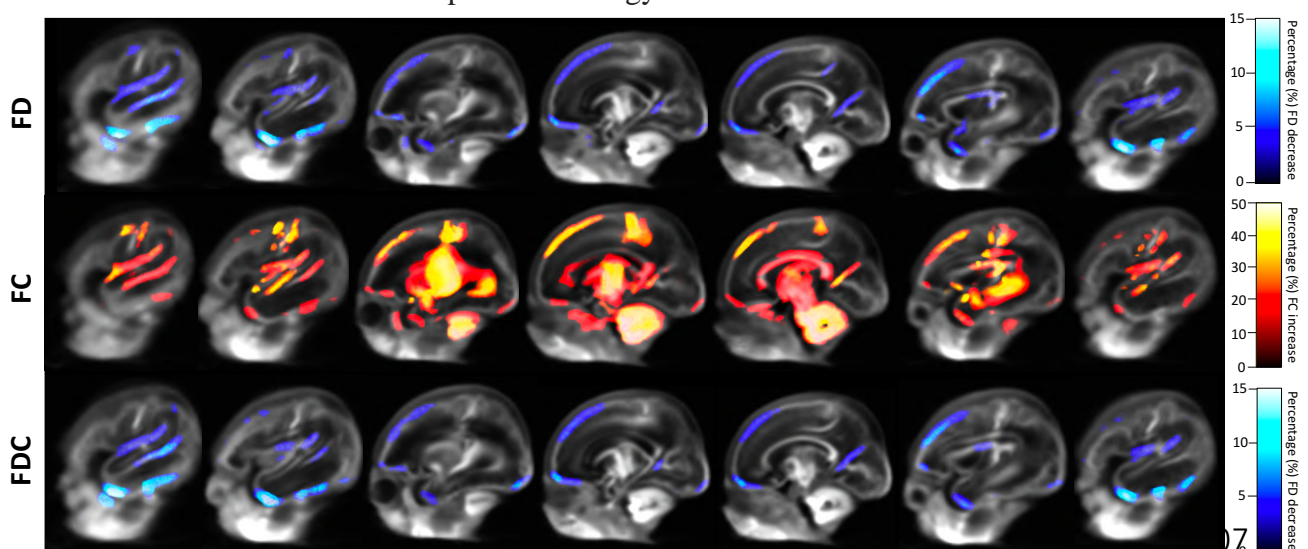
Fig. 1. **WM fibers with increased FD, FC and FDC from the 33th week GA to TEA in preterm infants' brain.** Population template axial views, from inferior to superior (left to right), of the streamline segments cropped from the template tractogram to include only streamline points that correspond to significant fixels ($p_{FWE} < 0.05$). Streamlines were coloured by direction (anterior-posterior: green, superior-inferior: blue, left-right: red) and percentage of relative effect size increase at TEA compared to the 33th week GA, for FD, FC and FDC. From the 33th week GA to TEA, there is an increase of FD, FC and FDC in all major cerebral WM fibers (commissural, association and projection tracts) bilaterally, as well as in the thalamus, brainstem, cerebellum and cerebellar peduncles.

3.1.2. Preterm brain cortical GM maturational changes from the 33th week GA to TEA

Longitudinally, in the preterm brain, from the 33th week GA to TEA there is a statistically significant increase of FC and decrease of FD and FDC ($p_{FWE} < 0.05$) in the following cortical GM regions: bilateral orbito-frontal cortex, dorsal superior frontal gyrus, medial frontal gyrus, precentral cortex, postcentral cortex, Heschl's gyrus, superior and inferior temporal gyrus, right middle temporal gyrus, bilateral insula, precuneus and posterior cingulate gyrus, inferior occipital gyrus, calcarine and lingual gyrus (Fig. 2).

During this period of early brain maturation, cortical GM macrostructural increases of FC are pronounced (until 50% of increase) and accompanied by decreases until 15% of FD and FDC in the same cortical regions. The highest FC increase occurred in the bilateral dorsal superior frontal gyrus, precentral cortex, postcentral cortex, Heschl's gyrus, superior temporal gyrus, insula and precuneus and posterior cingulate gyrus, whereas the highest FD and FDC decreases occurred in the bilateral temporal pole, inferior temporal gyrus, bilateral orbito-frontal cortex and left dorsal superior frontal gyrus.

Fig. 2. **Cortical GM regions with increased FC and decreased FD and FDC from the 33th week GA to TEA in the preterm brain.** Population template sagittal views, from the right to left hemisphere, including only points that correspond to significant fixels ($p_{FWE} < 0.05$). Streamlines were coloured by percentage or relative effect size increase at TEA in comparison to the 33th week GA, for FD, FC and FDC. From the 33th week GA to TEA there is an increase of FC (images colored in red) and decrease of FD and FDC (images colored in blue) in the following cortical GM areas: bilateral orbito-frontal cortex, dorsal superior frontal gyrus, medial frontal gyrus, precentral cortex, postcentral cortex, Heschl's gyrus, superior and inferior temporal gyrus, right middle temporal gyrus, bilateral insula, precuneus and posterior cingulate gyrus, inferior occipital gyrus, calcarine and lingual gyrus.

3.2.   Effect of prematurity on early brain development at TEA

3.2.1.   Whole-brain differences between PTC-TEA infants and FT newborns

At TEA, PTC infants evidenced a statistically significant ($p_{FWE} < 0.05$) decrease of FD, until 6%, in the body of corpus callosum, fornix bilaterally and left posterior limb of internal capsule, in comparison to FT newborns (Fig. 3). There were no regions with significant alterations of FDC or FC in PTC-TEA infants in comparison to FT newborns.
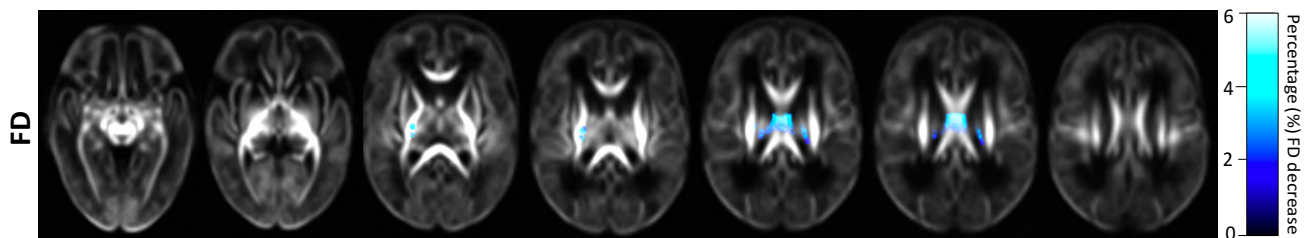
Fig. 3. **WM fibers with decreased FD in PTC infants in comparison to FT newborns.** Population template axial views, from inferior to superior (left to right), of the streamline segments cropped from the template tractogram to include only streamline points that correspond to significant fixels ($p_{FWE} < 0.05$). Streamlines were coloured by percentage of relative effect size decrease in PTC infants in comparison to FT newborns.

3.3. Effect of music on longitudinal brain maturation during early development

3.3.1. Effect of music on WM fibers FBA metrics

Fixel masks containing the segmented WM tracts with a significantly superior (pFWE < 0.05) FD, FC and FDC increase, from the 33th week GA to TEA, as well as tracts with a significantly FD decrease in PTC-TEA infants in comparison to FT newborns, were used for computing FBA metrics longitudinal changes and evaluate the effect of the music intervention on those WM fibers maturation. The fixel masks used comprised: corpus callosum (body, genu and splenium), anterior commissure, bilateral cingulum, superior longitudinal fasciculus, inferior fronto-occipital fasciculus/inferior longitudinal fasciculus, cortico-spinal tract, uncinate fasciculus, fornix, acoustic radiations and optic radiations. There were no significant statistical differences between PTM and PTC infants regarding FBA metrics longitudinal changes on the selected tracts (p > 0.05).

3.3.2. Effect of music on cortical GM FBA metrics

Fixel masks containing the cortical regions that evidenced a significant FC increase and FD and FDC decreases, from the 33th week GA to TEA, were used for computing FBA metrics longitudinal changes and evaluate the effect of the music intervention on cortical GM maturation specifically in those regions. The fixel masks used comprised: left and right orbito-frontal cortex, medial frontal gyrus, dorsal superior frontal gyrus, precentral cortex, Heschl's gyrus, superior temporal gyrus, inferior temporal gyrus, right middle temporal gyrus, left and right precuneus/posterior cingulate gyrus, insula and inferior occipital/lingual gyrus.

In comparison to PTC, PTM had a significantly superior increase from the 33th week GA to TEA of the FC in the left temporal pole ($F_{(1,32)}=4.507$, p=0.042), left OFC ($F_{(1,35)}=4.253$, p=0.047), right middle temporal gyrus ($F_{(1,35)}=4.852$, p=0.034), left insula ($F_{(1,35)}=5.068$, p=0.031) and right precuneus/posterior cingulate gyrus ($F_{(1,35)}=4.599$, p=0.039) (Fig. 4). No significant differences were found for the remaining cortical regions regarding FBA metrics longitudinal change between groups (p > 0.05).
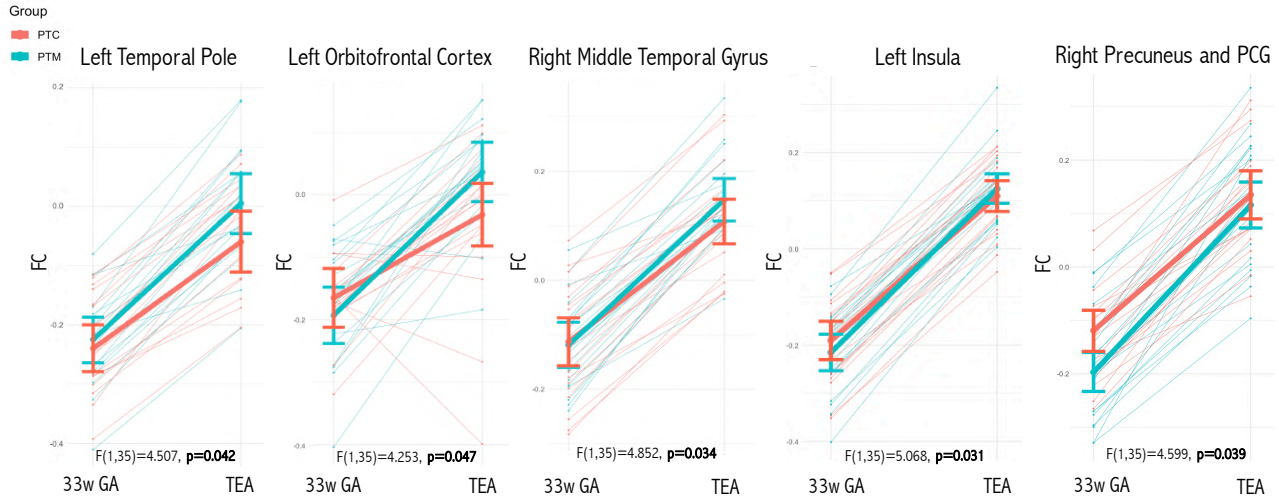
Fig. 4. **Cortical GM regions with a significantly superior longitudinal increase of FC in PTM in comparison to PTC, from the 33th week GA to TEA.** FC values were averaged across the GM cortical regions masks (left temporal pole, left orbito-frontal cortex, right middle temporal gyrus, left insula and right precuneus and posterior cingulate gyrus) for each subject and plotted against age. Repeated measures ANCOVA with correction for gestational age at MRI time-point 1, delta of the time between the two MRI and sex was performed. Mean and 95% confidence intervals are illustrated in blue for PTM and red for PTC infants.

3.3.3. Effect of music on cortical GM NODDI metrics

In order to better understand the microstructural changes related to the music effect on the cortical GM, masks containing the cortical regions that evidenced a significant superior longitudinal increase of FC in PTM in comparison to PTC infants were warped from the population template to the subject space, at each time point. These masks were used to evaluate NODDI parameters longitudinal evolution differences between both groups in these cortical regions from the 33th week GA and TEA. The masks used comprised: left orbito-frontal cortex, left temporal pole, right middle temporal gyrus, left insula and right precuneus/posterior cingulate gyrus.

For both groups, in all cortical regions evaluated, there was a significant ODI increase with time, from the 33th week GA to TEA (p<0.0001).

In comparison to PTC, PTM had a significantly superior increase from the 33th week GA to TEA of ODI in the left temporal pole ($F_{(1,33)}=5.201$, p=0.029) and left OFC ($F_{(1,33)}=4.973$, p=0.033). In the other cortical regions, namely the right middle temporal gyrus, left insula and right precuneus/posterior cingulate gyrus, there was a tendency for a

210

superior ODI longitudinal increase in the PTM vs PTC group, but without a statistically significant difference (Fig. 5). No significant differences between groups were found for v_{ic} in the same cortical regions ($p > 0.05$).
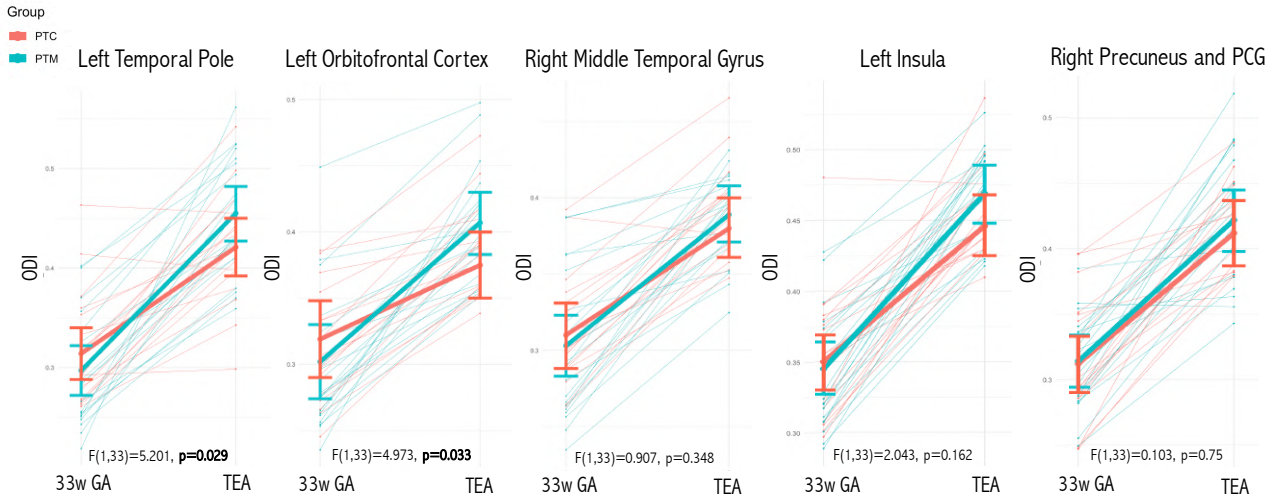
Fig. 5. **ODI longitudinal evolution, from the 33th week GA to TEA, in the cortical GM regions that had a significant longitudinal increase of FC in PTM in comparison to PTC.** ODI values were averaged across the GM cortical regions masks (left temporal pole, left orbito-frontal cortex, right middle temporal gyrus, left insula and right precuneus and posterior cingulate gyrus) for each subject and plotted against age. Repeated measures ANCOVA with correction for gestational age at MRI time 0, delta of the time between the two MRI and sex was performed. Mean and 95% confidence intervals are illustrated in blue for PTM and red for PTC infants.

4. Discussion

In this longitudinal study, we used FBA, a recent method that allows to investigate whole-brain fiber-specific changes, in order to characterize the whole-brain structural maturational alterations occurring during preterm infants' early development, from the 33th week GA to TEA, as well as the impact of preterm birth on structural brain development at TEA, in comparison to FT birth. Furthermore, we have evaluated longitudinally the impact of an early postnatal music intervention given to premature infants during neonatal stay, from the 33th week GA to TEA, on preterm infants' whole-brain maturation using FBA complemented with NODDI analysis.

The major findings from this study are: 1) from the 33th week GA to TEA, there is an important increase of FD, FDC and, specially, of FC in all major cerebral WM fibers bilaterally, as well as in the thalamus, brainstem, cerebellum and cerebellar peduncles, unveiling thus an important micro and, in particular, macroscopic WM fiber bundles maturation, with the projection fibers exhibiting the most prominent maturational changes; furthermore, in diverse cortical GM regions, there is an important increase of FC, accompanied by a parallel decrease of FD and FDC; 2) VPT-TEA infants evidence microscopic alterations of major commissural and projection WM fibers, characterized by a decreased FD, in comparison to FT newborns; 3) In PTM infants, there is a significantly superior increase of FC, from the 33th week GA to TEA, in specific cortical GM regions, namely the left temporal pole, left OFC, left insula, right middle temporal gyrus and right precuneus/posterior cingulate gyrus, accompanied by a significantly superior increase of ODI in left temporal pole and left OFC.

4.1. Premature infant's brain undergoes important micro and macrostructural maturational changes in both WM and GM during early brain development

By applying, for the first time in literature, a longitudinal fixel-based analysis to study early preterm brain development, we show that, from the 33th week GA to TEA, there is a significant longitudinal increase of FD, FC and FDC in all major cerebral WM fibers, as well as in the thalamus, brainstem, cerebellum and cerebellar peduncles, which proves that important micro and macroscopic maturational changes are taking place during this period in these brain regions.

The maturational changes occurring in WM fibers relate to the important axonal growth, neural organization, maturation and myelination processes occurring typically during the third trimester of pregnancy and leading to the establishment of long-range WM

connections, facilitating brain integration (Batalle et al., 2017; Kostovic and Jovanov-Milosevic, 2006; Kostovic and Judas, 2010a; Kostovic et al., 2014; van den Heuvel et al., 2015).

Our FBA results are in agreement with previous dMRI studies reflecting also an increase in WM fibers maturation during early brain development, translated by an increase of neurite density index (NDI) and fractional anisotropy (FA), accompanied by a decrease of mean diffusivity (MD), radial diffusivity (RD) and orientation dispersion index (ODI), in line with an increase in fiber organization, axonal coherence and preliminary myelination (Aeby et al., 2009; Batalle et al., 2017; Dean et al., 2017; Dubois et al., 2008; Huppi et al., 1998a; Kunz et al., 2014; Mukherjee et al., 2002; Nossin-Manor et al., 2013; Shim et al., 2012). FBA has been previously applied to investigate WM changes occurring in children and adolescents' brain development, revealing also an increase in FD, FC and FDC in the major cerebral WM fibers, supporting thus a continuous WM maturation throughout childhood (Dimond et al., 2020; Genc et al., 2018; Kelly et al., 2020).

Additionally, the detected increase in FD, FC and FDC occurring in thalamic regions supports that also deep GM undergoes important maturational processes, what is in line with the rapid growth and establishment of functional thalamo-cortical connections occurring during this critical period of early brain development (Batalle et al., 2017; Kostovic and Jovanov-Milosevic, 2006; Kostovic and Judas, 2010a; Krsnik et al., 2017; Pouchelon and Jabaudon, 2014).

Our results further show that WM fibers maturation during early brain development is characterized mainly by an important increase of FC, with values increasing until 50% from the 33th week GA to TEA, reflecting thus a predominant macroscopic spatial extent increase of the fiber bundles, along with an increase until 20% of FD, translating a microstructural axonal number expansion. This superior increase of FC in comparison to FD might be related to the maturational processes taking place during this period, namely myelination, leading to a prominent increase in fiber bundle diameter and thus increased ability to transfer information across brain regions (Baumann and Pham-Dinh, 2001; Volpe, 2001a). Also during early childhood, FC changes in WM were proven to be more widespread and to present a larger percentage increase than changes in FD, supporting thus that increases in fiber-bundle size might be the major contributor to WM maturation during this period (Dimond et al., 2020), in line with our present findings during early preterm development.

From all WM fibers, the central projection fibers are the ones revealing the highest rates of FD, FC and FDC increase. Such is in line with the expected developmental trajectory,

showing that myelination occurs primarily in central regions and in projection fibers (Kinney et al., 1988). Such might be related to the fact that earlier myelination in longer WM bundles might be necessary to compensate for brain growth and maintain similar communication latencies between brain regions (Salami et al., 2003).

Also for the first time in literature using FBA, we unveil important maturational changes occurring in the cortical GM during this early period of preterm brain maturation. A significant increase of FC accompanied by a decrease of FD and FDC is observed in various cortical GM regions distributed among the frontal, parietal, temporal, insula, cingulate and occipital cortices, including primary sensory-motor areas, namely the auditory, somatosensory, visual and primary motor cortex. These findings support that major cortical maturational processes are occurring during this period. In fact, cortical maturation during the third trimester of pregnancy is characterized by an important increase in dendritic arborisation and geometric complexity, with increasing number of neuronal connections, including in-growth of thalamo-cortical afferents, transformation of the radial glial cells into astrocytes, proliferation of glial cells and formation of basal dendrites cross-connections running parallel to the cortical surface, what leads to a complex multidirectional microstructural environment (Bystron et al., 2008; Cameron and Rakic, 1991; He et al., 2020). FD is computed by integrating the FOD amplitude, which is proportional to the volume of the fibers aligned in that direction (Raffelt et al., 2017). In GM, in particular, multiple cellular components are thought to contribute to the FOD amplitude, namely dendrites, axons and astrocytes processes, sharing the same orientation (Budde et al., 2011; Budde and Annese, 2013). Studies in both human and animal models have shown that the cortical FOD presents mostly a radial orientation, with variable degrees of complexity, with many regions exhibiting a pure radial arrangement and others a more complex pattern of perpendicular and parallel orientations in relation to the cortical surface (Aggarwal et al., 2015; Budde and Annese, 2013; Dudink et al., 2015; Heidemann et al., 2010; Kleinnijenhuis et al., 2013; Leuze et al., 2014), with the apical dendrites contributing importantly to the main radial orientation of the FOD and diffusion tensor (Assaf, 2019). The observed decrease of cortical FD and FDC, which are directionally-dependent metrics, from the 33th week GA to TEA, might thus reflect the important increase in dendritic arborisation and cortical geometrical complexification, as well as progressive disappearance of the radial glia and its transformation into astrocytes (Bystron et al., 2008; He et al., 2020), similarly to the reported cortical FA evolution, which diminishes during early cortical maturation (Ball et al., 2013b; Batalle et al., 2019; Eaton-Rosen et al., 2015; McKinstry et al., 2002). Indeed, the FA diminution in cortical GM during early brain maturation has been related to the occurring

typical cortical maturational processes, such as dendritic arborisation, synaptic formation, as well as myelination of intracortical axons, leading to the disruption of the well-organized radial glia scaffold and causing thus a decrease of FA (Assaf, 2019; McKinstry et al., 2002; Smyser et al., 2016). Furthermore, the decrease of fiber density in cortical GM is also in agreement with the reported decrease in cortical NDI and mean kurtosis (MK), as described during early brain development (Batalle et al., 2019), and which have been related to the cortical expansion occurring during this period (Huttenlocher, 1990), as well as cell death or apoptosis, leading to a reduction of the neuronal density in the cortical plate (Chan and Yew, 1998; Lossi and Merighi, 2003). The significant increase in cortical FC, accompanying mostly the regional FD and FDC decrease, might be related to an augmentation of the number of basal dendrites and glial cells in these cortical GM areas, as well as myelination of intracortical axons. Indeed, a decreased FC has been related to decreased myelination (Gajamange et al., 2018), what has been confirmed by histological staining (Malhotra et al., 2019). Interestingly, the highest FC increase was observed in primary sensorial and motor processing areas, namely in the precentral cortex, postcentral cortex and Heschl's gyrus, which have been proven to be the first cortical regions to demonstrate the presence of intra-cortical myelin (Huttenlocher and Dabholkar, 1997b; Rowley et al., 2017). Furthermore, the fact that the primary motor, somatosensory, visual and auditory cortices are among the regions with significant cortical maturational changes is in line with the establishment of the activity-dependent thalamo-cortical connectivity, transmitting the environmental extrinsic input through the sensory thalamic nuclei to the cerebral cortex, what may contribute to increased synaptogenesis and intra-cortical myelination. Our findings complement previous DTI and NODDI analysis that have proven a decrease of FA in the cerebral cortex, also a directionality-dependent metric, in relation with an increased dendritic density and general increase in cortical complexity (Ball et al., 2013b; McKinstry et al., 2002), as well as an increase in ODI, related to increased dendritic arborisation, mainly in motor and sensory areas, during the third trimester of development (Batalle et al., 2019).

4.2.   WM fibers evidence microstructural alterations related to premature birth

Our findings prove that, in comparison to full-term birth, preterm birth impacts the microstructural development of major cerebral WM fibers, translated by a decrease in FD, namely of the corpus callosum, fornix and the cortico-spinal tract passing through the posterior limb of internal capsule. These results are in line with previous literature showing a decreased

FD in these WM tracts in preterm infants at TEA, in comparison to full-term newborns or in association with lower GA (Pannek et al., 2018; Pecheva et al., 2019). Such supports a deleterious impact of prematurity in normal WM fiber bundles development, what might lead to an impaired information transfer across brain regions and contribute ultimately to the neurodevelopment impairments observed later in life. In comparison to these prior publications, our cohort of preterm babies did not present any brain lesions, which might explain the less extensive changes in FD and absence of significant differences regarding FC and FDC metrics, found in those previous studies. In fact, as we find a significant impairment in FD, but not in FC and FDC in preterm infants at TEA in comparison to FT newborns, such supports that prematurity impacts mainly FD in WM fiber bundles, what might be related to axonal packing and pre-myelination events defects, leading, for example, to an increased extra-axonal space. Such could justify the decrease in WM fibers FD and absence of differences regarding FC and FDC between groups at TEA.

4.3. Early music intervention enhances cortical GM maturation during early brain development

Our results suggest that an early postnatal music intervention impacts cortical GM brain regions undergoing significant longitudinal maturational changes from the 33th week GA to TEA. In particular, an increase of cortical FC, reflecting possibly an increase in the dendrites number and intra-cortical myelination, was found in the left OFC, left temporal pole, left insula, right middle temporal gyrus and right precuneus/posterior cingulate gyrus.

The left OFC, left temporal pole and left insula are paralimbic regions involved in sensory integration, processing of affective stimuli and evaluation of emotional association (Chang et al., 2013; Kringelbach, 2005; Mackes et al., 2018; Olson et al., 2007; Wildgruber et al., 2005). In fact, these three regions constitute what is called the insulo-orbito-temporopolar complex of the paralimbic brain, sharing the same heterogenic agranular-periallocortical structure with transitions to more fully developed isocortex, and sharing also functional similarities, constituting thus a paralimbic unit of cortical organization (Peters and Jones, 1985). Music listening has been shown to activate all these cortical regions in the human brain. In fact, music was shown to change activity in the main neural components of emotions (Koelsch, 2010; Koelsch, 2014). A previous study has proven, in particular, that the auditory cortex was functionally connected to a number of limbic and paralimbic regions, comprising

the OFC, temporal pole and insular cortices, when musical stimuli were eliciting emotions (Koelsch et al., 2018).

Our results support thus that the early postnatal music intervention in preterm infants during NICU stay has elicited the left insulo-orbito-temporopolar complex, leading to an increase of dendrites in these cortical regions, what is translated by an increase of the FC metric. Indeed, the third trimester of pregnancy is marked by an important activity-dependent neural plasticity and remodelling. The thalamocortical neurons, by bridging the cortical circuitry with sensory periphery, allow sensory-driven activity to modulate neuronal connections. Therefore, by providing an external organized auditory stimulus, in the form of music, during a critical period of activity-dependent brain maturation, cortical regions important for emotional processing were solicited, with an impact in its structural maturation.

These results are in line with our previous study, which had revealed that, in very preterm infants at TEA, this early postnatal music intervention during NICU stay led to a significant increase of FA in the uncinate fasciculus, a WM bundle connecting the OFC to the temporal pole, in comparison to preterm infants in the control group (Sa de Almeida et al., 2019). Additionally, also resting-state (rs) functional connectivity was studied in these preterm infants receiving the musical intervention and revealed that, in comparison to preterm infants in control group, those that received the intervention had a significantly higher functional connectivity between the salience network, in which the insula is a main component, with many other brain regions, namely the thalamus, precuneus and frontal regions (Lordier et al., 2019b). Indeed, previous evidence suggests that music training could lead to a significant reorganization of insula-based networks, potentially facilitating high-level cognitive and affective functions (Zamorano et al., 2017). The insula is actually thought to provide the basis for representations of signals from the external environment, namely external emotional stimuli, and to maintain the balance between internal and external information (Craig, 2004; Singer et al., 2009).

By modelling cortical maturation of regions thought to subserve emotional processing (Koelsch, 2014), an early postnatal music intervention may potentially enhance premature infants' later socio-emotional capacities. In fact, literature has shown that up to 25% of VPT infants evidence an atypical behavioral and socio-emotional development, comprising diminished social competences and self-esteem, emotional dysregulation, shyness and timidity, inattention, anxiety and internalizing problems (Anderson and Doyle, 2003; Arpi and Ferrari, 2013; Bhutta et al., 2002; Marlow, 2004; Montagna and Nosarti, 2016; Spittle et al., 2009; Spittle et al., 2011; Williams et al., 2010; Witt et al., 2014). In terms of brain structure, in

comparison to full-term newborns, preterm infants at TEA were shown to present a superior FA and MD in various cortical regions related to emotional processing, namely the frontal cortex, including the OFC (Rogers et al., 2012), and also parietal, occipital and temporal areas, suggesting an impaired cortical development in this population (Ball et al., 2013b). Structural alterations affecting the insulo-orbito-temporopolar complex have been further related to the later socio-emotional deficits observed in preterm born infants (Aanes et al., 2015; Anjari et al., 2007; Ball et al., 2012; Cismaru et al., 2016; Fischi-Gomez et al., 2015; Gimenez et al., 2006; Huppi et al., 1998a; Inder et al., 2005; Nosarti et al., 2014; Peterson et al., 2000; Rogers et al., 2012; Thompson et al., 2007; Thompson et al., 2013). Additionally, a previous study from our group has shown that preterm infants that have participated in a very similar music intervention during NICU stay presented fear-reactivity scores at 12-months and anger-reactivity scores at 24-months of age that were closer to full-term newborns, when compared to preterm infants from the control group (Lejeune et al., 2019b), supporting a positive long-term impact of the early music intervention in premature infants' socio-emotional development.

The right precuneus and posterior cingulate gyrus were also among the cortical regions with a significant longitudinal increase of FC in the preterm group exposed to music during NICU stay. The precuneus is situated in a strategic location with wide-spread connections and is known to support a variety of cognitive processes and behavioral functions (Cavanna and Trimble, 2006), as well as to be implicated in emotional processing (Maddock et al., 2003) and to influence an extensive network of cortical and subcortical structures involved in the elaboration of highly integrated and associative information (Cavanna and Trimble, 2006). Both the precuneus and the posterior cingulate cortex have been shown to be functional activated, together with the auditory cortex, when musical stimuli were eliciting emotions (Koelsch et al., 2018). Furthermore, these two brain cortical regions constitute the posterior part of "default mode network" (DMN), functionally linked to self-related processes (Cavanna and Trimble, 2006; Fransson and Marrelec, 2008), social cognition (Mars et al., 2012), inhibitory control (Fair et al., 2008; Whitfield-Gabrieli and Ford, 2012) and regulation of attentional states (Leech and Sharp, 2014; McKiernan et al., 2003). As referred above, preterm infants receiving this music intervention during NICU stay have revealed an increased rs-functional connectivity at TEA between the salience network and the precuneus (Lordier et al., 2019b). In addition, adult studies had also previously shown an increase in rs-functional connectivity between the salience network and DMN, in response to passive music listening (Sridharan et al., 2008). Therefore, our results support a structural impact of an early postnatal

music intervention in these cortical brain regions maturation, the precuneus and posterior cingulate gyrus, both implied in socio-emotional processes and constituting the posterior component of DMN, which was shown to have a decreased functional connectivity in the preterm population (Lordier et al., 2019b; Smyser et al., 2010; White et al., 2014). These results are thus also in line with the hypothesis that an early music intervention might contribute to mitigate the deficits in behavior and social-emotional cognition observed in the preterm population (Anderson and Doyle, 2003; Arpi and Ferrari, 2013; Bhutta et al., 2002; Marlow, 2004; Montagna and Nosarti, 2016; Spittle et al., 2009; Witt et al., 2014).

Additionally, also the right middle temporal gyrus revealed a significant longitudinal FC increase in preterm infants receiving the early postnatal music intervention. This region is part of the auditory association cortex and has been shown to be activated during passive music listening (Ohnishi et al., 2001) and when musical stimuli were eliciting emotions (Koelsch et al., 2018). Furthermore, it was shown that patients with lesions in middle temporal cortex have evidenced difficulty in interpreting the emotional tone of prosodic cues (Peretz et al., 1994).

Altogether, these findings support therefore that an early postnatal music intervention given to preterm infants during NICU stay might induce maturation of specific cortical regions, comprising the auditory processing association cortex, important paralimbic cortical regions: the insulo-orbito-temporopolar complex, and the posterior component of DMN: the precuneus and posterior cingulate gyrus. All these cortical regions were shown to undergo important maturational changes during the third trimester and have been shown to be elicited by music listening, to be implicated in emotional processing and to be affected at TEA by premature birth. Therefore, an early music intervention in preterm infants, by enriching the environmental input during a critical period of brain activity-depended maturation, might activate and contribute to the maturation of brain regions undergoing major changes during preterm development and that are implicated in emotional processing, what might help preterm infants to achieve its full potential, in particular regarding behavior and social-emotional cognition capacities.

4.4. Cortical ODI increase accompanies FC longitudinal increase after early music intervention

We used NODDI to better evaluate the microstructural modifications underlying the significant cortical FC increase following the early music intervention during early brain development. In fact, since this is the first study reporting that FC increases, while FD and

FDC decrease, in various cortical regions during the third trimester of brain development, we have further evaluated cortical microstructural changes using a NODDI analysis, in order to better elucidate the reason underlying the FBA metrics change.

In all the regions where the preterm group receiving the music intervention has evidenced a significantly superior FC longitudinal increase, also a significant longitudinal ODI increase was observed for both groups, from 33th week GA until TEA. This increase was significantly superior for the preterm group that listened to music in the left OFC and left TPO.

ODI relates to the degree of incoherence in fiber orientations (Zhang et al., 2012). In the cortical GM, ODI increases are generally related to an increased dendritic arborisation and consequent alteration of cortical geometrical structure. During early brain development, ODI was shown to increase until term age and then stabilize, supporting that until term-age cortical maturation is dominated by an increase in dendritic arborisation and complexity, congruent with the observed increase on cortical volume and curvature (Batalle et al., 2019; Eaton-Rosen et al., 2015). Indeed, human histology studies have proven that dendritic arborisation, glial proliferation, neuronal differentiation and synapse formation is occurring between 25 weeks and term age (Marin-Padilla, 1992; Mrzljak et al., 1988; Rakic, 2003).

This increase of ODI in these cortical regions, observed from the 33th week GA to TEA, supports thus an increase in dendrite arborisation occurring in the cortical plate during this period and, in particular, in left OFC and TPO in relation to the early music intervention. The ODI increase might explain the observed increase in cortical FC, since it supports that a higher number of dendrite branches is present when the cross-sectional plan is evaluated, as well as the parallel FD decrease, given that, as this is directional dependent metric, the complex cortical microstructure may affect its evaluation.

The absence of significant changes regarding v_{ic} (or tendency to its increase with increasing GA) is congruent with previous literature reporting that, in the cortex, while the ODI increases until term age, v_{ic} change does not differ significantly from 0, supporting that the major cortical changes occurring during this period are mostly related to geometry alteration and a more complex microstructure (Batalle et al., 2019; Eaton-Rosen et al., 2015).

Our results support thus the hypothesis that the early music intervention, by enriching the auditory environment of preterm infants during a critical period of cortical activity-dependent plasticity, might modify the establishment and remodelling of the incoming thalamo-cortical connections and impact cortical maturation, leading to an increase in cortical dendritic arborisation and complexity in brain regions important, in particular, for socio-emotional processing, which are known to be structurally impaired by preterm birth and related

to the behaviour and socio-emotional problems observed later in this population (Aanes et al., 2015; Anjari et al., 2007; Ball et al., 2012; Cismaru et al., 2016; Fischi-Gomez et al., 2015; Gimenez et al., 2006; Huppi et al., 1998a; Inder et al., 2005; Nosarti et al., 2014; Peterson et al., 2000; Rogers et al., 2012; Thompson et al., 2007; Thompson et al., 2013).

5. Conclusion

Using a longitudinal whole-brain FBA analysis, we have shown that important WM and GM maturational changes take place from the 33th week GA of preterm brain development to TEA. In particular, all major cerebral WM fibers undergo significant increases in microscopic fiber density and, specially, in macroscopic fiber bundle cross-section, with more pronounced changes in the central projection fibers, whereas in cortical GM, FBA metrics changes support an important increase in dendrite growth and arborisation with a consequent geometric structure complexification of multiple cortical regions, comprising, among others, the primary sensory-motor areas. We also show that preterm birth impacts, in particular, the microscopic maturation of main projection and commissural WM fibers, in comparison to full-term birth. Furthermore, an early music intervention given to preterm infants during NICU stay has led to a significantly superior longitudinal increase of dendrite growth and arborisation in cortical regions undergoing important maturational changes during preterm development and that are important for auditory, cognitive and, in particular, emotional processing. Early interventions aiming to enrich the sensory input given to preterm infants during this important period of activity-dependent brain plasticity might therefore play a role in these infants later clinical development. Music, in particular, may activate and modulate cortical regions implied in emotional processing and thus contribute to mitigate the later socio-emotional problems observed in preterm population, assisting preterm infants to achieve its full potential.

Acknowledgments

Funding

Competing interests

The authors declare no competing interests.

References

Aanes, S., et al., 2015. Memory function and hippocampal volumes in preterm born very-low-birth-weight (VLBW) young adults. Neuroimage. 105, 76-83.

Aeby, A., et al., 2009. Maturation of thalamic radiations between 34 and 41 weeks' gestation: a combined voxel-based study and probabilistic tractography with diffusion tensor imaging. AJNR Am J Neuroradiol. 30, 1780-6.

Aggarwal, M., et al., 2015. Probing region-specific microstructure of human cortical areas using high angular and spatial resolution diffusion MRI. Neuroimage. 105, 198-207.

Akazawa, K., et al., 2016. Probabilistic maps of the white matter tracts with known associated functions on the neonatal brain atlas: Application to evaluate longitudinal developmental trajectories in term-born and preterm-born infants. Neuroimage. 128, 167-179.

Anderson, P., Doyle, L.W., 2003. Neurobehavioral outcomes of school-age children born extremely low birth weight or very preterm in the 1990s. Jama-Journal of the American Medical Association. 289, 3264-3272.

Andersson, J.L.R., Skare, S., Ashburner, J., 2003. How to correct susceptibility distortions in spin-echo echo-planar images: application to diffusion tensor imaging. Neuroimage. 20, 870-888.

Andersson, J.L.R., et al., 2016. Incorporating outlier detection and replacement into a non-parametric framework for movement and distortion correction of diffusion MR images. Neuroimage. 141, 556-572.

Andersson, J.L.R., Sotiropoulos, S.N., 2016. An integrated approach to correction for off-resonance effects and subject movement in diffusion MR imaging. Neuroimage. 125, 1063-1078.

Andersson, J.L.R., et al., 2017. Towards a comprehensive framework for movement and distortion correction of diffusion MR images: Within volume movement. Neuroimage. 152, 450-466.

Anjari, M., et al., 2007. Diffusion tensor imaging with tract-based spatial statistics reveals local white matter abnormalities in preterm infants. Neuroimage. 35, 1021-7.

Arpi, E., Ferrari, F., 2013. Preterm birth and behaviour problems in infants and preschool-age children: a review of the recent literature. Developmental Medicine and Child Neurology. 55, 788-796.

Assaf, Y., 2019. Imaging laminar structures in the gray matter with diffusion MRI. Neuroimage. 197, 677-688.

Back, S.A., Miller, S.P., 2014. Brain Injury in Premature Neonates: A Primary Cerebral Dysmaturation Disorder? Annals of Neurology. 75, 469-486.

Ball, G., et al., 2012. The effect of preterm birth on thalamic and cortical development. Cereb Cortex. 22, 1016-24.

Ball, G., et al., 2013. Development of cortical microstructure in the preterm human brain. Proceedings of the National Academy of Sciences of the United States of America. 110, 9541-9546.

Bastiani, M., et al., 2019. Automated processing pipeline for neonatal diffusion MRI in the developing Human Connectome Project. Neuroimage. 185, 750-763.

Batalle, D., et al., 2017. Early development of structural networks and the impact of prematurity on brain connectivity. Neuroimage. 149, 379-392.

Batalle, D., et al., 2019. Different patterns of cortical maturation before and after 38 weeks gestational age demonstrated by diffusion MRI in vivo. Neuroimage. 185, 764-775.

Baumann, N., Pham-Dinh, D., 2001. Biology of oligodendrocyte and myelin in the mammalian central nervous system. Physiological Reviews. 81, 871-927.

Behrens, T.E.J., et al., 2003. Characterization and propagation of uncertainty in diffusion-weighted MR imaging. Magnetic Resonance in Medicine. 50, 1077-1088.

Bhutta, A.T., et al., 2002. Cognitive and behavioral outcomes of school-aged children who were born preterm - A meta-analysis. Jama-Journal of the American Medical Association. 288, 728-737.

Budde, M.D., et al., 2011. The contribution of gliosis to diffusion tensor anisotropy and tractography following traumatic brain injury: validation in the rat using Fourier analysis of stained tissue sections. Brain. 134, 2248-60.

Budde, M.D., Annese, J., 2013. Quantification of anisotropy and fiber orientation in human brain histological sections. Front Integr Neurosci. 7, 3.

Bystron, I., Blakemore, C., Rakic, P., 2008. Development of the human cerebral cortex: Boulder Committee revisited. Nat Rev Neurosci. 9, 110-22.

Cameron, R.S., Rakic, P., 1991. Glial-Cell Lineage in the Cerebral-Cortex - a Review and Synthesis. Glia. 4, 124-137.

Cavanna, A.E., Trimble, M.R., 2006. The precuneus: a review of its functional anatomy and behavioural correlates. Brain. 129, 564-583.

Chan, W.Y., Yew, D.T., 1998. Apoptosis and Bcl-2 oncoprotein expression in the human fetal central nervous system. Anatomical Record. 252, 165-175.

Chang, L.J., et al., 2013. Decoding the Role of the Insula in Human Cognition: Functional Parcellation and Large-Scale Reverse Inference. Cerebral Cortex. 23, 739-749.

Cismaru, A.L., et al., 2016. Altered Amygdala Development and Fear Processing in Prematurely Born Infants. Front Neuroanat. 10, 55.

Craig, A.D., 2004. Human feelings: why are some more aware than others? Trends in Cognitive Sciences. 8, 239-241.

Dean, D.C., 3rd, et al., 2017. Mapping White Matter Microstructure in the One Month Human Brain. Sci Rep. 7, 9759.

Dhollander, T., Raffelt, D., Connelly, A., 2016. Unsupervised 3-tissue response function estimation from single-shell or multi-shell diffusion MR data without a co-registered T1 image. ISMRM Workshop on Breaking the Barriers of Diffusion MRI. 5.

Dimond, D., et al., 2020. Early childhood development of white matter fiber density and morphology. Neuroimage. 210:116552.

Dubois, J., et al., 2008. Asynchrony of the early maturation of white matter bundles in healthy infants: quantitative landmarks revealed noninvasively by diffusion tensor imaging. Human brain mapping. 29, 14-27.

Dudink, J., et al., 2015. Recent advancements in diffusion MRI for investigating cortical development after preterm birth-potential and pitfalls. Frontiers in Human Neuroscience. 8.

Duvanel, C.B., et al., 1999. Long-term effects of neonatal hypoglycemia on brain growth and psychomotor development in small-for-gestational-age preterm infants. Journal of Pediatrics. 134, 492-498.

Eaton-Rosen, Z., et al., 2015. Longitudinal measurement of the developing grey matter in preterm subjects using multi-modal MRI. Neuroimage. 111, 580-589.

Fair, D.A., et al., 2008. The maturing architecture of the brain's default network. Proceedings of the National Academy of Sciences of the United States of America. 105, 4028-4032.

Fischi-Gomez, E., et al., 2015. Structural Brain Connectivity in School-Age Preterm Infants Provides Evidence for Impaired Networks Relevant for Higher Order Cognitive Skills and Social Cognition. Cereb Cortex. 25, 2793-805.

Fransson, P., Marrelec, G., 2008. The precuneus/posterior cingulate cortex plays a pivotal role in the default mode network: Evidence from a partial correlation network analysis. Neuroimage. 42, 1178-1184.

Gajamange, S., et al., 2018. Fibre-specific white matter changes in multiple sclerosis patients with optic neuritis. Neuroimage-Clinical. 17, 60-68.

Genc, S., et al., 2018. Development of white matter fibre density and morphology over childhood: A longitudinal fixel-based analysis. Neuroimage. 183, 666-676.

Gimenez, M., et al., 2006. Abnormal orbitofrontal development due to prematurity. Neurology. 67, 1818-1822.

Graven, S.N., Browne, J.V., 2008. Auditory Development in the Fetus and Infant. Newborn and Infant Nursing Reviews. 8, 187-193.

Grussu, F., et al., 2017. Neurite dispersion: a new marker of multiple sclerosis spinal cord pathology? Annals of Clinical and Translational Neurology. 4, 663-679.

He, L.X., et al., 2020. Synaptic development of layer V pyramidal neurons in the prenatal human prefrontal neocortex: a Neurolucida-aided Golgi study. Neural Regeneration Research. 15, 1490-1495.

Heidemann, R.M., et al., 2010. Diffusion Imaging in Humans at 7T Using Readout-Segmented EPI and GRAPPA. Magnetic Resonance in Medicine. 64, 9-14.

Hermoye, L., et al., 2006. Pediatric diffusion tensor imaging: normal database and observation of the white matter maturation in early childhood. Neuroimage. 29, 493-504.

Hernandez Fernandez, M., et al., 2017. cuDIMOT: a CUDA toolbox for modelling the brain tissue microstructure from diffusion MRI. In: GPU Technology Conference. Vol., ed.^eds., Munich, germany.

Huppi, P.S., et al., 1998a. Microstructural development of human newborn cerebral white matter assessed in vivo by diffusion tensor magnetic resonance imaging. Pediatric research. 44, 584-590.

Huppi, P.S., et al., 1998b. Quantitative magnetic resonance imaging of brain development in premature and mature newborns. Annals of Neurology. 43, 224-235.

Huttenlocher, P.R., 1990. Morphometric Study of Human Cerebral-Cortex Development. Neuropsychologia. 28, 517-527.

Huttenlocher, P.R., Dabholkar, A.S., 1997. Regional differences in synaptogenesis in human cerebral cortex. Journal of Comparative Neurology. 387, 167-178.

Inder, T.E., et al., 2005. Abnormal cerebral structure is present at term in premature infants. Pediatrics. 115, 286-94.

Kelly, C.E., et al., 2020. Long-term development of white matter fibre density and morphology up to 13 years after preterm birth. medRxiv. 2020.04.01.20049585.

Kinney, H.C., et al., 1988. Sequence of central nervous system myelination in human infancy. II. Patterns of myelination in autopsied infants. J Neuropathol Exp Neurol. 47, 217-34.

Kiss, J.Z., Vasung, L., Petrenko, V., 2014a. Process of cortical network formation and impact of early brain damage. Curr Opin Neurol. 27, 133-41.

Kiss, J.Z., Vasung, L., Petrenko, V., 2014b. Process of cortical network formation and impact of early brain damage. Current Opinion in Neurology. 27, 133-141.

Kleinnijenhuis, M., et al., 2013. Layer-specific diffusion weighted imaging in human primary visual cortex in vitro. Cortex. 49, 2569-2582.

Knickmeyer, R.C., et al., 2008. A Structural MRI Study of Human Brain Development from Birth to 2 Years. Journal of Neuroscience. 28, 12176-12182.

Koelsch, S., 2010. Towards a neural basis of music-evoked emotions. Trends in Cognitive Sciences. 14, 131-137.

Koelsch, S., 2014. Brain correlates of music-evoked emotions. Nat Rev Neurosci. 15, 170-80.

Koelsch, S., Skouras, S., Lohmann, G., 2018. The auditory cortex hosts network nodes influential for emotion processing: An fMRI study on music-evoked fear and joy. Plos One. 13.

Kostovic, I., Jovanov-Milosevic, N., 2006. The development of cerebral connections during the first 20-45 weeks' gestation. Seminars in fetal & neonatal medicine. 11, 415-422.

Kostovic, I., Judas, M., 2010. The development of the subplate and thalamocortical connections in the human foetal brain. Acta paediatrica (Oslo, Norway : 1992). 99, 1119-1127.

Kostovic, I., et al., 2014. Perinatal and early postnatal reorganization of the subplate and related cellular compartments in the human cerebral wall as revealed by histological and MRI approaches. Brain Struct Funct. 219, 231-53.

Kringelbach, M.L., 2005. The human orbitofrontal cortex: Linking reward to hedonic experience. Nature Reviews Neuroscience. 6, 691-702.

Krsnik, Z., et al., 2017. Growth of Thalamocortical Fibers to the Somatosensory Cortex in the Human Fetal Brain. Front Neurosci. 11, 233.

Kunz, N., et al., 2014. Assessing white matter microstructure of the newborn with multi-shell diffusion MRI and biophysical compartment models. Neuroimage. 96, 288-99.

Largo, R., et al., 1989. Significance of prenatal, perinatal and postnatal factors in the development of AGA preterm infants at five to seven years. Developmental Medicine & Child Neurology. 31, 440-456.

Lasky, R.E., Williams, A.L., 2005. The Development of the Auditory System from Conception to Term. NeoReviews. 6, e141-e152.

Leech, R., Sharp, D.J., 2014. The role of the posterior cingulate cortex in cognition and disease. Brain. 137, 12-32.

Lejeune, F., et al., 2019. Effects of an Early Postnatal Music Intervention on Cognitive and Emotional Development in Preterm Children at 12 and 24 Months: Preliminary Findings. Frontiers in Psychology. 10.

Leuze, C.W.U., et al., 2014. Layer-Specific Intracortical Connectivity Revealed with Diffusion MRI. Cerebral Cortex. 24, 328-339.

Lordier, L., et al., 2018. Music processing in preterm and full-term newborns: A psychophysiological interaction (PPI) approach in neonatal fMRI. Neuroimage.

Lordier, L., et al., 2019. Music in premature infants enhances high-level cognitive brain networks. Proceedings of the National Academy of Sciences of the United States of America. 116, 12103-12108.

Lossi, L., Merighi, A., 2003. In vivo cellular and molecular mechanisms of neuronal apoptosis in the mammalian CNS. Progress in Neurobiology. 69, 287-312.

Mackes, N.K., et al., 2018. Tracking emotions in the brain - Revisiting the Empathic Accuracy Task. Neuroimage. 178, 677-686.

Maddock, R.J., Garrett, A.S., Buonocore, M.H., 2003. Posterior cingulate cortex activation by emotional words: fMRI evidence from a valence decision task. Human Brain Mapping. 18, 30-41.

Malhotra, A., et al., 2019. Advanced MRI analysis to detect white matter brain injury in growth restricted newborn lambs. Neuroimage-Clinical. 24.

Marin-Padilla, M., 1992. Ontogenesis of the pyramidal cell of the mammalian neocortex and developmental cytoarchitectonics: a unifying theory. J Comp Neurol. 321, 223-40.

Marlow, N., 2004. Neurocognitive outcome after very preterm birth. Archives of disease in childhood. Fetal and neonatal edition. 89, F224-8.

Mars, R.B., et al., 2012. On the relationship between the "default mode network" and the "social brain". Front Hum Neurosci. 6, 189.

Martinet, M., et al., 2013. [Development and assessment of a sensory-motor scale for the neonate: a clinical tool at the bedside]. Arch Pediatr. 20, 137-45.

McKiernan, K.A., et al., 2003. A parametric manipulation of factors affecting task-induced deactivation in functional neuroimaging. J Cogn Neurosci. 15, 394-408.

McKinstry, R.C., et al., 2002. Radial organization of developing preterm human cerebral cortex revealed by non-invasive water diffusion anisotropy MRI. Cerebral Cortex. 12, 1237-1243.

Montagna, A., Nosarti, C., 2016. Socio-Emotional Development Following Very Preterm Birth: Pathways to Psychopathology. Frontiers in Psychology. 7.

Mrzljak, L., et al., 1988. Prenatal development of neurons in the human prefrontal cortex: I. A qualitative Golgi study. J Comp Neurol. 271, 355-86.

Mukherjee, P., et al., 2002. Diffusion-tensor MR imaging of gray and white matter development during normal human brain maturation. AJNR Am J Neuroradiol. 23, 1445-56.

Neil, J.J., et al., 1998. Normal brain in human newborns: apparent diffusion coefficient and diffusion anisotropy measured by using diffusion tensor MR imaging. Radiology. 209, 57-66.

Nosarti, C., et al., 2014. Preterm birth and structural brain alterations in early adulthood. Neuroimage-Clinical. 6, 180-191.

Nossin-Manor, R., et al., 2013. Quantitative MRI in the very preterm brain: Assessing tissue organization and myelination using magnetization transfer, diffusion tensor and T-1 imaging. Neuroimage. 64, 505-516.

Ohnishi, T., et al., 2001. Functional anatomy of musical perception in musicians. Cerebral Cortex. 11**,** 754-760.

Oishi, K., et al., 2010. MRI Atlas of Human White Matter Vol., Academic Press

Olson, I.R., Ploaker, A., Ezzyat, Y., 2007. The Enigmatic temporal pole: a review of findings on social and emotional processing. Brain. 130**,** 1718-1731.

Pannek, K., et al., 2018. Fixel-based analysis reveals alterations is brain microstructure and macrostructure of preterm-born infants at term equivalent age. Neuroimage-Clinical. 18**,** 51-59.

Pecheva, D., et al., 2019. Fixel-based analysis of the preterm brain: Disentangling bundle-specific white matter microstructural and macrostructural changes in relation to clinical risk factors. Neuroimage-Clinical. 23.

Peretz, I., et al., 1994. Functional Dissociations Following Bilateral Lesions of Auditory-Cortex. Brain. 117**,** 1283-1301.

Peters, A., Jones, E.G., 1985. Association and Auditory Cortices. Cerebral Cortex, Vol. 4, ed.^eds. Springer US.

Peterson, B.S., et al., 2000. Regional brain volume abnormalities and long-term cognitive outcome in preterm infants. Jama-Journal of the American Medical Association. 284**,** 1939-1947.

Pouchelon, G., Jabaudon, D., 2014. Nurturing the cortex's thalamic nature. Current Opinion in Neurology. 27**,** 142-148.

Radley, J.J., Morrison, J.H., 2005. Repeated stress and structural plasticity in the brain. Ageing Research Reviews. 4**,** 271-287.

Raffelt, D.A., et al., 2015. Connectivity-based fixel enhancement: Whole-brain statistical analysis of diffusion MRI measures in the presence of crossing fibres. Neuroimage. 117**,** 40-55.

Raffelt, D.A., et al., 2017. Investigating white matter fibre density and morphology using fixel-based analysis. Neuroimage. 144**,** 58-73.

Rakic, P., 2003. Developmental and evolutionary adaptations of cortical radial glia. Cereb Cortex. 13**,** 541-9.

Rogers, C.E., et al., 2012. Regional Cerebral Development at Term Relates to School-Age Social-Emotional Development in Very Preterm Children. Journal of the American Academy of Child and Adolescent Psychiatry. 51**,** 181-191.

Rose, S.E., et al., 2008. Altered white matter diffusion anisotropy in normal and preterm infants at term-equivalent age. Magnetic Resonance in Medicine. 60**,** 761-767.

Rowley, C.D., et al., 2017. Age-Related Mapping of Intracortical Myelin from Late Adolescence to Middle Adulthood Using T-1-Weighted MRI. Human Brain Mapping. 38**,** 3691-3703.

Sa de Almeida, J., et al., 2019. Music enhances structural maturation of emotional processing neural pathways in very preterm infants. Neuroimage. 207**,** 116391.

Salami, M., et al., 2003. Change of conduction velocity by regional myelination yields constant latency irrespective of distance between thalamus and cortex. Proceedings of the National Academy of Sciences of the United States of America. 100**,** 6174-6179.

Sarkamo, T., Tervaniemi, M., Huotilainen, M., 2013. Music perception and cognition: development, neural basis, and rehabilitative use of music. Wiley Interdisciplinary Reviews-Cognitive Science. 4**,** 441-451.

Shim, S.Y., et al., 2012. Altered Microstructure of White Matter Except the Corpus Callosum Is Independent of Prematurity. Neonatology. 102**,** 309-315.

Simmons, L.E., et al., 2010. Preventing Preterm Birth and Neonatal Mortality: Exploring the Epidemiology, Causes, and Interventions. Seminars in Perinatology. 34**,** 408-415.

Singer, T., Critchley, H.D., Preuschoff, K., 2009. A common role of insula in feelings, empathy and uncertainty. Trends in Cognitive Sciences. 13**,** 334-340.

Smith, R.E., et al., 2013. SIFT: Spherical-deconvolution informed filtering of tractograms. Neuroimage. 67**,** 298-312.

Smith, S.M., et al., 2004. Advances in functional and structural MR image analysis and implementation as FSL. Neuroimage. 23**,** S208-S219.

Smyser, C.D., et al., 2010. Longitudinal analysis of neural network development in preterm infants. Cereb Cortex. 20**,** 2852-62.

Smyser, T.A., et al., 2016. Cortical Gray and Adjacent White Matter Demonstrate Synchronous Maturation in Very Preterm Infants. Cereb Cortex. 26**,** 3370-3378.

Spittle, A.J., et al., 2009. Early Emergence of Behavior and Social-Emotional Problems in Very Preterm Infants. Journal of the American Academy of Child and Adolescent Psychiatry. 48**,** 909-918.

Spittle, A.J., et al., 2011. Neonatal white matter abnormality predicts childhood motor impairment in very preterm children. Dev Med Child Neurol. 53**,** 1000-6.

Sridharan, D., Levitin, D.J., Menon, V., 2008. A critical role for the right fronto-insular cortex in switching between central-executive and default-mode networks. Proc Natl Acad Sci U S A. 105**,** 12569-74.

Thompson, D.K., et al., 2007. Perinatal risk factors altering regional brain structure in the preterm infant. Brain. 130**,** 667-77.

Thompson, D.K., et al., 2013. Hippocampal shape variations at term equivalent age in very preterm infants compared with term controls: perinatal predictors and functional significance at age 7. Neuroimage. 70**,** 278-87.

Tournier, J.-D., Calamante, F., Connelly, A., 2010. Improved probabilistic streamlines tractography by 2nd order integration over fibre orientation distributions. Proc. Intl. Soc. Mag. Reson. Med. (ISMRM). 18.

Tournier, J.D., et al., 2019. MRtrix3: A fast, flexible and open software framework for medical image processing and visualisation. Neuroimage. 202**,** 116137.

van den Heuvel, M.P., et al., 2015. The Neonatal Connectome During Preterm Brain Development. Cerebral Cortex. 25**,** 3000-3013.

Vinall, J., et al., 2012. Neonatal pain in relation to postnatal growth in infants born very preterm. Pain. 153**,** 1374-1381.

Volpe, J.J., 2001. Neurology of the newborn (4th ed.), Vol., W.B. Saunders, Philadelphia.

Volpe, J.J., 2009. Brain injury in premature infants: a complex amalgam of destructive and developmental disturbances. Lancet Neurology. 8**,** 110-124.

Webb, A.R., et al., 2015. Mother's voice and heartbeat sounds elicit auditory plasticity in the human brain before full gestation. Proceedings of the National Academy of Sciences of the United States of America. 112**,** 3152-3157.

White, T.P., et al., 2014. Dysconnectivity of neurocognitive networks at rest in very-preterm born adults. Neuroimage-Clinical. 4**,** 352-365.

Whitfield-Gabrieli, S., Ford, J.M., 2012. Default Mode Network Activity and Connectivity in Psychopathology. Annual Review of Clinical Psychology, Vol 8. 8**,** 49-+.

Wildgruber, D., et al., 2005. Identification of emotional intonation evaluated by fMRI. Neuroimage. 24**,** 1233-1241.

Williams, J., Lee, K.J., Anderson, P.J., 2010. Prevalence of motor-skill impairment in preterm children who do not develop cerebral palsy: a systematic review. Dev Med Child Neurol. 52**,** 232-7.

Witt, A., et al., 2014. Emotional and effortful control abilities in 42-month-old very preterm and full-term children. Early Hum Dev. 90**,** 565-9.

Zamorano, A.M., et al., 2017. Insula-Based Networks in Professional Musicians: evidence for Increased Functional Connectivity during Resting State fMRI. Human Brain Mapping. 38**,** 4834-4849.

Zatorre, R.J., Peretz, I., Penhune, V., 2009. Neuroscience and Music ("Neuromusic") III: disorders and plasticity. . Annals of the New York Academy of Sciences. 1169**,** 1-2.

Zhang, H., et al., 2012. NODDI: Practical in vivo neurite orientation dispersion and density imaging of the human brain. Neuroimage. 61**,** 1000-1016.

Supplementary material

Supplementary Figures

Supplementary Fig. S1
Flow chart of the participant selection process
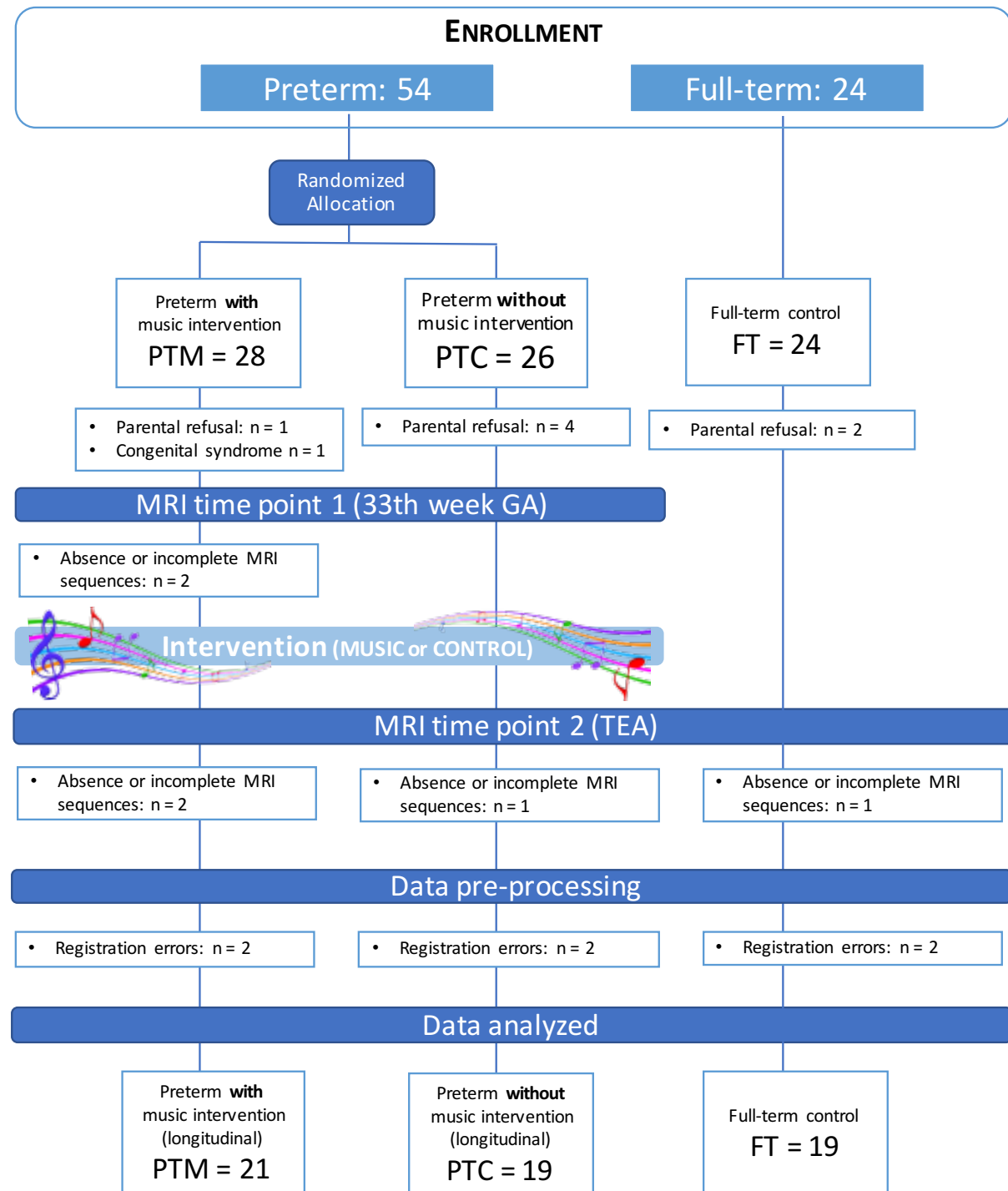
Supplementary Fig. S1: 54 very preterm infants (GA at birth <32 weeks) were recruited at the neonatal unit of the University Hospitals of Geneva (HUG), Switzerland, from 2017 to 2020, as part of a prospective randomized clinical trial entitled 'The effect of music on preterm infant's development' (NCT03689725). The 54 infants were randomized into two groups, 28 received a music intervention during NICU stay (PTM) and 26 received standard-of-care during NICU stay (PTC). Randomization was performed using an aleatory function for an unpredictable allocation sequence with concealment of that sequence until assignment occurred. The random allocation, enrolment of patients and assignment of patients to intervention was performed by the research assistant. Parents, music intervention providers, and caregivers were blinded to the group assignment. Additionally, 24 full-term (FT) infants were recruited at the maternity of HUG, from 2017 to 2019 as part of the same clinical trial. Inclusion criteria for full-term newborns included: birth after 37 weeks GA and an appropriate height, weight or head circumference (above the 5th and below the 95th percentiles), APGAR score > 8 at the 5th minute and absence of reanimation, infection or hospitalisation in neonatology unit. Exclusion criteria were similar to those used for preterm infants. Exclusion criteria for all infants comprised detection of severe brain lesions on MRI, such as intraventricular haemorrhage stage III-IV, hydrocephaly or leukomalacia, microcephaly or macrocephaly and presence of congenital syndrome.

Six preterm infants were excluded from the study due to parental refusal (1 PTM, 4 PTC) and genetic problems (1 PTM). Additionally, two full-term infants were excluded from the study due to parental refusal. Infants whose MRI protocol acquisition was incomplete (not comprising a T2-weighted image and/or complete multi-shell diffusion imaging (MSDI) sequence), without both longitudinal time-points (in preterm infants' case) or whose images presented registration issues during pre-processing, were excluded from the analysis. The final sample of infants used for the analysis consisted of: 40 VPT infants, from which 21 PTM and 19 PTC, and 19 FT infants.

Supplementary Fig. S2
Headphones adapted for preterm infant's head and preterm infants using the headphones set.

Supplementary Fig. 21: Photos of the headphones specifically designed for the project, adapted to preterm infants' head size. Headphones set (left top); very preterm infant participating in the intervention using the headphones in the NICU unit (left bottom); photo from a cover of a special issue from National Geographic, which included an article about our study (photo from Craig Cutler).